

# 13<sup>th</sup> International Conference on the **SCIENTIFIC AND CLINICAL APPLICATIONS OF MAGNETIC CARRIERS**

LONDON, UNITED KINGDOM

JUNE 14-17, 2022



Nguyen T. K. Thanh  
London, U.K.



Wolfgang Schutt  
Krems, Austria



Maciej Zborowski  
Cleveland, Ohio, U.S.A.



Urs Hafeli  
Vancouver, BC, Canada

The cover image was captured using a TEM at 40,000x magnification during work on the synthesis of iron oxide nanoflowers with outstanding heating efficiencies (ILP of  $8.4 \text{ nH m}^2/\text{kg}_{\text{Fe}}$  or SAR =  $2426 \pm 76 \text{ W/g}_{\text{Fe}}$ ) measured at a frequency of 488 kHz and a field strength of  $25 \text{ kA m}^{-1}$ . Each flower contains approximately 50 coalesced nanoparticles. (Storozhuk, L., Besenhard M. O., Mourdikoudis, S., LaGrow, A. P., Lees, M.R., Tung, L. D., Gavriilidis, A., **Thanh, N.T. K\*** (2021) Simple and Fast Polyol Synthesis of Stable Iron Oxide Nanoflowers with Exceptional Heating Efficiency. *Journal of Applied Materials and Interface*. **13**: 45870–45880). The work has become a finalist for 2022 The Royal Society of Chemistry Emerging Technologies Competition in Health category.



## Welcome Message

It is our great pleasure to welcome you all to the 13<sup>th</sup> International Conference on the Scientific and Clinical Applications of Magnetic Carriers. We are happy that it is now once again possible to have this wonderful meeting in-person to discuss our recent achievements in research on magnetic particles and their applications.

London is an excellent location to host such a conference and we are very fortunate that the selected venue, University College London, or UCL for short, is located right in the heart of the city. This allows easy access to a great variety of historical landmarks and areas around the city in reasonable time.

Unfortunately, the COVID-19 pandemic is not yet over, so while our conference will be held in person, we are basing our plans on you having received your vaccinations and booster shots, all of us wearing masks during the conference, and following all the local and UK national requirements regarding meetings and gatherings. Also, if you feel unwell during the conference or demonstrate COVID-19 symptoms, please perform a lateral flow test, and stay home if you are positive.

At our conference location, University College London (UCL), we will have a large auditorium so we can be well spaced out during the talks. In addition, the spaces for poster sessions, lunches and breaks are extensive enough for social distancing, and we also have a large outside space available.

We welcome you for a successful and interesting conference!

Your organizers,

Urs Hafeli, University of British Columbia, Vancouver, Canada,  
Nguyen T. K. Thanh, University College London, UK,  
Maciej Zborowski, Cleveland Clinic Foundation, Cleveland, USA,  
Wolfgang Schutt, IMC Krems, Austria & Rostock, Germany.

## Social Program

It has been said that science may never come up with a better system for communication than the coffee break. But why not also extend our social interactions beyond the conference venue? In this way, we will have fun, enjoy London, and get to know each other better.

### Tuesday, June 14

After the end of the first poster session, we will have a [reception](#) in the Wilkins Terrace, with lots of food and drinks. This traditional get-together is generously sponsored by **nanotherics**. Enjoy!

### Wednesday, June 15

At the end of the day, beer and Pretzels will be offered following the end of the second poster session. This is graciously supported by **micromod Partikeltechnology GmbH**.

### Thursday, June 16

During the day, there will be a spouse tour. This tour is complimentary and always fun. Spouses will meet at 9:00 at the registration desk in the UCL Wilkins building, in the North Cloisters. Spouses will be back at UCL latest at 17:15.

The traditional boat trip along the river Thames is generously sponsored by **Imagion Biosystems**. We will start at 17:30 with a double decker bus ride to Butlers Wharf Pier, board at 18:15 and cast off at 18:30 – please be on time! During the trip, we will enjoy a wonderful dinner, picturesque views of London and as always, a great time. The New Orleans style jazz band "The Blind Tigers" will keep us on our feet and is generously sponsored by **chemicell**. Our boat, the 'Dixie Queen' will be back at a different pier, the Tower Millenium Pier at 22:30. The buses will bring us back to UCL from there.



### Friday, June 17

The meeting will come to an end at 17:00. Please take the opportunity to explore the English capital on your own after the end of the conference!



# 13<sup>th</sup> International Conference on the Scientific and Clinical Applications of Magnetic Carriers

London, UK – June 14-17, 2022 – [magneticmicrosphere.com](http://magneticmicrosphere.com)

## 13th International Conference on the Scientific and Clinical Applications of Magnetic Carriers - London, UK

Tuesday, June 14, 2022

12:00	Registration desk opens in the Wilkins Building, North Cloisters		
	<b>Opening Session - Cruciform Building, Auditorium B304 - LT1</b>		
13:00	Parkin, Ivan	Opening of the conference and welcome address by Prof. Ivan Parkin the Dean of UCL MAFS (Faculty of Math Applied Phys Sci)	
13:10	Hafeli, Urs	Short review of the last 4 years of magnetic carriers research	Vancouver, BC, Canada Talk 0
	<b>Session 1 Nanoparticle Synthesis I</b>	<b>Chair: Thompson Mefford</b>	
13:30	Ablets, Yevhen	Synthesis and properties of Fe3N nanoparticles as alternative material for magnetic fluid hyperthermia	Darmstadt, Germany Talk 1
13:45	Bertuit, Enzo	Structure-Property-Function Relationships of Iron Oxide Multi-Core Nanoflowers in Magnetic Hyperthermia and Photohyperthermia	Paris, France Talk 2
14:00	Besenhard, Maximilian	Novel Reactor Concepts for the Reproducible and Scalable Synthesis of Fine-Tuned Magnetic Nanoparticles	London, UK Talk 3
14:15	Bleul, Regina	Micromixer synthesis for optimized manufacturing of single-core magnetic nanoparticles with tailored properties for versatile biomedical and clinical applications	Mainz, Germany Talk 4
14:30	<b>Coffee break - Wilkins Building North &amp; South Cloisters and Upper Terrace</b>		
	<b>Session 2 Nanoparticle Synthesis II</b>	<b>Chair: Nguyen Thanh</b>	
15:15	Durhuus, Frederik	Simulated clustering dynamics of magnetic nanoparticles	Copenhagen, Denmark Talk 5
15:30	Mefford, Thompson	Synthesis of polymer modified substituted ferrite nanomaterials guided by density functional theory and machine learning	Clemson, USA Talk 6
15:45	Roca, Alejandro	Fe3O4 Nanocubes as Multifunctional Theranostic Agents	Cerdanya del Valles, Spain Talk 7
16:00	Zabow, Gary	Micropatterning Magnetic Microparticles	Boulder, USA Talk 8
16:15	Zolochlevska, Kristina	Interaction of Ferritin Derivatives with Lysozyme Amyloid Fibrils	Kosice, Slovakia Talk 9
16:30	<b>Discussion with speakers from the Nanoparticle Synthesis session: Do we really still need new magnetic nanoparticle types?</b>		
17:15	<b>Poster session I (Posters 1-52) - In North Cloisters and Jeremy Bentham Room</b>		
18:30	<b>Reception in the Wilkins Building Upper Terrace with drinks and snacks. Generously sponsored by nanotherics!</b>		

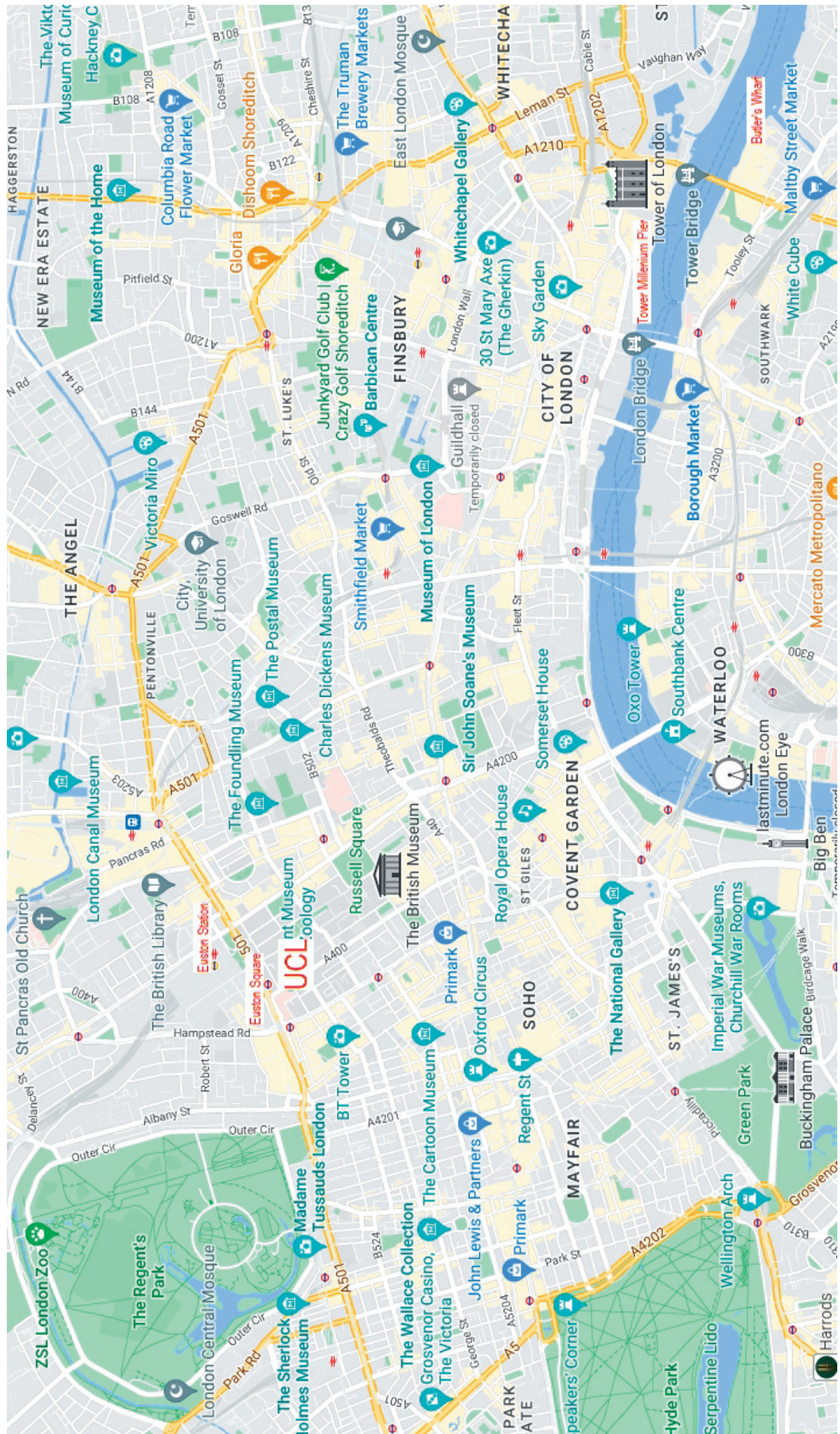
Wednesday, June 15, 2022

8:30	Registration desk opens in the Wilkins Building, North Cloisters		
8:45	Livesey, Karen	Tutorial about the basics of magnetic particles - Part I	Newcastle, Australia Tutorial 1
	<b>Session 3 Magnetic Imaging / MPI / MRI</b>	<b>Chair: Thilo Vierck</b>	
9:15	Schier, Peter	Quantitative Imaging of Magnetic Nanoparticles in Large Body Regions using Nonlinear Magnetorelaxometry	Hall in Tirol, Austria Talk 10
9:30	Rinaldi-Ramos, Carlos	Labeling T cells with a new tracer tailored for sensitive tracking using magnetic particle imaging (MPI)	Gainesville, USA Talk 11
9:45	Kim, Hoheyon	MPi image-based cancer hyperthermia therapy	Gwangju, South Korea Talk 12
10:00	<b>Coffee break - Wilkins Building North Cloisters, JBR and Upper Terrace</b>		
	<b>Session 4 Magnetic Imaging / MPI / MRI II</b>	<b>Chair: Carlos Rinaldi</b>	
10:45	Löwa, Norbert	Establishment of metabolic tracer based magnetic particle imaging	Berlin, Germany Talk 13
11:00	Arsalan, Soudab	Developing Magnetorelaxometry Imaging for Human Applications	Berlin, Germany Talk 14
11:15	Dutz, Silvio	A dynamic bolus phantom for the evaluation of the spatio-temporal resolution of MPI scanners	Ilmenau, Germany Talk 15
11:22	Oberdick, Samuel	Iron Oxide Nanoparticles as T1 Agents for Low-Field MRI	Boulder, CO, USA Talk 16
11:30	Schürle-Finke, Simone	Engineering Magnetic Nanorobots for Medicine	Zurich, Switzerland Invited Talk 1

12:15	<b>Lunch</b>			
13:15	<b>Session 5 Magnetic Drug Delivery</b>	<i>Chair: Quentin Parkhurst</i>		
13:30	Bizeau, Joelle	Innovative nanocomposites for protein release through magnetic hyperthermia	Strasbourg, France	Talk 17
13:45	Guidelli, Eder	Superparamagnetic Nanodevices as Single Oxygen Carriers for Cancer Therapy	Ribeirão Preto, Brazil	Talk 18
14:00	Howard, Faith	Bugs as drugs - Bacterial derived nanomagnets enhance tumour targeting and oncolytic activity of HSV-1 virus	Sheffield, UK	Talk 19
14:15	Marquina, Clara	Graphene-Encapsulated Magnetic Nanoparticles for Safe and Steady Delivery of Ferulic Acid in Diabetic Mice	Zaragoza, Spain	Talk 20
14:15	Zahn, Diana	Towards drug targeting to the eye using magnetic multilayer nanoparticles	Ilmenau, Germany	Talk 21
14:30	<b>Coffee break / Change posters to session II Magnetic Hyperthermia</b>	<i>Chair: Silvio Dutz</i>	<i>Zaragoza, Spain</i>	<i>Invited Talk 2</i>
15:15	Gutiérrez, Maruedo, Lucía	Beyond Classical Magnetic Hyperthermia: From Innovative Characterization Approaches to New Therapeutic Alternatives	Zaragoza, Spain	
16:00	Fratila, Raluca	Critical Parameters to Improve Pancreatic Cancer Treatment Using Magnetic Hyperthermia: Field Conditions, Immune Response, and Particle Biodistribution	Zaragoza, Spain	Talk 22
16:15	Ortega, Daniel	In silico safety analysis of different metallic implants in magnetic hyperthermia treatments	Madrid, Spain	Talk 23
16:30	Mues, Benedikt	Hyperthermia and Imaging Performance of Hybrid Stents with Incorporated Magnetic Nanoparticles for Tumor Ablation	Aachen, Germany	Talk 24
16:45	Storozhuk, Liudmyla	Iron Oxide Nanoflowers as Excellent Heating Agents for Magnetic Hyperthermia Cancer Therapy	London, UK	Talk 25
17:00	Telling, Neil	A magneto-optical microscope for investigating magnetisation dynamics of intracellular nanoparticles under hyperthermia conditions	Stoke-on-Trent, UK	Talk 26
17:15	<b>Session 6B - Short Talks Magnetic Hyperthermia</b>	<i>Chair: Silvio Dutz</i>	<i>Zaragoza, Spain</i>	
17:22	Bussolari, Francesca	Magnetic heating to trigger entrapped enzymes activity	Zaragoza, Spain	Talk 27
17:30	Cabriera, David	Nanoparticle-mediated magnetic hyperthermia enhances the breakdown of human blood clots by tissue plasminogen activator	Stoke-on-Trent, UK	Talk 28
17:37	Briero, Francesca	Magnetic Hyperthermia as an adjuvant cancer therapy in combination with carbon ions, protons and photons irradiation on pancreatic tumour cell cultures	Pavia, Italy	Talk 29
17:45	Castro, Jorge	Development of Handheld Induction Heaters for Magnetic Fluid Hyperthermia Applications and In-vitro Evaluation on Ovarian and Prostate Cancer Cells	Mayaguez, Puerto Rico	Talk 30
17:52	Milan, Angel	Local temperature gradients in intracellular magnetic hyperthermia	Zaragoza, Spain	Talk 31
18:00	Del Sol Fernández, Susel	Composition impacts the structural, magnetic, and heating efficiency of Mn <sub>x</sub> Fe <sub>3-x</sub> O <sub>4</sub> MNPs. An <i>in vitro</i> and <i>in vivo</i> study.	Zaragoza, Spain	Talk 32
19:30	<b>Poster session II (Posters 53-104) - In North Cloisters and Jeremy Bentham Room - with Beer and Pretzels generously sponsored by micromod!</b>			
<b>Thursday, June 16, 2022</b>				
8:30	<b>Registration desk opens in the Wilkins Building, North Cloisters</b>			
8:45	Livesey, Karen	<b>Tutorial about the basics of magnetic particles - Part II</b>	Newcastle, Australia	<b>Tutorial 2</b>
9:15	<b>Session 7 Analytical Techniques</b>	<i>Chair: Ron Goldfarb</i>	<i>Zurich, Switzerland</i>	<i>Invited Talk 3</i>
9:15	Scagnoli, Valerio	<b>Mapping the Structure and Behaviour of 3D Nanomagnetic Systems</b>	Garching, Germany	
10:00	Feektystov, Artem	On the mechanisms of magnetization reduction in iron oxide nanoparticles	Columbus, USA	Talk 33
10:15	<b>Coffee break</b>		Berlin, Germany	
11:00	Agarwal, Gunjan	Multimodal Magnetic Force Microscopy	Ghent, Belgium	Talk 34
11:15	Radon, Patricia	Harmonizing of static magnetization measurements using two commercial SQUID devices of the same type	Bilbao, Spain	Talk 35
11:30	<b>Session 8 Magnetic Force Optimizations</b>	<i>Chair: Frank Wierhorst</i>	<i>Montreal, Canada</i>	
11:45	Van Dume, Rikkert	Magnetic Force Optimization for Improved Magnetic Particle Targeting	London, England	<b>Invited Talk 4</b>
12:00	Villanueva Alvaro, Danny	Navigation control of Magnetotactic Bacteria by magnetic fields	Zaragoza, Spain	Talk 39
12:15	Li, Ning	Magnetic resonance navigation system for supra-selective embolization of the liver: <i>in vivo</i> demonstration with SPIONs	Wien, Austria	Talk 40
12:15	<b>Lunch - BBQ generously sponsored by nanoScale Biomagnetics!</b>			
13:15	Hart, Stephen	<b>Towards Gene Regulation and Editing</b>	Paris, France	<b>Talk 41</b>
14:00	Idiago-López, Javier	CRISPR - An Introduction to Gene Editing	San Diego, USA	<b>Talk 42</b>
14:15	Mostarac, Deniz	Combining bioorthogonal click chemistry and magnetic hyperthermia for siRNA transfection		
14:30	Slaugue, Jean-Michel	Characterisation of DNA Nano-Chamber Magnetic Filaments		
14:45	Proulx, Robert	Strain promoted azide alkyne click chemistry, an efficient surface functionalization strategy for microRNAs magnetic separation		
15:00	<b>Coffee break</b>	Magnetic Nanoparticles for Diagnostic Imaging: Getting into the Clinic		

Session 10		Biosensors	Chair: Wolfgang Schütt	
15:45	Deroo, Maikane	Innovative dynamic detection for early diagnosis with a lab-on-a-chip based on two-stage giant magnetoresistance sensors	Gif-sur-Yvette, France	Talk 43
16:00	Rösch, Enja	Sensitive DNA detection via strand displacement mediated disassembly of magnetic nanoclusters	Braunschweig, Germany	Talk 44
16:15	Christiansen, Michael	Development of Inductively Detectable Probes for Proteolytic Activity	Zurich, Switzerland	Talk 45
16:30	Wang, Jian-Ping	Handheld Magnetic Particle Spectroscopy (MPS) for Rapid, One-step, Wash-free Detection of SARS-CoV-2 Spike and Nucleocapsid Proteins in Liquid Phase	Minneapolis, MN, USA	Talk 46
16:45	Oh, Seungjun	Development of Magnetic Particle Spectroscopy That Integrates Both Conventional and Mixing Methods for Virus Detection	Gwangju, South Korea	Talk 47
17:00	<b>Talks will stop punctually at 17:00. Then transfer to the boat by Double Decker Bus.</b>			
18:30	<b>Boat tour with dinner from the Butler's Wharf Pier generously sponsored by Imagine Biosystems! And the New Orleans type band "Blind Tigers" is sponsored by Chemicell!</b>			
22:30	<b>Return to the Tower Millennium Pier (different pier!), travel back to UCL by Double Decker Bus.</b>			
Friday, June 17, 2022				
8:30	Registration desk opens in the Wilkins Building, North Cloisters			
8:45	Livesey, Karen	Tutorial about the basics of magnetic particles - Part III	Newcastle, Australia	Tutorial 3
Session 11		Biocompatibility Studies	Chair: Clara Margalida	
9:15	Ma, Yunn-Hwa	PEGylated Magnetic Nanoparticle-Induced Acute Hypersensitivity Reaction: Role of Bioactive Corona	Tao-Yuan, Taiwan	Talk 48
9:30	Mickolet, Frank	Biocompatibility studies and cellular interactions of biogenic magnetic nanoparticles	Bayreuth, Germany	Talk 49
9:45	Friedrich, Bernhard	Biomimetic capturing of pathogens using SPIONs functionalized with salivary agglutinin (GP-340)-derived peptides	Erlangen, Germany	Talk 50
10:00	Manshian, Bella	NP-cellular hitchhiking system for targeted combination therapy and diagnosis of glioblastoma	Leuven, Belgium	Talk 51
10:07	Gandaras, Lucia	Intracellular degradation of biosynthesized magnetic nanoparticles	Leioa, Spain	Talk 52
Session 12		Magnetic Characterization and Separation	Chair: Maciej Zborowski	
10:15	Coffee break			
11:00	Boelens, Peter	Use of peptide functionalized Dynabeads for the magnetic carrier separation of Rare Earth phosphors in low and high magnetic field gradients	Dresden, Germany	Talk 53
11:15	Makridis, Antonios	3D Printing of Polymer-Bonded Magnets	Thessaloniki, Greece	Talk 54
11:30	Goldfarb, Ron	Problems in Magnetic Characterization of Nanoparticles	Boulder CO, USA	Invited Talk 5
12:15	Lunch			
Session 13		Biological Applications I	Chair: Anna Roig	
13:15	Block, Findan	Magnetic bucket brigade networks as rails for single cell transportation	Kiel, Germany	Talk 55
13:30	Clement, Joachim	Passage of magnetic nanoparticles through a differentiating blood-placenta barrier	Jena, Germany	Talk 56
13:45	Fernández-Castañé, Alfred	Biomanufacturing magnetosomes: nanocarriers with versatile functionalisation for imaging and drug delivery applications	Birmingham, UK	Talk 57
14:00	Freis, Barbara	Active Targeting of Head and Neck Cancer Cells with Dendronized Iron Oxide Nanoparticles and Effect of the Size and Shape of Nanoparticles for Promoting Multimodal Therapy	Strasbourg, France	Talk 58
14:15	Coffee break			
Session 14		Biological Applications II	Chair: Lucia Gutiérrez	
15:00	Romero Uribe, Gabriela	Nanomagnetic Actuators for Neural Modulation	San Antonio, TX, USA	Invited Talk 6
15:45	Gárces, Victor	Heterobimetallic probiotic bacteria as new oral magneto-optical hyperthermia agents	Granada, Spain	Talk 59
16:00	Horák, Daniel	Antioxidant and Antibacterial Magnetic Nanoparticles: Design, Synthesis and Biological Effects	Prague, Czechia	Talk 60
16:15	Pasek-Alien, Jacqueline	Advancing Revarming for Cryopreservation through Scalable Polymer Coating of Iron Oxide Nanoparticles	Minneapolis, MN, USA	Talk 61
16:30	El Mousli, Shirine	Synthesis, Characterization and Cellular Internalization of Anisotropic Magnetic Nanoparticles	Paris, France	Talk 62
16:45	<b>Closing Comments: Nguyen Thanh &amp; Urs Hofel</b>			
17:00	Meeting ends			

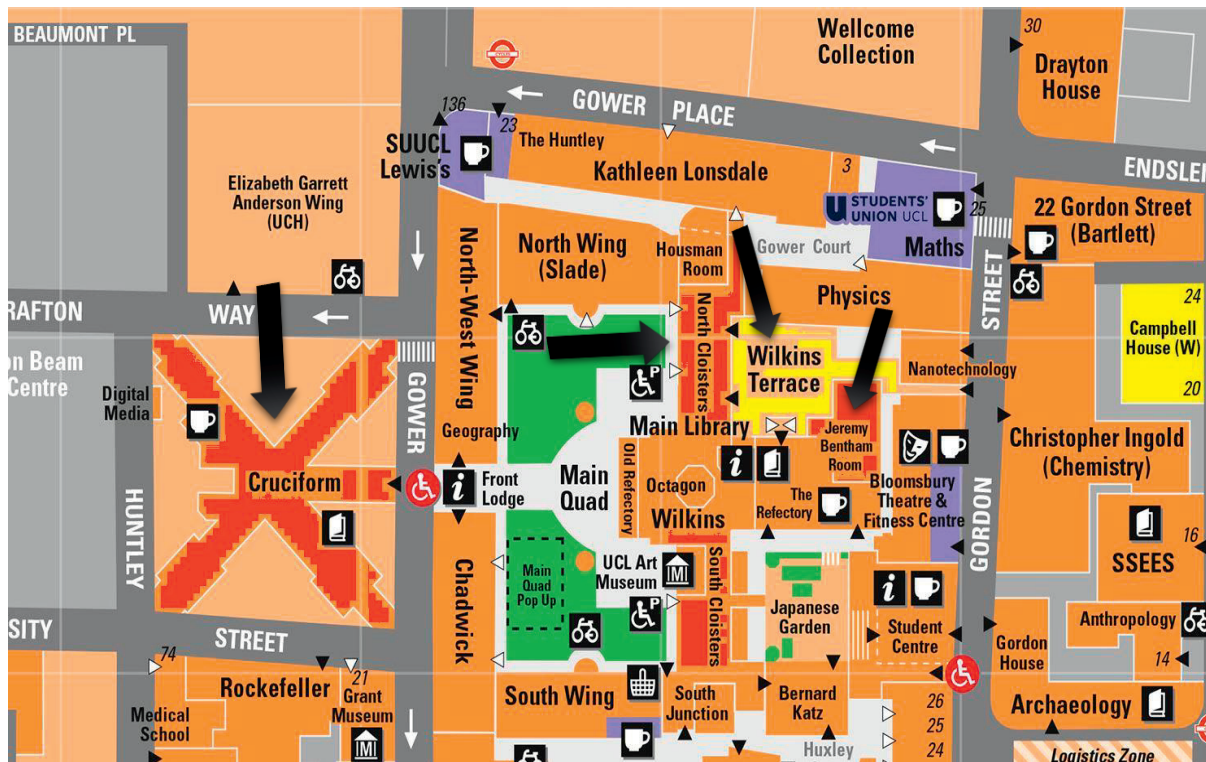
Map of London



## UCL Map



## Map of the Meeting Rooms at UCL





## INVITED TALK

### Engineering magnetic micro-and nanorobots for medicine

Simone Schürle<sup>1</sup>

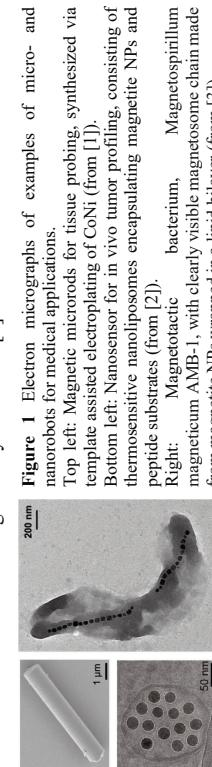
<sup>1</sup>Responsive Biomedical Systems Laboratory,  
Department for Health Sciences and Technology,  
ETH Zurich, Switzerland

e-mail: [simone.schuerle@hest.ethz.ch](mailto:simone.schuerle@hest.ethz.ch)

Engineering robots at the cellular scale could allow us to gain new insights into disease development and provide more targeted means for diagnostic and therapeutic interventions. Magnetic fields have proven to serve as safe strategy to wirelessly power magnetic microrobots for remote control in physiological environments. In this talk I will give an overview of three distinct examples of magnetic micro- and nanorobots for medical applications and describe their respective design and control schemes (Fig. 1).

First, I will present a method for 3D spatiotemporal probing of tissue models from a single cell perspective using microrobots. We fabricated rod-shaped magnetic microrods and leveraged 3D magnetic field generation, physical modeling, and image analysis to reveal local shear moduli and remotely apply mechanical stimuli [1]. The heterogeneous mechanical landscape of a tumor's extracellular matrix (ECM) is in part a result of increased local release of enzymes, in particular certain proteases, which degrades the ECM and is associated with tumor invasion. In a next example, I will describe nanorobots that are either activated or detected via magnetic fields and designed to report a tumor's proteolytic activity as novel diagnostic [2].

Last, I will show how an individual, synthetic and swarms of living magnetic microrobots can help to locally enhance transport of nanoparticles (NPs) mimicking drug carriers in a tissue model [3]. We employed two distinct micropropeller designs powered by rotating magnetic fields to increase diffusion-limited transport of NPs by enhancing local fluid convection. In the first approach, we use a single synthetic, magnetic microrobot, called an artificial bacterial flagellum, and in the second approach, we control swarms of magnetotactic bacteria to create a directable "living ferrofluid" by exploiting ferrohydrodynamics. With both strategies, we demonstrated the ability to locally and wirelessly drive convective transport in tissue models. The latter strategy has also shown to outperform synthetic ferrofluids in terms of ferrohydrodynamic coupling to drive NP transport (Fig.1) [4]. Lastly, I will share insights into how these living magnetic microrobots can be further engineered to function as therapeutic vectors themselves that can be magnetically controlled [5].



### References

- [1] Asgeirsson et al., *Lab Chip*, 21, 3850-3862, 2021
- [2] Schuerle et al., *Nano Lett.*, 16, 10, 6303-6310, 2016
- [3] Schuerle et al., *Sci. Adv.*, vol. 5, no. 4, eaav4803, 2019
- [4] Mirkhani, et al., *Adv. Funct. Mater.*, 2023912, 2020
- [5] Gwisi et al., bioRxiv, doi.org/10.1101/2022.01.03.473989, 2022

Invited Talk #1

## INVITED TALK

### Beyond Classical Magnetic Hyperthermia: from innovative characterization approaches to new therapeutic alternatives

Lucía Gutiérrez

<sup>1</sup>Departamento de Química Analítica, Instituto de Nanociencia y Materiales de Aragón (INMA), Universidad de Zaragoza-CSIC and CIBER-BBN, Zaragoza, Spain

email: [lu@unizar.es](mailto:lu@unizar.es)

Our work focuses on the use of iron oxide magnetic nanoparticles for pancreatic cancer treatment using hyperthermia. Along the journey from the material synthesis to the *in vivo* application, we have faced several drawbacks such as the difficulties characterizing the heat being produced in the tumors or the complex measurement of biological effects during the treatment. We have also developed interesting alternatives to solve some of these problems, so this talk will provide an overview of the advances we have achieved recently. Regarding the **nanoparticles characterization**, the first problem faced was the lack of standardized techniques and protocols to measure the heating properties of magnetic nanoparticles under the exposure to an AC magnetic field. The impact of the specific measurement settings leads to uncertainties when comparing results acquired with different equipment. In order to solve this, we have developed a fast protocol to calculate the SAR value based on zig-zag measurements (Fig. 1B up), obtaining more accurate results. We have also tracked the formation of reversible chains of magnetic nanoparticles during the SAR measurements (Fig. 1B down).

Once *in vivo*, knowledge on the transformations that magnetic nanoparticles suffer after their administration is a key parameter to design the therapeutic approach. The time frame in which the particles will produce an effect before they degrade is crucial to know whether a single administration can be used or repeated injections are needed. Using AC magnetic susceptibility measurements of tissue samples, we have tracked the transformations of particles in tumors and how these transformations may impact their heating properties (Fig. 1D).

In the specific case of **pancreatic cancer**, we have found that the heat produced during the magnetic hyperthermia treatment increased the permeability of the extracellular matrix (Fig. 1C). Using the particles to permeabilize the stroma could open the way for better outcomes from conventional chemotherapy, which hardly arrives to the inner parts of the tumor. We have also observed that the heat produced by the particles activates the release of immunogenic signals from the tumor cells (Fig. 1E), opening the way for further studies regarding the immune response of the body to this treatment.

Finally, we have prepared new materials with very interesting properties related to the production of heat.

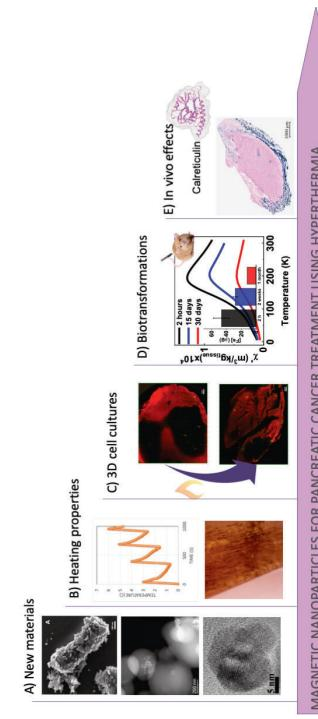
Bacteria loaded with magnetic and gold nanoparticles have been prepared as a particle carrier for oral administration (Fig. 1A up).

Enzymes have been trapped together with magnetic nanoparticles inside biomimetic silica shells to produce a drug in the tumor when a given temperature is reached (Fig. 1 A middle).

Manganese doped ferrites have been produced to improve the particles heating performance (Fig. 1 A down).

We have also been able to immobilize the particles into living cell membranes.

All these developments are small steps towards a better understanding of magnetic hyperthermia as a therapeutic strategy for cancer, aiming to achieve a successful treatment for pancreatic cancer in the near future.



**Acknowledgements:** Many people contributed to the work that will be presented in the talk. I am especially grateful to Yilian Fernández-Alonso, Laura Asín, Liliánn Beolí, Sílvia Solà, Javier Idiago, Sonali Correa, Lorena Betancor, Yadilen Portillo, Luis Porta, Miguel Castro, Víctor Garcés, José María Domínguez-Vera, Sergiu Ruta, David Serantes, Roy Chantrell, Domingo Barber, Puerto Morales, Sabino Veintemillas-Verdaguer, Jesús M. de la Fuente, María Moros, Valeria Grazu and Raluca Fratila.

Invited Talk #2

## INVITED TALK

### X-ray three-dimensional magnetic imaging

Valerio Seagnoli<sup>1,2</sup>

<sup>1</sup>Laboratory for Mesoscopic Systems, Department of Materials, ETH Zürich, Zürich, Switzerland.

<sup>2</sup>Laboratory for Multiscale Materials Experiments Paul Scherrer Institute, Villigen PSI 5232, Switzerland  
email: valerio.seagnoli@psi.ch

Three dimensional magnetic systems hold the promise to provide new functionality associated with greater degrees of freedom. For example, predictions suggest that the introduction of curvature into magnetic thin films could lead to unique properties such as curvature-induced anisotropy, magnetochirality, and domain wall automotive effects. Over the last years, we have worked towards developing methods to fabricate and characterize three-dimensional magnetic structures. Specifically, we have combined X-ray magnetic imaging with new iterative reconstruction algorithms to achieve X-ray magnetic tomography and laminography [1-4]. In a first demonstration, we have determined the three-dimensional magnetic nanostructure within the bulk of a soft Gd<sub>2</sub>O<sub>3</sub> magnetic micropillar with 100 nm spatial resolution and we have identified the presence of peculiar local magnetic configurations known as "Bloch points" [1, 3]. Subsequently, we have been able also to perform imaging of magnetic configurations in a time-resolved fashion determining the magnetization dynamics in a micrometer size GdCo disk. Therefore, X-ray magnetic three-dimensional imaging, with its recent extension to the soft X-ray regime [5], has now reached sufficient maturity that will enable to unravel complex three-dimensional magnetic structures for a range of magnetic systems, possibly including magnetic nanoparticles.

In this contribution, I will first give an overview of our recent results and review the current shortcomings of the magnetic tomography technique. Finally, I will discuss how diffraction-limited storage ring source, together with state of the art instrumentation, will allow three-dimensional magnetic nanotomography to thrive.

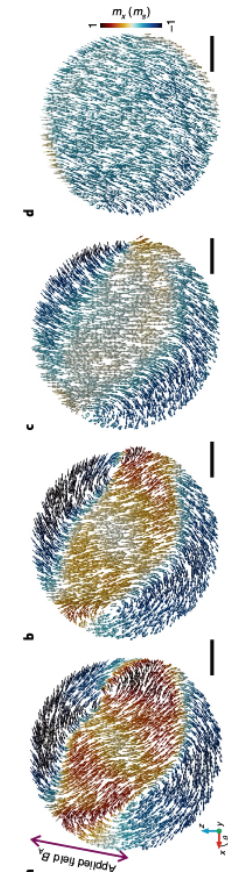


Figure: Non-invasive determination of the magnetic configuration of a GdCo disk. The scale bar corresponds to a length of 1  $\mu\text{m}$ . Several cross sections at different heights are presented. The magnetic moment orientation in the plane is represented by an arrow, whilst the component out of plane is illustrated with a colorbar. The magnetic material was grown such that there was no significant magnetic anisotropy at the bottom of the disk (panel **a** and **b**) leading to the formation of magnetic domains. In contrast the top part of the disk has a significant anisotropy leading to the formation of a configuration with magnetic moments almost completely in-plane (panel **c**) with parallel magnetization alignment (panel **d**) on the topmost part of the disk.

### References:

- [1] C. Donnelly et al., *Nature* **547**, 328 (2017), <https://doi.org/10.1038/nature23006>
- [2] C. Donnelly et al., *New J. Phys.* **20**, 083009 (2018), <https://doi.org/10.1088/1367-2630/aad35a>
- [3] C. Donnelly et al., *Nat. Phys.* **17**, 316 (2021), <https://doi.org/10.1038/s41567-020-01057-3>
- [4] C. Donnelly et al., *Nat. Nanotechnol.* **15**, 356 (2020), <https://doi.org/10.1038/s41565-020-0649-x>
- [5] K. Wite et al., *Nano Letters* **20**, 1305 (2020), <https://doi.org/10.1021/acsnanolett.9b04782>

## INVITED TALK

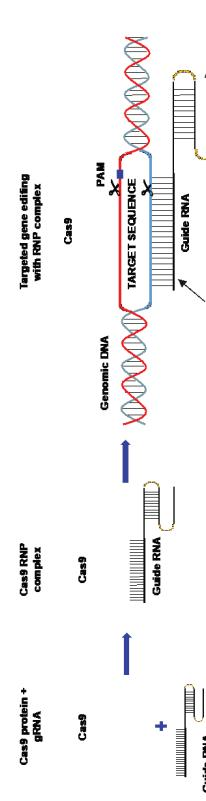
### CRISPR/Cas9 Correction of a Mutation in CFTR as a Potential Therapy for Cystic Fibrosis

Amy J. Walker<sup>1</sup>, Maximilian Woodall<sup>2</sup>, Ruhina Maeshima<sup>1</sup>, Carina Graham<sup>1</sup>, David Pearce<sup>3</sup>, Michelle O'Hara-Wright<sup>1</sup>, David J. Sanz<sup>4</sup>, Leana Guerrini<sup>1</sup>, Ahmad M. Aldossary<sup>1</sup>, Christopher O'Callaghan<sup>5</sup>, Deborah L. Baines<sup>2</sup>, Robin J McAnulty<sup>3</sup>, Patrick T. Harrison<sup>4</sup> & Stephen L. Hart<sup>1</sup>

<sup>1</sup>Genetics and Genomic Medicine Department, UCL Great Ormond Street Institute of Child Health, London, UK, <sup>2</sup>Institute for Infection and Immunity, St. George's, University of London, UK, <sup>3</sup>UCL Respiratory Centre for Inflammation and Tissue Repair, Rayne Building, London, UK, <sup>4</sup>Department of Physiology, BioSciences Institute, University College Cork, Cork, Ireland, <sup>5</sup>Infection, Immunity & Inflammation Department, UCL Great Ormond Street Institute of Child Health, London, UK

Gene editing by CRISPR/Cas9 is a rapidly developing area of gene therapy technologies. It offers opportunities to correct disease causing mutations for a wide range of diseases. Essentially, an RNA guided nuclease, CRISPR, can be used to knockout genes, to repair them with a high degree of specificity, or to replace regions of DNA including complete cDNA coding sequences. We are focused on developing CRISPR strategies to develop novel therapies for cystic fibrosis. Cystic Fibrosis is an autosomal recessive disorder caused by mutations in the CFTR gene. It mainly affects the lung causing production of thick sticky mucus leading to infection and inflammation and loss of lung function. CF-causing mutations of CFTR have been well characterised of which there are approximately 300. The 10th most common mutation, 3849+10kb C>T, generates a cryptic splice site within an intron, leading to a faulty mRNA producing a truncated CFTR protein. We are developing CRISPR to delete this mutation in the intron. This therapy would need to be delivered to the lung by inhalation of an aerosolised formulation of nanoparticles carrying the CRISPR repair molecules.

We have developed a non-viral, receptor-targeted nanocomplex (RTN) formulation to deliver the CRISPR formulation. CF cells with the splice site mutation were transfected with the nanoparticle leading to more than 60% correction efficiency. Normal processing of the CFTR mRNA was restored leading to normal CFTR protein production. We then showed that the repaired protein behaved correctly as a chloride channel in treated CF cells. Finally, we showed that the nanoparticle can deliver CRISPR to the lungs of mice.



## INVITED TALK

### Problems in Magnetic Characterization of Nanoparticles

Ron B. Goldfarb  
Ron.goldfarb@nist.gov

National Institute of Standards and Technology, Boulder, Colorado 80305, USA

In 1955, Bean<sup>1</sup> first applied the term “super-paramagnetic” to ensembles of small, single-domain, ferromagnetic particles that reach equilibrium through thermal activation, noting that “the particles ... act as paramagnetic particles of very large moment.” The following year, Bean and Jacobs<sup>2</sup> showed how the magnetization followed a Langevin function of magnetic field  $H$  and temperature  $T$ , and “that curves measured at different temperatures should be approximately superposable when plotted with respect to  $H/T$ .<sup>3</sup>” This scaling is characteristic of superparamagnetism and distinguishes it from simple anisotropic ferromagnetism.

An exponential dependence of magnetization relaxation time on single-domain particle size and temperature and the concept of blocking were originally developed by Neel.<sup>4</sup> An Arrhenius or Vogel-Tulcher relationship between  $f$  and  $T_B$ , where  $f$  is the frequency in alternating-field susceptibility measurements and  $T_B$  is the blocking temperature, is indicative of superparamagnetism.<sup>4</sup>

Like a ferrimagnet above its Curie temperature  $T_C$  and an antiferromagnet above its Néel temperature  $T_N$ , the low-field susceptibility  $\chi$  of a superparamagnet follows a Curie-Weiss law,  $\chi = C/(T - \theta)$ , between  $T_N$  and  $T_C$ . This gives rise to the well-known linear dependence of reciprocal susceptibility,  $1/\chi$ , on temperature  $T$ . The slope of the linear fit gives the reciprocal of the Curie constant,  $1/C$ , from which the average magnetic moment per particle can be calculated. The temperature-axis intercept of the linear extrapolation, the superparamagnetic Curie temperature  $\theta$ , is an indication of the interaction among superparamagnetic particles,<sup>5</sup> spins in spin glasses,<sup>6</sup> or superparamagnetic clusters in alloys.<sup>7</sup> Additionally,  $\theta$  may depend on packing fraction, particle diameter, applied field,<sup>8</sup> and distribution of particle sizes and  $T_B$ .<sup>9</sup>

Many articles hastily invoke superparamagnetism based on a single magnetization-vs.-field curve or a pair of zero-field-cooled and field-cooled magnetization-vs.-temperature curves, without verifying scaling of magnetization at zero-field and  $T$ , Néel relaxation, or Curie-Weiss behavior above  $T_B$ . Virtually always ignored in Curie-Weiss plots is that the value of  $\theta$  depends on the demagnetizing factor of the specimen under test. The effect may be significant for samples of particles such as iron, magnetite, and maghemite that have large magnetization at low fields and, therefore, small reciprocal susceptibilities:  $\chi^{-1} = \chi_e^{-1} - N$ , where  $\chi_e$  is the internal volume susceptibility characteristic of the material,  $\chi_e$  is the external volume susceptibility characteristic of the sample, and  $0 \leq N \leq 1$  is the demagnetizing factor of the sample (in SI units). An impediment to correction for demagnetizing factor is that, as functions of temperature, most published data are of magnetic moment, mass or molar susceptibility, or susceptibility in arbitrary units instead of susceptibility referenced to particle volume.<sup>10</sup>

For magnetic characterization, superparamagnetic particles are often packed in capsules or dispersed in films. The effective demagnetizing factor  $N_{eff}$  for specimens that consist of exchange-decoupled particles may be estimated from classical effective-medium theories,<sup>10</sup> one of which yields a simple interpolation formula.<sup>11,12</sup> The correction for demagnetizing factor will increase  $\theta$  and, if  $N_{eff}$  is large enough relative to  $\chi_e^{-1}$ , can even result in a change in sign of  $\theta$  from apparently negative (indicative of antiferromagnetic interparticle interactions) to positive (indicative of ferromagnetic interactions).<sup>4</sup>

#### References

1. C. P. Bean, *J. Appl. Phys.* **26** (1955) 1381–1383; doi: 10.1063/1.1721912.
2. C. P. Bean, I. S. Jacobs, *J. Appl. Phys.* **27** (1956) 1448–1452; doi: 10.1063/1.1722287.
3. L. Néel, *Ann. Geophys.* **5** (1949) 99–136; N. Kurti, *Selected Works of Louis Néel*. Gordon & Breach (1988) 407–427.
4. J. L. Dommann, L. Bessais, D. Fiorani, *J. Phys. C* **21** (1988) 2015–2043; doi: 10.1088/0022-3719/21/10/019.
5. K. O’Grady et al., *J. Magn. Magn. Mater.* **31–34** (1983) 958–960; doi: 10.1016/0304-8853(83)90755-2.
6. C. N. Guy, *J. Phys. F: Met. Phys.* **7** (1977) 1505–1519; doi: 10.1088/0305-4608/7/8/018.
7. R. B. Goldfarb, C. E. Patton, *Phys. Rev. B* **24** (1981) 360–373; doi: 10.1103/PhysRevB.24.360.
8. R. W. Chantrell, E. P. Wohlfarth, *J. Magn. Magn. Mater.* **40** (1983) 1–11; doi: 10.1016/0304-8853(83)90002-1.
9. M. El-Hilo et al., *J. Magn. Magn. Mater.* **117** (1992) 21–28; doi: 10.1016/0304-8853(92)90286-W.
10. A. Shrivastava, *Electromagnetic Mixing Formulas and Applications*. London, U.K.: Inst. Electrical Engineers (1999).
11. B. Blaney, R. A. Hull, *Proc. Roy. Soc. London A* **176** (1941) 86–92; doi: 10.1098/rspa.1941.0045.
12. R. Skomski et al., *IEEE Trans. Magn.* **43** (2007) 2956–2958; doi: 10.1109/TMAG.2007.893798.

## INVITED TALK

### Nanomagnetic Actuators for Neural Modulation

Gabriela Romero Uribe  
gabrielaromero.uribe@utsa.edu  
Department of Biomedical Engineering and Chemical Engineering, The University of Texas at San Antonio, San Antonio, TX, 78249 USA

The ability to modulate neural activity on-demand is essential for understanding the basic biology of neural circuit dynamics and to develop novel therapies for neurological disorders and psychiatric conditions. Existing technologies for the control of neural circuits offer only limited possibilities. Manipulation of neural signaling via chemical agents is restricted by the blood-brain barrier, the rapid cerebrospinal fluid clearance, and the lack of cell-type specificity, resulting in poor cell response and adverse drug reactions [1]. Microelectronic and optogenetic technologies have opened the possibility for stimulation through direct control of brain circuit dynamics and for simultaneous cell activity recording. However, they require implantable devices that are damaging to biological tissues [2,3].

Transduction of external stimuli by nanomaterials, particularly magnetic nanoparticles (MNPs) has been studied for the wireless control of cellular signaling [4]. The weak magnetic properties and low electrical conductivity of tissues allow alternating magnetic fields (AMFs) to reach deep into the body [5], making MNPs particularly promising to actuate on deep tissues. Single domain MNPs and MNPs with a vortex state configuration may act as transducers for AMFs remote stimulation by dissipating heat or exerting mechanical forces. Both transduction mechanisms have been studied due to its potential applications in cancer research and therapies [6]. In this contribution, I will give an overview of our recent results in the development of magnetic nanotechnologies for the modulation of biothermal, magnetomechanical and chemomagnetic nanoactuation. Finally, I will review the current challenges, limitations and prospects of magnetic nanotechnologies in neuroengineering.

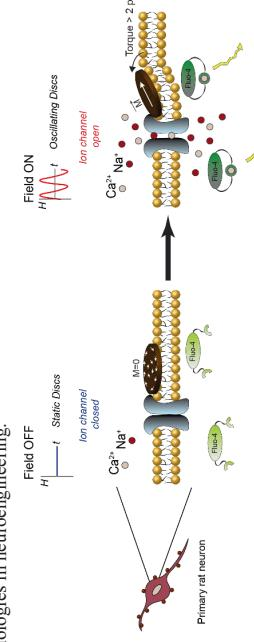


Figure: Overview of magnetomechanical neuromodulation mechanism. Functionalized magnetic nanodisks (MNMs) in co-culture with primary rat neurons. Upon exposure to AMFs, the torque produced by MNMs triggers the response of mechanosensitive ion channels located in the cell membrane.

#### References

- [1] C. Hamani, J. S., et al., *Operative Neuromodulation: Volume 2*. Springer Vienna, Vienna 2007, 127.
- [2] R. Chen, et al., *Neural recording and modulation technologies*, Vol. 2, 2017.
- [3] T. Knöpfel, *Nature Reviews Neuroscience* **2012**, 13, 687.
- [4] R. Chen, et al., *Science* **2015**, 347, 1477.
- [5] Y. Shen, et al., *Theranostics* **2017**, 7, 1735.
- [6] Q. A. Pankhurst, et al., *Journal of Physics D: Applied Physics* **2009**, 42, 224001 1.

## Synthesis and properties of Fe<sub>3</sub>N nanoparticles as alternative material for magnetic fluid hyperthermia

Yevhen Ablets<sup>1\*</sup>, Najma Sultana Shaik<sup>1,2</sup>, Esmaeil Adabifiroozjai<sup>2</sup>, Leopoldo Molina-Luna<sup>2</sup>, Oliver Gutfleisch<sup>1</sup>, Imants Dirba<sup>1</sup>

<sup>1</sup>Materials Science, Functional Materials, Technical University of Darmstadt, 64287 Darmstadt, Germany

<sup>2</sup>Materials Science, Advanced Electron Microscopy, Technical University of Darmstadt, 64287 Darmstadt, Germany  
email: yevhen.ablets@tu-darmstadt.de

Magnetic fluid hyperthermia (MFH) is one of the modern individual and adjuvant methods for cancer treatment<sup>[1]</sup>. Usually, iron oxide nanoparticles (IONP) are used for this purpose due to their chemical stability, non-toxicity, well-established and cost-effective production, well-known metabolism of iron in the human body. However, the heating performance of IONP is limited due to moderate values of saturation magnetization and magnetocrystalline anisotropy<sup>[2]</sup>. Using particles with enhanced magnetic properties<sup>[3]</sup> will enable more effective tumor treatment, as particles heat to higher temperatures with the same alternating current (AC) magnetic field amplitude ( $H$ ) and frequency conditions ( $f$ ). As well, enhanced particles will be used in smaller concentration, which will lead to less cytotoxic load on the human body.

In this work, a new synthesis method of crystalline Fe<sub>3</sub>N nanoparticles (Fig. 1) is demonstrated. Metal-organic compound iron pentacarbonyl is thermally decomposed in the presence of polyisobutylene succinimide (PS) under continuous ammonia flow. Varying by gas flow concentrations and type of surfactant (oleic acid, PS, oleyamine) Fe<sub>3</sub>O<sub>4</sub>, Fe<sub>3</sub>N and Fe homogeneous spherical particles were obtained with an average diameter of 13.5 nm. Fe<sub>3</sub>N particles show higher saturation magnetization and hence better heating performance (at  $H=300$  Oe,  $f=402$  kHz) compared to Fe<sub>3</sub>O<sub>4</sub> (Fig. 2).

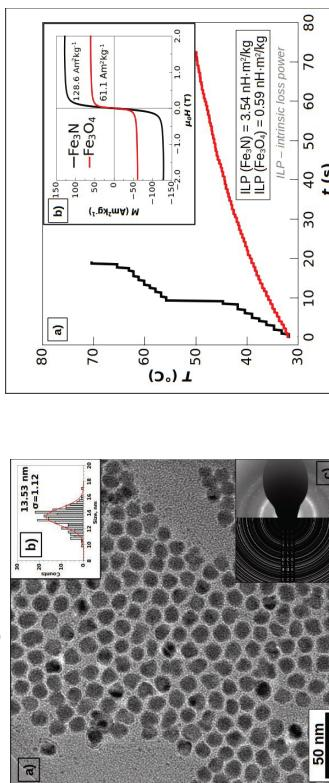


Fig. 1: TEM image (a) of Fe<sub>3</sub>N nanoparticles with particle size distribution (b) and SAED pattern (c).

### References:

- C. Blanco-Andujar, F. J. Teran, D. Ortega, in *Iron Oxide Nanoparticles for Biomedical Applications*, Elsevier, 2018 pp. 197–245.
- J. Carrey, B. Meldaoui, M. Respaud, *Journal of Applied Physics* **2011**, *109*, 083921.
- I. Dirba, C. K. Chandra, Y. Abiles, J. Kohout, T. Kmiec, O. Kaman, O. Gutfleisch, *Evaluation of Fe-Nitrides, -Borides and -Carbides for Enhanced Magnetic Fluid Hyperthermia*, Social Science Research Network, Rochester, NY, 2022.

## Structure-Property-Function Relationships of Iron Oxide Multi-Core Nanoflowers in Magnetic Hyperthermia and Photothermia

Enzo Bertuui<sup>4</sup>, Emilia Benassai<sup>1</sup>, Guillaume Mériguet<sup>4</sup>, Jean-Marc Grenache<sup>4</sup>, Benoit Baptiste<sup>#</sup>, Sophie Neveu<sup>5</sup>, Claire Wilhelm<sup>5</sup> and Ali Abou-Hassan<sup>1,\*</sup>

<sup>1</sup>Sorbonne Université, CNRS, Physico-chimie des Électrolytes et Nano-systèmes Interfaciaux (PHENIX), F-75005 Paris, France

<sup>2</sup>Université du Maine, UMR CNRS 6283, Institut des Molécules et Matériaux du Mans (INMM), Avenue Olivier Messiaen, 72085 Le Mans Cedex 9, France

<sup>3</sup>Sorbonne Université, UMR 7590 CNRS – Sorbonne Université – IRD-MNHN, Institut de Minéralogie, de Physique des Matériaux et des Cosmochimie (IMPMC), Case 115, 4 Place Jussieu, 75252 Paris Cedex 5, France

\*Corresponding author: ali.abou-hassan@sorbonne-universite.fr

Due to their unique physico-chemical properties, multi-core iron oxide nanoparticles (NPs) also called nanoflowers (NFs), are used as functional materials in many applications, including for diagnosis and therapy in biomedical field.<sup>1</sup> NFs are efficient magnetic resonance imaging (MRI) contrast agents and permanent nano-heaters in magnetic hyperthermia (MHT), with specific loss powers (SLP) values amongst the highest reported ones for magnetic materials.<sup>2</sup> More recently, magnetic NFs have been proved to be promising materials for photothermal therapy (PTT) thanks to their absorption in the first (around 808 nm for maghemite) and second (around 1064 nm for magnetite) infrared biological windows.<sup>3</sup> However, how the fine structure features of NFs at the nanoscale govern their properties and their collective function in MHT and PTT still needs to be elucidated.

In the present work,<sup>4</sup> we investigate in a multi-scale approach the role of many parameters of the polyol synthesis on the final NFs size, shape, chemical composition, number of cores and crystallinity. These nanofeatures are later correlated to the magnetic, optical and electronic properties of the NFs as well as their collective macroscopic thermal properties in MHT and PTT to find relationships between their structure, properties and function. We evidence the critical role of iron(II) and heating ramps on the elaboration of well-defined NFs with high number of cores. While MHT efficiency is found to be proportional to the average number of magnetic cores within the assemblies, the optical responses of the NFs and their collective photothermal properties depend directly on the mean volume of the cores (as supported by optical cross sections numerical simulations) and strongly on the structural disorder in the NFs, rather than the stoichiometry. The concentration of defects in the nanostructures, evaluated by time-resolved photoluminescence and Urbach energy ( $E_U$ ) measurements, evidences a switch in the optical behavior for a limit value of  $E_U = 0.4$  eV where a discontinuous transition from high to poor PT efficiency is also observed.

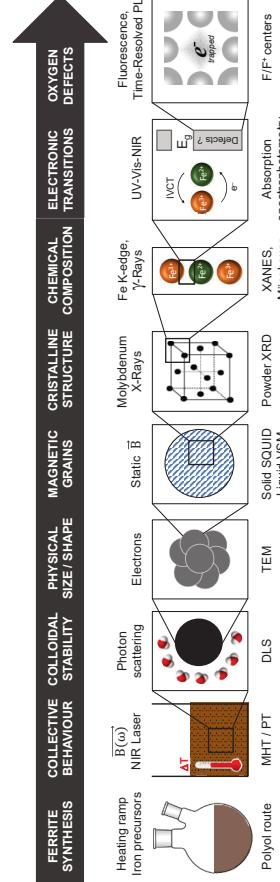


Figure 1. Diagram summarizing the multi-scale materials-science approach used in this work, from the batch polyol synthesis of iron oxide nanoflowers and their collective behavior in colloidal suspensions to their sub-atomic level characteristics.

### References

- Cocito, A., Silva, A. K. A., Cabana, S., Espinosa, A.; Baptiste, B., Menguy, N.; Wilhelm, C.; Abou-Hassan, A. *Iron Oxide Nanoflowers @ CuS Hybrids for Cancer Tr-THERAPY: Interplay of Photothermal Therapy, Magnetic Hyperthermia and Photodynamic Therapy*. *Theranostics* **2019**, *9* (5), 1288–1302. <https://doi.org/10.7150/thno.30238>.
- Huguenin, P.; Levy, M.; Alayon, D.; Lartigue, L.; Dubois, E.; Cabuil, V.; Ricolleau, C.; Roux, S.; Wilhelm, C.; Gazeau, F.; Buzzi, R. *Iron Oxide Monocrystalline Nanoflowers for Highly Efficient Magnetic Hyperthermia*. *J. Phys. Chem. C* **2012**, *116* (29), 15702–15712. <https://doi.org/10.1021/jp3025478>.
- Cabana, S.; Cocito, A.; Michel, A.; Wilhelm, C.; Abou-Hassan, A. *Iron Oxide Mediated Photothermal Therapy in the Second Biological Window: A Comparative Study between Maghemite Magnetite Nanospheres and Nanoflowers*. *Nanomat. 2020*, *10* (3), 1548. <https://doi.org/10.3390/nano10031548>.
- Bertuui, E.; Benassai, E.; Mériguet, G.; Grenache, J.-M.; Baptiste, B.; Neveu, S.; Wilhelm, C.; Abou-Hassan, A. *Structure-Property-Function Relationships of Iron Oxide Multi-Core Nanoflowers in Magnetic Hyperthermia and Phototherapy*. *ACS Nano* **2022**, *16* (1), 271–284. <https://doi.org/10.1021/acsnano.1c06212>.

## Novel Reactor Concepts for the Reproducible and Scalable Synthesis of Fine-Tuned Magnetic Nanoparticles

**Maximilian O. Besenhard,<sup>1,\*</sup> Liudmyla Storozukh,<sup>2</sup> Nguyen T.K. Thanh,<sup>2,3,4</sup> Asterios Gavrilidis<sup>1</sup>**

<sup>1</sup> Department of Chemical Engineering, University College London, Torrington Place, London, WC1E 7JE, UK

<sup>2</sup> UCL Healthcare Biomaterials Laboratories, University College London, 21 Albemarle Street, London W1S 4BS, UK

<sup>3</sup> UCL Nanomaterials Laboratory, University College London, 21 Albemarle Street, London W1S 4BS, UK

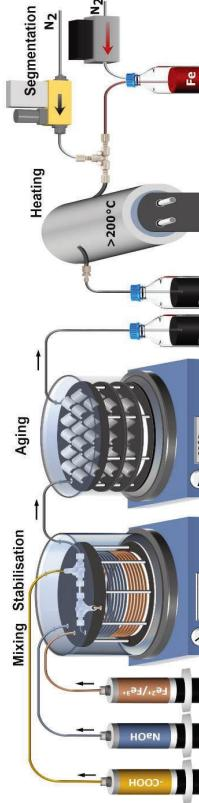
<sup>4</sup> Biophysics Group, Department of Physics and Astronomy, UCL, Gower Street, London, WC1E 6BT, UK

\*Email: m.besenhard@ucl.ac.uk

Despite the wide usage of magnetic nanoparticles, their reproducible synthesis with the desired properties remains challenging at all scales. Hence, the (re)-development and fine-tuning of synthetic protocols remains an unfortunate burden for each project involving magnetic nanoparticles. Scale-up is commonly considered as the logical step following the proof of principle, but up-scaling lab scale syntheses is everything but trivial. This is why scalability and pilot production (at throughput below full-scale production) are crucial to bring research across the so called “Valley of Death” (the gap between research and commercialisation) in high-cost, and high-risk areas such as nanotechnology. Novel reactor concepts, such as flow reactors, are known for their potential to improve mass transfer, reagent mixing, heating and cooling rates, and facilitate precisely timed reagent addition (especially for rapid reactions). In addition, their inherently continuous operation facilitates large scale production via longer operation times, i.e., the same or similar reactors can be used for development and pilot production.

The continuous synthesis of magnetic nanoparticles, however, is not trivial as particle formation mechanisms are complex with limited knowledge of reaction kinetics, and rapid mixing and/or high temperatures are required. Therefore, we have developed a new family of flow reactors, specifically designed for the synthesis of iron oxide nanoparticles (IONP) via i) co-precipitation, ii) partial oxidation, and iii) thermal decomposition. These novel reactors, overcame the engineering challenges for each synthetic procedure and allowed not only for robust and reproducible IONP syntheses, but also to gain new insights into the particle formation mechanisms by “freezing” transient reaction locally. This made it possible to characterise the intermediate oxide phases formed during co-precipitation and study particle morphology at early reaction stages. Furthermore, the flow reactors facilitated synthetic procedures with no batch equivalent, synthesising (without any growth promoting or inhibiting additives) IONPs  $\leq 5$  nm showing excellent T1 contrast via co-precipitation, colloidally stable 20-30 nm particles with good heating characteristics for magnetic hyperthermia via partial oxidation, and all particle sizes between 2- and 20 nm via a high temperature polyol synthesis using the same precursor solution. To further extend the application range of flow-chemistry for magnetic nanoparticle synthesis, a highly sensitive flow magnetometer was developed to characterise magnetic nanoparticles in solution, in-situ and in real-time using alternating current susceptibility.

This holistic engineering approach resulted not only to new ways for magnetic nanoparticle synthesis, large scale production, synthesis monitoring and control, but also paves the way towards high-throughput screening and self-optimised reactors using artificial intelligence to produce magnetic nanoparticles with properties tuned specifically for each application.



Schematics of co-precipitation (left) and high-temperature (right) flow reactors to synthesise  $\leq 5$  nm IONPs

## Micromixer synthesis for optimized manufacturing of single-core magnetic nanoparticles with tailored properties for versatile biomedical and clinical applications

Regina Bleul<sup>1\*</sup>, Abdulkader Bakı<sup>1</sup>, Amani Remmo<sup>2</sup>, Norbert Löwa<sup>2</sup>, Olaf Koisch<sup>2</sup>, Frank Wiekhorst<sup>2</sup>

<sup>1</sup>Fraunhofer Institute for Microengineering and Microsystems IMM, Carl-Zeiss-Str. 18-20, Mainz, Germany

<sup>2</sup>Physikalisch-Technische Bundesanstalt, Abbestr.2-12, 10587 Berlin, Germany

Email: regnabeule@imm.fraunhofer.de

For every biomedical application of magnetic nanoparticles (MNP), their structural and magnetic characteristics have to be adjusted specifically to the requirements of the envisaged use [1]. For instance, for magnetic particle imaging (MPI), single core MNP with core sizes between 25-30 nm are postulated to achieve optimal performance, whereas ultrasmall iron oxide MNP with core sizes below 5 nm are aimed for to be used as positive contrast agent in MRI. Thus, tailoring core size of MNP while sustaining colloidal stability even in physiological environment with high ionic strength using a reliable and reproducibly synthesis route still remains a challenging task. Microfluidic nanoparticle production has experienced a remarkable boom during the actual pandemic for synthesis of lipid nanoparticles as a vaccine carrier. However, even the existing technologies often suffer from non-reliable production and lack from direct scale up capability without the need of parallelization. As compared to lipid nanoparticles, the production of MNP in a continuous microfluidic system is even more challenging due the high risk of clogging of the devices.

We established a micromixer process based on an aqueous synthesis route without using any organic solvents or high temperatures. Single-core MNP with a core size of about 25 nm are produced at a synthesis temperature of max.  $T_s=55$  °C already within a few minutes reaction time  $t_r$  [2]. Optionally, the resulting single-core MNP can subsequently be coated with serum albumin to enhance colloidal stability in physiological environment [3] or be further functionalized to change surface coating to hydrophobic thus obtaining starting material for encapsulation in hydrophobic region of polymeric or lipid structures as well as particles.

The variation of the two main process parameters temperature  $T_s$  and residence time  $t_r$  (see figure 1), enables us to precisely adjust the core size [2]. We furthermore show that the reaction progress can be monitored magnetically by online magnetic particle spectroscopy measurements (Online-MPS) [4]. Evaluation of the produced nanoparticles reveal their high potential in different biomedical applications such as MPI, MRI, and magnetic fluid hyperthermia [5]. Combing the high imaging capability (MRI or MPI) with the excellent hyperthermia performance will advance theranostic applications of MNP.

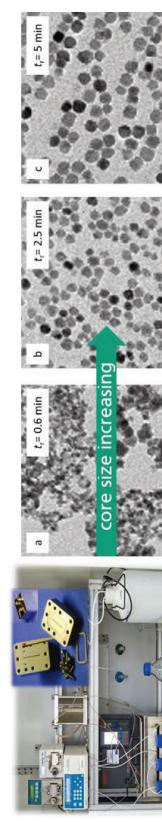


Figure 1: Setup of the micromixer synthesis platform (left). Adjustment of residence time  $t_r$  enables to control of particle growth and to adjust the particle core size. TEM images of MNP after  $t=0.6$  min (a),  $t=2.5$  min (b), and  $t=5$  min (c) at  $T_s=52.5^\circ\text{C}$  [2]

### References:

- [1] A. Bakı, F. Wiekhorst, R. Bleul: Advances in Magnetic Nanoparticles Engineering for Biomedical Applications – A Review, *Bioengineering* 2021, 8(10), 134.
- [2] A. Bakı et al.: Micromixer Synthesis Platform for a Tunable Production of Magnetic Single-Core Iron Oxide Nanoparticles, *Nanomaterials* 2020, 10(9), 1845.
- [3] A. Bakı et al.: Albumin-coated single-core iron oxide nanoparticles for enhanced molecular magnetic imaging (MRI/MPI), *Int. J. Mol. Sci.* 2021, 22(12), 6235.
- [4] N. Löwa et al.: Novel Benchtop Magnetic Particle Spectrometer for Process Monitoring of Magnetic Nanoparticle Synthesis, *Nanomaterials* 2020, 10(11), 2277.
- [5] R. Bleul et al.: Continuously manufactured single-core iron oxide nanoparticles for cancer theranostics as valuable contribution in translational research, *Nanoscale Adv.*, 2020, 2, 4510.

## Simulated clustering dynamics of magnetic nanoparticles

Frederik Laust Durhus<sup>1</sup>, Marco Boleggia<sup>2</sup>, Cathrine Frandsen<sup>1</sup>

<sup>1</sup>DTU Physics, Technical University of Denmark, Denmark

<sup>2</sup>Department of Physics, University of Modena and Reggio Emilia, Italy

Corresponding author, fraca@fysik.dtu.dk

Magnetic nanoparticles (MNPs) in liquid suspension may spontaneously aggregate, forming a plethora of complex structures. This clustering affects system properties like average magnetisation and hysteresis, which are crucial for applications, e.g. in magnetic hyperthermia [1]. Also, understanding clustering enables control over bottom-up self-assembly of desired structures.

In a recent study [2], we used Langevin dynamics simulations to study the clustering of single-domain spherical MNPs, free to move and rotate in 3D. The model contains magnetic dipole interaction, van der Waals forces, Brownian motion, viscous drag and steric repulsion. We have shown how the relative importance of all these effects can be tuned through the radius of the magnetic core,  $R_m$ , and of the surfactant layer,  $R_h$ . We find that dipole interaction favors linear structures like rings and chains, while van der Waals forces favour compact clusters and Brownian motion may induce dissociation into single particles. In this talk, we will illustrate how these competing dynamics play out for MNP ensembles through snapshots and 3D animations of  $R_m$  and  $R_h$ . The results are in general agreement with cryo-TEM experimental work [3]. Besides helping interpret experiments, the generated clusters form a useful basis for further theoretical studies linking cluster structures to their magnetic properties.

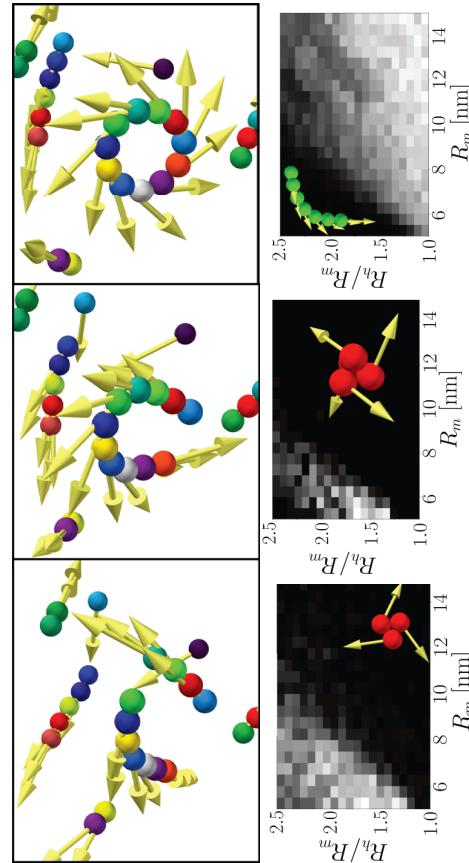


Figure 1: Simulations of single-domain cementite MNPs (Fe<sub>3</sub>C) with saturation magnetisation  $M_s = 1.49 \cdot 10^6$  A/m. Arrows represent magnetic moments. **Top :** Snapshots of MNPs aggregating into a ring. **Bottom :** Distribution of specific clusters as a function of hydrodynamic- and magnetic radius ( $R_h$ ,  $R_m$  respectively). **Left:** 3-particle ring. **Center:** tetrahedron. **Right:** Chains of 3 or more MNPs.

- [1] C. Blanco-Andujar et al. *Nanoscale*, **7**:1768–1775, 2015.
- [2] F. L. Durhus et al. *Nanoscale*, **13**:1970–1981, 2021.
- [3] K. Buttner et al. *Nature materials*, **2**:88–91, 2003.

## Synthesis of polymer modified substituted ferrite nanomaterials guided by density functional theory and machine learning

Zichun Yan<sup>1</sup>, Paul Meza-Morales, Venkata Rohit Punyapu, Anish Chahvadi<sup>1,2</sup>, Sara FitzGerald<sup>3</sup>, Thomas M. Crawford<sup>3</sup>, Rachel B. German<sup>2</sup>, and O. Thompson Mefford<sup>1</sup>

Metal substituted ferrite nanoparticles ( $\text{Me}_x\text{Fe}_{3-x}\text{O}_4$ ,  $\text{Me} = \text{Mn}, \text{Co}, \text{Ni}$ , and  $\text{Zn}$ , etc.) have been utilized in a variety of biomedical applications, including magnetic hyperthermia, drug delivery, and magnetic resonance imaging (MRI) contrast agents. Additional applications include magnetic induction for selective reduction of  $\text{CO}_2$ , high frequency inductors for energy conversion, and environmental remediation tools. In most these applications the likelihood of success is dependent upon the magnetic properties of these composite materials as well as ability to modify the surface with a strongly anchored polymeric brush that provides sufficient steric repulsion to insure colloidal stability.

The most significant magnetic properties include magnetic saturation and magnetic anisotropy. For these materials, those properties are most depended on the composition of the ferrite core. Therefore, by manipulating the atomic composition, materials can be intelligently designed to have the appropriate magnetic properties for a given application. Normally, to produce such materials is a rather Edistonian where multiple samples synthesized and characterized seeking the optimal composition. For this work we have utilized we use a combination of Density Functional Theory (DFT) and machine learning (ML) to learn the relationship between composition and magnetic performance of substituted ferrites. Magnetic saturations and anisotropies are calculated for ~1,000 substituted ferrite bulk structures (with  $x$  ranging from 0.0625 to 1) using DFT. Substitutions are made at the octahedrally coordinated  $\text{Fe}^{2+}$  sites. DFT values are input to machine-learning (ML) to correlate the magnetic properties to composition. Specifically, an XGBoost algorithm is used to produce multi-dopant ferrite nanoparticle databases and do not require further calculations.

To produce multi-dopant ferrite nanoparticles, the Extended LaMer<sup>®</sup> and seed-mediated growth techniques were combined by first utilizing traditional thermal decomposition of metal acetylacetones to produce seed particles, followed by a continuous injection of metal oleate precursors to increase the volume of the seed particles. With the choice of precursors for the seeding and dripping stage. Combining transmission electron microscopy, energy-dispersive x-ray spectroscopy, x-ray diffraction, and vibrating sample magnetometry, we conclude that the seed-mediated drip method is a viable method to produce multi-dopant ferrite nanoparticles, and the size of the particles was mostly determined by the seeding stage, while the magnetic properties were more affected by the dripping stage.

Finally, the effect of stabilizing polymer brushes on the surface of the nanocomposites will be discussed. Specially, calculations of the energetics between the particles accounting for the magnetic interactions are applied to determine the molecular weight of the stabilizing polymer brush. In addition, surface moieties for additional imaging, therapy, and targeting will be covered as avenues of investigation.

## Fe<sub>3</sub>O<sub>4</sub> Nanocubes as Multifunctional Theranostic Agents

Alejandro G. Roca<sup>1</sup>, Javier Muro-Cruces<sup>1</sup>, Alberto López-Ortega<sup>2</sup>, Elvira Fantech<sup>3</sup>, Miryana Hemadi<sup>4</sup>, Claudio Sangregorio<sup>5</sup>, Borja Sepúlveda<sup>3</sup>, Josep Nogués<sup>1,6</sup>

<sup>1</sup>Catalan Institute of Nanoscience and Nanotechnology (ICN2) CSIC and BIFI, 08193 Barcelona, Spain

<sup>2</sup>Dept. Ciencias & Institute for Advanced Materials and Mathematics INAMAT2, Univ. Pública de Navarra, 31006 Pamplona, Spain

<sup>3</sup>Dipartimento di Chimica and INSTM, Università degli studi di Firenze, Sesto Fiorentino (FI) I-50019, Italy.

<sup>4</sup>ITODYS – Interfaces, Traitements, Organisation et Dynamique des Systèmes, Sorbonne Paris Cité, CNRS-UMR 7086, Université Paris Diderot, Paris, France.

<sup>5</sup>Institut de Microelectrónica de Barcelona (IMB-CNM, CSIC), Campus UAB, Bellaterra, Barcelona 08193, Spain

\*Email: alejandro.gomez@icn2.cat; Mobile:+34 675123694

The performance of a specific nanomaterial for its intended use in biomedicine is the result of different interrelated factors such as the nanomaterial dimensions, interaction with cells and also the inherent physical properties. The control of particle dimensions and reactivity are devoted to the synthesis step.

In the case of magnetic iron oxide nanoparticles, the evolution of the colloidal synthetic methods has been a hot topic for more than 30 years since the publication of the synthesis of iron oxide nanoparticles by coprecipitation. During this time, the demands from the biologists and medical sector has motivated the introduction of new colloidal synthetic routes and evolution of the conventional ones resulting in nanoparticles with narrow size distribution, high crystallinity and absence of impurities. However, most of the research performed in iron oxide nanoparticles has been carried out on isotropic spherical particles.<sup>[1]</sup>

Here we present a rational designed synthesis route based on thermal decomposition of iron (III) acetylacetone which leads to high quality nanocubes over a wide size range (10-80 nm).<sup>[2]</sup> This synthesis route can be extended to other spinel ferrites (Co, Mn and Zn). In the past it has been reported the synthesis of magnetite nanocubes over 20 nm but below, these synthesis routes fails leading to non-regular nanoparticles.<sup>[1]</sup> We have shown that 17 nm nanocubes still show a great colloidal stability, excellent magnetic hyperthermia, and better NMR performance (much better than their spherical counterparts). Moreover, Fe<sub>3</sub>O<sub>4</sub> nanocubes are outstanding heat mediators for photothermal in the near infrared biological windows (680-1350 nm). In addition, the magnetic and optic anisotropies of the nanocubes have been exploited for a relatively new approach for *in situ* local temperature sensing.

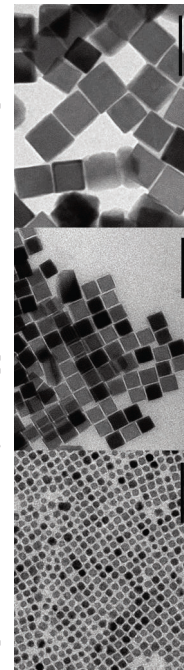


Fig. 1. TEM images of magnetite nanocubes with different average sizes (left 10 nm, centre 17 nm and right 30 nm).

## References

- [1] A. G. Roca *et al.* *Adv. Drug Del. Rev.* **2019**, *138*, 68–104.
- [2] J. Muro-Cruces *et al.* *ACS Nano*, **2019**, *13* (7), 7716–28.

## Micropatterning Magnetic Microparticles

Gary Zabow

National Institute of Standards and Technology (NIST), Boulder, Colorado, 80305, USA  
Email: [zabow@boulder.nist.gov](mailto:zabow@boulder.nist.gov)

The value of magnetic nano and microparticles for in-vitro and in-vivo applications derives from their ability to be remotely controlled, including remotely directed translation, rotation, and magnetization. These functionalities are directly determined by the particle size, shape, and composition. Spherical magnetic particles are most commonly used because they are easiest to synthesize but their high symmetry / more anisotropic particles. Considerable work is therefore now also directed towards less symmetric / more anisotropic particles. These include different shaped particles such as cubes, rods, and ellipsoids, particles and asymmetric particle clusters, which may function as rotational micromotors / microswimmers, and hemispherically coated particles, such as Janus particles with novel bi-directional properties. Here a new approach towards increasing particle functionalization is introduced that reverts back to widely available spherical particles but that instead breaks symmetry via tailored micropatterning of the microparticle surfaces. The highly curved surfaces of microparticles precludes their patterning with conventional microlithographic tools because such equipment is limited to operation on only flat, planar 2-dimensional surfaces. Here, however, the surface patterning are enabled via a newly developed transfer micropatterning approach which uses reflowable materials to transport pre-fabricated micropattern designs. The flexibility of the reflowable materials allows for normally microfabricated, initially planar designs to be transferred over to, and directly wrapped onto, the microparticle surfaces. By thus leveraging the power and precision resolution of existing planar semiconductor lithographic tools, the approach allows for arbitrary surface patterning, extending design and magnetic control options beyond those of more common homogeneous or two-sided Janus-like patterning. The process also allows for parallel patterning of many microparticles simultaneously. This presentation will describe how this new process works and potential applications, illustrated through examples of new magnetically patterned microspheres, some of which are shown in the sample figure below.



Figure: **Micropatterned microparticles.** Scanning electron micrographs of micropatterned microparticles showing: (a) top down view of sub-micron magnetic disks arrayed over a set of microsphere, (b) side-angled view of individual spheres patterned like miniature hot-cross buns, and (c) smiley faces imprinted onto microspheres. Scale bars in all images are ~2 microns.

## Interaction of Ferritin Derivatives with Lysozyme Amyloid Fibrils

Ján Gombos<sup>1</sup>, Lucia Balejčíková<sup>2</sup>, Peter Kopáčský<sup>3</sup>, Mariána Bartková<sup>3</sup>, Katarína Šipošová<sup>3</sup>, Jozef Kováč<sup>3</sup>, Kristína Zolochovská<sup>3</sup>, Ivo Šafárik<sup>4,5</sup>, Alícia Lokajová<sup>6</sup>, Dušan Dobrota<sup>1</sup>, Oliver Štěrbák<sup>6</sup>

- <sup>1</sup> Department of Medical Biochemistry, Jessenius Faculty of Medicine, Comenius University, Martin, Slovakia
- <sup>2</sup> Institute of Hydrology, Slovak Academy of Sciences, Bratislava, Slovakia
- <sup>3</sup> Institute of Experimental Physics, Slovak Academy of Sciences, Kosice, Slovakia
- <sup>4</sup> Department of Nanobiotechnology, Biology Centre, ICB, Czech Academy of Sciences, České Budějovice, Czech Republic
- <sup>5</sup> Regional Centre of Advanced Technologies and Materials, Czech Advanced Technology and Research Institute, Palacky University Olomouc, Czech Republic
- <sup>6</sup> Biomedical Center Martin, Jessenius Faculty of Medicine, Comenius University, Martin, Slovakia

Free iron is at physiological conditions occurring in two oxidation states. The first one is a relatively soluble but highly toxic ferrous ( $\text{Fe}^{2+}$ ) form, and the second one is a very insoluble but non-toxic ferric ( $\text{Fe}^{3+}$ ) state. Magnetic mineral core in magnetoferritin (as a model system of pathological ferritin) produce more toxic ferrous ions in the presence of reducing agents (vitamins B<sub>2</sub> and C) than ferrihydrite mineral core in native ferritin [1]. Neurodegenerative processes are also associated with the presence of abnormal protein aggregates, forming very organized fibrils known as plaques. To simulate the formation of amyloid plaques or fibrils, we used lysozyme amyloid fibrils. We used ferritin derivatives as model systems to study their interaction with lysozyme amyloid fibrils (LAF). To accomplish that, we have successfully synthesized magnetoferritin and reconstructed ferritin as well as lysozyme amyloid fibrils, using controlled in vitro synthesis. To reveal the potential adverse effect of ferritin derivatives with LAF interaction, we determined the time dependence of ferrous ions release from the ferritin envelopes. Ferrous ions are highly toxic to the cell. Therefore, any excess iron currently not needed for the metabolic processes must be eliminated by translocation to ferric state and stored, e.g. in ferritin. From the comparison of the average and median values (Figure 1), it is clear that the release of toxic ferrous ions occurs to a greater extent during the interaction of ferritin derivatives with LAF. From this point of view, the LAF behaves like a mineral core reducing agent, similar to vitamins B<sub>2</sub> and C [1].

Induction of increased ferrous ions release from the ferritin envelope during interaction with LAF can cause increased oxidative stress and more significant damage for the cells. On the other hand, we found destructive effect of ferritin derivatives on the LAF.

These findings can help better understand the biochemistry behind the pathological processes associated with the iron accumulation and magnetic mineralization, e.g. in neurodegenerative disorders.

[1] Štěrbák, O.; Balejčíková, L.; Kmetová, M.; Gombos, J.; Trancikova, A.; Pokusa, M.; Kopáčský, P. Quantification of iron release from native ferritin and magnetoferritin induced by vitamins B2 and C. *Int. J. Mol. Sci.* (2020), 21, 632.

## Quantitative Imaging of Magnetic Nanoparticles in Large Body Regions using Nonlinear Magnetotrlaxometry

Peter Schier<sup>1\*</sup>, Aaron Jaufenthaler<sup>1</sup>, Maik Liebl<sup>2</sup>, Uwe Steinhoff<sup>2</sup>, Frank Wiekhorst<sup>2</sup>, Daniel Baumgarten<sup>1</sup>

<sup>1</sup> Institute of Electrical and Biomedical Engineering, UMIT TIROL - Private University for Health Sciences, Medical Informatics and Technology, Hall in Tirol, Austria

<sup>2</sup>Physikalisch-Technische Bundesanstalt (PTB), Berlin, Germany

\*Email: peter.schier@umit-tirol.at

Magnetotrlaxometry (MRX) imaging enables the noninvasive detection and quantification of magnetic nanoparticles (MNPs). An MRX measurement process consists of (i) an excitation phase, where a set of external coils produces inhomogeneous magnetic fields, aligning the MNPs along the resulting field and (ii) a relaxation phase, measuring the decaying net magnetic moment of the particles with a highly sensitive sensor system after rapidly deenergizing the excitation coils. The state-of-the-art imaging process itself involves the solution to the inverse problem of the linear MRX forward model. This linear model is valid within the (approximately) linear magnetization regime of the MNPs for weak magnetic excitation fields and holds for small fields of view (FOVs) (roughly 10 cm in diameter, depending on the MRX setup). In this case, it is typically possible to magnetize particles in the center of the FOV still strong enough such that they produce a measurable relaxation signal at nearby sensor locations, without leaving the linear magnetization regime in any part of the FOV. However, when aiming for larger FOVs (e.g., torso size), larger excitation fields need to be employed to produce measurable relaxation signals in all areas of the FOV that inevitably drive areas close to the coils into the nonlinear magnetization regime, thereby invalidating the linear MRX forward model and preventing accurate reconstructions of the MNP ensembles.

In this contribution, we not only extend the linear MRX forward model by a nonlinear, excitation field dependent magnetization factor that enables simulating realistic relaxation responses for large magnetic fields, but we also present a novel MRX spatial encoding scheme that exploits this nonlinearity by employing different driving coil currents which allows for more accurate MNP imaging than obtainable by the standard imaging approach. The nonlinear magnetization factor was empirically tuned using real measurement data from MNPs magnetized with different magnetic field strengths. The proposed approach is tested in simulations on a  $40 \times 20 \times 30 \text{ cm}^3$  torso-shaped volume, using four large excitation coils and eight sensors with two sensitive axes, respectively, inspired by dual axis optically pumped magnetometers (OPMs) (see Figure 1a). The FOV is discretized into cubic voxels with a side length of 2.5 cm for imaging several different MNP phantoms with clinically relevant MNP concentrations used in both the linear MRX model and the nonlinear approach applying multiple different coil currents. Realistic model errors (differing voxel sizes for measurement simulation and reconstruction, as well as positioning and orientation deviations of coils and sensors in the range of few millimeters and degree, respectively) and measurement noise ( $1 \text{ pT}/\sqrt{\text{Hz}}$ ) which is appropriate for OPMs was added in the simulations, resulting in an adequate signal-to-noise ratio for MRX imaging of approximately 20 dB. It is evident throughout all reconstructions that the nonlinear approach yields more accurate reconstructions by introducing additional information to the inverse problem through the nonlinear spatial encoding scheme (see Figure 1b). Specifically, this is useful since large coil sizes are necessary to generate strong magnetic excitation fields for large FOVs. However, large coil sizes hamper good spatial encoding of the FOV due to their more homogeneous magnetic fields compared to smaller coils. Thus, the proposed approach counteracts this loss of spatial information to some degree. These theoretical findings will be validated in experiments in the near future.

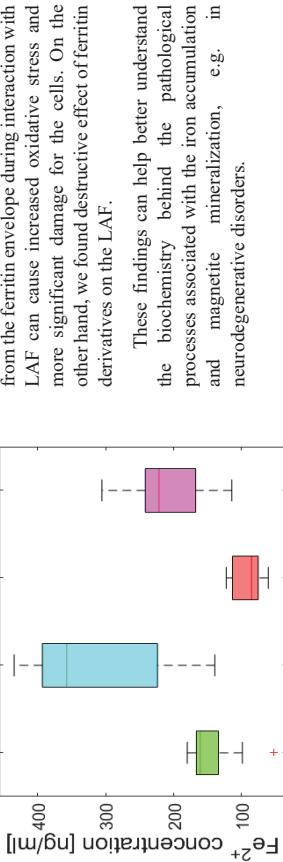


Figure 1. Median of ferrous ion release from ferritin derivatives themselves and during the interaction with LAF in 11 days.

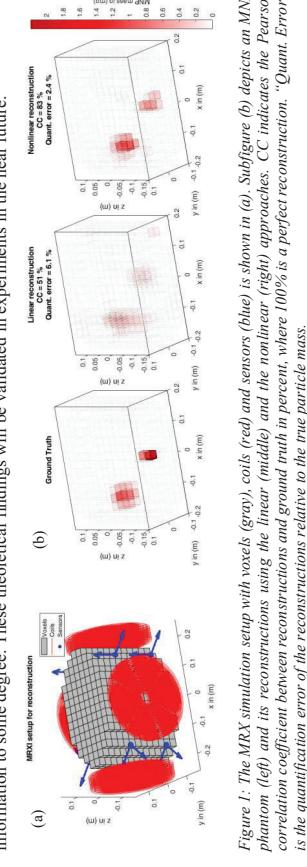


Figure 1: The MRX simulation setup with voxels (gray), coils (red) and sensors (blue) is shown in (a). Subfigure (b) depicts an MNP phantom (left) and its reconstructions using the linear (middle) and the nonlinear (right) approaches. CC indicates the Pearson correlation coefficient between reconstructions and ground truth in percent, where 100% is a perfect reconstruction. "Quant. Error" is the quantification error of the reconstructions relative to the true particle mass.

### Acknowledgements

Financial support by the Austrian Science Fund (FWF, grant I 4357-B) and the German Research Foundation (grant WI 4230/4-1) is gratefully acknowledged.

## Labelling T cells with a new tracer tailored for sensitive tracking using magnetic particle imaging (MPI)

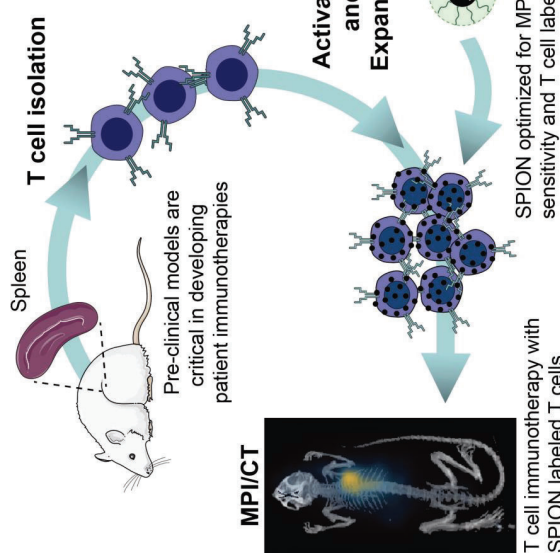
Angelie Rivera-Rodriguez<sup>1</sup>, Sitong Liu<sup>2</sup>, Bo Yu<sup>2</sup>, Hayden Good<sup>2</sup>, Lan Hoang-Minh<sup>3</sup>, Duane A. Mitchell<sup>3</sup>, and Carlos M. Rinaldi-Ramos<sup>3</sup>

<sup>1</sup>U. Crayton Pruitt Family Department of Biomedical Engineering, University of Florida

<sup>2</sup>Department of Chemical Engineering, University of Florida

<sup>3</sup>Department of Neurosurgery, University of Florida

Magnetic Particle Imaging (MPI) is a new molecular imaging technology capable of unambiguous and quantitative tomographic imaging of the distribution of superparamagnetic iron oxide nanoparticle (SPION) tracers *in vivo*. One exciting application of MPI is in tracking adoptive cell transfer (ACT) therapies. The modification and use of patient's T cells to attack cancer is of great interest due to the potential of eradicating not only primary tumors but also metastases. However, T cell cancer immunotherapy suffers many challenges in treating solid tumors, including achieving accumulation and persistence of ACT T cells at the site of the tumor. Development and evaluation of ACT T cell therapies would benefit tremendously from non-invasive and quantitative imaging of T cell biodistribution. We previously demonstrated tracking of T cells labeled with the commercially available SPION ferucarbotran in mice using MPI, with an estimated cell sensitivity of ~50,000 T cells. Here we report labeling T cells with an optimized MPI tracer, RL-1, coated with the anionic polymer poly(maleic anhydride-alt-1-octadecene) (PMAO). Various labeling strategies were studied, resulting in varying degrees (~5-15 pg<sub>Fe</sub>/cell) of T cell labeling with the MPI tracer, without affecting T cell viability, phenotype, or cytotoxic function, and resulting in T cell sensitivity of 5,000 T cells labeled with RL-1 PMAO tracer, a 10x improvement relative to labeling with ferucarbotran. MPI was further used to evaluate the extent of SPION exocytosis, degradation, and dilution in T cells, and to monitor long-term clearance of nanoparticles after systemic administration, alone or inside T cells. Furthermore, the therapeutic efficacy of RL-1 PMAO labeled T cells *in vivo* was not hampered by nanoparticle labeling, thus enabling non-invasive quantitative tracking of T cell cancer without affecting their intended function. These results illustrate the value of optimizing tracers for high signal and efficient T cell labeling and illustrate the potential of MPI for unambiguous, sensitivity, and quantitative tracking of T cell cancer immunotherapy.



T cell immunotherapy with SPION labeled T cells

## MPI image-based cancer hyperthermia therapy

Hohyun Kim<sup>1</sup>, Thanh-Luu Cao<sup>1</sup>, Bui Minh Phu<sup>1</sup>, Dongwhi Kim<sup>2</sup>, Tuan-Anh Le<sup>1</sup>, Yun-Hee Kim<sup>2</sup>, Daehong Kim<sup>2</sup> and Jungwon Yoon<sup>1,\*</sup>

<sup>1</sup> School of Integrated Technology, Gwangju Institute of Science and Technology, Gwangju 61005, Republic of Korea;

<sup>2</sup> National Cancer Center, Goyang-si, Gyeonggi-do, Republic of Korea;

\*Email: jyoon@gist.ac.kr Mobile: 82-10-2402-6904

Appropriate treatment after detection of cancer is an important factor in improving the quality of life. Magnetic hyperthermia is localizable and non-invasive treatment among various therapies for cancer treatment. Magnetic hyperthermia is receiving great attention in a variety of medical applications due to its deep penetration and reproducibility<sup>1</sup>. The alternating magnetic field induces the release of thermal energy from magnetic nanoparticles located at the target site. Magnetothermal therapy can be used to treat cancer due to its local heating and high temperature. However, temperature and particle distribution parameters should be controlled for effective treatment.

The temperature of nanoparticles *in vivo* requires accurate measurement for preclinical applications, but it is practically impossible to directly measure the target site. Therefore, a temperature prediction model using the characteristics of nanoparticles and experimental verification is essential. The amount of magnetic particle to be injected can be controlled through the temperature prediction model, and the biodistribution of particles can be measured using the MPI (Magnetic Particle Imaging). The distribution information obtained by MPI can be utilized to predict the temperature of the target site and can provide additional treatment strategies by controlling the particles to be injected.

In this study, a temperature prediction was built in a 3D tumor model for cancer treatment and predicted the temperature of hyperthermia. The model was validated by ex-vivo experiments and the SLP value was calculated. The obtained initial SLP value allows predicting the concentration distribution of particles *in vivo* due to the linearity of the MPI signal. Figure (a) shows the heat transfer equations in the constructed 4 layers breast cancer tumor model. To apply the built model *in vivo*, particle distribution information is required, and this information was measured using the MPI signal in Figure (b). Figure (c) shows the measured particle distribution to an *in-vivo* cancer model before and after hyperthermia. With an MPI image, the thermal effect of the target area can be predicted and further treatment can be decided.

Based on temperature prediction and MPI feedback, one can increase the therapeutic effect at the target site while minimizing side effects to surrounding undesired healthy tissue. The potential of technologically integrated systems demonstrated through *in vivo* experiments can support existing clinical applications of magnetic carriers.

Figure. Hyperthermia simulation model and magnetic particle imaging. (a) Temperature prediction model of magnetic hyperthermia. (b) Linear relation of acquired MPI signal intensity and mass of nanoparticle inside target position. (c) Initial MPI image of nanoparticle inside tumor and nanoparticle image after 1 week.

1. J. Kim, D. Heo, J. Wang, H. Kim, S. Oh, Y. Takemura, C. Huh, S. Bae, Pseudo-single domain colloidal superparamagnetic nanoparticles designed at a physiologically tolerable AC magnetic field for clinically safe hyperthermia. *Nanoscale* **13**, 19484–19492 (2021).

## Establishment of metabolic tracer based magnetic particle imaging

Norbert Löwa<sup>1</sup>, Staffan Hildebrand<sup>2</sup>, Hendrik PaySEN<sup>1</sup>, Olaf Kosch<sup>1</sup>, Laia R. Salisa<sup>3</sup>, Stephanie F. Preuss<sup>3</sup>, Georg Kasparis<sup>4,5</sup>, Thithawat Trakoolwiliwan<sup>4,5</sup>, Nguyen Thi Kim Thanh<sup>4,5</sup>, Alexander Pleiter<sup>2</sup>, Frank Wiekhorst<sup>1</sup>

<sup>1</sup> Physikalisch-Technische Bundesanstalt, 8.23 Metiology for Magnetic Nanoparticles, Berlin, Germany;  
<sup>2</sup> Rheinische Friedrich-Wilhelms-Universität Bonn, Institut für Pharmakologie & Toxikologie, Bonn, Germany;  
<sup>3</sup> German Cancer Research Center, Division of Vascular Oncology and Metastasis, Heidelberg, Germany;  
<sup>4</sup> Biophysics Group, Department of Physics and Astronomy, University College London, London, UK;  
<sup>5</sup> UCL Healthcare Biomagnetics and Nanomaterials Laboratories, University College London, London, UK.

\*Email: Norbert.loewa@ptb.de

Radiation-free imaging techniques are beneficial for the development of brown adipose tissue (BAT)-centered therapies. Magnetic Particle Imaging (MPI) is such non-radioactive quantitative 3D imaging technique specifically detecting magnetic nanoparticles (MNP) in biological systems. Here, we present quantitative MPI imaging of BAT metabolic activity using MNP-loaded lipoproteins<sup>1</sup>. Artificial lipoprotein particles (metabolic MPI-tracer) were synthesized by mixing phosphatidylcholine, triglycerides, and cholesterol and then loaded with Zn-doped iron oxide MNP. Initial suitability testing of the metabolic MPI-tracer for imaging was performed using a commercial MPS device, a zero-dimensional variant of MPI. MPS-based quantification on organ samples also supported in vivo studies to optimize the pharmacokinetic properties of the metabolic MPI-tracer. Subsequent quantitative imaging of the new MPI tracer was carried out using a preclinical MPI system (Bruker). Complementary anatomic scans were acquired using a preclinical 1T MRI system (Bruker).

MPS evaluation of the metabolic MPI tracer revealed excellent stability, good MPI performance, and that their magnetic properties were nearly independent of the surrounding physiological environment. Although lipoprotein encapsulation of MNP resulted in slightly reduced spatial resolution, the measured MPI-signal intensity scaled linearly with tracer amount, indicating their suitability for quantitative MPI. We used BAT activation by acute cold exposure of mice as a model for induced tissue-specific lipoprotein (metabolic MPI-tracer) uptake. Using MPS quantification, we demonstrated that the amount of metabolic MPI-tracer in BAT samples was significantly increased when mice were kept at 4°C for 20 h (see Figure 1). Moreover, metabolic tracer allowed clear MPI-visualization of the uptake of lipoproteins in active BAT. In contrast, no accumulation in the BAT region was detected in mice treated with the MPI gold standard Resovist<sup>®</sup>. We showed for the first time that lipoproteins loaded with MNP facilitate in vivo MPI tracking of lipid uptake and metabolic activity of BAT. If human-sized MPI scanners become available, this opens the possibility of studying lipid uptake and metabolic activity of BAT in humans without radiation exposure.

metabolic MPI-tracer injection



Figure. Metabolic imaging procedure using MPI.

### Acknowledgement:

This project was funded by the Deutsche Forschungsgemeinschaft (DFG) within the research grants "Matrix in Vision" SFB 1340/1 2018, no 372486779, project A02, "cellMPI" (455706279), FOR917, 397484323 SFB 759 TFR 259/1, and DAAD (57172123).

### References:

- [1] Hildebrand, S., Löwa, N., PaySEN, H., Fratila, R., de la Fuente, I., Reverte-Salisa, L., Trakoolwiliwan, T., Niu, Z., Kasparis, G., Preuss, S.F., Kosch, O., de la Fuente, J.M., Thanh, N.T.K., Wiekhorst, F. & Pleiter, A. (2020). Quantification of Lipoprotein Uptake in Vivo Using Magnetic Particle Imaging and Spectroscopy. ACS Nano, 15(1), 434–446. DOI: 10.1021/acsnano.0c03229

## Developing Magnetorelaxometry Imaging for Human Applications

Soudabeh Arsalan<sup>1\*</sup>, Patricia Radon<sup>1</sup>, Mark Liebl<sup>1</sup>, Uwe Steinhoff<sup>1</sup>, Aaron Jauenthaler<sup>2</sup>, Peter Schier<sup>2</sup>, Daniel Baumgarten<sup>2</sup>, Frank Wiekhorst<sup>1</sup>

<sup>1</sup>Physikalisch-Technische Bundesanstalt, Abbestrasse 2-12, D-10587 Berlin, Germany  
<sup>2</sup>Institute of Electrical and Biomedical Engineering, UMIT, Medical Informatics and Technology, Hall in Tirol, Austria

\*Email: soudabeh.arsalan@ptb.de

Magnetic nanoparticles (MNPs) due to their unique magnetic properties, exhibit an excellent potential in biomedical applications such as cancer therapy and diagnosis. For therapy applications such as hyperthermia and drug delivery, it is necessary to quantify the distribution of MNPs in the body before, during and after treatment to improve therapy efficiency and reduce unwanted side effects. Several techniques such as magnetorelaxometry imaging (MRXI), magnetic particle imaging (MPI), and AC susceptibility biosusceptometry (ACB) exist that are capable to provide this information. However, none of these imaging modalities has been established yet for quantitative imaging of MNPs over a human body in a clinical environment.

We aim to improve our MRXI setup, which originally was developed for in vitro investigations of animal models (see Figure 1), to provide the technology and infrastructure required to establish MRXI for monitoring of MNPs in human cancer therapies. This requires on the development of a novel imaging infrastructure and measurement procedures to detect MNPs in specific human body regions (e.g., brain, prostate, breast, etc.). MRXI shall be applied in personalized therapy for online monitoring of MNP distributions focusing on fast and direct feedback to the clinicians. Additionally, we explore the MRXI capability for molecular imaging by mapping of MRXI signal features to local viscosity, mobility and MNP density within body regions to investigate physiological and biological processes. We present novel hardware and equipment developments addressing phantom and excitation coil arrangement, the potential of optically pumped magnetometers (OPM) as alternative magnetic sensors for MRXI, and the workflow for online data analysis of MRXI measurements in human.

As a first realistic model for MRXI in humans, we deploy a head phantom simulating a glioblastoma multiforme (GBM) tumor. For this setup, we developed a reference hollow head phantom and measured MRXI using the PTB 304 channel SQUID system with 55 excitation coils for inducing the relaxation of the MNP moments mimicking a GBM tumor of 4 cm<sup>3</sup> volume (composed 1 cm<sup>3</sup> cubes of EMG 700 MNPs, Ferrotec, embedded in silicone, iron concentration 20 mg/ml).

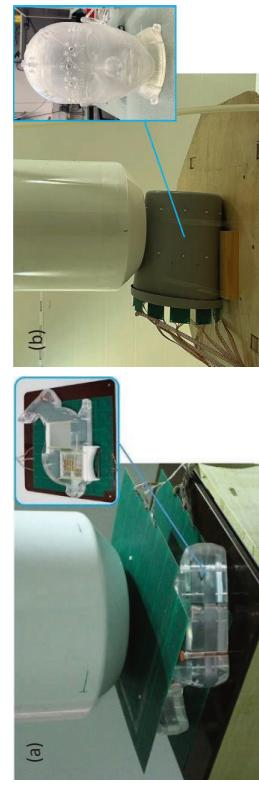


Figure 1: (a) Setup for preclinical MRXI in animal models; (b) Head phantom for human MRXI investigations.

## A dynamic bolus phantom for the evaluation of the spatio-temporal resolution of MPI scanners

Silvio Dutz<sup>1\*</sup>, Anton Stang<sup>1</sup>, Lucas Wöckel<sup>1</sup>, Olaf Kosch<sup>2</sup>, Patrick Vogel<sup>3</sup>, Volker C. Behr<sup>3</sup>, Frank Wiekhorst<sup>2</sup>

<sup>1</sup>Institut für Biomedizinische Technik und Informatik, Technische Universität Ilmenau, Germany

<sup>2</sup>Physikalisch-Technische Bundesanstalt Berlin, Berlin, Germany

<sup>3</sup>Department of Experimental Physics 5 (Biophysics), University of Würzburg, Würzburg, Germany

E-mail: silvio.dutz@tu-ilmenau.de

Magnetic Particle Imaging (MPI) is an imaging modality providing good spatial and high temporal resolution, allowing the 3D visualization of time-critical phenomena such as arterial bolus tracking under realistic conditions. Several different types of MPI scanners have been presented, which use the non-linear magnetization response of magnetic nanoparticles (MNP) exposed to a time varying external magnetic field for the determination of the MNP distribution. To facilitate a consistent assessment of results obtained from different MPI scanners, reference objects with well-defined imaging properties are mandatory. Mostly, static phantoms realized by a defined volume filled with a liquid tracer of known MNP concentration are used. Beside this, MNP embedded into a stiff matrix or 3D-printed magnetic materials are also used for the preparation of such static phantoms. But these phantoms do not offer the possibility to assess time dependent properties of MPI signal acquisition and data analysis. Therefore, we developed a dynamic bolus phantom, which provides movable liquid objects of different size, tracer concentration, and velocity.

This dynamic phantom is based on segmented flow of a cylindrically shaped bolus (permag®; MNP dispersion) within a liquid carrier material (silicon oil). A hydrophobic liquid (carrier) is filled into a flexible tube system with different diameters, into which a bolus of an aqueous MNP dispersion (tracer) is added. Due to the high surface tension between both liquid phases, the tracer bolus is stabilized within the carrier and can be moved accurately through the tube system by pumping the hydrophobic carrier liquid. Different geometries (trajectories) of the moving bolus were realized by mounting the tube into two different 3D-printed tube holders. The velocity of moving boluses was adjusted to be 1 cm/s, 5 cm/s, 10 cm/s, 20 cm/s, and 40 cm/s, which represent realistic blood flow velocities within the body. The moving boluses were imaged by two different MPI scanner types (MPI 25/20FF, Bruker BioSpin operated at Charité University Medicine and TWMPI prototype V1, operated at Würzburg).

Both scanners successfully imaged all moving boluses, showing an increasing blurring with increasing bolus velocity, see figure. We conclude that the obtained temporal imaging resolution is determined by the bolus dimensions as well as the achievable spatial resolution. Thus, our phantom is capable to assess the correlation of spatial and temporal resolution for moving objects of different size and velocity and is suited to evaluate and compare the performance of different MPI scanner architectures under different imaging parameters such as field modulation frequencies and acquisition times.

### Acknowledgements

This work was supported by Deutsche Forschungsgemeinschaft (DFG) in the frame of the projects "quantMPI" (DU293/6-1 and TR 4089-1) and "Development of a relaxation based technique for highly sensitive spectroscopy and imaging of magnetic nanoparticles and corresponding measurement sequences" (BE 5293/1-1).

\*Corresponding author

## Iron Oxide Nanoparticles as T1 Agents for Low-Field MRI

Samuel D. Oberdick<sup>1,2</sup>, Kalina V. Jordanova<sup>2</sup>, Giacomo Parigi<sup>3</sup>, Gary Zabow<sup>2</sup>, Kathryn E. Keenan<sup>2</sup>

<sup>1</sup>Physics Department, University of Boulder, Colorado, USA

<sup>2</sup>National Institute of Standards and Technology, Boulder, USA

<sup>3</sup>Magnetic Resonance Center (ERM), University of Florence, Italy

Low-field magnetic resonance imaging (MRI) has the potential to revolutionize accessibility of MRI for patient diagnosis and care. The magnetic fields used in these scanners can be a fraction of the field used in current clinical-field MRI scanners, operating at 1 mT – 100 mT compared to 3 T for clinical scanners. The lower fields can be generated using permanent magnets, and therefore require less power, space, and accompanying infrastructure than clinical-field scanners. These scanners are highly portable, needing only to be plugged into a conventional wall socket, and are also small enough that they can be wheeled next to a patient's bedside, enabling new modes of MRI-based point-of-care diagnostics (Figure 1a). In the low-field regime, the physics of MRI contrast generation can change considerably compared to clinical fields. Therefore, as low-field scanners are adopted for new imaging procedures, there will be a critical need to develop of MR contrast agents with properties uniquely designed for low-field applications. To this end, we have performed a series of experiments aimed at exploring the efficacy of iron oxide nanoparticles (IONPs) as T1 agents using a commercially available and FDA-approved, low-field (64 mT) MRI scanner produced by Hyperfine.

We have characterized magnetite ( $\text{Fe}_3\text{O}_4$ ) nanoparticles with a range of sizes (5 nm to 16 nm) using 64 mT MRI, magnetometry and nuclear magnetic resonance dispersion (NMRD) to evaluate T1 contrast at 64 mT. We find that IONPs can be efficient longitudinal relaxation agents, producing bright contrast in T1-weighted images compared to control samples (Figure 1b). The particles have longitudinal relaxation rates that are size dependent and, in some cases, outperform commercial Gd-based agents or Feridex (Figure 1c). We correlate the magnetic and structural properties of the particles with models of nanoparticle relaxivity to explain optimal parameters for generation of T1 contrast. Additional engineering may be necessary for *in vivo* use, particularly with regards to colloidal stability and capping ligands. Still, these experiments suggest that IONPs have desirable magnetic properties for future, exciting applications as T1 agents at low fields.

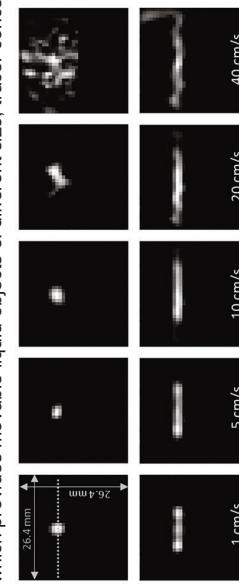


**Figure:** MPI images of moving boluses with 0.8 mm diameter and length (upper row) as well as 3.2 mm diameter and 9.6 mm length (lower row) at flow velocities from 1 to 40 cm/s, from MPI 25/20 FF.

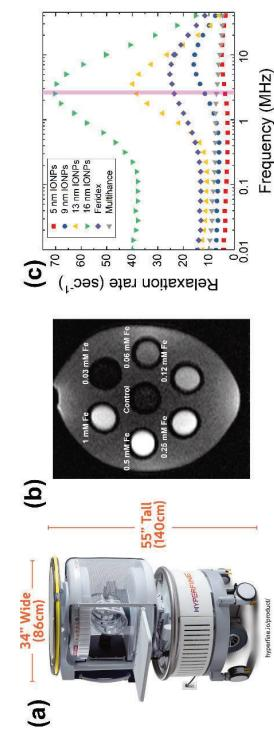


**Figure 1.** (a) Picture of 64 mT Swoop Hyperfine MRI scanner with scale bars showing overall dimensions. (b) T1-weighted fast spin echo image of 9 nm IONPs, taken in Hyperfine scanner at 64 mT (T1 = 700 msec). (c) NMRD profiles showing IONP size-dependence of T1 relaxation rates as a function of frequency (log scale). Also displayed are relaxation rates of commercial contrast agents, Multihance (Gd-based) and Feridex. Pink-shaded line vertical shows 64 mT (2.7 MHz).

Disclaimer: Any mention of commercial products within NIST web pages is for information only; it does not imply recommendation or endorsement by NIST.

## Innovative nanocomposites for protein release through magnetic hyperthermia

Joëlle Bizeau<sup>1,\*</sup>, Alexandre Adam<sup>1</sup>, Clémence Nadal<sup>1</sup>, Grégoire Francus<sup>2</sup>, David Simiscaico<sup>2</sup>, Matthias Pauly<sup>3</sup>, Sylvie Bégin-Colin<sup>1</sup>, Damien Mertz<sup>1,\*</sup>

<sup>1</sup> Institut de Physique et Chimie des Matériaux de Strasbourg (IPCMS), UMR-7504 CNRS-Université de Strasbourg, 23 rue du Loess, BP 34 67034, Strasbourg Cedex 2, France.

<sup>2</sup> Laboratoire de Chimie Physique et Microbiologie pour les Matériaux et l'Environnement (LCPME), UMR 7564 CNRS-Université de Lorraine, 405 rue de Vandoeuvre, 54600 Villerupt-lès-Nancy, France.

<sup>3</sup> Université de Strasbourg, CNRS, Institut Charles Sadron (I2R22), 23 rue du Loess, 67034 Strasbourg Cedex 2, BP 84047, France

\*E-mails: joelle.bizeau@ipcms.unistra.fr; damien.mertz@ipcms.unistra.fr

A well-known interest of using nanoparticles to deliver drugs is the controlled delivery of the contained therapeutic agents activated by external fields such as magnetic field or light. But these nanosystems are even more interesting if they combine several modalities. In our group, such combination has been used to obtain imaging and magnetic hyperthermia. The system consisted in an iron oxide nanoparticle encapsulated in a stellate mesoporous silica shell (IO@STMS) and was already reported to be a promising bimodal imaging probe when functionalized with quantum dots and coated with Human Serum Albumin (HSA) [1]. Herein, the aim of our work was to optimize the surface of such IO@STMS NPs in order to make them promising agents for the loading and controlled delivery of proteins for tissue engineering through magnetic hyperthermia.

For this purpose, in a first study, the ability of isobutyrainide (IBAM)-grafted STMS was assessed, as this IBAM group has been shown to act as a "glue" able to load a wide range of biomolecules (proteins, nucleic acid, polysaccharide and polypeptide [2]) in a large amount. Thus, the stability of protein coating through the IBAM strategy has been studied using four different proteins and several detection techniques. Then, the stability of this protein loading over scaling-up and washings was assessed prior to investigate the thermo-induced release ability of such system. AFM -force spectroscopy was finally used in order to decipher the interactions at play between the particles and the proteins [3].

In a second study, it was hypothesised that the combination of the IO@STMS with thermo-responsive (bio)polymers will allow the release of the protein through magnetic hyperthermia-induced conformational change, as represented in Figure 1. Several thermo-responsive polymers were then studied, as well as several anchoring strategies on the particles, such as covalent grafting or polymer adsorption through the IBAM strategy [4].

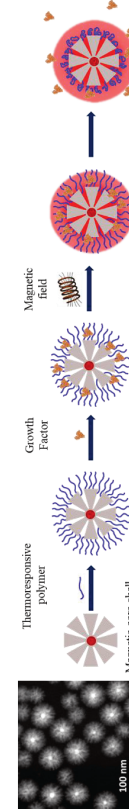


Figure 1: Schematic representation of the release of protein through magnetic hyperthermia by thermo-responsive polymer-functionalized IO@STMS

[1] F. Perton, M. Tassio, G. A. Muñoz Medina, M. Menard, C. Blanco-Andújar, E. Portiansky, M. B. Fernández van Raap, D. Bégin, F. Meyer, S. Bégin-Colin, D. Mertz, Applied Materials Today 2019, 16, 301-314

[2] D. Mertz, P. Tan, Y. Wang, T. K. Goh, A. Blencowe, F. Caruso, Adv. Mater. 2011, 23, 5668-5673

[3] J. Bizeau, A. Adam, C. Nadal, G. Francus, D. Simiscaico, M. Pauly, S. Bégin-Colin, D. Mertz, Int. J. Pharm., submitted

[4] J. Bizeau, A. Adam, S. Bégin-Colin, D. Mertz, Eur. J. Inorg. Chem. 2021, 2021(46), 4799-4805

## Superparamagnetic Nanodevices as Singlet Oxygen Carriers for Cancer Therapy

Isabella Nevoní Ferreira and Eder José Guidelli\*

<sup>1</sup> Departamento de Física, Faculdade de Filosofia Ciências e Letras de Ribeirão Preto, Universidade de São Paulo, Brazil

Considering the treatments available for cancer, radiotherapy is one of the most used. Magnetic hyperthermia, which heats up the cancer cells with alternated magnetic fields and superparamagnetic nanoparticles, can also be employed as cancer treatment. Photodynamic therapy can also be used. In this case, a photosensitizer is responsible to produce reactive oxygen species, such as singlet oxygen ( ${}^1\text{O}_2$ ), that causes cell damage.

The purpose of this work is to sensitize iron oxide nanoparticles covered with a shell of aromatic compounds that can be guided through the body until the tumor to deliver  ${}^1\text{O}_2$ . In this context, aromatic compounds can be employed, once they are able to trap  ${}^1\text{O}_2$  and subsequently release it upon heating. Considering the presence of a superparamagnetic core, the heating could be achieved by magnetic hyperthermia. Therefore,  ${}^1\text{O}_2$  release is expected only when the nanoparticles achieve the target tumor cells and are heated by alternated magnetic fields.

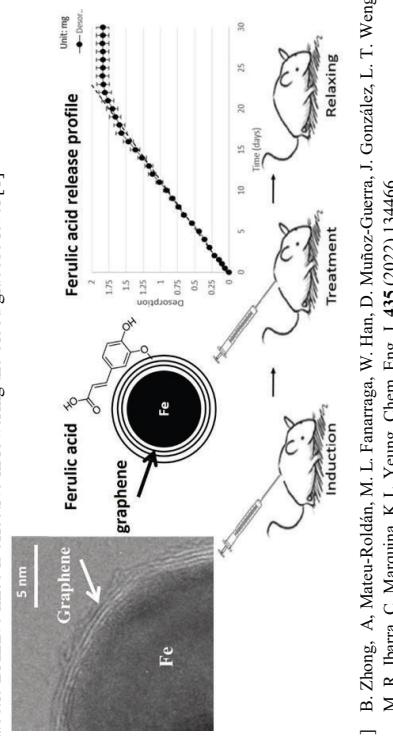
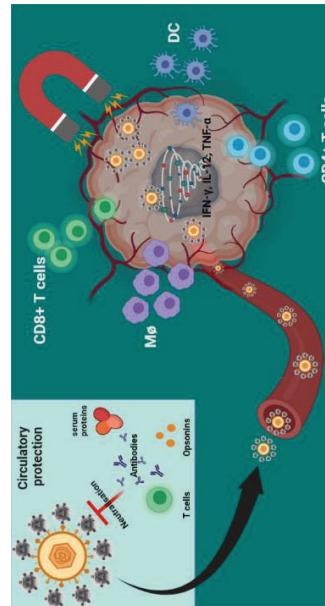
Iron oxide nanoparticles, doped with zinc or not, were synthesized and covered with anthracene or naphthalene. The nanoparticles doped with zinc presented smaller sizes compared to the undoped ones. Dynamic light scattering results indicated the growth of an anthracene or naphthalene shell around the magnetic core. The hybrid nanoparticles were then mixed with methylene blue (MB) and exposed to light of appropriate wavelengths so that the nanoparticles could trap the  ${}^1\text{O}_2$  produced by the photosensitizer. The  ${}^1\text{O}_2$  trapping was monitored by fluorescence spectroscopy, as evidenced by the characteristic fluorescence quenching of the aromatic emission after trapping the  ${}^1\text{O}_2$ , thereby demonstrating the potential use of these hybrid nanoparticles as  ${}^1\text{O}_2$  carriers. More interesting, the magnetic core increased the  ${}^1\text{O}_2$  loading rate and capacity. The posterior  ${}^1\text{O}_2$  release was stimulated by heating the sample on a vacuum oven and monitored by fluorescence spectroscopy. Also, an evaluation of the toxicity of the samples was performed by adding the magnetic nanoparticles covered with naphthalene to a bacterial culture and analyzing the difference in the bacterial growth curves after the samples were heated to mild temperatures (37 – 46 °C). Decreased bacterial growth rate was observed only for samples containing hybrid nanoparticles loaded with  ${}^1\text{O}_2$ , further suggesting that iron oxide nanoparticles covered with naphthalene can be used as biocompatible nanodevices to increase efficiency in cancer treatments combining, in an unexplored way in the literature, photodynamic therapy and magnetic hyperthermia.

## Bugs as drugs – Bacterial derived nanomagnets enhance tumour targeting and oncolytic activity of HSV-1 virus

Faith H N Howard<sup>1</sup>, Haider Al-Janabi<sup>1</sup>, Priya Patel<sup>1</sup>, Katie Cox<sup>1</sup>, Emily Smith<sup>2</sup>, Jayakumar Vadakekolathu<sup>3</sup>, A. Graham Pockley<sup>3</sup>, Joe Conner<sup>4</sup>, James F Nohli<sup>5</sup>, Dan A Allwood<sup>5</sup>, Cristal Collado-Rojas<sup>6</sup>, Aneurin Kennerley<sup>6</sup>, Sarah Staniland<sup>7</sup> and Munita Muthana<sup>1</sup>

<sup>1</sup>Department of Oncology and Metabolism, Mellanby Centre for Bone Research, University of Sheffield; Cancer Research Centre, Centre for Health, Ageing and Understanding Disease (CHAUD), School of Science and Technology, Nottingham Trent University, Nottingham, UK. <sup>2</sup>John van Geest Scotland, <sup>3</sup>Department of Materials Science and Engineering, University of York, York, UK. <sup>4</sup>Virtru Biologics Ltd, BioCity, Newcastle, UK. <sup>5</sup>Department of Chemistry, University of York, York, UK. <sup>6</sup>Department of Chemistry, University of Sheffield; Sheffield, UK.

The survival strategies of infectious organisms have inspired many therapeutics over the years. Indeed the advent of oncolytic viruses (OVs) exploits the uncontrolled replication of cancer cells for production of their progeny resulting in a cancer-targeting treatment that leaves healthy cells unharmed. Their success against inaccessible tumours however, is highly variable due to inadequate tumour targeting following systemic administration. To address this, we have combined these nanobugs with biological nanomagnets for the generation of a magnetised OV with enhanced targeting to the tumour site as well as protection from systemic, inactivating immune mechanisms. Co-assembling herpes simplex virus (HSV1/16) with biocompatible magnetic nanoparticles derived from magnetotactic bacteria enables tumour targeting from circulation with magnetic guidance, protects the OV against neutralising antibodies and thereby enhances viral replication within tumours. This approach additionally enhanced the intratumoural recruitment of activated immune cells, promoted anti-tumour immunity and immune cell death, induced tumour shrinkage and increased survival in a syngeneic mouse model of breast cancer by 50%. Exploiting the properties of such a nanocarrier, rather than tropism of the virus, for active tumour targeting offers an exciting, novel approach for enhancing the efficacy of tumour immunotherapies for disseminated neoplasms.



Talk #19

## Graphene-Encapsulated Magnetic Nanoparticles for Safe and Steady Delivery of Ferulic Acid in Diabetic Mice

Baihua Zhong<sup>1</sup>, Adrián Mateu-Roldán<sup>2,3</sup>, Mónica L. Fanarraga<sup>4</sup>, Wei Han<sup>5</sup>, Débora Muñoz-Guerra<sup>4</sup>, Jesús González<sup>2,6</sup>, Lu Tao Weng<sup>7</sup>, M. Ricardo Ibarra<sup>8</sup>, Clara Marquina<sup>8</sup>, King Lun Yeung<sup>1,5</sup>

\*clarat@unizar.es

<sup>1</sup>Department of Chemical and Biological Engineering, The Hong Kong University of Science and Technology, Clear Water Bay, Kowloon, Hong Kong, China

<sup>2</sup>Instituto de Nanociencia y Materiales de Aragón INMA, CSIC-Universidad de Zaragoza 50009-Zaragoza, Spain.

<sup>3</sup>Departamento de Física de la Materia Condensada, Universidad de Zaragoza, 50009-Zaragoza, Spain.

<sup>4</sup>Grupo de Nanomedicina, Instituto Valdecilla-IDIVAL, Universidad de Cantabria, 39011-Santander, Spain.

<sup>5</sup>Division of Environment and Sustainability, The Hong Kong University of Science and Technology, Clear Water Bay, Kowloon, Hong Kong, China

<sup>6</sup>Departamento de Ciencias de la Tierra y Física de la Materia Condensada (CITIMAC), Universidad de Cantabria, 39005-Santander, Spain

<sup>7</sup>Material Preparation and Characterization Facility, The Hong Kong University of Science and Technology, Clear Water Bay, Kowloon, Hong Kong, China

<sup>8</sup>Laboratorio de Microscopías Avanzadas (LMA), Universidad de Zaragoza, 50018-Zaragoza, Spain

New therapies demand drug delivery systems with added functionalities and proven safety, stability, and biocompatibility to achieve effective drug delivery and uptake. Herein, a magnetic nanovector (Fe@C) was designed by encapsulating iron nanoparticles within a shell of 3-10 concentric graphene layers, structure that was exhaustively characterized through a wide range of techniques. The shell serves as an impervious barrier, mitigating toxicity and enhancing the biocompatibility of Fe@C. Its internalization, subcellular behavior, biocompatibility, and influence on cell viability and proliferation were investigated. Studies on human lung (adenocarcinoma human alveolar basal epithelial) and skin (epidermoid carcinoma) cells indicate Fe@C is less toxic and more biocompatible than the magnetite nanoparticles coated by an amorphous carbon (Fe<sub>3</sub>O<sub>4</sub>@C), a popular drug carrier. As advanced HR-TEM and Raman spectroscopy suggest, Fe<sub>3</sub>O<sub>4</sub>@C exhibited more signs of degradation than Fe@C when exposed to murine macrophages (mouse monocyte-macrophages J774). Unlike Fe<sub>3</sub>O<sub>4</sub>@C, Fe@C has a high drug loading capacity (0.18 g/g) for ferulic acid, an active pharmaceutical ingredient found in the traditional Chinese herb *Angelica sinensis* and releases the drug at a constant dosing rate of 8.75 mg/g/day over 30 days. Ferulic acid released by Fe@C injected subcutaneously in diabetic BALB/c mice is effective in lowering the blood glucose level [1]

Talk #20

[1] B. Zhong, A. Mateu-Roldán, M. L. Fanarraga, W. Han, D. Muñoz-Guerra, J. González, L. T. Weng, M. R. Ibarra, C. Marquina, K.L. Yeung, Chem. Eng. J. **435** (2022) 134466.

## Towards drug targeting to the eye using magnetic multicore nanoparticles

Diana Zahn<sup>1\*</sup>, Kaija Klein<sup>1</sup>, Patricia Radon<sup>2</sup>, Edgar Nagel<sup>1,4</sup>, Michael Eichhorn<sup>3</sup>, Frank Wiekhorst<sup>2</sup>, Silvio Dutz<sup>1</sup>

<sup>1</sup> Institut für Biomedizinische Technik und Informatik, Technische Universität Ilmenau, Ilmenau, Germany

<sup>2</sup> Physikalisch-Technische Bundesanstalt Berlin, Berlin, Germany

<sup>3</sup> Instituut für Anatomie, LSH, Universität Erlangen-Nürnberg, Erlangen, Germany

\*E-mail: diana.zahn@tu-ilmenau.de

If a pharmaceutical agent is needed inside a patient's eye, an injection directly into the vitreous body is a common and effective strategy, but comes with severe risks and discomfort for the patient, so that an alternative strategy to target the drug would be beneficial. Therefore, we are evaluating the possibility of magnetic drug targeting into the eye by using magnetic nanoparticles (MNP) as vehicles. For this approach, magnetic multicore iron oxide nanoparticles were synthesised by a wet co-precipitation method under slow addition of alkaline medium to enable the formation of a multicore structure. These optimized particles where coated with several adsorptive coatings, namely starch (S), carboxymethylcellulose (CMD), dextrane (DEX), citric acid (CA), polyethylene glycol (PEG), and trisodium citrate (NaZ). Magnetic and structural properties of the particles were characterized using VSM, DLS and TEM. The stability of the coated particles was evaluated in different biological media (water for injections, NaCl solution and artificial tears) by means of turbidimetry using an UV/VIS spectrophotometer, showing superior stability of starch coated particles. Numerical simulations performed in a previous study revealed a maximum possible magnetic field gradient of 20 T/m at the side of the eye, resulting from superconducting magnets placed aside/behind the head. This gradient was resembled by a simple permanent magnet setup for ex-vivo laboratory targeting experiments using a 3D printed two-chamber setup (fig. a). By placing the permanent magnet behind the target chamber, particles can be pulled through the tissue sample from the reservoir into the target chamber. The amount of particles that had passed the tissue after 24 h was measured with quantitative magnetic particle spectroscopy relating the amplitude of the measured third harmonic ( $A_3$ ) to the amount of iron in calibration samples. Measurements revealed that only starch coated particles where able to penetrate sclera tissue samples (fig. b) with a mean rate of 5.4 ng/mm<sup>2</sup> within 24 h, while no particles passed cornea samples. Despite the rather small amounts of targeted particles, the results are a promising proof of principle and open the door for future magnetic drug targeting to the eye.

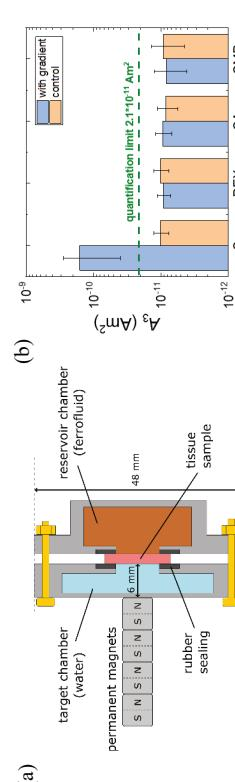


Fig. (a) scheme of the two-chamber setup (b) amount of particles in the target chamber, quantified by the amplitude of third harmonic  $A_3$  in MPS measurements, for four different coating materials and sclera as the tissue sample

### Acknowledgements

This work was supported by the "Thüringer Innovationszentrum für Medizintechnik-Lösungen" (ThIMEDOP; FKZ IZN 2018 0002) and by the Freistaat Thüringen Development Fund (ERDF). It was co-financed from the European Union in the frame of the "European Regional Development Fund (ERDF)". Funding was provided by the DFG core facility, grant number KO321/3 and grant number TR408/11 for the MPS quantification measurements.

## Critical Parameters to Improve Pancreatic Cancer Treatment Using Magnetic Hyperthermia: Field Conditions, Immune Response, and Particle Biodistribution

Lilianne Beola<sup>a,c</sup>, Valeria Graziu<sup>a\*</sup>, Yilian Fernández-Afonso<sup>a,b</sup>, Raluca M. Fratila<sup>a,b</sup>, Marcelo de las Heras<sup>c</sup>, Jesús M. de la Fuente<sup>a</sup>, Lucía Gutiérrez<sup>a,b\*</sup>, and Laura Asín<sup>a\*</sup>

<sup>a</sup>Instituto de Investigación Biomédica en Red (IIM&D), CSIC, Universidad de Zaragoza, Zaragoza, Spain; <sup>b</sup>CIBER-BBN, 50018 Zaragoza, Spain.

<sup>c</sup>Department of Analytical Chemistry, Smart Bio-Interfaces, Viale Rinaldo Piaggio 34, 56025 Pontedera, Italy

<sup>d</sup>Department of Animal Pathology, Universidad de Zaragoza, 50009 Zaragoza, Spain

\*E-mail: lgraziu@unizar.es, lucin@unizar.es, lasin@unizar.es

Magnetic hyperthermia (MH) has been proposed as a promising therapy for the localized treatment of cancer. Under the exposure to an external alternating magnetic field (AMF), magnetic nanoparticles (MNPs) act as heating agents inducing cell death and/or sensitizing the cells against other conventional treatments. Despite the advantages of this experimental treatment, researchers working in the field of MH still face several challenges and practical problems such as the difficulty in achieving enough magnetic material in the tumors or the heterogeneous distribution of the particles in the whole tumor volume even after intratumoral injection. In addition, there are still many knowledge gaps in the frame of *in vivo* MH applications, such as the cytotoxicity mechanisms triggered directly by the heat or the immune response activation stimulated by the treatment.

In this work, several AMF conditions were evaluated using three-dimensional (3D) cell culture models of a pancreatic tumor cell line (MiaPaCa), loaded with MNPs, to determine which of them produced the strongest effect on the cell viability. Then, the MH treatment was tested in a heterotopic xenograft mouse model using the optimal AMF conditions. MNP biodistribution, cell death and immune response triggered by MH were evaluated through different techniques: magnetic measurements, flow cytometry, confocal microscopy and histological staining. Our results point out several factors that should be considered to improve the treatment effectiveness of pancreatic cancer by magnetic hyperthermia, like the great importance the MNPs biodistribution after intratumoral injection in the treatment effectiveness (Figure).

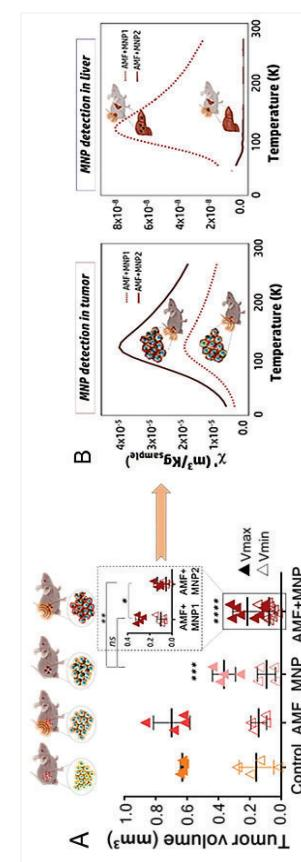


Figure: (A) Tumor evolution represented as minimum and maximum volume reached during the experiment (B) MNP detection by AC magnetic susceptibility 30 days after their intratumoral injection. Significance differences with respect to the control were performed using a two-way ANOVA. GraphPad Prism v7. *ACS Appl. Mater. Interfaces* 2021, 13, 12982–12996

## In silico safety analysis of different metallic implants in magnetic hyperthermia treatments

Irene Rubia-Rodríguez<sup>1</sup>, Luca Zilberti<sup>2</sup>, Alessandro Arduino<sup>2</sup>, Oriano Bottauscio<sup>2</sup>, Mario Chiampi<sup>2</sup>, Daniel Ortega<sup>1,3,4\*</sup>.

<sup>1</sup>IMDEA Nanoscience, Faraday 9, 28049 Madrid, Spain

<sup>2</sup>Istituto Nazionale di Ricerca Metrologica (INRIM), Strada delle Cacce 91, 10135 Turin

<sup>3</sup>Condensed Matter Physics department, Faculty of Science, 15100 Puerto Real, Spain

<sup>4</sup>Institute of Research and Innovation in Biomedical Sciences of the Province of Cádiz (INIBICA), 11002 Cádiz, Spain

\* e-mail of presenting author: [daniel.ortega@uca.es](mailto:daniel.ortega@uca.es)

Magnetic hyperthermia (MH) is a nanoparticle-driven therapy that uses the heat released by magnetic nanoparticles under the exposure of an alternating magnetic field to induce apoptosis in cancerous cells. It has and is being trialed as an adjuvant for the standard of care to successfully treat several types of localized tumours [1, 2]. Computer simulations (*in silico* testing) in MH can predict the thermal dose of several clinical setups in a cheap and fast way. This allows for analysing the treatment safety in terms of dosimetry and temperature rise, as well as assessing possible hot spots due to induced currents, leading MH on its way towards personalized medicine.

The versatility of the simulations to evaluate many clinical situations allows us to study the actual risks of the current exclusion criteria [1, 3]. Nowadays, bearing any kind of metallic object, such as orthopaedic implants, constitutes an absolute contraindication for the treatment. This is based on the knowledge obtained from MRI related studies, but there is an important lack in the literature about the quantification of these risks in the context of clinical MH. In this work, we studied the actual risks of potential MH patients carrying different metallic prostheses using computer simulations. We also analysed the influence of the presence of these objects in the effective magnetic field during the therapy. We have considered different treatment setups varying target sites, implant types and materials to evaluate the temperature increase and the dosimetric values in the major tissue groups. Finally, using these safety parameters, a multi-criteria decision analysis has been performed to assess a risk index for each tissue group in every clinical situation analysed [4, 5].

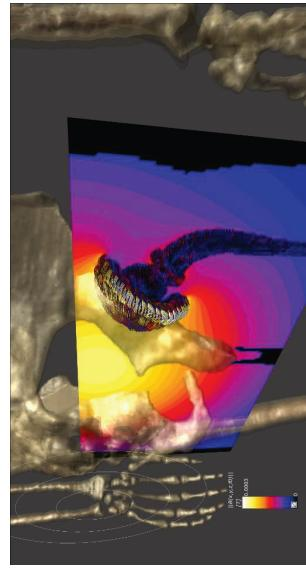


Figure. Possible heating of a hip implant during a magnetic hyperthermia treatment.

## References

- [1] M. Johannsen et al. *Int. J. Hyperthermia* **21** (2005), 637; M. Johannsen et al. *Int. J. Hyperthermia* **23** (2007), 315; D. Ortega, Q. A. Pankhurst, in *Nanoscience: Vol. I: Nanostructures through Chemistry* (2013), 60.
- [2] [www.nocanther-project.eu](http://www.nocanther-project.eu)
- [3] Maier-Hauff et al. *J. Neurooncol.* **103** (2011), 317
- [4] I. Rubia-Rodríguez et al. *Int. J. Hyperthermia* **38** (2021), 846
- [5] I. Rubia-Rodríguez et al. *Int. J. Hyperthermia* (In preparation)

## Hyperthermia and Imaging Performance of Hybrid Stents with Incorporated Magnetic Nanoparticles for Tumor Ablation

Benedikt Mues<sup>1</sup>, Benedict Bauer<sup>2</sup>, Anjali A. Roeth<sup>3</sup>, Thomas Gries<sup>2</sup>, Thomas Schmitz-Rode<sup>1</sup>, and Ioana Slabu<sup>1\*</sup>

<sup>1</sup>Institute of Applied Medical Engineering, Helmholtz Institute, Medical Faculty, RWTH Aachen University,

Pauwelsstr. 20, 52074 Aachen, Germany

<sup>2</sup>Institut für Textilechnik, RWTH Aachen University, Otto-Blumenthal-Str. 1, 52074 Aachen, Germany

<sup>3</sup>Department of General, Visceral and Transplant Surgery, RWTH Aachen University Hospital,

Pauwelsstr. 30, 52074 Aachen, Germany

E-mail: mues@ame.rwth-aachen.de | \*slabu@ame.rwth-aachen.de

Magnetic nanoparticles (MNP) are used as additives for the development of hybrid stents in order to enable local hyperthermia treatment e. g. for endoluminal tumor therapy (esophagus adenocarcinoma or bile duct Klatskin tumors) [1]. In this way, tumor cells can be destroyed in close vicinity to the stent preventing a re-closure of the endoluminal site by tumor tissue ingrowth. Additionally, the MNP can also be used as contrast agents in magnetic resonance imaging (MRI) or as tracers in magnetic particle imaging (MPI) which makes the visualization of the whole stent and a monitoring of its function *in vivo* possible.

Because of the manufacturing process of the hybrid stents, MNP agglomerations occur influencing the magnetic relaxation properties of the MNP. Since the performance of medical technologies like hyperthermia and imaging depends on Néel and Brownian relaxations, it is expected that the MNP agglomerations will have a significant impact. To characterize this impact, we performed parameter studies with the above-mentioned technologies not only for hybrid stents but also for ferrohydrogels. The latter are model systems consisting of immobilized but non-agglomerated MNP in hydrogels. The hybrid stents had two different sizes (corresponding to the size of the oesophagus and bile duct) and were made of hybrid melt-spun polypropylene (PP) fibers incorporated with different MNP types (core diameter of 10 nm, 100 nm and 300 nm). Six different MNP concentrations up to 12 wt% were investigated. The MNP concentrations inside the hybrid fibers were examined by thermogravimetric analysis. Figure 1 exemplarily shows the hyperthermia and MRI imaging ability of a typical oesophagus stent incorporated with 4.4 wt% MNP of 10 nm core size. The latter are model systems consisting of immobilized MNP in hydrogels. The hybrid stents had two different sizes (corresponding to the size of the oesophagus and bile duct) and were made of hybrid melt-spun polypropylene (PP) fibers incorporated with different MNP types (core diameter of 10 nm, 100 nm and 300 nm). Six different MNP concentrations up to 12 wt% were investigated. The MNP concentrations inside the hybrid fibers were examined by thermogravimetric analysis. Figure 1 exemplarily shows the hyperthermia and MRI imaging ability of a typical oesophagus stent incorporated with 4.4 wt% MNP of 10 nm core size. Figure 1a displays a photograph of the hybrid stent. Under an alternating magnetic field ( $f = 270$  kHz and  $H = 13$  kA/m) the stents surface reached a temperature of ca. 43 °C (Figure 1b). Using a 3T MRI  $T_2$  weighted spin echo sequence, the cross-section of the hybrid stent can be visualized (Figure 1c). Based on the data collected from the parameter studies, it was possible to create a multi-dimensional map displaying the heating power and saturation temperature as a function of the alternating magnetic field parameters (frequency, amplitude), MNP concentration and MNP type. MRI measurements produce accurate images of the hybrid stents, especially at the low MNP concentrations. The MPI measurements provide high-resolution images for all hybrid fibers, even for those with high MNP concentration. However, MPI imaging succeeds so far only for hybrid fibers and not for braided hybrid stents.

The hybrid stents represent the basis of a new technology providing the necessary local heating for tumor therapy in a controlled, localized and reproducible manner. The possibility of postoperative visualization of the hybrid stent via MRI and MPI increases the patient safety for future clinical use.

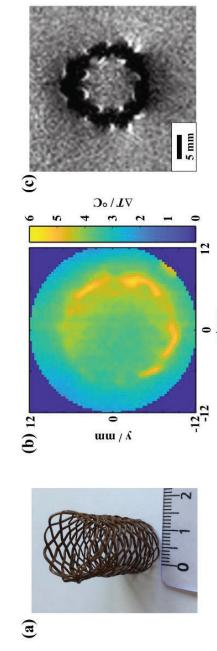


Figure 1: (a) Photograph of an exemplary hybrid stent. (b) Temperature profile 4T of the hybrid stent after 900 s under an AMF  $f = 270$  kHz and  $H = 13$  kA/m. (c) MRI image of the stents' cross-section using a spin echo sequence.

- [1] Mues et al. Nanomagnetic Actuation of Hybrid Stents for Hyperthermia Treatment of Hollow Organ Tumors. *Nanomaterials*, **2021**, *11* (3), 618.

## Iron Oxide Nanoflowers as Excellent Heating Agents for Magnetic Hyperthermia Cancer Therapy

Liudmyla Storozhuk<sup>1,2</sup>, Maximilian O. Besenhard<sup>3</sup>, Stefanos Mourtikoudis<sup>1,2</sup>, Alec P. LaGrow<sup>4</sup>, Martin R. Lees<sup>5</sup>, Le Due Tung<sup>1,2</sup>, Asterios Gavrilidis<sup>3</sup>, and Nguyen Thi Kim Thanh<sup>1,2\*</sup>

<sup>1</sup> UCL Healthcare Biomagnetics and Nanomaterials Laboratories, 21 Albermarle Street, London W1S 4BS, UK

<sup>2</sup> Biophysics Group, Department of Physics and Astronomy, University College London, London, WC1E 6BT, UK

<sup>3</sup> Department of Chemical Engineering, University College London, London, WC1E 7JE, UK

<sup>4</sup> International Iberian Nanotechnology Laboratory, Braga 4715-330, Portugal

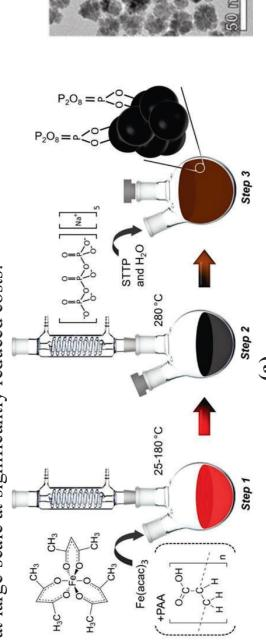
<sup>5</sup> Superconductivity and Magnetism Group, Physics Department, University of Warwick, Coventry CV4 7AL, UK

E-mail: l.storozhuk@ucl.ac.uk; nth.thanh@ucl.ac.uk

In this context, the optimisation of IONP properties for magnetically induced hyperthermia (MIH) for cancer treatment is still a very active research area. The heating ability is considered a critical factor in MIH and is usually prioritised when developing synthesis of IONPs destined for this application. However, there is a bottle neck for wide acceptance of MIH therapy due to the quality limitations of commercial iron oxide nanoparticles (IONPs), which display sub-optimal heating efficiency and are associated with high preparation costs.

We recently overcame these limitations with our novel synthetic procedure for iron oxide nanoflowers (IONFs) exhibiting heating rates that are 3 times higher than those of any commercially available nanoparticle alternative. The experimental scheme is shown in the Figure (a) below. Polyol process yielded biocompatible single core nanoparticles and nanoflowers (Figure (b)). The effect of parameters such as the precursor concentration, polyol molecular weight as well as reaction time was studied, aiming to isolate NPs with the highest possible heating efficiency. Adding polyacrylic acid (PAA) facilitated the formation of excellent nanohating agents IONFs within 30 min.

The progressive increase of the size of the IONFs through applying seeded growth approach resulted in outstanding enhancement of their heating ability with intrinsic loss parameter (ILP) up to  $8.49 \text{ nJ m}^2 \text{ kg}_{\text{Fe}}^{-1}$ . Apart from their exceptional heating efficiency, our IONFs feature exceptional colloidal stability (more than 3 months) and can be synthesised reproducibly via simple protocols in short time, hence, they have good potential for production at large-scale at significantly reduced costs.



(a) Schematic of simple one-pot thermal decomposition of  $\text{Fe}(\text{acac})_3$  polyol synthesis yielding single core IONPs (without PAA) and IONFs (with PAA) in Step 1 and Step 2. (b) TEM images of the IONFs synthesized with PAA via seeded growth, 2nd feeding step.

**Acknowledgement:** EPSRC (EP/M015157/1), EPSRC IAA D2U (KE12021-01).

**Reference:** ACS Appl. Mater. Interfaces 2021, 13, 38, 45870–45880. <https://doi.org/10.1021/acsmami.1c12323>

## A magneto-optical microscope for investigating magnetisation dynamics of intracellular nanoparticles under hyperthermia conditions

M.E. Sharifabadi<sup>1</sup>, R. Soucaille<sup>2</sup>, M. Rotherham<sup>1</sup>, T. Loughran<sup>2</sup>, J. Everitt<sup>1</sup>, D. Cabrera<sup>1</sup>, R. J. Hickie<sup>2</sup> and N. Delling<sup>1,\*</sup>

<sup>1</sup>School of Pharmacy and Bioengineering, Keele University, Guy Hilton Research Centre, Thornburrow Drive, Stoke-on-Trent ST4 7QB, United Kingdom

<sup>2</sup>Department of Physics and Astronomy, University of Exeter, Stocker Road, Exeter EX4 4QL, United Kingdom

\*n.delling@keele.ac.uk

Nanoparticle-mediated magnetic hyperthermia treatment is a promising cancer therapy that enables selective heating of cancerous tissues to slow or stop tumour growth, whilst also increasing tumour sensitivity to chemotherapy and radiotherapy. The importance of magnetic hyperthermia has fuelled interest in the development of biocompatible magnetic nanomaterials. However, previous experiments have suggested that the association of nanoparticles with cells modifies their magnetic response, thus dramatically altering heating efficiency. To explain this behaviour and inform on new design configurations for intracellular hyperthermia, the development of new characterisation tools capable of assessing nanoparticles under relevant biological conditions is required.

Here we present a novel magneto-optical microscope based on the Faraday effect, that enables the study of magnetisation dynamics of nanoparticles in cellular environments under hyperthermia conditions, in combination with fluorescence lifetime measurements (Fig. 1). The developed system is capable of mapping localised AC magnetic susceptibility, magnetometry and fluorescence lifetime, under magnetic fields generated at frequencies up to 1 MHz for AC susceptibility (500 kHz for AC magnetometry) and amplitudes of up to 50 mT (dependent on frequency). The intracellular magnetic properties can be probed *in situ* with  $<0.5 \mu\text{m}$  resolution, and the system can also be used to probe nanoparticles in liquid suspensions.

Using this microscope, we present direct observations revealing the influence of cellular environment on the AC magnetic properties of nanoparticles in both fixed and living cancer cells. Sub-micron measurements of magnetization dynamics are discussed, as well as the first demonstration of AC susceptibility microscopy. Crucially, these experiments reveal huge variability as a function of nanoparticle cellular location and AC field frequency, demonstrating the importance of this new optical approach for understanding the magnetic behavior of intracellular nanoparticles for hyperthermia. The results also show how such methods could be used more generally to probe nanoscale magnetism in biology.

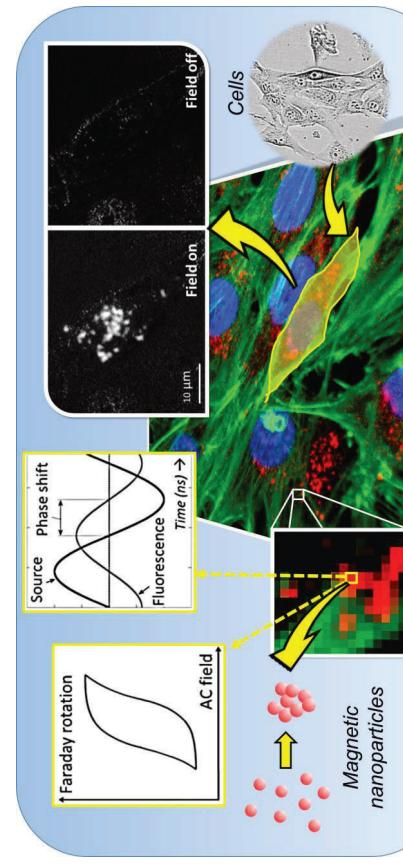


Figure 1: Concept of the combined scanning magneto-optical and fluorescence lifetime microscope. The inset shows AC susceptibility (amplitude) images obtained from nanoparticles localised to the perinuclear region of osteosarcoma cancer cells.

## Magnetic heating to trigger entrapped enzymes activity

Francesca Bussolari<sup>1\*</sup>, Beatriz Torres<sup>1</sup>, Ilaria Armenta<sup>1</sup>, Fernando López-Gallego<sup>2</sup>, María del Puerto Morales<sup>3</sup>, Lorena Betancor<sup>4</sup>, Jesús Martínez de la Fuente<sup>1,5</sup>, Valeria Grazio<sup>1,5</sup>,

<sup>1</sup> BioNanoSurf Group, Aragón Materials Science Institute (ICMA), CSIC/Universidad de Zaragoza, c/ Edificio I+D, Mariano Esquillor Gómez, 50018 Zaragoza, Spain.

<sup>2</sup> HetBioCat Group, CIC biomaGUNE, Miramon, Pasealeku 132, 20014, Donostia, Gipuzkoa, Spain

<sup>3</sup> Mambo Group, Instituto de Ciencia de Materiales de Madrid (ICMM), CSIC, Calle Serrano 61, 28049, Madrid, Spain.

<sup>4</sup> Departamento de Biotecnología, Facultad de Ingeniería, Universidad ORT Uruguay, Mercedes 1237, 11100, Montevideo, Uruguay.

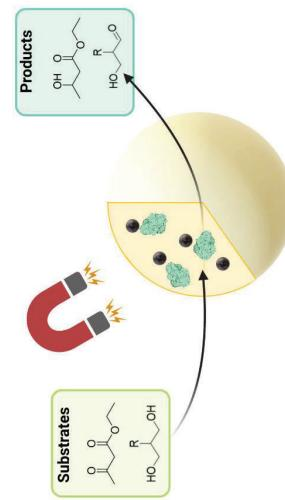
<sup>5</sup> Centro de Investigación Biomédica en Red de Biotecnología, Biomateriales y Nanomedicina (CIBER-BBN), Avenida Monforte de Lemos, 3-5, 28029 Madrid, Spain

\*fbussolari@unizar.es

Enzyme immobilization for industrial application is a wide used but challenging strategy to increase enzyme stability and reusability. Especially, silica matrix has been widely reported in literature as support for enzymatic reaction [1].

The synthesis of nanostructured particles via catalysis of a polyamine molecule in presence of silic acid in mild and biocompatible conditions has been already studied, and recently, the possibility to incorporate magnetic nanoparticles has been demonstrated [2]. In this work, we reported the experimental conditions required for the co-entrapment of different MNPs with different organic coating and Alcohol dehydrogenase from *Thermus thermophilus* (TADH) and from *Bacillus stearothermophilus* (BsADH). Both of them are thermophilic enzyme, that we entrapped with superparamagnetic nanoparticles, and activated thanks to the capability of the MNPs to generate heat in presence of an external alternating magnetic field (AMF). A first screening of MNPs with different size, coating, and heating capacity, has been performed in order to identify the most suitable for encapsulation, expressed activity and AMF activation. Initially, enzymes immobilization, expressed activity and entrapped iron yields was evaluated to obtain a small selection of the original MNPs panel. Then, the most interesting MNPs were evaluated for AMF triggered heating efficiencies, to find the most adequate one to locally reach the optimal ADHs temperature (70-80°C).

Preliminary results suggest it as a versatile tool for the development of a new concept of industrial biocatalyst remotely controlled by magnetic field.



### References

- [1] E. Jackson, *Methods Mol Biol* 2020; 2100, 259-270.
- [2] S. Correa, *PLOS ONE* 2019;14, e0214004.

### Acknowledgements

The research for this work has received funding from the European Union (EU) project HOTZYMEs (grant agreement n° 829162) under EU's Horizon 2020 Programme Research and Innovation actions H2020-FETOPEN-2018-2019-2020-01. Authors also thank Spanish MINECO project BIO2017-84246-C2-1-R and DGA and Fondos Feder (Bionanosurf E15\_17R).

## Nanoparticle-mediated magnetic hyperthermia enhances the breakdown of human blood clots by tissue plasminogen activator

David Cabreira<sup>1\*</sup>, Maneea E Sharifabadi<sup>1</sup>, Neil D Telling<sup>1</sup> and Alan GS Harper<sup>2</sup>

<sup>1</sup> School of Pharmacy and Bioengineering and <sup>2</sup> School of Medicine, Keele University, UK.  
\* d.c.cabreira@keele.ac.uk

Thrombolysis is a front-line treatment for stroke. Intravenous injection of the clot-busting agent, tissue plasminogen activator (tPA), is used to enzymatically breakdown a blood clot and re-establish blood flow through the blocked cranial vessel. However use of thrombolytic is currently limited by its short time window of efficacy. Here, we investigated whether platelet-targeted magnetic hyperthermia (MH) induced by Iron Oxide Nanoparticles (IONPs) could be used to enhance the efficacy of tPA-mediated thrombolysis. Platelet-targeted IONPs were created by conjugation to PAC-1, an antibody that specifically binds to activated platelets. *Ex vivo* generated human blood clots were exposed to tPA in the presence or absence of MH. MH was found to enhance the clot-dissolving activity of tPA, reducing the weight of tPA + MH treated clots to  $75.6 \pm 1.5\%$  of untreated control clots, compared to  $81.3 \pm 2.2\%$  clots treated with tPA alone ( $n = 15$ ,  $P < 0.05$ ). Platelet-targeted MH was found to increase permeability of blood clots to 70 kDa fluorescent dextran, which has a similar molecular weight to that of tPA (Figure 1). Electron microscopy images revealed that localised MH enhances tPA-mediated clot disruption. Remarkably, viability tests evidenced no increase in cell death of 3D endothelial cell cultures when exposed to f-IONP-mediated MH – indicating that MH does not injure this internal layer of blood vessels. Platelet-targeted magnetic nanoparticles could act as an adjuvant to enhance the efficacy of tPA through the induction of localised MH. Clot-targeted MH could improve the treatment of cardiovascular conditions such as Venous Thromboembolism.

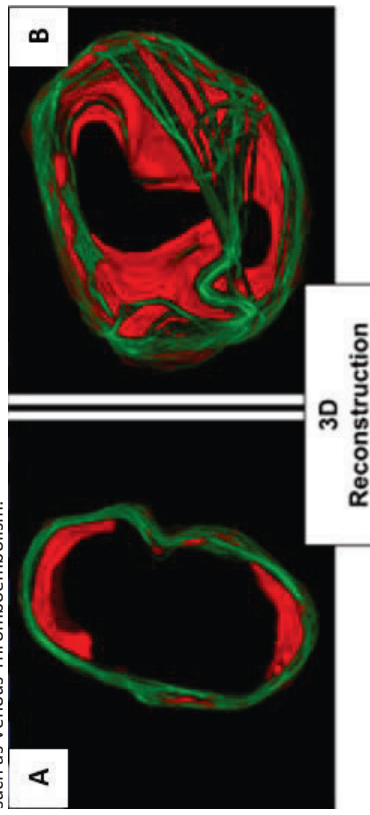


Figure 1. 3D reconstruction of a blood clot (A) untreated or (B) treated with nanoparticle-mediated magnetic hyperthermia. Green colour: Blood clot contour; Red colour: fluorescent dextran with similar molecular weight to that of clot-busting enzymes.

## Magnetic Hyperthermia as an adjuvant cancer therapy in combination with carbon ions, protons and photons irradiation on pancreatic tumour cell cultures

**Francesca Biero<sup>1\*</sup>, Martín Albino<sup>2</sup>, Antonio Antocia<sup>3</sup>, Paolo Airolo<sup>4</sup>, Matteo Berardinelli<sup>5</sup>, Daniela Bettiga<sup>4</sup>, Paola Calzolari<sup>6</sup>, Mario Ciocca<sup>6</sup>, Maurizio Corti<sup>6</sup>, Angelica Facchetti<sup>6</sup>, Salvatore Gallo<sup>7</sup>, Flavia Groppi<sup>7</sup>, Andrea Guerini<sup>2</sup>, Claudia Innocenti<sup>2,8</sup>, Cristina Lenard<sup>4,9</sup>, Silvia Locardi<sup>9</sup>, Simone Manenti<sup>7</sup>, Renato Marchesini<sup>9</sup>, Manuel Mariani<sup>1,5</sup>, Francesco Orsin<sup>1</sup>, Emanuele Pignoli<sup>10</sup>, Claudio Sangregorio<sup>2,8</sup>, Ivan Veronesi<sup>8</sup>, Alessandro Lascialfari<sup>1,5</sup>**

<sup>1</sup>National Institute of Nuclear Physics-INFN, Pavia 27100, Italy  
<sup>2</sup>Department of Chemistry, University of Florence, Sesto F. no 50019, Italy  
<sup>3</sup>Department of Science and INFN, Roma Tre University, Roma 00146, Italy  
<sup>4</sup>Department of Physics and INFN, University of Milano, Milano 20133, Italy  
<sup>5</sup>Department of Physics, University of Pavia, Pavia 27100, Italy  
<sup>6</sup>CNAO Foundation, Pavia 27100, Italy  
<sup>7</sup>Department of Physics and INFN-UNIMI laboratory LASA, Segrate 20090, Italy  
<sup>8</sup>IICCOM-CNR, Sesto F. no 50019, Italy  
<sup>9</sup>C.I.M.A.L.Na., Milano 20133, Italy  
<sup>10</sup>IRCCS National Cancer Institute Foundation, Milano 20133, Italy

\*Email: francesca.biero@unipi.it. Mobile: +39 0382 987483

Magnetic fluid hyperthermia (MFH) is used in clinics as an anti-cancer therapy, especially thanks to the reached increment of the magnetic nanoparticles' (MNPs) thermal efficiency and the promising synergy between MFH and the more traditional tumour treatments. Thanks to the elevation of tumour temperature to  $42\text{--}44^{\circ}\text{C}$  by exposing MNPs to an alternating magnetic field, MFH can induce cancer cell death (apoptosis). MNPs commonly have a core-shell structure, with an iron-oxide based core, and a biocompatible shell and can be directly injected into the tumour with high concentrations (c.a.  $30\text{--}40\text{ mg}/\text{cm}^3$  of the target volume). Here we present the combination of MNPs assisted hyperthermia and carbon ions/photon irradiation on human pancreatic adenocarcinoma cell cultures (BxPC3 cells). Hyperthermia made use of spherical  $\text{Fe}_3\text{O}_4$  core coated with meso-2,3-dimercaptosuccinic acid with Specific absorption rate (SAR) of  $110 \pm 30\text{ W/greson}$  under an alternating magnetic field of frequency  $f = 109.8\text{ kHz}$  and amplitude  $\mu\text{H} = 19.5\text{ mT}$ . Cell cultures irradiation with carbon ions and protons was performed using the synchrotron-based clinical scanning beams at the National Center for Oncological Hadron Therapy (CNAO) in Pavia (Italy), and the photons beam was delivered by using a 6 MV linear accelerator at the Fondazione IRCCS Istituto Nazionale dei Tumori in Milano (Italy). The clongenic survival assay was used to evaluate the effectiveness of the combined treatment; the BxPC3 cells were treated with 3 different protocols: (i) simple irradiation (carbon ions/protons/photons), (ii) magnetic nanoparticles (MNPs) administration and irradiation and (iii) MNPs administration plus irradiation and subsequent hyperthermia (Hyp). Briefly, our results (see Biero, Francesca, et al. *Nanomaterials*, **10**, 16 (2020); **19**/9 for experiments with carbon ions irradiation) show a significant effect of MNPs administration and hyperthermia for all irradiation protocols, *i.e.* an enhancement of the cell death rate induced by the irradiation alone. These encouraging results pave the way to further *in vivo* investigations for finally testing this new combined therapy (hadron irradiation and MNP assisted hyperthermia) in view of its translation to clinics.

## Development of Handheld Induction Heaters for Magnetic Fluid Hyperthermia Applications and In-vitro Evaluation on Ovarian and Prostate Cancer Cells

**Jorge L. Castro-Torres<sup>1</sup>, Janet Méndez<sup>2</sup>, Madeline Torres-Lugo<sup>2</sup> and Eduardo J. Juan<sup>3</sup>**

<sup>1</sup>Bioengineering Graduate Program, University of Puerto Rico-Mayagüez  
<sup>2</sup>Department of Chemical Engineering, University of Puerto Rico-Mayagüez  
<sup>3</sup>Department of Electrical Engineering, University of Puerto Rico-Mayagüez

Magnetic fluid hyperthermia (MFH) is a cancer treatment that takes advantage of the efficient, clean, and accurate method of delivering heat by induction heating and the intrinsic physicochemical characteristics of magnetic nanoparticles (MNPs). When in the presence of an external alternating magnetic field (AMF), MNPs elevate the temperature of the desired target (tumor site) to around  $41\text{--}47^{\circ}\text{C}$ , inducing various mechanisms of cell death depending on therapeutic conditions. Applying these magnetic fields with high spatial resolution is still a challenge in the field. Large magnetic fields will heat unwanted parts of the body if there are metallic implants, pacemakers, or other magnetically susceptible materials, as well as MNPs outside the target area. One solution is to miniaturize induction heating system down to the level of small tumors, potentially limiting the resulting damage to only the tumorigenic tissue. To our knowledge, such instruments have not yet been reported in the medical setting. Therefore, the purpose of this work was to develop a novel laparoscopic induction heater (LIH) and a transrectal induction heater (TRIH), both capable of applying high-frequency, high-intensity AMFs in hard-to-reach places within the human body.

A 20-turn and a 30-turn miniature multilayer "pancake" coils were wound using Litz wire. These coils, which were aimed at laparoscopic and transrectal applications for cancer, were inserted into 3D printed enclosures. Both enclosures mimic known medical instruments and include water circulation to remove heat, electrical connection for the coil, and a fiber optic sensor to monitor the temperature at the center of the coil. Figure 1 shows a conceptual diagram of the laparoscopic induction heater. Maximum values of magnetic field intensities reached by the laparoscopic and transrectal induction heaters were  $42\text{ kA/m}$  at  $328\text{ kHz}$  and  $25\text{ kA/m}$  at  $302\text{ kHz}$ , respectively. The first potential application of the LIH was thought to be on intraperitoneal malignancies which are regarded as silent killers. The TRIH was designed for prostate cancer after feedback from many surgical oncologists. Therefore, ovarian cancer cell lines (SKOV-3, A2780) and prostate cancer cell lines (PC-3, LNCaP) were used to evaluate the instruments' capabilities in killing cancer cells. The normal cell line, NIH3T3, was also used to observe how healthy cells respond to MFH treatment as compared to abnormal cells.

Figure 2 (left) displays the results from utilizing the laparoscopic induction heater on NIH3T3, SKOV-3 and A2780, while Figure 2 (right) shows the results of the transrectal induction heater on LIH and  $43^{\circ}\text{C}$  by the TRIH. Both instruments successfully accomplished killing cancer cells, with minimal effects on normal cells, by applying a relatively strong, yet localized, magnetic field to magnetic nanoparticles. We successfully designed a laparoscopic induction heater and a transrectal induction heater and evaluated them on ovarian and prostate cancer cell lines, respectively. These innovations could become an enabler for the development of medical treatments that would require non-contact heating approaches inside the body of a patient.

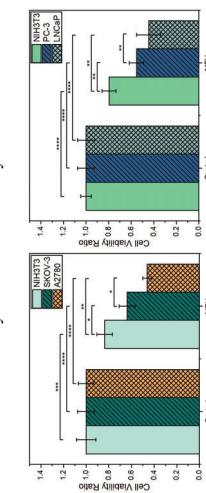


**Figure 1** Conceptual diagram of the laparoscopic induction-heating instrument. The (a) coil leads, (b) peristaltic tubing, and (c) thermocouples run the length of the instrument (tube). Five input/output accesses are included for the (d) peristaltic tubing, (e) thermocouples, (f) water, and (g) coil terminals. Once the peristaltic pump is turned on, water starts filling the interior of the instrument through (d), until it reaches the top, and exits through (f).

Figure 2 (left) displays the results from utilizing the laparoscopic induction

heater on NIH3T3, SKOV-3 and A2780, while Figure 2 (right) shows the results of the transrectal induction heater on LIH and  $43^{\circ}\text{C}$  by the TRIH. Both instruments

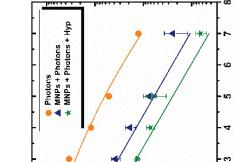


**Figure 2** Cell viability ratio of the control and experimental (MFH) groups obtained using Trypan Blue assay by manual counter. Only one control group and the MFH group are shown for simplicity. Each error bar represents the standard error of nine samples from three different cell lines: NIH3T3, SKOV-3 and A2780 for the LIH experiments (left), and PC-3 and LNCaP for the TRIH experiments (right). Temperatures reached were  $41^{\circ}\text{C}$  (left) and  $43^{\circ}\text{C}$  (right).

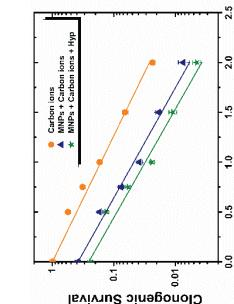


Figure. Clonogenic survival of BxPC3 cells culture for 3 different protocols (see text): carbon ions/photon irradiation (orange circles), carbon ions/protons administration (blue triangles) and carbon ions/photon irradiation + MNPs administration + Hyp (green stars).

## Local temperature gradients in intracellular magnetic hyperthermia

Ángel Millán,<sup>1,\*</sup> Yanyan Gu,<sup>1,2</sup> Rafael Piñol,<sup>1</sup> Raquel Moreno-Loshuertos,<sup>3</sup>

Carlos D.S. Brites,<sup>4</sup> Justyna Zeler,<sup>4,5</sup> Abelardo Martínez,<sup>6</sup> Guillaume Maurin,<sup>1</sup>

Patrício Fernández-Silva,<sup>3</sup> Joaquín Marco-Briallal,<sup>3</sup> Pedro Tellez,<sup>1</sup> Rafael Cases,<sup>1</sup> Rafael Navarro Beltrú,<sup>7</sup> Débora Bonvin,<sup>7</sup> Luis D. Carlos<sup>4</sup>

<sup>1</sup> INMA, Instituto de Nanoscience y Materiales de Aragón (INMA-CSIC)/University of Zaragoza) Zaragoza, Spain. <sup>2</sup> Centro de Investigación Biomédica en red en Bioingeniería, Biomaterias y Nanomedicina (CIBER-BBN), Zaragoza, Spain. <sup>3</sup> Universidad de Zaragoza, Organic Chemistry Department. <sup>4</sup> Institute of Applied Sciences and Intelligent Systems, Naples, Italy. <sup>5</sup> Institute of Materials Science in Madrid (ICMM-CSIC), Spain.

<sup>6</sup> Departamento de Biología Molecular y Celular, and Instituto de Biocomputación y Física de Sistemas Complejos, Universidad de Zaragoza, C. Pedro Cerbuna 10, 50006 Zaragoza (Spain).

<sup>4</sup> Phantommg, CICECO-Aveiro Institute of Materials, Department of Physics, University of Aveiro Campus de Santiago, 3810-193 Aveiro, Portugal.

<sup>5</sup> Faculty of Chemistry, University of Wrocław, 14, F. Joliot-Curie Street, 50-383 Wrocław, Poland

<sup>6</sup> Departamento de Electrónica de Potencia, 13A, Universidad de Zaragoza, 50018 Zaragoza, Spain

<sup>7</sup> Powder Technology Laboratory, Institute of Materials, Ecole Polytechnique Fédérale de Lausanne, 1015 Lausanne, Switzerland

\* Email: amillan@unizar.es Mobile: +34 672312859

Exogenous and endogenous heat generation inside cells is a subject of intense debate in recent times. In particular the generation of temperature gradients on nanoparticles heated externally by a magnetic field is of crucial importance in magnetic hyperthermia therapy of cancer. In the absence of reliable direct measurements of local temperatures on cell-internalized nanoheaters, a controversy has been established between those who predict that it is not physically possible to reach substantial temperature increments between the source of heat, and those who adhere to the possibility of large temperature gradients. Here, we have measured the variation of the local temperature on magnetic nanoheaters under an external alternating magnetic field using a luminescence molecular ratometric thermometer placed on the nanoheater surface. Moreover, we have also measured the temperature at intracellular sites at some distance from the magnetic heaters and on the outside of the cell membrane. Even for moderate magnetic fields ( $H_f=2.4 \times 10^6 \text{ A} \cdot \text{m}^{-1} \cdot \text{s}^{-1}$ ,  $f=30 \text{ mT}$ ,  $F=100 \text{ kHz}$ ), temperature increments of about  $11^\circ\text{C}$  have been found in the nanoheaters. The  $T(t)$  curve shows a steep initial increase and then it reaches a plateau. However, at some distance from the nanoheaters, the temperature increases constantly to values of about  $4.5^\circ\text{C}$ . In the meantime, the temperature at the cell membrane does not show any appreciable increment indicating that the generated heat is too small to produce an increase of the overall temperature of the cells. It was found that these local temperature increments are sufficient to produce noticeable cell apoptosis. When we increased the  $H_f$  values close to this limit ( $4.8 \times 10^6 \text{ A} \cdot \text{m}^{-1} \cdot \text{s}^{-1}$ ,  $f=60 \text{ mT}$ ,  $F=100 \text{ kHz}$ ), the specific absorption rate (SAR) increased from 45 to  $150 \text{ W/g(Fe}_3\text{-O}_4\text{)}$  and, then, the apoptosis ratio increased to 60%, that is already relevant for the final goal of therapeutic performance. In conclusion, our *in vitro* results are indicating that the approach of focal hyperthermia therapy suggested as an improved alternative to actual global heating hyperthermia could be feasible.

## Composition impacts the structural, magnetic, and heating efficiency of $\text{Mn}_x\text{Fe}_{3-x}\text{O}_4$ MNPs. An *in vitro* and *in vivo* study.

S. Del Sol-Fernández<sup>1</sup>, G. Tommasini<sup>1</sup>, P. Martínez-Vicente<sup>1</sup>, P. Gomollón-Zucco<sup>1</sup>, J. M. de la Fuente<sup>1,2</sup>, R. M. Fratila<sup>1,2,3</sup>, C. Tortajone<sup>4</sup>, P. Morales<sup>5</sup> and M. Moros<sup>1,2</sup>

<sup>1</sup> Institute of Nanoscience and Materials of Aragón (INMA-CSIC)/University of Zaragoza) Zaragoza, Spain. <sup>2</sup> Centro de Investigación Biomédica en red en Bioingeniería, Biomaterias y Nanomedicina (CIBER-BBN), Zaragoza, Spain. <sup>3</sup> Universidad de Zaragoza, Organic Chemistry Department. <sup>4</sup> Institute of Applied Sciences and Intelligent Systems, Naples, Italy. <sup>5</sup> Institute of Materials Science in Madrid (ICMM-CSIC), Spain. <sup>6</sup> Email: sdelsol@unizar.es and moros@unizar.es

Manganese-iron oxide ( $\text{Mn}_x\text{Fe}_{3-x}\text{O}_4$ ) systems have unique properties, such as high magnetic moment values of *c.a.*  $5 \mu_B$  per unit cell, excellent chemical stability, and a surface suitable for ligand functionalization and bioconjugation, which make them particularly promising in biomedical applications. In this work, we present a systematic approach for tuning the composition of a set of  $\text{Mn}_x\text{Fe}_{3-x}\text{O}_4$  with control over the size and shape through one-step thermal decomposition method. The composition ( $x$ ) of the  $\text{Mn}_x\text{Fe}_{3-x}\text{O}_4$  nanoparticles, ranging from 0.07 to 1.4, has been carefully tailored by adjusting the  $(\text{Fe(acac})_3/\text{Mn(acac})_2$  precursor ratio. The effects of the nanoparticles composition and its impact on the magnetic properties were studied from static magnetic measurements, X-ray Diffraction, Transmission Electron Microscopy (TEM) analysis and infrared spectroscopy (FTIR). Moreover, the synthesis method has been refined to obtain NPs with polyhedral morphology and suitable magnetic anisotropy, which significantly improves their magneto-thermal behaviour. The heating performance has been investigated using two different combinations of alternating magnetic fields (AMFs): high amplitude and low frequency (96 kHz, 60 mT) or with low amplitude and high frequency (10 mT, 763 kHz) in water and in glycerol. A linear increase between the  $\text{Mn}^{2+}$  content and the heating performance was obtained in samples where  $x < 0.6$ , while for  $x > 0.7$  a deterioration of the magnetic output was found, leading to a marked reduction of the magnetothermal efficiency. Interestingly, the heating performance does not change when the samples are dispersed in environments of high viscosity, which is an important requirement for a successful intracellular heating. Selected  $\text{Mn}_x\text{Fe}_{3-x}\text{O}_4$  nanoparticles with the lowest, medium, and highest  $\text{Mn}^{2+}$  content ( $x = 0.07, 0.4$  and  $0.6$ ) and thus, different magnetic heating performance were studied in two biological models, *in vitro* and *in vivo*: pancreatic tumoral cells and the freshwater invertebrate model organism *Hydra vulgaris*. In both systems the toxicology and the internalization of the different MNPs were assessed. Moreover, the biological effects after applying mild magnetic hyperthermia were studied, both to kill tumoral cells and enhance *Hydra* regeneration.

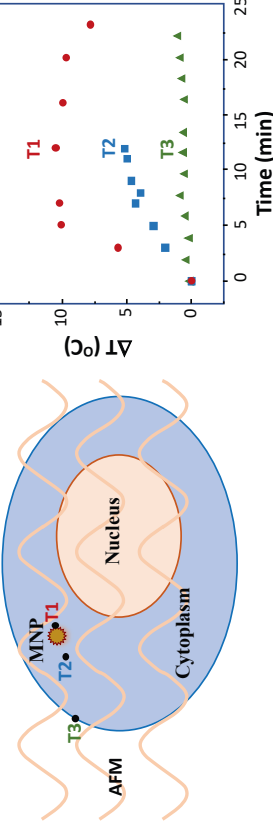


**Figure 1.** Overview of the work. Fine control over composition of  $\text{Mn}_x\text{Fe}_{3-x}\text{O}_4$  impacts their heating performance and thus, their biological performance in two different models.

Figure. Local temperature variation on the magnetic nanoparticle (T<sub>1</sub>) surface, at some distance in the cytoplasm (T<sub>3</sub>), and on the exterior of the cell membrane (T<sub>2</sub>), during the application of an alternating magnetic field to a cell culture.

## On the mechanisms of magnetization reduction in iron oxide nanoparticles

T. Köhler<sup>1,2,3</sup>, A. Feoktystov<sup>1</sup>, O. Petracic<sup>2</sup>, E. Kentzinger<sup>2</sup>, T. Bhatnagar-Schoffmann<sup>2,3,4</sup>, M. Feygenson<sup>5,6</sup>, N. Nandakumaran<sup>2,3</sup>, J. Landers<sup>7</sup>, H. Wende<sup>7</sup>, A. Cervellino<sup>8</sup>, U. Rücke<sup>2</sup>, A. Kovács<sup>4</sup>, R.E. Dunin-Borkowski<sup>4</sup>, Th. Brückel<sup>2,3</sup>

<sup>1</sup> Forschungszentrum Jülich GmbH, Jülich Centre for Neutron Science JCNS at Heinz Maier-Leibnitz Zentrum MLZ, Garching, Germany

<sup>2</sup> Forschungszentrum Jülich GmbH, Jülich Centre for Neutron Science JCNS-2 and Peter Grünberg Institute PGI-4, JARA-FIT, Jülich Centre for Microscopy and Spectroscopy with Electrons and Peter Grünberg Institute PGI-4, JARA-FIT, Jülich, Germany

<sup>3</sup> Forschungszentrum Jülich GmbH, Ernst Ruska-Centre for Microscopy and Spectroscopy with Electrons and Peter Grünberg Institute PGI-4, JARA-FIT, Jülich, Germany

<sup>4</sup> Forschungszentrum Jülich GmbH, European Spallation Source ERIC, Lund, Sweden

<sup>5</sup> Faculty of Physics and Center for Nanoimaging Duisburg-Essen (CENIDE), University of Duisburg-Essen, Duisburg, Germany

<sup>6</sup> Paul Scherrer Institut, Swiss Light Source, Villigen, Switzerland

\*E-mail: a.feoktystov@fz-juelich.de

Iron oxide nanoparticles are presently considered as promising objects for various medical applications including targeted drug delivery and magnetic hyperthermia. The nanoparticle solution in water has to be free of large aggregates to avoid blocking of capillaries and simultaneously the nanoparticles have to possess large enough saturation magnetization to react to an external magnetic field. However, there remain several unsolved questions regarding the effect of size onto the overall magnetic behavior of nanoparticles. One aspect is the reduction of magnetization as compared to bulk samples. A detailed understanding of the underlying mechanisms of this reduction will allow one to improve the particle performance in the applications.

There are several proposed models for the spatial distribution of the magnetization, which include the presence of a magnetic core-shell structure, spin disorder around defects and a reduced magnetization in the core due to reversed moments and frustration. In this work [1] we combine neutron and synchrotron X-ray scattering techniques with magnetometry, transmission electron microscopy (TEM), elemental analysis and Mössbauer spectroscopy to study nanoparticles of various sizes and to obtain an as complete as possible picture of their properties. We find that the nanoparticles possess a macroscopically reduced saturation magnetization, mostly due to the presence of antiphase boundaries as observed with high-resolution TEM (HRTEM) and X-ray scattering and to a lesser extent due to a small magnetically depleted surface layer and cation vacancies.

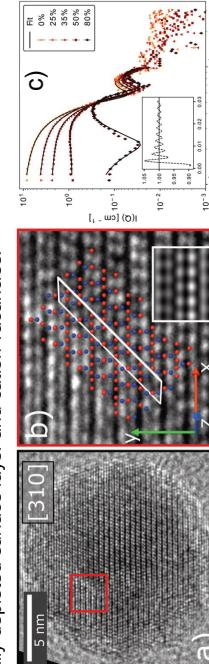


Figure. (a) HRTEM micrograph of an isolated nanoparticle viewed along [310]. A region with an antiphase boundary is marked with the red square. (b) Marked region of (a) with a schematic of the crystal structure. The lattice plane along which the translation occurs is indicated with the white rectangle. (c) small-angle neutron scattering of polarized neutrons for 5 different contrasts. The black line represents the best fit of a core-shell model with a sticky hard sphere potential (inset on the lower left). [1] *Nanoscale* (2021) **13**, 6965–6976. <https://doi.org/10.1039/DONR08615K>

## Multimodal Magnetic Force Microscopy

Kevin J. Walsh<sup>a</sup>, Joshua Sifford<sup>b</sup>, Owen Shiflett<sup>b</sup>, Sheng Tong<sup>c</sup>, Gang Bao<sup>c</sup> and Gunjan Agarwal<sup>a,b</sup>

<sup>a</sup> Biophysics Graduate Program and <sup>b</sup> Department of Mechanical and Aerospace Engineering, The Ohio State University, Columbus OH

<sup>c</sup> Department of Bioengineering, Rice University, Houston, Texas 77005, United States  
Email: [agarwal.60@osu.edu](mailto:agarwal.60@osu.edu) Phone: 1-6142924213

Magnetic force microscopy (MFM) is a scanning probe technique that can map nanoscale magnetic domains in a sample. MFM employs a magnetically coated probe to track the sample topography and detect long-range forces due to magnetic stray fields at user defined lift heights above the sample. Although MFM is widely used in solid-state devices, there are several challenges in application of MFM for biological samples. These include, contamination of the MFM probe by sticky biological materials, topological cross-talk in MFM images and incompatibility in a fluid environment.

In this study we developed two methods to overcome the limitations of MFM towards making it amenable to biological samples. In our first approach, we developed a novel indirect-MFM (ID-MFM) technique to detect fluorescently labeled nanoparticles. In ID-MFM an ultrathin silicon-nitride window is used to create a physical barrier between the sample and the probe. The window prevents direct contact between the sample and the probe thereby eliminating probe contamination and topological cross-talk. We show how ID-MFM does not dampen the MFM signal and the samples prepared on silicon-nitride windows are amenable to multi-modal analysis by fluorescence or transmission electron microscopy (TEM).

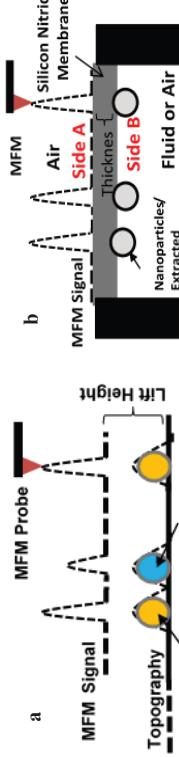


Figure: (a) In conventional (direct) MFM, a first scan is performed at a user-defined lift height ( $z$ ) to determine the topology of the sample. A second scan is performed at a user-defined lift height ( $z$ ) to determine long-range magnetic probe-sample interactions. In indirect MFM (ID-MFM), the sample is immobilized under an ultrathin silicon-nitride membrane and the MFM probe scan the top surface. Long-range magnetic interaction is detected through the membrane. The silicon-nitride windows are transparent to light and electron optics (Sifford et al. *Nanoscale Advances*, 2019)

In our second approach we analyzed rodent spleen tissue sections via conventional MFM. We investigated how scan rate and surface roughness can impact the topological cross-talk in MFM experiments. We elucidate how thin sections with reduced surface roughness (as that used for TEM) can minimize the topographical cross-talk. In addition thin sections can be compatible for multimodal microscopy analysis via both conventional (direct) and ID-MFM.

Taken together our work has advanced the use of MFM for imaging and mapping nanoscale iron-oxide deposits in biological samples. Future work along these directions could enable MFM analysis of physiological and pathological iron deposits in tissues sections in a label-free, multimodal and high throughput manner.

## Harmonizing of static magnetization measurements using two commercial SQUID devices of the same type

Patricia Radon<sup>1</sup>, Zvonko Jagličić<sup>2</sup>, Uwe Steinhoff<sup>1</sup>, Frank Wiekhorst<sup>1</sup>

<sup>1</sup> Physikalisch-Technische Bundesanstalt (PTB), Berlin, Germany  
<sup>2</sup> Institute of Mathematics, Physics and Mechanics & Faculty of Civil and Geodetic Engineering  
 University of Ljubljana (MFNM), Ljubljana, Slovenia

E-mail: patricia.radon@ptb.de

The characterization of magnetic nanoparticles (MNP) is an important issue, which demands for reliable and sensitive magnetic measurement techniques. Nevertheless, there exists no internationally accepted protocol for reliable and reproducible determination of their magnetic properties. Static magnetization measurements using highly sensitive superconducting quantum interference devices (SQUIDs) are commonly used to characterize MNP. While the continuous verification of the proper operation of SQUID devices within one laboratory is state of the art, interlaboratory comparisons are not common. Here, we conducted a comparison of static magnetization measurements of MNP on two commercial SQUID devices of the same type using the same palladium (Pd) calibration reference sample at IMFM Ljubljana and PTB Berlin.

Initial magnetization curves and hysteresis loops of a Pd reference sample were recorded at 298K using identical SQUID devices (MPMS-XL-5, Quantum Design Inc). The Pd measurement data were used to calibrate the external magnetic field values. With these corrections the static magnetization measurements of an identical MNP sample on both devices were corrected and compared to assess the accuracy of magnetic moment determination. The analysis of the paramagnetic Pd curves reveal non-linear deviations of the external magnetic field values from the nominal field experienced by the sample leading to implausible effects like inverted hysteretic behaviour as reported by other groups, before [1]. This is found for both devices but to varying degrees. Applying the field correction on MNP measurements resulted in a significant reduction of the total difference between the MNP magnetization curves measured in the two laboratories. In the low field region, the differences in the magnetic moment decreased from about 15% down to about 1.5% after field correction.

The corrections validated by our interlaboratory comparison help to harmonize magnetic measurement techniques for the characterization of magnetic nanoparticles and demonstrate the importance of interlaboratory comparisons between different laboratories working and using the same magnetic measurement devices. This is an important step towards establishing a reference measurement site for static magnetization of MNP at PTB.

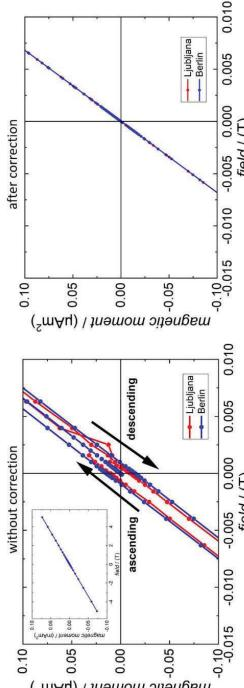


Figure 1: Comparison of the measurement of the initial magnetization curve and the hysteresis loop of the paramagnetic palladium reference sample at 298 K and between  $\pm 10$  mT. Left: Without correction. The inset shows the whole hysteresis loops over  $\pm 5$  T. The branches of the hysteresis loop are inverted: The descending hysteresis branches cut the field axis in the positive and the ascending branches in the negative field range. Right: After correction. The descending and the ascending hysteresis branches overlay

[1] McElfresh, M., et al. *Quantum Design Application Note*. 1-37.

## Magnetic Force Optimization for Improved Magnetic Particle Targeting

Rikert Van Durme<sup>\*</sup>, Guillaume Crevecoeur<sup>1,2</sup>, Luc Dupré<sup>1</sup>, and Annelies Coene<sup>1,2,3</sup>

<sup>1</sup> Department of Electromechanical Systems and Metal Engineering, Ghent University, 9000 Ghent, Belgium

<sup>2</sup> EEDT Decision & Control, core lab Flanders Make, 3920 Lommel, Belgium

<sup>3</sup> Cancer Research Institute Ghent, 9000 Ghent, Belgium

\* Email: [Rikert.vandurme@ugent.be](mailto:Rikert.vandurme@ugent.be)

Setups with electromagnets to move magnetic micro- or nanoparticles from a distance have been widely researched [1]. They can be used in magnetic drug targeting applications, in which magnetic particles attached with therapeutics are injected into the human body to treat diseases. External electromagnets surrounding the particles in the vascular network are activated such that magnetic forces acting upon the particles make them move towards a targeted site, improving therapy efficacy while reducing patient side effects. During movement other intervening forces such as blood drag, buoyancy and gravity, interaction forces, etc. affect the particles' trajectories. It is beneficial for treatment if as many as possible particles overcome some of these forces and end up in the targeted region instead of taken away by the bloodstream.

We have applied a constrained optimization of the magnetic force on a particle in a given direction with respect to the electromagnet currents. As such, the trajectory of the particles is manipulated to guide them to the targeted region. We added a constraint that limits the divergence of the magnetic force to keep the particles together while moving (Figure 1). This greatly reduces particle scattering and increases the amount of particles at the target. It is shown with simulations on bifurcated vessel branches that the optimized forces move particles into the targeted branch at velocities increased by 20% compared to without optimization.

Secondly, an optimization was conducted to find time-dependent electromagnet currents that make a particle and surrounding particles travel towards a target location over a finite time interval. Here also the divergence constraint was included. Simulations demonstrate that under the optimized magnetic fields in a considered time interval, groups of particles reach the target with reduced spreading and increased amounts by 10 times compared to without divergence limitation.

The discussed methods can be readily applied to any setup with electromagnets.

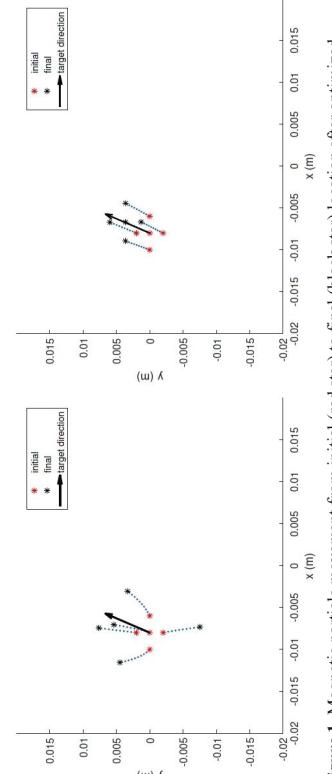


Figure 1. Magnetic particle movement from initial (red star) to final (black star) location after optimized electromagnet currents are applied, without (left) and with (right) divergence constraint. The black arrow is the set direction along which the optimization of the magnetic force is executed. When the force divergence is constrained (right), the surrounding particles also move in the target direction, improving targeting performance.

[1] Liu, Ya-Li, et al. "A review of magnet systems for targeted drug delivery." *Journal of Controlled Release* 302 (2019): 90-104.

## Navigation control of Magnetotactic Bacteria by magnetic fields

Danny Villanueva-Alvarez<sup>1\*</sup>, Alicia G. Gubieda<sup>2</sup>, Nerea Lete<sup>1</sup>, David Gandia<sup>3</sup>, Eduardo Fernández<sup>2</sup>, Alfredo García-Arrabias<sup>1,3</sup>, Ana Abad<sup>2</sup>, Jorge Feuchtwanger<sup>1,4</sup>, David de Cos<sup>5</sup>, Mª Luisa Fdez-Gubieda<sup>1,3</sup>

<sup>1</sup>Dpto. Electricidad y Electrónica, Universidad del País Vasco (UPV/EHU), 48904 Leioa, Spain.

<sup>2</sup>Dpto. Immunología, Microbiología y Parasitología, Universidad del País Vasco (UPV/EHU), 48904 Leioa, Spain.

<sup>3</sup>Basque Center for Materials Applications and Nanostructures (BCMat) (BCMaterials), 48904 Leioa, Spain.

<sup>4</sup>Ikerbasque, Basque Foundation for Science, 48009 Bilbao, Spain.

<sup>5</sup>Dpto. de Física, Universidad del País Vasco (UPV/EHU), Spain.

\*Email: danny.villanueva@ehu.eus

Magnetotactic bacteria (MTB) are biological microorganisms with the ability to align and navigate along geomagnetic field lines to reach hypoxic regions. To develop this ability, MTB biomimic magnetic nanoparticles, called magnetosomes, that organize forming a chain to respond optimally to an external magnetic field. The intrinsic properties of MTB, such as self-propulsion, aerotaxis, and their capability to grow and proliferate in regions with low oxygen concentrations, make them suitable as biogents for potential anticancer applications. In addition, the presence of the magnetic chain allows control in their navigation. All these characteristics explain why MTB are considered a promising nanobiorobots for biological applications [1,2]. The latter indicates that MTB nanobiobots could be employed as localized drug transport, tumor monitoring agent, and even in cancer treatments (magnetic hyperthermia) [3,4].

However, its activity as a nanorobot is fundamentally limited by its navigation control [5]. Trying to shed light on this matter, in order to study their mobility we have developed software algorithms to the analysis of detection and tracking of magnetotactic bacteria, applying image sequencing techniques to the analysis of videos acquired by optical microscopy. We have worked with two different species (*Magnetospirillum gryphiswaldense* and *Magnetospirillum magnetum*) in different biological media, supplying controlled flows to emulate blood stream. In addition, we have precisely controlled the magnitude and direction of the external magnetic field applied to regulate navigation and evaluate their swimming capacity. Preliminary results are shown in Fig.1.

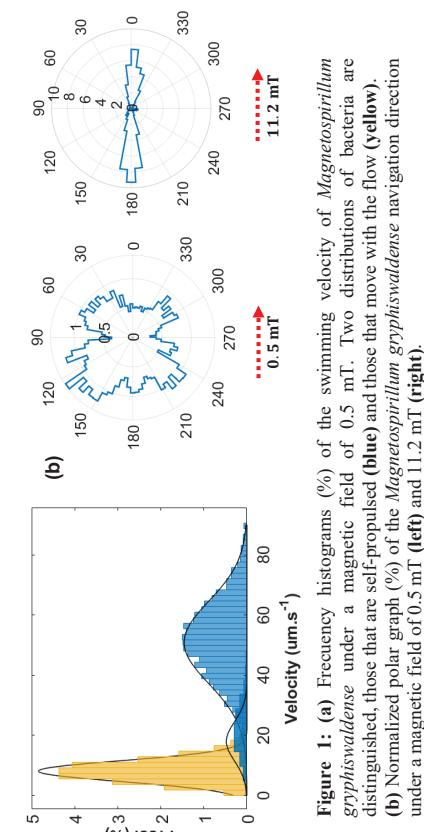


**Figure 1:** (a) Frequency histograms (%) of the swimming velocity of *Magnetospirillum gryphiswaldense* under a magnetic field of 0.5 mT. Two distributions of bacteria are distinguished, those that are self-propulsed (blue) and those that move with the flow (yellow). (b) Normalized polar graph (%) of the *Magnetospirillum gryphiswaldense* navigation direction under a magnetic field of 0.5 mT (left) and 11.2 mT (right).

## References

- [1] M.L. Fdez-Gubieda, *et al.* J. Appl. Phys. 128, 070902 (2020).
- [2] D. Kurzajewska, *Biology* 9(5), 102 (2020).
- [3] A. Muclà, *et al.* J. Phys. Chem. C 120, 42, 24437-24448 (2016).
- [4] D. Gandia, *et al.* Small 15, 1902626 (2019).
- [5] S. Rismann, *et al.* Small 1702982, (2017).

## Magnetically navigating superparamagnetic particles using MRI in phantom and swine chemoembolization model

Ning Li<sup>1,2</sup>, Cyril Tous<sup>1,2</sup>, Ivan P. Dimov<sup>1,2</sup>, Philip Fei<sup>1,2</sup>, Simon Lessard<sup>1,2</sup>, Zeynab Nosrati<sup>3</sup>, Katayoun Saatchi<sup>3</sup>, An Tang<sup>1,2</sup>, Samuel Kadoury<sup>4</sup>, Urs O. Häfeli<sup>2</sup>, Sylvain Martel<sup>1</sup>, and Gilles Soulez<sup>1,2\*</sup>

<sup>1</sup>Centre de recherche du Centre Hospitalier de l'Université de Montréal (CRCHUM), Montréal, Québec, Canada;

<sup>2</sup>Université de Montréal, Montréal, Québec, Canada; <sup>3</sup>University of British Columbia, Vancouver, BC, Canada;

<sup>4</sup>Polytechnique Montréal, Montréal, Québec, Canada.

\*Email: gilles.soulez.med@ssss.gouv.qc.ca

Superparamagnetic nanoparticles (SPIONs) can be combined with tumor chemoembolization agents to form magnetic drug-eluting beads (MDEBs), which can be navigated magnetically in the MRI scanner through the vascular system.

Magnetic resonance navigation (MRN) uses the outstanding imaging properties of MRI to detect liver tumors, the  $B_0$  magnetic field to magnetize MDEBs, and the imaging gradient generated by imaging gradient coils to steer them in the targeted vessels. In this paper, the MDEBs ( $200 \pm 12 \mu\text{m}$ ) were fabricated using  $\text{Fe}_3\text{O}_4$  SPIONs ( $12 \pm 3.6 \text{ nm}$ ) coated with  $\text{C}_{12}\text{-bisphosphonate}$  and poly(lactic-co-glycolic) acid (PLGA), and then we demonstrated the feasibility of MDEBs MRN *in vivo* and *in vitro*.

The experimental setup is shown in Figure (a). Before MRN, the swine was rotated (the target lobar and segmental vessel in a decline position) to combine magnetic and gravitational forces. The MDEBs were injected using a partially inflated balloon catheter. After balloon inflation, the blood flow rate in the proper hepatic artery was measured at  $\leq 1.0 \text{ mL/s}$  using the 2D cine phase-contrast sequence. The artifacts. The experimental results reveal that the combination of the magnetic and gravitational forces steering gradient durations were 8 ms in the left (+X) and down (-Y) direction for amplitudes of 26.5 mT/m and 18 mT/m, yielding a 32 mT/m nominal amplitude for 29.5% duty cycle given TR = 14 ms and  $G_{\text{max}} = 43 \text{ mT/m}$ . In each MRN cycle, an MDEB aggregate (20 MDEBs) was released from our injector and followed by the opening of the pre-set MRN sequence. The sequence would last 20 s for each MRN cycle. A volumetric interpolated breath-hold examination (VIBE) sequence (radio-frequency-spoiled 3D gradient-echo sequence) was used to locate the MDEBs *in vivo* using their MRI artifacts. The experimental results reveal that the combination of the magnetic and gravitational forces can navigate the MDEBs into the targeted vessel branches shown in Figure (c).

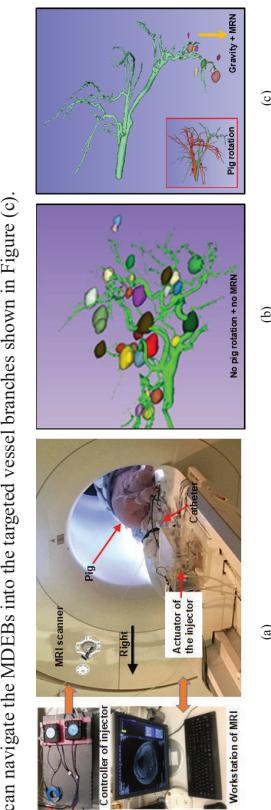


**Figure 2:** (a) Setup of the MRN of the MDEBs in the pig liver. The MDEB aggregates are formed in a particle injection system. The catheter, inserted into the hepatic artery of a living swine, is connected to the MRI-compatible injection system to allow the injection of the MDEB aggregates into the proximal proper hepatic artery. MRI workstation controls the MRN sequence and receives the TI-VIBE-based MR images. (b) Accumulation of aggregates (green arrow) in both lobes without MRN and optimization of gravitational forces (green arrow) showing the optimization of gravitational forces. (c) Accumulation of aggregates in the left lobe can be observed after MRN combined with optimization of gravitational forces (pig positioned in left decubitus); in the red box, projection of a 3D angiography in supine (orange) and left decubitus (green) showing the optimization of gravitational forces.

## Combining bioorthogonal click chemistry and magnetic hyperthermia for siRNA transfection

Javier Idiato-López<sup>a,b</sup>, Daniela Ferreira<sup>c,d</sup>, Laura Asín<sup>a,b</sup>, María Moros<sup>a,b</sup>, Eduardo Moreno-Antolín<sup>a</sup>, Valeria Grazú<sup>a,b</sup>, Alexandra R. Fernandes<sup>c,d</sup>, Jesús M. de la Fuente<sup>a,b</sup>, Pedro V. Baptista<sup>c,d</sup> and Raluca M. Fratila<sup>a,b,e</sup>  
Email: jidillo@unizar.es

<sup>a</sup> Institute of Nanoscience and Materials of Aragon, INMA (CSIC-University of Zaragoza), Zaragoza, Spain. <sup>b</sup> Centro de Investigación Biomédica en Red de Bioingeniería, Biomateriales y Nanomedicina (CIBER-BBN), Spain. <sup>c</sup> Associate Laboratory i4HB - Institute for Health and Bioeconomy, NOVA School of Science and Technology, NOVA University Lisbon, Portugal. <sup>d</sup> UCBiO – Applied Molecular Biosciences Unit, Department of Life Sciences, NOVA School of Science and Technology; NOVA University Lisbon, Portugal. <sup>e</sup> Organic Chemistry Department, Facultad de Ciencias, Zaragoza, Spain.

The heat generation by magnetic nanoparticles (MNPs) in the presence of an alternating magnetic field (AMF) has traditionally been studied for cancer treatment applications upon the accumulation of MNPs inside target cells. Herein, we developed an innovative approach to apply localized heating onto living cell membranes for inducing changes of membrane biophysics. Our approach is based on the covalent immobilization of MNPs on the cell membranes via bioorthogonal click chemistry, more specifically the strain-promoted [3+2] azide-alkyne cycloaddition (SPAAC) between azide-labelled cell membranes and strained alkyne-functionalized MNPs.

First, the expression of azide reporters on human breast adenocarcinoma cells (MCF7) was optimized through metabolic glycoengineering. Then, 13 nm iron oxide MNPs were decorated with two different strained alkynes with different reactivity towards azides, namely cyclooctyne (CO) and dibenzocyclooctyne (DBCO). Their bioorthogonal reactivity was assessed in suspension, onto artificial azide substrates and their attachment to the cell membrane was confirmed with electron microscopy, flow cytometry and elemental mass analysis.

Finally, upon the application of an AMF, these MNPs acted as “hotspots” to generate a very localized heating of the cell membrane, leading to changes in cell membrane fluidity that promoted the intracellular delivery of a siRNA to silence the expression of a Green Fluorescent Protein. Our transfection approach led to a silencing effect comparable to the one observed using a commercially available siRNA transfection reagent; however, it resulted notably less toxic for the cells. Therefore, our approach overcomes one of the most limiting aspects of existing transfection strategies, i.e. impact on cell viability.

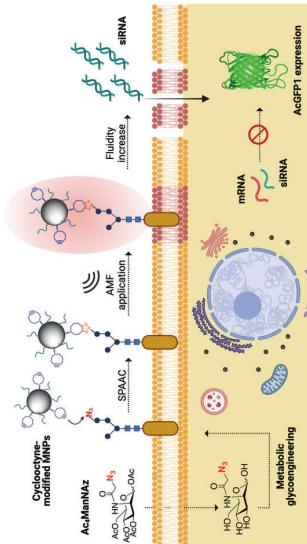


Figure 1. Scheme of the application of localized MH onto cell membranes for cell transfection.

## Characterisation of DNA Nano-Chamber Magnetic Filaments

D. Mostarac<sup>1</sup>; O. Gang<sup>2</sup>; S. Kantorovich<sup>1</sup>

<sup>1)</sup> University of Vienna, Faculty of Physics, 1080 Vienna, Austria  
<sup>2)</sup> Columbia University, New York, USA

DNA nano-objects are one of the most prominent building blocks for engineering self-assembled morphologies that can broadly be classified as supra-molecular polymers. These polymers can carry nanoscopic cargos, can serve for changing optical and rheological properties. We previously reported on the directional assembly of DNA nanocuboids (DNCs) with tailorabile multi-linking bonds into long polymer-like chains.[1,2] In this contribution we treat directional assembly as a platform for synthesis of polymer-like magneto-responsive materials, namely magnetic filaments (MFs).

By comparative analysis of equilibrium properties of DNC filaments functionalised with magnetic nanoparticles (DNC MFs) under compression in constant homogeneous magnetic fields, we quantify the impact of cubic monomer shape and bonding mechanism of DNC. DNC MFs have a surprisingly smooth, and controllable response to compression. Furthermore, combining MD and Lattice-Boltzmann method we study the effects of monomer shape and magnetic nature of colloid on the behaviour of MFs subjected to the simultaneous action of shear flow and a stationary external magnetic field perpendicular to the flow. External magnetic field strongly inhibits tumbling only for filaments with ferromagnetic monomers, with an orientation angle independent of monomer shape. Reorientational dynamics of MFs with super-paramagnetic monomers, are not inhibited by applied magnetic fields, but enhanced, particularly for cubic monomer shape. The latter finding suggests the DNC filaments might be ideal candidates to create magnetically responsive polymers.

[1] Lin, Zhiwei, et al. "Engineering organization of DNA nano-chambers through dimensionally controlled and multi-sequence encoded differentiated bonds." Journal of the American Chemical Society 142.41 (2020): 17531-17542.

[2] Xiong, Yan, et al. "Divalent Multilinking Bonds Control Growth and Morphology of Nanopolymers." Nano Letters (2021).

## Strain promoted azide alkyne click chemistry, an efficient surface functionalization strategy for microRNAs magnetic separation

Djamila Kechkeche<sup>1,2</sup>, Shirine El Mousli<sup>1</sup>, Claire Poujouly<sup>2</sup>, Emilie Secret<sup>1</sup>, Vincent Dupuis<sup>1</sup>, Marie-Emmanuelle Goriot<sup>3</sup>, Julien Stracusa<sup>2</sup>, Sébastien Banzet<sup>2</sup>, Jean Gamby<sup>2</sup>, Jean-Michel Siaugue<sup>1</sup>

<sup>1</sup> Physico-chimie des Électrolytes et Nanosystèmes Interfaçaux (PHENIX), Sorbonne Université, CNRS, Paris, France

<sup>2</sup> Centre de Nanosciences et de Nanotechnologies (C2N), Université Paris-Saclay, CNRS, Palaiseau, France

<sup>3</sup> Institut de Recherche Biomédicale des Armées (IRBA), INSERM, Clamart, France  
Contact: jean-michel.siaugue@sorbonne-universite.fr

Magnetic nanoparticles, used in biological and biomedical assays, like magnetic particle spectroscopy-based applications [1], are made of a superparamagnetic iron oxide core capped with an organic or inorganic layer, to prevent aggregation and to improve their physicochemical stability. Precise surface bio-functionalization is also mandatory to allow highly selective chemical interactions with the biological target to quantify.

In this work,  $\gamma\text{-Fe}_2\text{O}_3@\text{SiO}_2$  core-shell nanoparticles [2] were used to anchor single strand nucleic acid (ssDNA) using two surface functionalization strategies. A comparison of two grafting protocols (figure 1), one based on maleimide chemistry and the other on strain promoted azide alkyne click chemistry (SPAAC) reveals that the SPAAC strategy allows for a higher grafting yield and a more accurate control of the amount of the grafted ssDNA.

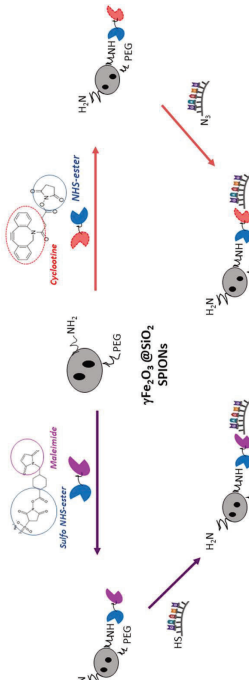


Figure 1: surface functionalization strategies.

Optimized SPAAC grafting protocol enables the grafting of six different ssDNA, complementary of miRNA sequences specific of liver (miR 122), skeletal (miR 133b, 206) and/or cardiac (miR 208a, 133a, 1) muscles, as they are promising biomarkers.

Magnetic separation of the complementary miRNA sequences in model buffer solution results in the rapid capture of miRNAs, corresponding to 50–60% of ssDNA's hybridization. Furthermore, capture experiments carried out in complex biological media (fetal bovine serum or rat plasma) reveal only a slight decrease in the amount of miRNA extracted. Finally mismatch experiments using miR 133a and 133b sequences, which differ only by one nucleic acid, indicate a fairly good selectivity.

Dehybridization of captured miRNAs is now being studied in a lab-on-a-chip format using mild magnetic hyperthermia conditions [3] to quantify miRNAs on the surface of microelectrodes, as part of the DIMELEC and e-miRGeny projects, funded by the French National Research Agency, and the Labex NanoSaclay, respectively.

[1] Wu K. *et al.* (2020), Magnetic Particle Spectroscopy: A Short Review of Applications, *ACS Appl. Naturat.*

[2] Horny M.-C. *et al.* (2021), Magnetic Hyperthermia on  $\gamma\text{-Fe}_2\text{O}_3@\text{SiO}_2$  Core-Shell Nanoparticles for mi-RNA 122 Detection, *Nanomaterials*.

[3] Horny M.-C. *et al.* (2021), Release and Detection of microRNA by Combining Magnetic Hyperthermia and Electrochemistry Modules on a Microfluidic Chip, *Sensors*.

## Magnetic Nanoparticles for Diagnostic Imaging: Getting Into the Clinic

Proulx, R., Zhang, M., Jayalakshmi, Y. – Imagion Biosystems

Iron oxide nanoparticles have been used in preclinical and clinical research as imaging agents for decades because of their magnetic properties and their known safety profile. Few, however, have made it through clinical development and regulatory approval to be made commercially available. We have developed iron oxide nanoparticles for both non-targeted and targeted uses, including an anti-HER2 conjugated nanoparticle currently being investigated in a Phase I study for lymph nodal staging. We propose reviewing some of the challenges associated with developing iron oxide nanoparticles for clinical diagnostic imaging, and provide examples of their use in three forms of imaging: magnetic resonance imaging (MRI), Magnetic Particle Imaging (MPI), and Magnetic Relaxometry (MRX).

## SPIONs AS IMAGING AGENTS

### Magnetic Particle Imaging (MPI)

- Use an oscillating magnetic field (the drive field to generate a signal by exciting the iron - linear magnetization of magnetic nanoparticle tracer. A superimposed magnetic gradient field (the selection field) localizes the signal, allowing image formation.

### Magnetic Resonance Imaging (MRI)

- Nanoparticles cause changes in the T2 lifetime of local hydrogen nuclei resulting in negative contrast (dark regions) in T2-weighted (transverse relaxation) images.

### Magnetic Relaxometry (MRx)

- Localizes the differential relaxation rate of nanoparticles caused by targeted delivery and binding to the tumor.
- Particles bound to tumor cells relax more slowly.
- Requires a targeted nanoparticle.

Image courtesy of Imagion Biosystems Inc.  
12-3D MRx image showing location of tumor in magnetic field after injection of magnetic SPIONs.

Imaging the particles and measuring the response takes about 3 sec.

IMAGIONBIOSYSTEMS.COM | 2

## Innovative dynamic detection for early diagnosis with a lab-on-a-chip based on “two-stage” giant magnetoresistance sensors

M. Derou<sup>1</sup>, M. Giraud<sup>1</sup>, F.D. Delapierre<sup>1</sup>, M. Jeckelmann<sup>1</sup>, P. Bonville<sup>1</sup>, A. Solignac, M. Thévenin<sup>1</sup>, F. Conegg<sup>1</sup>, E. Paul<sup>1</sup>, S. Simon<sup>2</sup>, C. Fernon<sup>1</sup>, C. Ferandet-Tarisse<sup>2</sup> and G. Jasmin-Lébras<sup>1\*</sup>

<sup>1</sup>CEA/DRF/IRAMIS/SPEC/LNO : CEA Orme des merisiers bat 772 CP 135 - 91191 GIF-SUR-YVETTE France

<sup>2</sup>CEA/DRF/DMTS/JOLIOT/SPULERI : CEA - SPI Bât 136 - 91191 GIF-SUR-YVETTE France

\*Email : gaelle.jasmin-lebras@cea.fr

The development of early diagnosis techniques, that are fast, sensitive, inexpensive and point of care, is a challenge in the field of health but also in the field of defense or the environment. Currently, among the easy-to-use early diagnostic devices, there are strip tests in which the targets migrate in the cellulose. Other methods used routinely in biology laboratories, such as ELISA or PCR tests, have better sensitivities but require a qualified staff. Optical detection is still not suitable for some opaque matrices and electrochemical or static magnetic detection have too many non-specific interactions. In this context, we propose a patented biochip, based on Giant Magnetoresistance (GMR), to detect biological objects in very small quantities, in complex matrices without a prior washing step. This approach is based on the use of magnetic nanoparticles functionalized by monoclonal antibodies, directed against target biological objects. Their dynamic detection, after interaction with the magnetic nanoparticles, is carried out using GMR sensors which allow to count the magnetically targeted biological objects one by one.

Very promising results were obtained with a first GMR biochip [1] based on GMR sensors placed under the microfluidic channel, developed on a eukaryotic cell model, allowing reaching sensitivities and specificities equivalent to those obtained on the same biological model in ELISA tests, with a greater ease of use and a slight time gain. Until now, the main limitation has been the bead aggregates that lead to false positives. The new patented biochip [2] (Figure 1A) has sensors arranged face to face on either side of the microfluidic channel, which allow each magnetic object to be detected simultaneously (Figure 1B). For the first time, thanks to this technique, it is possible to determine the magnetic moment of the objects flowing in the channel and thus to discriminate the aggregates of beads from the targeted biological objects. This detection technique allows to obtain a sensitivity 30 times higher than that obtained with the ELISA test or with the first prototype making this biochip very competitive.

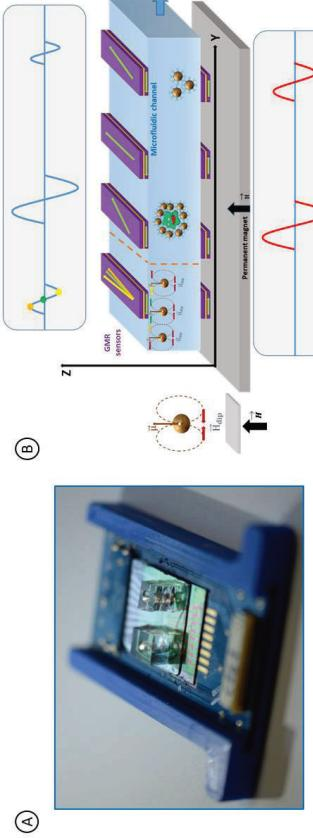


Figure 1 - A: New biochip; B: New biochip principle. A cell labelled with several magnetic beads (about 60 beads) is detected simultaneously by both sensors. A single bead passing very close to one of the two sensors will only be detected by one of the two sensors but if it passes in the middle of the channel it will not be detected at all. Aggregates of beads (no more than 20 beads) passing in the middle of the channel will be detected by both sensors but with a lower magnetic moment than for a labelled cell.

[1] Giraud, M. and al. G. Evaluation of In-Flow Magnetoresistive Chip Cell Counter as a Diagnostic Tool. In: Biosensors. Vol. 9, n° 3, pp. 105. 31st August 2019. [2] C. Fernon and al. Patent n° 1855217.

## Point-of-need detection of pathogen-specific nucleic acid targets using magnetic particle spectroscopy

Enja Laureen Rösch<sup>1</sup>, Jing Zhong<sup>1</sup>, Aldin Lak<sup>1</sup>, Zhe Liu<sup>2</sup>, Markus Etzkorn<sup>2</sup>, Meinhard Schilling<sup>1</sup>, Frank Ludwig<sup>1</sup>, Thilo Vierreck<sup>1</sup> and Birka Lakens<sup>3</sup>

<sup>1</sup> Institute for Electrical Measurement Science and Fundamental Electrical Engineering and Laboratory for Emerging Nanometrology (LENA), TU Braunschweig, Germany

<sup>2</sup> Institute of Applied Physics, TU Braunschweig, Wendeelsohnstraße 2, 38106 Braunschweig, Germany

<sup>3</sup> Institute of Semiconductor Technology and Laboratory for Emerging Nanometrology (LENA), TU Braunschweig, Langer Kamp 6a/b, 38106 Braunschweig, Germany

Email: enja.roesch@tu-braunschweig.de

The pandemic caused by severe acute respiratory syndrome coronavirus 2 (SARS-CoV-2) strongly demonstrates the need for a sensitive, fast and reliable pathogen diagnostics tool. While reverse-transcription polymerase chain reaction (RT-PCR) can detect down to single copies of virus DNA, this comes at high cost, several hours of preparation and evaluation time, need for qualified personnel, and well-equipped laboratories.

Here, we present a rapid, easy-to-handle, and cost-efficient diagnostic assay for detection of pathogen-specific nucleic acids based on Magnetic Particle Spectroscopy (MPS). In MPS, magnetic nanoparticles (MNPs) are exposed to alternating magnetic fields. Upon binding to biological targets, the relaxation process of the MNPs changes, which is reflected in the higher harmonics of the MPS spectrum. In this study, MNPs and polystyrene beads were functionalized with single-stranded (ss)DNA. By the addition of a specific target ssDNA sequence, the particles and beads are crosslinked, resulting in increased particle hydrodynamic size and retarded Brownian relaxation mechanism, causing a decrease of odd higher harmonics in the MPS spectrum (Fig. 1A). To exclude the effect of particle concentration,  $3^{rd}/1^{st}$  harmonics ratio is calculated (Fig. 1B). Our preliminary study shows that ssDNA can be detected in a concentration-dependent manner, providing the means to quantify the results, with a limit of detection of 280 pM (Fig. 1C). We show that not only synthetic DNA with an arbitrary sequence, but also RNA can be detected. In addition, SARS-CoV-2-specific DNA, as well as saliva as a sample medium can be used for an accurate assay.

Our proof-of-principle experiments demonstrate the potential of MPS-based assays for a reliable and fast diagnostic of pathogens like SARS-CoV-2 in a point-of-need fashion without the need of complex sample preparation.

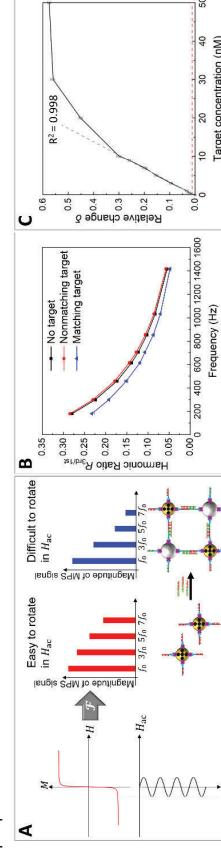


Figure 1 A) Measurement and assay principle of MPS. B) Exemplary result of the harmonic ratio. C) Target concentration dependence of the relative change  $\delta$  (difference between the measured harmonic ratio with target present and the blank probe).

Acknowledgement:  
This work was supported by the Deutsche Forschungsgemeinschaft (DFG, German Research Foundation) under Germany's Excellence Strategy – EXC-2123 QuantumFrontiers – 390837967, the DFG Research Training Group 1952 Metrolgy for Complex NanoSystems ZH 78/2-1 and "Niedersächsisches Vorab" through "Quantum- and Nano-Metrolgy (QUANOMET)" initiative within the projects NI-1 (Bl) and NI-2 (TV).

## Development of Inductively Detectable Probes for Proteolytic Activity

Michael G. Christiansen<sup>1</sup>, Ines Oberhuber<sup>1</sup>, Matej Vizovísek<sup>1</sup>, Dragana Dubey<sup>1</sup>, Lucien Stöcklin<sup>2</sup>, Manuel Strahm<sup>3</sup>, Simonne Schuerle<sup>1\*</sup>

<sup>1</sup> Dept. of Health Sciences and Technology, ETH Zurich, 8092, Switzerland

<sup>2</sup> Dept. of Biosystems Science and Engineering, ETH Zurich, 8092, Switzerland

<sup>3</sup> Dept. of Information Technology and Electrical Engineering, ETH Zurich, 8092, Switzerland  
simone.schuerle@ethz.ch

Inductive detection of magnetic nanoparticles (MNPs) via time-changing magnetization in response to applied fields is the basis of technologies including magnetic particle imaging and magnetic particle spectroscopy. Because inductive readouts may be advantageous for the development of low cost, point-of-care devices, they have also been considered for diagnostic sensing of biomolecules. Most often, this has involved the selective binding of an analyte to the surface of the MNPs, resulting in a subtle shift in frequency-dependent susceptibility. Additionally, modulation of aggregation behavior by chemical linkers and sensing saturation characteristics with high amplitude alternating magnetic fields has been shown to produce robust changes in inductive signal. Nevertheless, these approaches have not yet become competitive methodologies for commonplace analyte detection. Alternative methods, including sensing paradigms that lower the cost and required power of associated electronics, should be explored.

Here, we develop and evaluate an inductive sensing concept for detecting proteolytic cleavage. In addition to acting as a highly informative class of biomarkers with early and underlying roles in disease, proteases are inherently catalytically amplified and offer a combinatorial space of peptide substrates that can be tailored for selective response. In our scheme (Fig. a), MNPs are covalently bound to larger nonmagnetic scaffold nanoparticles via cleavable peptide linkers. With transmission electron microscopy, we show that these structures are indeed formed (Fig. b) and that they undergo disassembly in response to nonspecific proteolytic cleavage by a blend of Proteinase K and Chymotrypsin (Fig. c-d). To detect whether MNPs are in a bound or free state, we developed a prototype pulsed field magnetometer with adjustable pulse width and magnitude (Fig. e). The design directly incorporates the drive coil, sense coil, and compensation coil into a printed circuit board (Fig. f). A proof-of-concept test with samples containing MNPs in a solid or liquid matrix to mimic the free and bound states show that during the rising and falling edges of the pulse, the MNPs produce signals that depend on whether they are bound or freely suspended in solution (Fig. g). Parameters such as the magnitude of the pulse can be selected to maximize the change in voltage signal distinguishing the free and bound states (Fig. h).

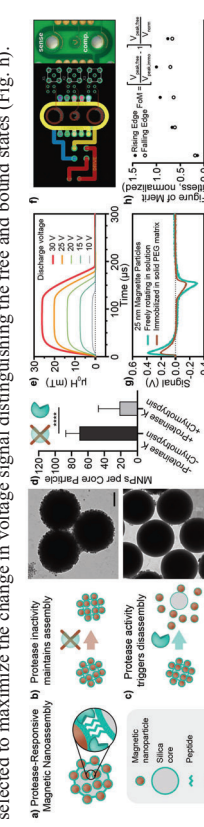


**Figure 1.** (a) The concept for inductively detectable protease responsive magnetic nanoassemblies (PRIMAs) is shown. Under conditions of enzymatic cleavage, MNPs dissociate from a central nonmagnetic scaffold particle. (b) Representative TEM of PRIMAs incubated overnight without proteases. (c) Representative TEM of PRIMAs incubated overnight with 1.8  $\mu$ M active Proteinase K and 1.8  $\mu$ M Chymotrypsin. Scale bar: 200 nm (d) The number of MNPs visible on the perimeter of  $n=25$  randomly selected PRIMAs was found with and without exposure to cleavage conditions. Error bars show standard deviation and \*\*\* indicates  $p<0.0001$  in an unpaired t-test. (e) Pulses resulting from a 100  $\mu$ s trigger and various discharge capacitor charging voltages are shown. (f) The schematic of a printed circuit board incorporating the pulse, sense, and compensation coils is shown. (g) The inductive signals from a 100  $\mu$ L solid and liquid sample of Ocean Nanotech 25 nm MNPs at 500  $\mu$ g/mL is shown for a 15 V, 100  $\mu$ s pulse. (h) A figure of merit defined to maximize the change in signal observed between bound and free states is evaluated over a range of pulse amplitudes.

## Handheld Magnetic Particle Spectroscopy (MPS) for Rapid, One-step, Wash-free Detection of SARS-CoV-2 Spike and Nucleocapsid Proteins in Liquid Phase

Kai Wu<sup>1</sup>, Vinit Kumar Chugh<sup>1</sup>, Venkataranana D. Krishna<sup>2</sup>, Timothy Dean Gordon<sup>3</sup>, Pat Keady<sup>3</sup>, Maxim C.-J. Cheeran<sup>2</sup>, Jian-Ping Wang<sup>1,\*</sup>

<sup>1</sup> Department of Electrical and Computer Engineering, University of Minnesota, Minneapolis, MN 55455, United States

<sup>2</sup> Department of Veterinary Population Medicine, University of Minnesota, St. Paul, MN 55108, United States

<sup>3</sup> Aerosol Devices Inc., Fort Collins, CO 80524, United States

\*Presenter and corresponding author. E-mail: jpwang@umn.edu (J.-P. W.)

With the ongoing global pandemic of coronavirus disease 2019 (COVID-19), there is an increasing quest for more accessible, easy-to-use, rapid, inexpensive, and high accuracy diagnostic tools. Traditional disease diagnostic methods such as qRT-PCR (quantitative reverse transcription-PCR) and ELISA (enzyme-linked immunosorbent assay) require multiple steps, trained technicians, and long turnaround time that may worsen the disease surveillance and pandemic control. In sight of this situation, a rapid, one-step, easy-to-use, and high accuracy diagnostic platform will be valuable for future epidemic control especially for regions with scarce medical resources. Herein, we report a magnetic particle spectroscopy (MPS, see Fig. 1) platform for detection of SARS-CoV-2 biomarkers: spike and nucleocapsid proteins. This technique monitors the dynamic magnetic responses of magnetic nanoparticles (MNPs) and uses their higher harmonics as a measure of the nanoparticles' binding states. By anchoring polyclonal antibodies (pAbs) onto MNP surfaces, these nanoparticles function as nanoprobes to specifically bind to target analytes and form nanoparticle clusters. This binding event causes detectable changes in higher harmonics and allows for quantitative and qualitative detection of target analytes in liquid phase. We have achieved detection limits of 1.56 nM (equivalent to 125 fmole) and 3.13 nM (equivalent to 250 fmole) for detecting SARS-CoV-2 spike and nucleocapsid proteins, respectively. This MPS platform combined with one-step, wash-free, nanoparticle clustering-based assay method is intrinsically versatile and allows for the detection of a variety of other disease biomarkers by simply changing the surface functional groups on MNPs.

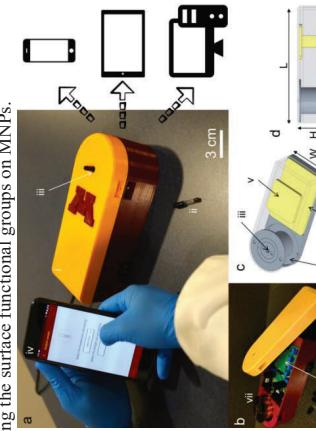


**Fig. 1.** (a) Photograph of the MPS portable device with a smartphone application. The overall dimensions of device are 212 mm (L)  $\times$  84 mm (W)  $\times$  72 mm (H). (b) Photograph of the internal structures of the MPS device. (c) and (d) are the 3D models of the device.

Reference: ACS Applied Materials & Interfaces 13 (37), 44136-44146

## Development of Magnetic Particle Spectroscopy That Integrates Both Conventional and Mixing Methods for Virus Detection

**Seungjum Oh<sup>1</sup>, Minh Phu Bu<sup>1</sup>, Tuan-Anh Le<sup>1</sup>, Ali Dimari<sup>1</sup>, and Jungwon Yoon<sup>\*</sup>**

<sup>1</sup> School of Integrated Technology, Gwangju Institute of Science and Technology, Gwangju 61005, Republic of Korea.

\*Email : [jyoon@gist.ac.kr](mailto:jyoon@gist.ac.kr), Mobile : +82-10-2402-6904

Infectious diseases spread by viruses can be quite lethal. Viruses usually have a high rate of spread, which has been made obvious by the Covid-19 pandemic. Early detection of disease causing viruses using sensitive, rapid and accurate methods is very important for efficient reaction. In this regard, various technologies for detecting viruses are being researched, but there are still many aspects of this work that need to be improved, such as the long time requirement, high cost and poor accuracy. Compared to other techniques for virus detection, Magnetic Particle Spectroscopy (MPS) is a novel magnetic detection technique that has many advantages, such as portability, high-sensitivity, ease of use, low-cost, non-invasiveness and avoidance of radiation exposure. Through the use of superparamagnetic iron oxide nanoparticles (SPIONs) and a sinusoidal magnetic field at high frequency, harmonic components can be obtained, which can be used to indicate the bound states of the SPIONs. Coupling the virus receptors at the surface of the SPIONs by using conjugation methods can make magnetic nanoparticles (MNPs) for virus detection. In this case, the functionalized SPIONS can form clusters with the virus and lead to changes in the hydrodynamic volume of the SPIONs. This technology can be used for virus detection as it causes a phase delay to be detected in the MPS. There are two kinds of MPS; the conventional MPS that uses one sinusoidal magnetic field to excite the SPIONs and the mixing method that uses two sinusoidal magnetic fields with distinct frequencies. Each type of MPS has different strengths and weaknesses. In this paper, we present a MPS that can handle both conventional and mixing methods for virus detection, and provide guidelines for choosing the appropriate method. Our integrated MPS system and its connection diagram are shown in Figure 1. The excitation coil used in the proposed system has 2 layers of 18 turns each and the drive coil has 4 layers of 18 turns each. The excitation and drive coils can generate magnetic fields of 20mT and 9.6mT, respectively. In future works, the developed model will be tested and verified through experiment.

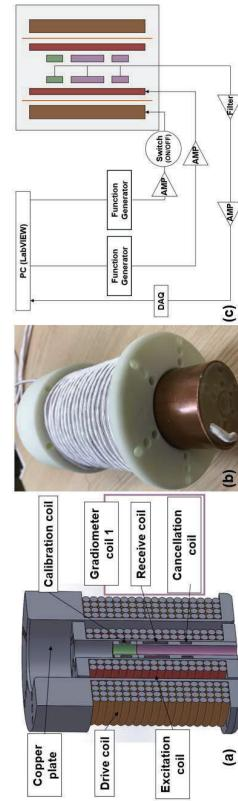


Figure 1. (a) Cross-section view and (b) photograph of the integrated MPS system. A copper plate is sandwiched between the excitation and drive coils to remove external noise. (c) Connection diagram of the integrated MPS system. We can control the driving mode through a switch and a software running in LabVIEW® controls the system operation.

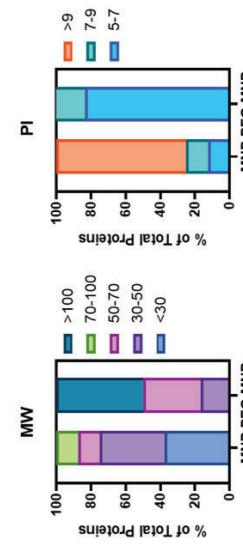
## PEGylated Magnetic Nanoparticle-Induced Acute Hypersensitivity Reaction:

### Role of Bioactive Corona

Yunn-Hwa Ma

Department of Physiology and Pharmacology, College of Medicine, Chang Gung University,  
Taoyuan, Taiwan, Republic of China  
Email: [yhma@mail.cgu.edu.tw](mailto:yhma@mail.cgu.edu.tw)

Polyethylene glycol (PEG) is a common surface modulator that increases the half-life of nano-drugs in circulation; however, intravenous administration of PEGylated pharmaceuticals often induces acute hypersensitivity reactions (HSR) with symptoms including systemic hypotension, followed by tachyphylaxis with unknown mechanism. We hypothesize that the formation of protein corona with a composition specific to PEGylated nanoparticles induces transient microvascular occlusion that entrains hemodynamic effects. In anesthetized rats, administration of PEGylated magnetic nanoparticles (PEG-MNPs), but not the pristine MNPs, induced a transient decrease in arterial pressure and cardiac output, which was associated with a reduction in blood flow of the kidney and cremaster muscle, as demonstrated by ultrasound flowmetry and laser speckle contrast imaging, respectively, which were subjected to tachyphylaxis in response to the 2nd dose. Calculated renal vascular resistance was significantly increased with a reduction in cross-sectional area of the renal vasculature, suggesting PEG-MNPs-induced hypotension is unlikely due to dilation of resistant vessels. Nevertheless, histological analysis reveals no iron retention in the kidney. Proteomic analysis of the hard corona demonstrated much more complement proteins on PEG-MNPs vs. MNPs, suggesting a more vigorous complement activation occurred on the surface of PEG-MNPs in circulation. After i.v. administration of PEG-MNPs, the remaining plasma proteins with high affinity to PEG-MNPs were greatly reduced, suggesting consumption of the corona proteins with repeated exposure. In conclusion, bioactive corona of nano-drugs may directly or indirectly participate in the hemodynamic responses associated with HSRs; such information may be amendable to prediction and/or prevention of the adverse effects of, especially PEGylated nanomedicines.



Talk #48

Talk #47

## Biocompatibility studies and cellular interactions of biogenic magnetic nanoparticles

Frank Mickoleit<sup>1</sup>, Cornelia Jörke<sup>2</sup>, Stefan Geimer<sup>3</sup>, Jörg P. Müller<sup>4</sup>, Dirk Schüller<sup>1</sup>, Joachim H. Clement<sup>2</sup>

<sup>1</sup> Dept. Microbiology, University of Bayreuth, D-95447 Bayreuth, Germany

<sup>2</sup> Dept. Hematology and Oncology, Jena University Hospital, D-07747 Jena, Germany

<sup>3</sup> Dept. Cell Biology and Electron Microscopy, University of Bayreuth, D-95447 Bayreuth, Germany

<sup>4</sup> Institute of Molecular Cell Biology, Center for Molecular Biomedicine (CMB),

Jena University Hospital, D-07745 Jena, Germany

E-mail: frank.mickoleit@uni-bayreuth.de

Biogenic nanoparticles are an intriguing example for a biomaterialization process. Magnetotactic bacteria like the model organism *Magnetospirillum gryphiswaldense* are capable of synthesizing so-called magnetosomes, single-domain nanocrystals of chemically highly pure magnetite that are enveloped by a biological membrane. Magnetosome biosynthesis is genetically highly controlled, thereby generating nanoparticles with extraordinary properties (such as high crystallinity, strong magnetization and uniform shape and size). Moreover, the magnetosome membrane is accessible to genetic engineering, which enables the selective and controlled functionalization of the particle surface with reactive moieties.<sup>[1]</sup> Due to these unique characteristics, bacterial magnetosomes have the potential to yield promising agents for (bio)medical applications in diagnosis as well as magnetic imaging techniques or as drug carriers.<sup>[2]</sup> In order to comprehensively evaluate the biocompatibility of isolated magnetosomes when administered to mammalian cell lines (cancer cells and primary cells), different cytotoxicity assays were performed. For the magnetosome-treated cell lines FaDu, BeWo, HCC78, and hPC-PL, concentration-dependent effects on cell viability were observed, however, even increased particle concentrations of up to  $400 \mu\text{g mL}^{-1}$  were considered to be biocompatible. Using different microscopy techniques, we could demonstrate that the particles are internalized and accumulate in endlysosomal vesicles in the vicinity of the nucleus. Remarkably, even upon short-term incubation magnetosomes – cell interactions were strong enough to allow for magnetic cell sorting, with  $\sim 60\%$  of the treated FaDu cells being magnetically separated.<sup>[3]</sup>

In order to enhance these interactions and to address distinct cancer cell types, genetic engineering techniques will be used for the display of specific anticancer peptides on the magnetosome surface. Thereby we will generate a set of multifunctional magnetic nanoparticles that provide a flexible “tool” with potential in e.g. the targeting of circulating tumour cells.

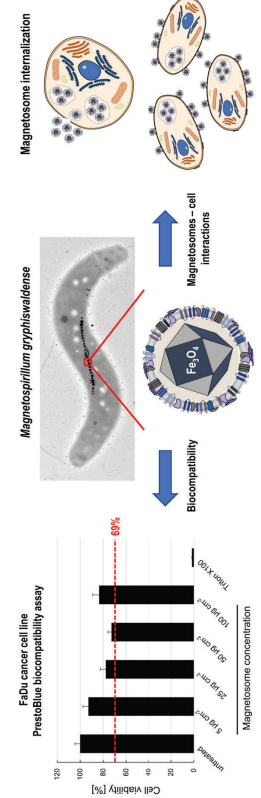


Figure 1: Principle of SPION-APTES-Pep enhanced diagnostic time and potential treatment.  
Acknowledgement: This work is supported by the Dr. Robert-Pfleger-Stiftung, Bamberg.

- [1] Uebel R., Schüller D. *Nat. Rev. Microbiol.* 2016, *14*, 621
- [2] Vargas G., et al. *Molecules* 2018, *23*, 2438
- [3] Mickoleit F., et al. *Nanoscale Adv.* 2021, *3*, 3799

## Biomimetic capturing of pathogens using SPIONs functionalized with salivary agglutinin (GP-340)-derived peptides

Bernhard Friedrich<sup>1</sup>, Christina Janko<sup>1</sup>, Harald Untenwege<sup>1</sup>, Regine Brox<sup>2</sup>, Silvio Dutz<sup>2</sup>, Floris J. Bilkner<sup>1</sup>, Lars Fester<sup>5</sup>, Holger Hackstein<sup>2</sup>, Richard Strauß<sup>6</sup>, Aldo R. Boccaccini<sup>7</sup>, Christian Bogdan<sup>8</sup>, Christoph Alexiou<sup>1</sup>, Stefan Lyer<sup>1</sup>, Rainer Tieze<sup>1\*</sup>

<sup>1</sup> Department of Otorhinolaryngology, Head and Neck Surgery, Section of Experimental Oncology and Nanomedicine (SEON), Else Kirdorf-Fresenius-Stiftung-Professorship, Universitätsklinikum Erlangen, Germany. <sup>2</sup> Department of Transfusion Medicine and Hemostaseology, Universitätsklinikum Erlangen, Germany. <sup>3</sup> Institute of Biomaterials, Ilmenau University of Technology, Germany. <sup>4</sup> Department of Oral Biochemistry, Academic Centre for Dentistry Amsterdam (ACTA), University of Technology, Germany. <sup>5</sup> The Netherlands. <sup>6</sup> Institute of Anatomy and Cell Biology, Friedrich-Alexander-Universität Erlangen-Nürnberg, Germany. <sup>7</sup> Department of Medicine 1, Universitätsklinikum Erlangen, Germany. <sup>8</sup> Institute of Biomaterials, Department of Materials Science and Engineering, Friedrich-Alexander-Universität (FAU) Erlangen-Nürnberg, Germany. <sup>\*</sup>Microbiologisches Institut – Klinische Mikrobiologie, Immunologie und Hygiene, Universitätsklinikum Erlangen, Friedrich-Alexander-Universität (FAU) Erlangen-Nürnberg, Germany.  
E-mail: rainer.tieze@uk-erlangen.de

Sepsis and other blood stream infections still pose a significant treat in modern clinical practice. The treatment consists of broad-spectrum antibiotics and simultaneous fluid therapy, vasoactive drugs, respiratory and metabolic support. Improving the time to diagnosis sepsis remains the most important task and is essential for the treatment. A new approach using a biomimetic interface for the separation of bacterial pathogens from for example blood lies in the use of peptides from the broad-spectrum binding motif of human GP-340, a pattern recognition molecule for mucosal protection. Peptides derived from this protein were therefore bound to SPIONs. The obtained SPION-APTES-Pep are highly efficient in separating various pathogens, especially at low and thus clinically relevant concentrations. It was shown that captured bacteria can be recultured without the need of conventional blood culture methods before plating them out. A drastic reduction of diagnostic times by using SPION-APTES-Pep for quality control of blood and blood products as well as for patients with suspected bloodstream infections to accelerate targeted antibiotic therapy can be achieved as seen in Figure 1.

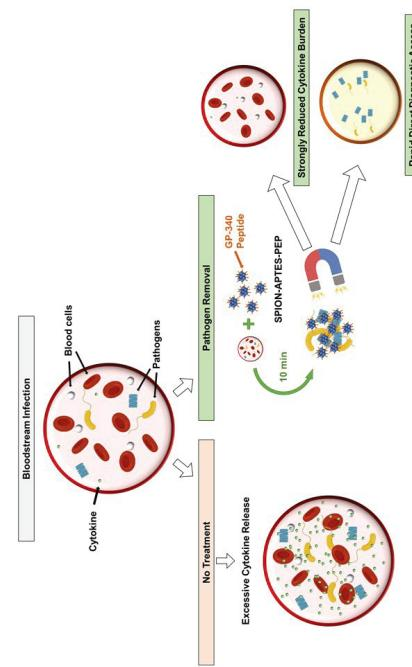


Figure 1: Principle of SPION-APTES-Pep enhanced diagnostic time and potential treatment.  
Acknowledgement: This work is supported by the Dr. Robert-Pfleger-Stiftung, Bamberg.

## NP-cellular hitchhiking system for targeted combination therapy and diagnosis of glioblastoma

Xanthippi Koutsoumpou<sup>1</sup>, Steven De Vleeschouwer<sup>2</sup>, Jeff Rozenzki<sup>4</sup>, Teresa Pellegrino<sup>5</sup>, Stefaan J. Soenens<sup>1</sup>, Bella B. Manshian<sup>1,3</sup>

Email: bella.manshian@kuleuven.be

1. NanoHealth and Optical Imaging Group, Department of Imaging and Pathology, KU Leuven, Leuven, Belgium.  
 2. Department of Neurosurgery, University Hospitals Leuven, Leuven, Belgium.  
 3. Translational Cell and Tissue Research Unit, Department of Imaging and Pathology, KU Leuven, Leuven, Belgium.  
 4. Rega Institute for Medical Research, Department of Pharmaceutical and Pharmacological Sciences, KU Leuven, B3000 Leuven, Belgium.  
 5. Nanomaterials for Biomedical Applications, Istituto Italiano di Tecnologia, Via Morego 30, 16163 Genova, Italy.

Zeta potential, TEM, HPLC and ICP-MS. The NPs were screened for toxic effects in relevant human and mouse cell lines, namely, monocytes, endothelial cells and glioma cells, using high content screening and image based flow cytometry systems. The optimal ratio of NP-cell conjugation was determined. Next, SPIO nanocubes, approximately 20 nm in size were loaded into the PLGA NPs. MRI measurements of SPIO loaded PLGA NPs or U87 cells incubated with SPIO-loaded NPs revealed the increase of  $r_2$  relaxation rates with increasing Fe concentrations. *In vivo* chemotaxis was investigated using optical imaging with the IVIS Spectrum and via intravital microscopy in subcutaneous and orthotopic glioma tumors following intravenous injection of NP conjugated monocytes. Tissue slices from tumors and major organs were investigated for targeting and therapeutics using H&E staining and immunohistochemistry. In general, formulation showed homing ability towards GBM tumors, *in vivo*, promising a potential for targeted GBM treatment.

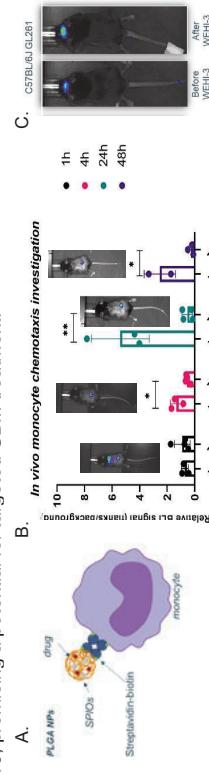


Figure 1. A) A representative sketch of the proposed NP-cell formulation. B) *In vivo* homing of NPCHS in subcutaneous glioma tumors. C) *In vivo* homing of NPCHS in orthotopic glioma tumors.

## Intracellular degradation of biosynthesized magnetic nanoparticles

Lucía Gandarias<sup>1\*</sup>, Alicia Gascón Guibeda<sup>1</sup>, Ana Abad<sup>1</sup>, Mª Luisa Fernández-Gubieda<sup>2</sup>, Alicia Muñoz<sup>1</sup>, and Ana García-Prieto<sup>3</sup>  
<sup>1</sup> Depto. Inmunología, Microbiología y Parasitología, Universidad del País Vasco (UPV/EHU), 48940 Leioa, Spain,  
<sup>2</sup> Dept. Electricidad y Electrónica, Universidad del País Vasco (UPV/EHU), 48940 Leioa, Spain,  
<sup>3</sup> Depto. Física Aplicada, Universidad del País Vasco (UPV/EHU), 48013 Bilbao, Spain  
 \*Email: lucia.gandarias@ehu.eus

Most proposed biomedical applications for magnetic nanoparticles need them to be internalized by cells (Figure 1A,B). Therefore, it is essential we understand the intracellular process that nanoparticles undergo long-term in order to establish their effective time after internalization and to determine if the released products cause cytotoxicity.

In our group we work with magnetosomes, magnetic nanoparticles synthesized by magnetotactic bacteria. In particular we work with *Magnetospirillum gryphiswaldense* (MSR-I) that synthesizes magnetic ( $\text{Fe}_3\text{O}_4$ ) nanocrystals of 40 nm arranged in one chain that they use to orientate along the Earth's magnetic field. Magnetosomes have shown several advantages when compared to chemically synthesized magnetic nanoparticles and are good candidates for magnetic hyperthermia<sup>1-3</sup>.

In this work we present the long-term fate of magnetosomes in two cellular models: A549 lung carcinoma cells and RAW 264.7 macrophages. By means of SQUID magnetometry we observed that in both cell types the saturation magnetic moment decreased with time implying that magnetosomes were being expelled from or degraded by the cells (Figure 1A,C). Moreover, X-ray absorption near edge spectroscopy (XANES, at CLAESS (ALBA) and BM23 (ESRF) synchrotron beamlines) on the Fe K-edge allowed us to identify the iron phases that were being formed in the magnetosome degradation process. In Figure 1 (C, D) the results of linear combination fitting of the XANES spectra are displayed. In both cell types, there is a first oxidation of magnetosomes to maghemite and a later appearance of ferrhydrite, the iron mineral phase stored in the cores of ferritin, the protein involved in the storage of Fe. In the present case we have used Horse Spleen Ferritin (HsF) as the ferrhydrite reference. Both cell types were able to degrade around 50 % of the magnetite, in 9 days the RAW 264.7 and 21 days the A549.

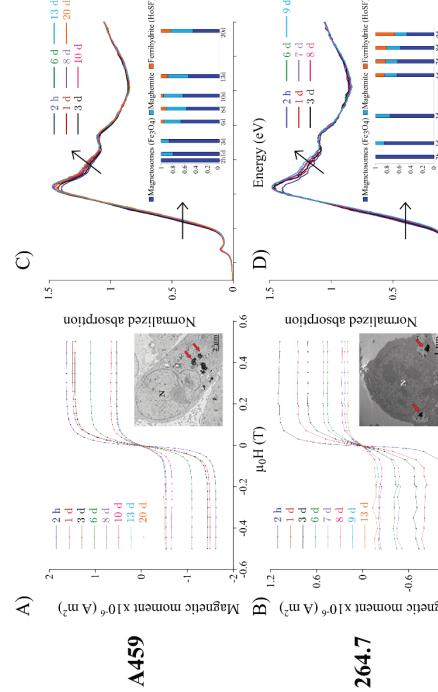


Figure 1. A, B) Hysteresis loops of A549 cells and RAW 264.7 macrophages along time after the magnetosome internalization (Inset: TEM images of a cell with magnetosomes stored in endosome-like vesicles); C, D) XANES spectra measured at the Fe K-edge of cells measured at different time points (Inset: linear combination fitting results showing the percentages of iron species at each time point).

## References

1. Muñoz, A. et al. *J. Phys. Chem. C* **120**, 24437–24448 (2016).
2. Gandia, D., Gandarias, L., et al. *Small* **15**, 1902626 (2019).
3. Jefremovas, E. M. et al. *IEEE Access* **9**, 99552–99561 (2021).

## Use of peptide functionalized Dynabeads for the magnetic carrier separation of Rare Earth phosphors in low and high magnetic field gradients

Peter Boelens<sup>1</sup>, Caroline Bobeth<sup>1</sup>, Zhe Lei<sup>2</sup> and Franziska Lederer<sup>1</sup>

<sup>1</sup>Helmholtz-Zentrum Dresden-Rossendorf, Helmholtz Institute Freiberg for Resource Technology, Freiberg, Germany

<sup>2</sup>Helmholtz-Zentrum Dresden-Rossendorf, Institute of Fluid Dynamics, Dresden, Germany

### ABSTRACT

Superparamagnetic composite beads are widely used as magnetic carriers in biotechnological processes, including the purification of biomolecules, organelles and cells [1,2]. Their wide range of applications include diagnostic, as well as industrial purposes. Furthermore, the immobilization of surface-binding peptides can render highly specific surface properties to composite beads and facilitate their selective interaction with target particles. In this context, peptide functionalized composite beads have been shown to be promising tools for environmental applications, including biomining and wastewater treatment [3-5]. Nevertheless, to the best of our knowledge, their use has so far only been investigated in low magnetic field gradients, on a milliliter scale.

The waste of fluorescent lamps contains several valuable Rare Earth phosphors in the form of fine particles that are hard to separate and therefore lack efficient recycling schemes [6]. Our junior research group, Biokolllekt, has previously identified selectively surface-binding peptides that interact with the Rare Earth phosphor LaPO<sub>4</sub>:Ce, Tb [7]. Recently, we have chemically immobilized the identified peptides and have tested their interaction with several target phosphors [8], we have thoroughly characterized a range of Rare Earth phosphors and we have shown their compatibility with an upscaleable High-Gradient Magnetic Separator [9], which was specifically designed for biotechnological separations with superparamagnetic carriers [10].

In this work, we investigate the use of Dynabeads® M-270, functionalized with previously identified peptides, for the separation of Rare Earth phosphors. First, we characterize the physical properties of functionalized and unfunctionalized beads. Subsequently, we examine the ‘beads’ selectivities towards various Rare Earth phosphors in an LGMS setup. Finally, we compare the carrier behaviour of the beads in low and high magnetic field gradients by the use of an optical microscopic setup. A special focus is placed on the magnetically induced chain formation by sets of beads. Finally, this work can shine a light on the future perspectives of peptide functionalized superparamagnetic composite beads for a selective and upscalable separation process of fine particles.

### REFERENCES

1. Leong, S.; Yeap, S.P.; Lim, J.K. Working principle and application of magnetic separation for biomedical diagnostic at high- and low-field gradients. *Interface Focus*. 2016; 6: doi:10.1088/rsfs.2016.0048.
2. Bergensmeier, S. Magnetic Particles for the Separation and Purification of Nucleic Acids. *Appl. Microbiol. Biotechnol.* 2007; 73: 495-504, doi:10.1007/s00253-006-0675-0.
3. Cetinel, S.; Shen, W.-Z.; Aminpour, M.; Bhowmik, P.; Wang, F.; Boruyeni, E.; Sharma, K.; Nayebi, N.; Montemagno, C. Biomining of MoS<sub>2</sub> with Peptide-based Smart Biomaterials. *Scientific Reports*. 2018; 8: doi:10.1038/s41598-018-21692-4.
4. Vreuls, C.; Genin, A.; Zorchi, G.; Boschini, F.; Cloots, R.; Gilbert, B.; Martel, J.; Weerdt, C. Generally engineered polymeric tools for inorganic nano-particles separation in water based media. *J. Mater. Chem.* 2011; 21: 13841-13846, doi:10.1039/CJFM12440D.
5. Pollmann, K.; Kutschke, S.; Matys, S.; Raft, J.; Hlawacek, C.; Lederer, F.; Schröder, C. Bio-recycling of metals: recycling of technical products using biological applications. *Biotechnol. Adv.* 2018; 36: doi:10.1016/j.biotechadv.2018.03.006.
6. Binnemann, K.; Jones, P. Perspectives for the recovery of rare earths from end-of-life fluorescent lamps. *Journal of Rare Earths* 2014; 32, 195-200, doi:10.1016/S1002-0721(14)60051-X.
7. Lederer, F.; Curtis, S.; Bachmann, S.; Dunbar, S.; MacGillivray, R. Identification of lanthanum-specific peptides for future recycling of rare earth elements from compact fluorescent lamps: Peptides for Rare Earth Recycling. *Biotechnol. Bieng.* 2016; 114, doi:10.1002/bit.26240.
8. Schrader, M.; Bobeth, C.; Lederer, F. Quantification of Peptide-Bound Particles: A Phage Mimicking Approach via Site-Selective Immobilization on Glass. *ACS Omega*. 2021; XXXX, doi:10.1021/acsomega.0c04343.
9. Boelens, P.; Lei, Z.; Drobott, B.; Rudolph, M.; Li, Z.; Franzreb, M.; Eckerl, K.; Lederer, F. High Gradient Magnet Separator. *Minerals* 2021; 11, doi:10.3390/min1101116.
10. Hoffmann, C.; Franzreb, M.; Hall, W.H. A novel high-gradient magnetic separator (HGMS) design for biotech applications. *IEEE Transactions on Applied Superconductivity* 2002; 12, 963-965, doi:10.1109/TASC.2002.1018560.

### 3D Printing of Polymer-Bonded Magnets

A. Makridis<sup>a</sup>, D. Trygontakis<sup>a</sup>, N. Okkalidis<sup>b</sup>, M. Angelakakis<sup>a</sup>  
<sup>a</sup>Magnetic Nanostructure Characterization: Technology and Applications (*MagnaCharita*) Center  
for interdisciplinary Research and Innovation (CIRI-AUTh) 57001 Thessaloniki, Greece  
<sup>b</sup>Morphé, Praxitelous 1, Thessaloniki, 54641, Greece

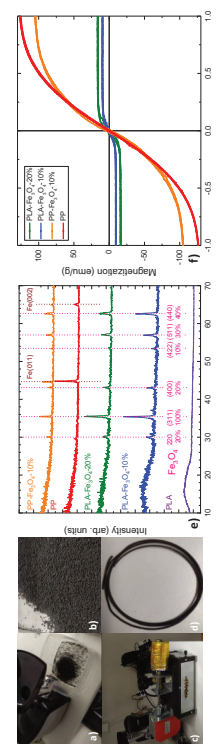


Figure 1. Main process for the filament extraction: a) After cutting PLA filament to pieces, a grinder is used to make PLA granules. The b) mixed material is used for feed stock of c) the single screw extruder to produce the resulted magnetic filament. e) X-ray diffraction patterns of fabricated magnetic filaments: PLA and PP (Proto-Pasta) filaments are also shown as reference. f) 300 K hysteresis measurements of the fabricated magnetic filaments. PP hysteresis loops is also given as reference.

Acknowledgments: This work was supported by European Union's Horizon 2020 research and innovation programme under grant agreement No 857502 (MaNaCa)

## Magnetic bucket brigade networks as rails for single cell transportation

Findan Block<sup>1\*</sup>, Finn Klingbeil<sup>1</sup>, Umer Sajjad<sup>1</sup>, Christine Arndt<sup>2</sup>, Sandra Sintd<sup>2</sup>, Dennis Seidler<sup>1</sup>, Christine Selhuber-Unkel<sup>2</sup>, and Jeffrey McCord<sup>1</sup>

<sup>1</sup> Nanoscale Magnetic Materials and Magnetic Domains, Institute for Materials Science, Kiel University, Kaiserstraße 2, 24143 Kiel, Germany

<sup>2</sup> Institute for Molecular Systems Engineering (IMSE), Heidelberg University, Im Neuenheimer Feld 253, 69120 Heidelberg, Germany

\*Email: fib@tf.uni-kiel.de Mobile: +49-17687925360

A key feature for all kind of transport mechanisms is a comprehensive and flexible infrastructure. The invention of railway switches was crucial to transform single railroad lines to a transportation network. Bucket brigades represent an efficient concept for the handling of water buckets or goods, or also for analogue delay lines e.g. in CCD cameras. Transferring these concepts to a microscopic structure level allows a flexible and efficient transfer of single microparticles and biological cells to different destinations located on a microchip.

Single cell control is an important feature in modern biomedicine as for example in fields as immunology, gene sequencing, cell force analysis, or tissue engineering. The combination of magnetic labelling and lithographically structured thin films out of hard-magnetic or soft-magnetic materials enables particle guidance along predefined tracks or flexible motion within element arrays. Changing external field sequences with in- and out-of-plane components, generate a great variety of possible movement patterns.

Here, a versatile flow less transport scheme of microbeads and cells by a network of lined up magnetic elements is presented, where magnetic motion is enabled through different radii of curvatures of the magnetic elements. Simple oval structures form the basic transport elements, exhibiting a rectifying motion scheme along only one direction leading to a linear bucket brigade like transportation scheme. Changing only the rotation sense of an external magnetic field, the single elements are transformed from transport routes to breakpoints, and the switchable motion across bifurcations and unification lines is achieved. The flexible magnetic transport route networks are used to program the movement of microspheres and rat embryonic fibroblasts over long distances. The platform constitutes an easy integrable multifunctional system featuring a backflow free transport scheme with great capabilities for future lab-on-a-chip technologies.

MB + Cell

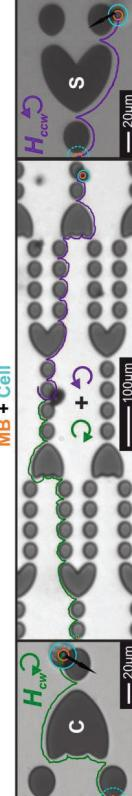


Figure. Transport of fibroblast cells carried by magnetic beads (MB) along arrays of ferromagnetic elements.  
(a) Cell trajectories around collecting (C) and (b) switching (S) elements for a clockwise or a counter-clockwise rotating magnetic fields are shown. (b) Transport of a fibroblast cell along a network of multiple elements using a combination of magnetic field rotation directions is performed.  
J.M. and F.B. acknowledge funding through the Deutsche Forschungsgemeinschaft grants DEG MC 9/13-2.

- [1] F. Block, F. Klingbeil, S. Deshpande, U. Sajjad, D. Seidler, C. Arndt, S. Sintd, C. Selhuber-Unkel and J. McCord, *Appl. Phys. Lett.* **118**, (2021).

## Passage of magnetic nanoparticles through a differentiating blood-placenta barrier

Alexander Trinks<sup>1</sup>, Patricia Radon<sup>2</sup>, Lena Belfi<sup>1</sup>, Malika Suttor<sup>1</sup>, Diana Zahn<sup>3</sup>, Frank Wickhorst<sup>2</sup>, Silvio Dutz<sup>3</sup>, Andreas Hochhaus<sup>1</sup>, Joachim H. Clement<sup>1</sup>

<sup>1</sup> Dept. Hematology and Medical Oncology, Jena University Hospital, D-07747 Jena, Germany

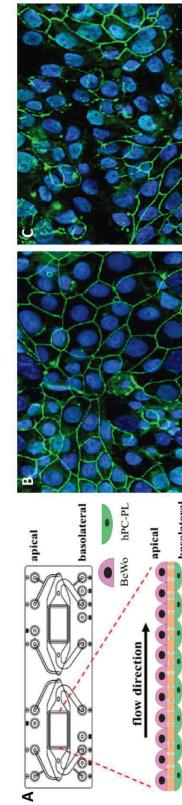
<sup>2</sup> Physikalisch-Technische Bundesanstalt (PTB), D-10587 Berlin, Germany

<sup>3</sup> Institut für Biomedizinische Technik und Informatik (BMTI), Technische Universität Ilmenau, D-98693 Ilmenau, Germany

E-mail: joachim.clement@med.uni-jena.de

The application of nanomaterials in a medical context is rapidly progressing within the past years. However, there is still the necessity to understand the interaction between nanomaterials and the human body in more detail, especially at cellular barriers. Since clinical trials on pregnant women are difficult to perform, physiologically appropriate models of the human placenta to study nanoparticle-placenta interactions *in vitro* are needed. The placenta delivers nutrients from the maternal blood to the fetus and clears metabolites in reverse direction. This organ is furthermore responsible for the protection of the fetus from harmful substances. Various cell types form the blood-placenta barrier (BPB), e.g. cytotrophoblasts, endothelial cells, placental macrophages (Hofbauer cells), and pericytes. During pregnancy, the placenta is highly dynamic in its morphology and composition, e.g. the cytotrophoblasts fuse and form the syncytiotrophoblast. The aim of our investigations is to gain a better understanding of the interactions of nanomaterials, especially magnetic nanoparticles (MNP), with the blood-placenta barrier. Recently, we studied the interaction of different magnetic nanoparticles under fluidic conditions in a microfluidic biochip with special focus on extended incubation times and passaging abilities of the MNPs [1,2]. In the present study, we investigated whether the fusion of cytotrophoblasts to syncytiotrophoblasts affects MNP passage through the barrier.

The *in vitro* BPB was established in a microfluidic chip by using the cytotrophoblast cell line BeWo and human primary placental pericytes. After 6 days the integrity of the barrier was confirmed by sodium fluorescein permeability (permeability coefficient: empty chip > 3.0E-5 cm/s; BeWo/pericyte barrier < 6.0E-6 cm/s). The fusion of the cytotrophoblasts was induced with 20  $\mu$ M forskolin for 24h. The morphological changes were confirmed by fluorescence microscopy and qPCR. The fused BeWo cell layer was incubated with citrate-coated MNP for 24h. Magnetic Particle Spectroscopy was used to determine the MNP distribution in the apical and basolateral compartment as well as in the cell layer. The penetration rate of MNP was not affected by the formation of syncytiotrophoblasts. In the basolateral compartment no significant difference in MNP content was measured between the untreated setting ( $2.3\% \pm 2.0\%$ ) and after cytotrophoblast fusion induced by forskolin ( $2.4\% \pm 1.6\%$ ). We demonstrate that MNPs pass a cytotrophoblastic cell layer as well as a syncytiotrophoblast.



A: Schematic representation of the BPB in the microfluidic chip and the localization of BeWo cells and pericytes (hPC-PL). B: Untreated BeWo cells with well-structured and tight cell borders (green). C: BeWo cells after treatment with 20  $\mu$ M forskolin for 24h to induce cytotrophoblast fusion. Cell membranes are largely degraded (green dots). Cell nuclei are stained with DAPI (blue); Cell membranes are stained with phalloidin (green). Magnification 20x

- [1] Gräfe, C., et al. *Phys. Sci. Rev.* 2020, doi: 10.1515/psr-2019-0114

- [2] Gresing, L., et al. *J. Magn. Magn. Mater.* 2021, 521, 167535

## Biomanufacturing magnetosomes: nanocarriers with versatile functionalisation for imaging and drug delivery applications

Alfred Fernández-Castañé<sup>1,\*</sup>, Cyrielle Durand<sup>1,2</sup>, Marta Masó-Martínez<sup>1,2</sup>, Kavita Yadav<sup>1,2</sup>, Dimitri Albert<sup>3</sup>, Benjamin Peacock<sup>2</sup>, Rebecca Lees<sup>3</sup>, Graham A Rance<sup>4</sup>, Michael W Fay<sup>4</sup>, Hong Li<sup>5</sup>, Owen RT Thomas<sup>5</sup>, Tim W Overton<sup>5,6</sup>

<sup>1</sup> Energy and Bioproducts Research Institute, Aston University, Birmingham, B4 7ET, UK

<sup>2</sup> Aston Institute of Materials Research, Aston University, Birmingham, B4 7ET, UK

<sup>3</sup> NanofCM Co. Ltd, Nottingham, NG9 6BH, UK

<sup>4</sup>Nanoscale and Microscale Research Centre, University of Nottingham, Nottingham, NG7 2RD, UK

<sup>5</sup> School of Chemical Engineering, College of Engineering and Physical Sciences, University of Birmingham, Edgbaston, Birmingham, B15 2TT, UK

<sup>6</sup> Institute for Microbiology and Infection, University of Birmingham, Edgbaston, Birmingham, B15 2TT, UK

\*Email: alfernandez-castañel@aston.ac.uk

Magnetosomes are functional magnetic nanoparticles (MNPs) generated by magnetotactic bacteria (MTB) and are arranged as single-domain magnetic crystals individually wrapped in a phospholipid membrane. Magnetosomes have advantageous properties when compared to chemical synthetic MNPs: they are ferrimagnetic; have narrow size distribution; are coated in organic material, preventing aggregation; and can be functionalized *in vivo* using genetic engineering tools, allowing one-step manufacture of functionalized particles. In addition, the presence of different chemistries on the surface of magnetosomes such as amino and carboxyl groups, makes them amenable for different functionalisation strategies. Therefore, magnetosomes can be used as versatile magnetic nanocarriers.

On the other hand, biosynthesis of magnetosomes is a clean process carried out at mild temperatures and generates safe waste. Magnetosomes therefore have highly attractive prospects as "smart materials" for biotechnology and nanomedicine uses. However, their true potential to become the next generation nanomaterials hangs the ability to develop high-yield and robust bioprocesses.

Here, we address the challenges and opportunities in magnetosome biomannufacturing and present our strategy to biomannufacture magnetosomes in bench-top bioreactors. Our findings demonstrate that the employment of process analytical technologies (PAT) during the production, purification and formulation stages are key to not only to understand the influence of external stimuli on the process yield but also to ensure the magnetosome quality attributes (e.g., size, chain length, membrane integrity, stability and residual impurities). As examples of the numerous potential applications of magnetosomes, we present how (i) genetic engineering approaches can be used to express functional peptides on the surface of magnetosomes capable of binding fluorescent molecules and (ii) electrostatic interactions can be useful in the application of magnetosomes for the delivery of antimicrobial polymers.

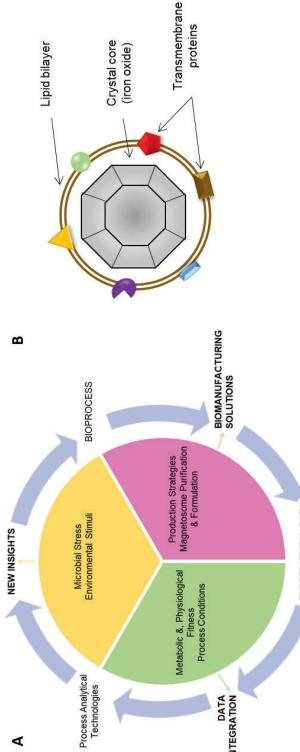


Figure. (A) Circular approach to the development of high-yield and robust magnetosome biomannufacturing. (B) Schematic representation of a single magnetosome composed by a magnetic iron oxide crystal core encapsulated by a phospholipid bilayer. Magnetosome membrane contains magnetosome-associated transmembrane proteins. Variation of shape and colour denote the diversity of proteins.

## Active Targeting of Head and Neck Cancer Cells with Dendronized Iron Oxide Nanoparticles and Effect of the Size and Shape of Nanoparticles for Promoting Multimodal Therapy

Barbara Freis<sup>1,2</sup>, Sonia Furgiuele<sup>3</sup>, Celine Kiefer<sup>1</sup>, Maria De Los Angeles Ramirez<sup>1</sup>, Marianna Tasso<sup>1</sup>, Christine Affalter-Zbarszczuk<sup>4</sup>, Sébastien Boutry<sup>5</sup>, Lionel Larbanov<sup>6</sup>, Florent Meyer<sup>4</sup>, Céline Henoumont<sup>2</sup>, Sven Saussay<sup>2</sup>, Sylvie Laurent<sup>2\*</sup>, Sophie Beguin-Colin<sup>1\*</sup>

(1) Université de Strasbourg, CNRS, Institut de Physique et Chimie des Matériaux, UMR CNRS-UJS 7504, 23 Rue du Loess, BP 43, 67034 Strasbourg, France.

(2) Laboratoire de NMR et d'imagerie moléculaire, Université de Mons, Avenue Maistrail 19, B-7000 Mons, Belgique.

(3) Service d'Anatomie et d'Oncologie Expérimentale, CHU de Mons, Avenue du Champ de Mars 6, 7000 Mons, Belgique.

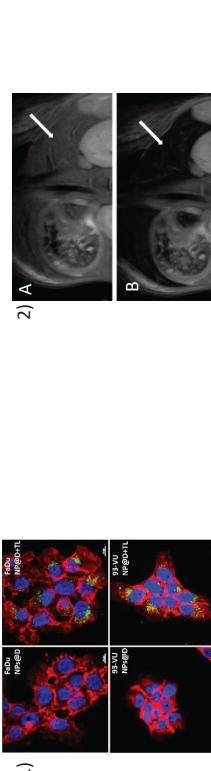
(4) Inserm U1321, Centre de recherche en biomédecine de Strasbourg, 1 rue Eugène Boeckel, CS 60026, 67084 Strasbourg Cedex, France.

(5) Inserm U1109, Centre de recherche en biomédecine de Strasbourg, 1 rue Eugène Boeckel, CS 60026, 67084 Strasbourg Cedex, France.

(6) Center for Microscopy and molecular imaging, Université de Mons, B-6041, Gosselies, Belgique, France.

Head and neck cancers (HNC) represent 4% of all cancer worldwide and are hard to treat due to their location especially for children. Developing multimodal theranostic nanoparticles (NPs) to speed up targeted diagnosis and increase its sensitivity, reliability and specificity is a promising tool for a better management of the disease. Besides being excellent T2 contrast agents for MRI, iron oxide NPs are promising as therapeutic agents by magnetic hyperthermia when correctly designed (high magneto-crystalline anisotropy) and they also have an interest for photothermal treatment and ultrasound therapy thanks to ROS activation. Another challenge is to specifically target cancer cells by coupling targeting ligand at the surface of NPs to enhance the NPs accumulation in tumoral cells.

In that context, we develop dendronized iron oxide NPs with a mean size of 10 nm, which have been proved along several *in vivo* studies to present a very good biodistribution with no captation by the RES<sup>[1]</sup>. Recently, we have developed a strategy to couple targeting ligand (peptide 22) at their surface and proved a specific internalization in two HNC cell lines. *In vivo* studies were as well conducted both in mice and zebrafish to investigate the biodistribution of NPs and check the effect of the presence of the targeting ligand and evaluate the T2 contrasting properties of the NPs. Then, we have studied the internalization in cells of dendronized iron oxides NPs with different sizes (10 and 20 nm) and shapes (nanocubes and plates) synthesized by the thermal decomposition method by tuning synthesis parameters such as the reaction temperature, the heating rate and the nature of surfactant. These dendronized NPs were found biocompatible without cytotoxicity up to 150 µg/ml and after coupling of targeting ligand, internalized in cells with amounts depending on their size and shape. Finally, NPs behaviors towards different kinds of therapies (magnetic and photo-thermia and sonotherapy) were investigated both in suspension in water and in cells. The photothermal efficiency was found to not depend on the NP's size and shape when differences were observed with other therapeutic modes. Such study allowed to establish the optimal NPs design to combine different therapeutic modes to be able during tumor treatment to test different therapies for a better management of diseases.



1- Confocal images of Fadu cell lines (top) and 93-VU cell lines (bottom) with dendronized particles with our without targeting ligand (respectively left and right). 2- Magnetic resonance images of CD-45 mice taken at 9.4T A) pre-injection, B) 3 min after IV injection with 12nm dendronized NPs at a dose of 45 µmol/kg body weight. White arrows point the liver.

References:[1] Colin, G. et al. Unveiling the role of surface, size, shape and defects of iron oxide nanoparticles for theranostic applications Nanoscale, 13, 145 (2021)

This project received funding from ANR (EURO-NANO-MED 2020 Research and Innovation, N72370 of the EU Horizon 2020 Research and Innovation.

## Heterobimetallic probiotic bacteria as new oral magneto-optical hyperthermia agents

**Víctor Garcés<sup>1,\*</sup>, Ana González<sup>1</sup>, Natividad Gálvez<sup>1</sup>, José M. Delgado-López<sup>1</sup>, José J. Calvino<sup>2</sup>, Susana Trasobares<sup>2</sup>, Yilian Fernández-Afonso<sup>3</sup>, Lucía Gutiérrez<sup>3</sup>,  
José M. Domínguez-Vera<sup>1</sup>**

<sup>1</sup> Departamento de Química Inorgánica and Instituto de Biotecnología, Universidad de Granada, 18071 Granada, Spain.

<sup>2</sup> Departamento Ciencia de Materiales e Ingeniería Metalúrgica y Química Inorgánica, Universidad de Cádiz, 11510 Cádiz, Spain

<sup>3</sup> Departamento de Química Analítica, Instituto de Nanociencia de Aragón, Universidad de Zaragoza y CIBER-BBN, 50018 Zaragoza, Spain.

\*E-mail: [vigaro@ugr.es](mailto:vigaro@ugr.es)

Probiotic bacteria were used as carriers of gold nanoparticles (AuNPs) and superparamagnetic magnetite nanoparticles (MNP) to develop innovative oral agents for hyperthermia cancer therapy. The adsorption of metallic nanoparticles takes place in the biofilm, an extra-bacterial conglomeration of products, composed mainly of extropolysaccharides (EPS), that surrounds the bacterial wall of the probiotic bacterium. Two synthetic strategies were used to produce the different therapeutic agents. First, the probiotic bacterium *Lactobacillus fermentum* was simultaneously loaded with MNP and AuNPs to produce AuNPs+MNP-bacteria systems with both types of nanoparticles arranged in the same layer of bacterial EPS. In the second approach, the probiotic was first loaded with AuNPs to form AuNPs-bacteria and subsequently loaded with MNP-EPS to yield AuNPs-bacteria-EPS-MNP with the MNP and AuNPs arranged in two different EPS layers. This second strategy has never been reported and exploits the specific EPS-EPS recognition, which allows the layer-by-layer formation of structures on the bacterial external wall. The potential of AuNPs+MNP-bacteria and AuNPs-bacteria-EPS-MNP as magnetic hyperthermia or photothermal therapy agents was assessed, validating their capacity to produce heat either during exposure to alternating magnetic fields or near-infrared light. Interestingly, *Lactobacillus fermentum* is marketed as an oral supplement to reinforce the gut microbiota and has already been proposed as an oral drug carrier, able to overcome the stomach medium and deliver drugs to the intestines. Therefore, our results open the way for the development of novel therapeutic strategies using these new heterobimetallic AuNPs/MNP-bacteria systems in the frame of gastric diseases, using them as oral agents for magnetic hyperthermia and photothermal therapy [1].

## Heterobimetallic probiotic bacteria as new oral magneto-optical hyperthermia agents

### Antioxidant and Antibacterial Magnetic Nanoparticles: Design, Synthesis and Biological Effects

Daniel Horák<sup>1\*</sup>, Yun-Hwa Ma<sup>2</sup>, Małgorzata Świertek<sup>1</sup>, Anastasia Shatov<sup>1</sup>, MakSYM Moskvín<sup>1</sup>

<sup>1</sup> Institute of Macromolecular Chemistry CAS, 162 06 Prague, Czech Republic

<sup>2</sup> Chang Gung University, Taoyuan 33302, Taiwan

\* Email: horak@imc.cas.cz

Due to the population aging, disorders associated with high oxidative stress and inflammation, such as cancer, atherosclerosis, diabetes, Alzheimer's disease, microbial infections, are becoming main challenges of modern medicine. Considering this trend, the development of improved therapeutic and diagnostic approaches for the management of aforementioned disorders is of utmost importance.

From a broad spectrum of functional nanoparticles, the superparamagnetic iron oxides (SPIONs) are promising for theranostics due to a unique combination of properties. In particular, the SPIONs are biocompatible and biodegradable, their synthesis is well-controlled, and the surface can be readily modified by a plethora of functional agents; the particles can be manipulated and targeted by a magnet, producing heat under alternating magnetic field, and are traceable by magnetic resonance imaging. However, their colloidal stability has to be improved by coating with various polymers to minimize nonspecific protein adsorption in biological media. In this paper, we have developed 10–20 nm SPIONs functionalized with antioxidants (tannic acid or CrO<sub>2</sub>) and bactericides (poly[2-(dimethylamino)ethyl methacrylate (PDMAEMA)-co-2-*tert*-butylaminoethyl methacrylate] or Ag) for suppression of oxidative stress and treating bacterial infections, respectively (Figure 1). The SPIONs were also coated with synthetic (silica, poly(ethylene glycol), poly(L-lysine), or polyethylenimine) or natural (chitosan or heparin) shells containing the agents. Both the antioxidant or antibacterial activity of SPIONs, including their cellular internalization enhanced with magnetic field, was confirmed by assays and flow cytometry using mouse fibroblasts and human brain glioblastoma cells or *S. Aureus* and *E. Coli* bacteria, respectively.

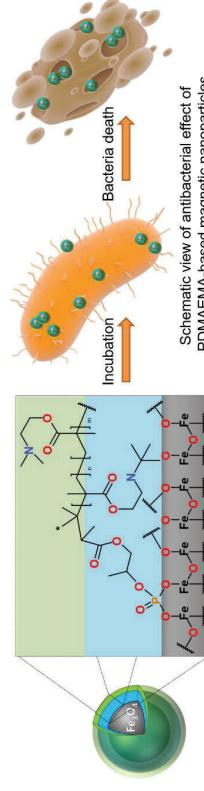


Figure 1.

Support of the Czech Science Foundation No. 20-02177J is acknowledged.  
[1] V. Garcés, A. González, N. Galvez, J. M. Delgado-López, J. I. Calvino, S. Trasobares, Y. Fernández-Afonso, L. Gutiérrez and J. M. Domínguez-Vera, *Nanoscale*, 2022, DOI: 10.1039/DNRM08513A.

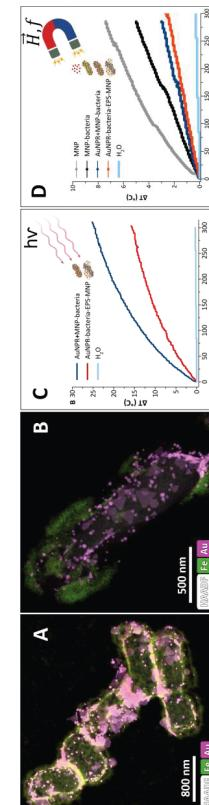


Figure 1. A) HAADF-STEM/EDX image of the AuNPs+MNP-bacteria (Au, pink; Fe, green). B) HAADF-STEM/EDX image of the AuNPs-bacteria-EPS-MNP-bacteria (Au, pink; Fe, green). C) Heating curves obtained after laser irradiation of 2 mg/ml of AuNPs+MNP-bacteria and AuNPs-bacteria-EPS-MNP, plus water as a control sample. D) Temperature variation over time for MNP, MNP-bacteria, AuNPs+MNP-bacteria and AuNPs-bacteria-EPS-MNP at 0.5 mgFe/mL after exposing during 5 min the samples to a high-frequency alternating magnetic field.

## Advancing Rewarming for Cryopreservation through Scalable Polymer Coating of Iron Oxide Nanoparticles

Jacqueline L. Pasek-Allen<sup>1</sup>, Zhe Gao<sup>2</sup>, Randall K. Wilharm<sup>3</sup>, Valerie C. Pierre<sup>3</sup>, John C. Bischof<sup>1,2</sup>  
1. Department of Biomedical Engineering, University of Minnesota, 2. Department of Mechanical Engineering, University of Minnesota 3. Department of Chemistry, University of Minnesota

Donated organs have a short time limit for preservation after collection leading to shortages, morbidity, and mortality of transplant recipients. We have successfully rewarmed vitrified, cryopreserved (<140 °C – indefinite storage) organs using radiofrequency (RF) excited iron oxide nanoparticles (IONPs) in cryoprotective agents (CPAs).<sup>1</sup> CPAs are aqueous solutions containing high concentrations of salts, sugars, and organics such as dimethylsulfoxide (DMSO), formamide, and propylene glycol. We previously demonstrated that although scalable silica-coated ONPs form stable colloidal suspension in CPAs, these suspensions were limited in iron concentration to 15–20 mg Fe/ml, depending on the silica shell thickness.<sup>2</sup> Herein, we present biocompatible polymers (i.e. polyethylene glycols, PEG) coated IONPs via a phosphonate linker (PLink) that is stable in CPAs, increases saturation concentration, and is inexpensive for scale-up (>1 g per batch).<sup>3</sup>

PLink displaces the initial coating on commercial IONPs (Ferrotec Inc.) such as EMG-1200 (hydrophobic) and EMG-308 (hydrophilic) and allows attachment of the polymers of interest, in a simple ligand exchange step. Plinked-PEG increases colloidal stability and decreases aggregation of EMG-1200 in water and CPAs from minutes (uncoated) to up to 2 weeks. PLink has high affinity for iron oxide due to the phosphonate anchoring moiety and a carboxyl chemical handle for ligand attachment. The heating of coated EMG-1200 was enhanced significantly comparing to uncoated hydrophobic EMG-1200 (20 to 150 W/g Fe in H<sub>2</sub>O) due to better dispersion and colloidal stability in the solution, while the heating of coated EMG-308 was the same as the hydrophilic EMG-308 indicating the polymer coating did not affect IONP core's heating capability. The concentrations of IONP in VSS5 (a common CPA) reached 25 mg Fe/ml of 308-PEG5000 and 60 mg Fe/ml of 1200-PEG5000, which is significantly above our previously published capabilities of siONP at 10 mg Fe/ml. Further, at these concentrations cryopreserved human dermal fibroblast cells were successfully nanorewarmed at an applied field of 360 kHz and 20 kA/m, with higher viability as compared to convective rewarming in a water bath and a heating rate close to 200 °C/min, 2.5 times faster than our previous tests with IONPs. PLink-coated IONPs have since been scaled to over 10 g synthesis and used to nanorewarm rat kidneys at and above these rates.<sup>3</sup>

The PLink coating allows for facile, inexpensive, and scalable synthesis of PEG-functionalized IONPs for, as needed for human scale organ cryopreservation. In future experiments, PLink IONPs will be tested at higher Fe concentration in various CPAs, maximizing the heating rates with EMG308 IONPs and translating nanorewarming to transplantation.

- Sharma, A.; Rao, J. S.; Han, Z.; Gangavar, L.; Namstai, B.; Gao, Z.; Ring, H. L.; Magnuson, E.; Etheridge, M.; Wowk, B.; Fahy, G. M.; Garwood, M.; Finger, E. B.; Bischof, J. C.; Vitrification and Nanorewarming of Kidneys. *Advanced Science* **2021**, *8* (19), 2101691.
- Gao, Z.; Ring, H. L.; Sharma, A.; Namstai, B.; Tran, N.; Finger, E. B.; Garwood, M.; Haynes, C. L.; Bischof, J. C.; Preparation of Scalable Silica-Coated Iron Oxide Nanoparticles for Nanorewarming. *Advanced Science* **2020**, *7* (4), 1901624.
- Pasek-Allen, J.; Wilharm, R.; Gao, Z.; Pierre, V. C.; Bischof, J.; Phosphonate Coating of Commercial Iron Oxide Nanoparticles for Nanorewarming Cryopreserved Samples. *Journal of Material Chemistry B* **2022** in Press.

## Synthesis, Characterization and Cellular Internalization of Anisotropic Magnetic Nanoparticles

Sirine El Mousli, Emile Secret and Jean-Michel Staigue

Physico-chimie des Électrolytes et Nanosystèmes Interfaçants, PHENIX, Sorbonne Université,  
CNRS, F-75005 Paris, France

Contact: [sirine.el\\_mousli.sciada@sorbonne-universite.fr](mailto:sirine.el_mousli.sciada@sorbonne-universite.fr)

Magnetic nanoparticles (MNPs) are widely studied for bio-applications such as magnetic hyperthermia or cellular engineering. MNPs with elongated shape such as nanorods are of great interest for these applications as they notably exhibit higher heating efficiencies and a prolonged retention in tumour sites than their spherical counterparts.<sup>1</sup> The main issue during cells internalization is to avoid endosomal entrapment of nanoparticles, which prevent them from interacting with intracellular components and decrease their heating efficiency. Membrane translocation phenomena have already been observed with some anisotropic nanoparticles. Such process allows the internalization of these objects directly in the cytoplasm, without being trapped in endosomes.<sup>2</sup>

In this study, a two-step robust synthesis<sup>3</sup> method was optimized to produce magnetic nanorods of controlled composition in a large range of lengths and diameters. Water-soluble magnetite nanorods with high aspect ratios were obtained and then coated with a fluorescent silica shell. Core-shell magnetic nanorods were subsequently functionalized either with polyethylene glycol (PEG) or with zwitterionic molecules for their antifouling properties. The cellular internalization of these elongated MNPs and of spherical core-shell MNPs<sup>4</sup> was thoroughly studied by confocal microscopy. At 4°C when endocytosis is blocked, elongated nanoparticles are still observed inside the cells whereas spherical nanoparticles are no longer internalized, confirming that the shape is a determining factor in the internalization of nanoparticles. Those first results suggest that elongated MNPs can enter cells through passive diffusion. Finally, transmission electron microscopy observations will help elucidate the mechanisms involved in the nanorods internalization.

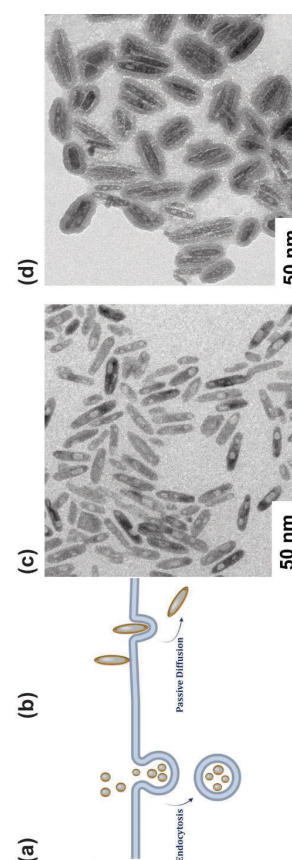


Figure 1: Scheme of nanoparticles internalization: (a) Endocytosis of magnetic nanospheres (b) passive diffusion of magnetic nanorods. TEM micrographs of (c) magnetic nanorods ( $Fe_3O_4@SiO_2$ ) magnetic core silica shell nanorods ( $Fe_3O_4@SiO_2$ )

References:

- [1] a) Srikanth H. *et al.* (2016), Tunable High Aspect Ratio Iron Oxide Nanorods for Enhanced Hyperthermia. *J. Phys. Chem. C* ; b) Shukla S. *et al.* (2015), The Impact of Aspect Ratio on the Biodistribution and Tumour Homing of Rigid Soft-Matter Nanorods. *Adv. Healthcare Mater.*
- [2] a) Kostarelos K. *et al.* (2007), Cellular Uptake of Functionalized Carbon Nanotubes, *Nature Nanotechnology*; b) Millot N. *et al.* (2015), Dispersion of Titania Nanotubes for nanomedicine: comparison of PEI and PEG nano-hybrids, *Dalton Trans.*
- [4] Mohapatra J. *et al.* (2015), Iron oxide nanorods as high-performance magnetic resonance imaging contrast agents, *Nanoscale*.
- [5] Georgelin T. *et al.* (2010), Nanoparticles-mediated delivery of bleomycin, *Angew. Chem. Int. Ed.*





## Poster Session I - Tuesday, June 14, 2022

First Author	Title	Corresponding Author	City, Country
1 Arsalan, Saeideh	Hybrid Magnetic Nanoparticles As Molecular Agents In Magneto-Motive Ultrasound Imaging	Arsalan, Saeideh	Ribeirão Preto, Brazil
2 Bassam, Jameel	Ultrasound Spectroscopy For Studying Pickering Emulsions Stabilized By Magnetic Nanoparticles	Bassam, Jameel	Poznan, Poland
3 Das, Arpita	Negative Differential Capacitance (Ndc) And Hysteresis Achieved In Dna Added Cobalt Ferrite Magnetic Nanoparticles	Das, Arpita	Kolkata, India
4 Kaman, Ondrej	Gold Nanoshells With Magnetic Cores For Multimodal Imaging And Sensing	Kaman, Ondrej	Praha, Czechia
5 Arenas, Maria	Development of multimodal phantoms for Magnetic Resonance Imaging and Magnetic Particle Imaging	Löwa, Norbert	Berlin, Germany
6 Mickoleit, Frank	Generation Of Reusable Nano-Biocatalysts By Genetic Engineering And Functionalization Of Bacterial Magnetic Nanoparticles	Mickoleit, Frank	Bayreuth, Germany
7 Nasser, Amal	Structural And Magnetic Characterization Of Citrate-Coated Spions For Magnetically Controlled Immune Therapy	Nasser, Amal	Munich, Germany
8 Smela, Denisa	TIO2 Magnetic Nanotubes For RNA Isolation From Complex Biological Samples	Smela, Denisa	Pardubice, Czechia
9 Armenia, Ilaria	Combining Iron Oxide Nanoparticles And Fluorescent Protein For Selective Magnetic Nanoheating Studies	Armenia, Ilaria	Zaragoza, Spain
10 Fernández Afonso, Yilian	Magnetic Nanoparticle Transformations And The Effect On Their Heating Properties	Fernández Afonso, Yilian	Zaragoza, Spain
11 Fernández Afonso, Yilian	Reversible Chain Formation During Magnetic Hyperthermia Experiments	Fernández Afonso, Yilian	Zaragoza, Spain
12 Idiago-Lopez, Javier	Cell Membrane Hyperfluidization With Localized Magnetic And Optical Hyperthermia	Fratila, Raluca	Zaragoza, Spain
13 Bielas, Rafal	Pickering Emulsions Stabilized By Magnetite Particles In A Rotating Magnetic Field	Józefczak, Arkadiusz	Poznan, Poland
14 Reisen, Oliver	Temperature-Controlled Drug Release From Magnetic Pga Nanospheres Enabling Efficient Treatment Of Pancreatic Cancer Cells	Slabu, Ioana	Aachen, Germany
15 Lozano Pedraza, Claudia	Photothermal Therapy For In Vitro Multimodal Treatment Of Peritoneal Carcinomatosis	Lozano Pedraza, Claudia	Madrid, Spain
16 Chen, Hao	Tuning The Dynamics In Fe3O4 Nanoparticles For Hyperthermia	Majetich, Sara	Pittsburgh, USA
17 Molcan, Matus	The Impact Of Alternating And Rotating Regimes On The Heating Characteristics Of Magnetic Colloids And Dense Cellulose Structures	Molcan, Matus	Kosice, Slovakia
18 Ruta, Sergiu	Sar Determination From Temperature Measurement Using Repeated Heating-Cooling Cycles	Ruta, Sergiu	Sheffield, UK
19 Serantes, David	On The Effective Uniaxial Anisotropy Of Magnetite Nanoparticles	Serantes, David	Santiago de Compostela, Spain
20 Singh, Sarbjit	Magnetic Heating Of Superparamagnetic KfeO2 Nanoparticles For Treatment Of Cancer	Singh, Sarbjit	Tarn Taran, India
21 Sojková, Tereza	Magnetic Properties Of Iron Oxide Feo/Fe3O4 Core-Shell Nanocubes Tuned By The Preparation Method	Sojková, Tereza	Brno, Czechia
22 Çitoglu, Senem	Dmsa-Coated Cubic Iron Oxide Nanoparticles As Potential Therapeutic Agents	Thanh, Nguyen	London, UK
23 Wang, Lilin	Synergistic Effect Of The Doxorubicin Loaded Thermal And Ph-Sensitive Nanocarriers On The Different Cell Lines	Thanh, Nguyen	London, UK
24 Torres, Teobaldo	Determining The Key Parameters To Reach Synergistic Effects Between Magnetic Hyperthermia And Ros Production In Znxfe3-xfo4 Magnetic Nanoparticles	Torres, Teobaldo	San Carlos de Bariloche, Argentina

25	Valdés, Daniela	Untangling The Influence Of Particle-Intrinsic Parameters And Experimental Conditions In Magnetic Fluid Hyperthermia	Valdés, Daniela	Bariloche, Argentina
26	Wang, Xuyiling	Investigation Of Ac Hysteresis From Magnetic Nanoparticle Suspensions Using Magneto-Optical Methods	Wang, Xuyiling	Stoke-on-Trent, UK
27	Wells, James	Multifrequency Hyperthermia Characterisation By Calorimetry And Dynamic Magnetisation	Wiekhorst, Frank	Berlin, Germany
28	Le, Tuan-Anh	Theoretical Three-Dimensional Predictions For Spatial Focusing Of Magnetic Hyperthermia Using Field-Free Point/Line Concept	Yoon, Jungwon	Gwangju, South Korea
29	Arijomandi, Sarah	Capturing Magnetic Nanoparticles With External Magnetic Fields In The Fluidic Flow	Arijomandi, Sara	Milan, Italy
30	Manipuntee, Chonnavee	Visible Light-Driven Amide Synthesis From Thioacid And Amine With Cdse Qds-Coated Magnetic Pmma Nanocomposites In An Aqueous Solution	Insin, Numpon	Bangkok, Thailand
31	Löwa, Norbert	Highly Selective Separation Of Magnetic Nanoparticles Using Dynamic Magnetic Fields: A Novel Approach For Mpi Tracer Purification	Löwa, Norbert	Berlin, Germany
32	Löwa, Norbert	Magnetic Anisotropy In Polymeric Magnetic Hybrid Material Induced By Vat Photopolymerization Additive Manufacturing	Löwa, Norbert	Berlin, Germany
33	Queirolos Campos, Jordy	Improved Magneto-Microfluidic Separation Of Nanoparticles Through Formation Of The Beta-Cyclodextrin-Curcumin Inclusion Complex	Queirolos Campos, Jordy	Nice, France
34	Mirkhani, Nima	A Scalable Magnetic Control Strategy To Suppress Off-Target Nanoparticle Transport	Schürle, Simone	Zurich, Switzerland
35	Moore, Lee	Red Blood Cell Magnetophoresis As A Function Of Oxygen Partial Pressure.	Zborowski, Maciej	Cleveland, USA
36	Abolfathi, Kiana	Magnetic Bio-Hybrid Microrobots For Targeted Stem Cell Delivery	Hoshtiar, Ali K.	Colchester, UK
37	Bernad, Sandor	Magnetoresponsive Nanocomposite Aggregation During Magnetic Targeting	Bernad, Sandor	Timisoara, Romania
38	Grondzak, Tomas	The Effect Of Spions Modified By Aluminium Nanoparticles On The Growth Of S. Aureus And E. Coli	Grondzak, Tomas	Prague, Czechia
39	Cepova, Jana	The Effect Of Spions Modified By Silver Nanoparticles And Vancomycin On The Growth Of S. Aureus And E. Coli	Grondzak, Tomas	Prague, Czechia
40	Manipuntee, Chonnavee	Biodegradable Pga-Based Magnetic Nanocomposites For Magnetic Target Retention And Sustained Release Of Triamcinolone Acetonide From Detachable Microneedles	Insin, Numpon	Bangkok, Thailand
41	Ionica, Maria-Cristina	The Magnetic Field Generated By Single Or Multiple Magnets For The Magnetic Drug Targeting Process	Ionica, Maria-Cristina	Lugoj, Romania
42	Lachowicz, Dorota	Molecular Insights of the Oxidation Process of Copper-Zinc Ferrites Nanoparticles Coated by a Polymer Layer	Lachowicz, Dorota	Krakow, Poland
43	Koutsoumpou, Xanthippi	NP-Cellular Hitchhiking System for Targeted Combination Therapy and Diagnosis for Glioblastoma	Manshian, Bella	Leuven, Belgium
44	Mandal Goswami, Madhuri	Trifunctional Fluorescent Cobalt Ferrite Nanoparticles For Hyperthermia Therapy, Cell Probing And Drug Delivery	Mandal Goswami, Madhuri	Kolkata, India
45	Adam, Alexandre	Hybrid Iron Oxide Core@Mesoporous Silica Shell Nanoparticles For Magnetic Hyperthermia, Phototherapy And Drug Delivery	Mertz, Damien	Strasbourg, France
46	Petrus, Jakub	Lc-Ms/Ms As A Study Method Of The Release Kinetics Of Remdesivir From Magnetic Nanoparticles	Petrus, Jakub	Prague, Czechia
47	Pfister, Felix	Functionalization Of Primary T Cells With Magnetic Nanoparticles For Guided Immunotherapy	Pfister, Felix	Erlangen, Germany
48	Son, Boyoung	Magnetic Nanoparticle Focusing System On The Blood Vessel Using An Array Of Permanent Magnets	Yoon, Jungwon	Gwangju, South Korea
49				
50				
51				
52				

## Poster Session II - Wednesday, June 15, 2022

#	First Author	Title	Corresponding Author	City, Country
53	Kim, Yonggyu	A Novel Guidance Scheme For Magnetic Particles Inspired By The Artificial Potential Field	Yoon, Jungwon	Gwangju, South Korea
54	Hunter, Arabella	Quantitative Measurements Of The Influence Of Polymer Brush Length On Magnetic Nanoparticle Interactions And Signal Enhancement During Linear Aggregation Via Magnetic Particle Spectroscopy	Mefford, Thompson	Clemson, USA
55	Janssen, Klaas-Julian	Temperature Imaging With A Single Harmonic Magnetic Particle Imaging Approach	Ludwig, Frank	38106 Braunschweig, Germany
56	Jaufenthaler, Aaron	Human-Head-Sized Magnetorelaxometry Imaging Of Magnetic Nanoparticles Using Optically Pumped Magnetometers	Jaufenthaler, Aaron	Hall in Tirol, Austria
57	Kosch, Olaf	Tracer Comparison Including Mpi Scanner Characteristics By 2-Voxel-Analysis	Kosch, Olaf	Berlin, Germany
58	Kubickova, Lenka	Probing Relaxation Characteristics Of Magnetic Nanoparticles By A Home-Made Magnetic Particle Spectroscopy Setup	Kubickova, Lenka	Prague, Czechia
59	Porru, Margherita	Core-Shell Structured Mnps: Coating Effect On The 1H-Nmr Relaxation Properties	Porru, Margherita	Pavia, Italy
60	Remmo, Amani	Magnetic Particle Imaging For Cell Tracking: Establishing Quality And Effectiveness In Magnetic Cell Labeling	Remmo, Amani	Berlin, Germany
61	Salamzadeh, Sadaf	Optimising Excitation Field Frequency For Handheld Defects Of Magnetic Nanoparticles	Salamzadeh, Sadaf	Enschede, Netherlands
62	Sasayama, Teruyoshi	Estimation Accuracy Improvement Of Magnetic Nanoparticle Tomography By Combining Inverse Solution Methods	Sasayama, Teruyoshi	Fukuoka, Japan
63	Schoonenen, Max	The Impact Of Mnp Agglomerations Inside Magnetic Fibers On Mri, Mpi And Hyperthermia Performance	Slabu, Ioana	Aachen, Germany
64	Besenhard, Maximilian	Small Iron Oxide Nanoparticles As Mri T1 Contrast Agent	Storozhuk, Liudmyla	London, UK
65	Baffa, Oswaldo	Low Frequency Ac Susceptometry With Optically Pumped Magnetometers	Baffa, Oswaldo	Ribeirão Preto, Brazil
66	Everaert, Katrijn	Tabletop Setup For Thermal Noise Magnetometry Of Magnetic Nanoparticles Based On Optically Pumped Magnetometers	Everaert, Katrijn	Gent, Belgium
67	Hovorka, Ondrej	Characterising Magnetic Nanoparticles Using Data-Driven Methods	Hovorka, Ondrej	Southampton, UK
68	Ackers, Justin	Construction Of A Broadband 3D Magnetic Particle Spectrometer	Justin, Ackers	Lübeck, Germany
69	Pourshahidi, Ali M.	Resolving Ambiguities In Core Size Determination Of Magnetic Nanoparticles From Magnetic Frequency Mixing Data	Krause, Hans-Joachim	Jülich, Germany
70	Martin, Éléonore	Monte Carlo And Experimental Study Of The Magnetic Behaviour Of Superparamagnetic Nanoparticles	Martin, Éléonore	Mons, Belgium
71	Sepehri, Sobhan	Nanorheology Monitoring Using Magnetic Nanoparticles And Ac Susceptometry	Sepehri, Sobhan	Göteborg, Sweden
72	Cabriera, David	Novel Methodologies To Determine The Magnetic Anisotropy Of Iron Oxide Nanoparticles In Colloidal Suspensions	Terán, Francisco J.	Madrid, Spain
73	Friedrich, Bernhard	Portable Mips Device For Radical Innovation In Medical Point-Of-Care Diagnostics	Vogel, Patrick	Würzburg, Germany
74	Kim, Hohyeon	Characterization Of Physical Properties Of Commercial Nanoparticle For Biomedical Application	Yoon, Jungwon	Gwangju, South Korea
75	Park, Myungjin	Studies Aggregation Mechanism Of Magnetic Nanoparticles Under Possible Scenarios During Magnetic Drug Targeting	Yoon, Jungwon	Gwangju, South Korea
76	Makridis, A.	Iron-Cementite Nanoparticles In Carbon Matrix: Synthesis, Features And Biomedical Perspectives	Angelakeris, Makis	Thessaloniki, Greece
77	Chowdhury, Mohammad S.	Mind The Solvent Impurity And Never Give Up On Catechol Anchor: 3D Nano-Assembly And Aqueous Dispersion Of Cobalt-Ferrites	Chowdhury, Mohammad Suman	Braunschweig, Germany
78	Freis, Barbara	Effects Of Size, Shape And Defects Of Iron Oxide Nanoparticles On Photothermal And Magnetothermal Therapies	Freis, Barbara	Strasbourg, France
79	Harvell-Smith, Stanley	Synthesis Of Size-Controlled Iron Oxide Nanocubes For Mpi-Mfh Applications	Thanh, N. T. K.	London, UK
80	Nemec, Sebastian	A Tunable Acid-Etching Procedure For The Preparation Of Partially Hollow Magnetic Nanostructures	Kralj, Slavko	Ljubljana, Slovenia

81	Adhikari, Samyog	Synthesis And Characterisation Of Batio3 – Cofe2O4 Magnetolectric Nanoparticles For Biomedical Applications.	Thanh, N. T. K.	London, UK
82	Rafe, Diana	Synthesis Of Flower-Like Manganese Ferrite Nanostructures For Enhancing Chromium Bio-Reduction By Shewanella Oneidensis	Thanh, N. T. K.	London, UK
83	Çitoglu, Senem	Effect Of Iron Oxide Nanoparticle Surface Chemistry On Magnetic Property And Cytotoxicity On Hela Cells	Onur, Mehmet A.	Ankara, Turkey
84	Shah, Wiqar	Competing Interactions, And Magnetization Dynamics In Doped Rare-Earth Manganites Nanostructural System	Shah, Wiqar	Islamabad, Pakistan
85	Shlapa, Yuliia	"Core-Shell"-Like Fe3O4/Ceo2 Nanocomposites For Perspective Application In Medicine: Synthesis, Physical-Chemical Characterization And Bio-Activity	Shlapa, Yuliia	Kyiv, Ukraine
86	Göpfert, Lennart	Millifluidic Two-Phase System For The Continuous Automated Manufacturing Of Mnp	Slabu, Ioana	Aachen, Germany
87	Stein, René	Synthesis And Characterization Of Gold-Coated Superparamagnetic Iron Oxide Nanoparticles For Magnetic Drug Targeting Treatment	Alexiou, Christoph	Erlangen, Germany
88	Zahn, Diana	Magnetic Microspheres: A Toolbox For Hyperthermia, Drug Delivery And Immunomagnetic Separation	Dutz, Silvio	Ilmenau, Germany
89	Zahn, Diana	Ferrimagnetic Iron Oxide Nanoparticles For Heating Applications: Large Single Domain Particles Prepared By The Green Rust Method	Dutz, Silvio	Ilmenau, Germany
90	Bielas, Rafal	Colloidal Microcapsules Fabricated From Pickering Droplets Using Alternating Magnetic Fields	Bielas, Rafal	Poznan, Poland
91	Chiriac, Horia	Stem Cells Carriers Of Fe-Cr-Nb-B Ferromagnetic Particles For Cancer Cell Destruction By Magneto-Mechanical Actuation	Chiriac, Horia	Iasi, Romania
92	Lafuente, Aritz	Ferromagnetic Drug Loaded Biodegradable Nanocapsules For Externally Controlled And Non-Invasively Monitored Nanotherapies.	Lafuente, Aritz	Barcelona, Spain
93	Castro-Hinojosa, C.	Oriented Immobilization Of Cadherin Fragments On Magnetic Nanoparticles As Novel Magneto-Mechanical Cell Actuators	Moros, Maria	Zaragoza, Spain
94	Nucci, Giulia Eugenia Paola	Magnetic Hyperthermia As A Combinatorial Tool To Develop New Therapies Against Cancer	Pellegrino, Teresa	Genova, Italy
95	Ramirez, Maria de los Angel	Dendronized Iron Oxide Nanoparticles Used As Theragnostic Agents For Breast Cancer Treatment	Ramirez, Maria de los Angeles	Strasbourg, France
96	Santander, Sergio	Synthesis And Characterisation Of Fe@FePt Core-Shell Nanocubes For Synergistic Magneto-Phototherapy	Thanh, N. T. K.	London, UK
97	Gwisi, Tinotenda	Using Magnetic Torques To Enhance Tumor Infiltration Of Cargo-Carrying Magnetotactic Bacteria	Schuerle, Simone	Zurich, Switzerland
98	Le Jeune, Matilde	Poly-Histidine Functionalized Fe2O3@SiO2 Nanoparticles To Access The Cell Cytoplasm	Secret, Emilie	Paris, France
99	Engelmann, Ulrich	Optimal Particles For Highly Sensitive Biosensing Application In Mixed Frequency Excitation: Insights From A Fundamental Simulative Approach	Engelmann, Ulrich	Jülich, Germany
100	Kahmann, Tamara	Optimizing Virus Detection With Magnetic Nanoparticles	Kahmann, Tamara	Braunschweig, Germany
101	Rösch, Enja	Point-On-Need Detection Of Pathogen-Specific Nucleic Acid Targets Using Magnetic Particle Spectroscopy	Rösch, Enja	Braunschweig, Germany
102	Su, Diqing	Ultra-Flexible Giant Magnetoresistance Biosensors For Realtime Monitoring Of Tumor Cells: Method For Future Lab-On-A-Needle Biopsies	Wang, Jian-Ping	Minneapolis, USA
103	Rosenberg, Margaret	Understanding The Dynamic Susceptibility Of Magnetic Nanoplatelet Suspensions	Kantorovich, Sofia	Vienna, Austria
104	Ivan, Novikau	The Influence Of Spatial Crosslinker Distribution On The Magnetic Properties Of Magnetic Nanogels	Kantorovich, Sofia	Vienna, Austria
105	Hannon, Gary	Safety and efficacy assessment of iron oxide nanoparticles intended for magnetic hyperthermia: a translational story	Hannon, Gary	Dublin, Ireland
106				
107				

## Hybrid Magnetic Nanoparticles as Molecular Agents in Magneto-motive Ultrasound

### Imaging

<sup>1</sup>Saeideh Arsalani,<sup>2</sup>Soudabeh Arsalani,<sup>1</sup>Mileni Isikawa,<sup>1</sup>Eder J Guidelli,<sup>1</sup>Ernesto E Mazon,<sup>3</sup>André Bakuzis,<sup>1</sup>Theo Pavan,<sup>1</sup>Oswaldo Baffa, and<sup>1</sup>Antonio Adilton O Carneiro

<sup>1</sup>Department of Physics, FFCLRP, University of São Paulo, Av. Bandeirantes 3900, Ribeirão Preto, SP, 14040-901, Brazil

<sup>2</sup>Physikalisch-Technische Bundesanstalt, Abbestrasse 2-12, D-10587 Berlin, Germany

<sup>3</sup>Instituto de Física-Universidade Federal de Goiás, Goiânia, 74690-900, Brazil

\*Email: arsalani@usp.br

Studies of nanostructures have been established as promising approaches in the diagnosis and therapy of cancer through the last decades. Magnetic nanoparticles (MNPs) and gold nanorods (GNRs) are known as the most widely used nanomaterials due to their considerable physicochemical properties. Herein, using simultaneously a combination of magneto-optical NPs provides new prospects in various medical fields.

In this study, we used negatively charged citrate-coated manganese ferrite and synthesized positively charged GNRs coated by CTAB to produce hybrid NPs of GNRs and  $\text{CIMnFe}_2\text{O}_4$ . These hybrid NPs were developed as contrast agents in magneto-motive ultrasound imaging (MMUS). In this regard, two different samples were made: the first one contained just  $\text{CIMnFe}_2\text{O}_4$  (0.8 wt. %), and the second one was made of hybrid NPs of GNRs (0.4 wt. %) and  $\text{CIMnFe}_2\text{O}_4$  (0.8 wt. %). Moreover, several characterizations were performed including UV-Visible spectrometry, transmission electron microscopy (TEM), and magnetic separation (SEPMAG) to examine the interaction of GNRs and  $\text{CIMnFe}_2\text{O}_4$ . The MMUS setup is depicted in Figure 1a which consisted of a magnetic coil with a steel core, and a capacitor bank that is charged by a half-drive inverter. After the charging of this capacitor, the magnetic field pulse is generated by an electronic switching device.

The results showed the hybrid NPs interacted electrostatically and small nanoclusters were generated with an average size of 55 nm. These NPs homogeneously embedded in a tissue-mimicking phantom reported a larger displacement of 19.42  $\mu\text{m}$  rather than using just  $\text{CIMnFe}_2\text{O}_4$  (8  $\mu\text{m}$ ) in MMUS when exposed to an external oscillating magnetic field of 740 mT. The MMUS image of the sample containing just  $\text{CIMnFe}_2\text{O}_4$  is illustrated in Figure 1b, and the regions presenting higher displacements indicate where the NPs are located. Thus, based on the achieved results, GNRs and  $\text{CIMnFe}_2\text{O}_4$  hybrid NPs can be considered as potential contrast agents in MMUS.

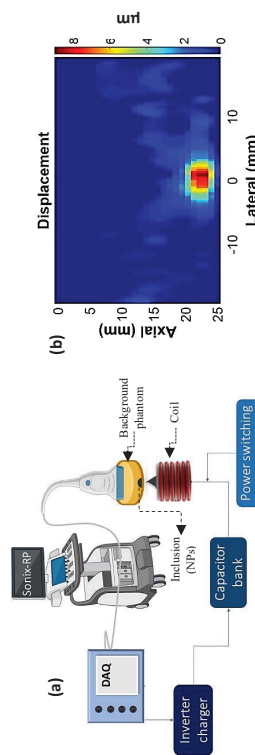


Figure 1: Experimental setup of MMUS (a) and MMUS image of the phantom containing  $\text{CIMnFe}_2\text{O}_4$  (b). Partial Financial Support: CAPES, FAPESP, and CNPq.

## ULTRASOUND SPECTROSCOPY FOR STUDYING PICKERING EMULSIONS STABILIZED BY MAGNETIC NANOPARTICLES

Bassam Jameel\*, Tomasz Horowski, Rafał Bielaś and Arkadiusz Józefczak

Chair of Acoustics, Faculty of Physics, Adam Mickiewicz University in Poznań  
Uniwersytetu Poznańskiego 2, 61-614 Poznań, Poland

\*e-mail: bassam@amu.edu.pl

Magnetic nanoparticles (MNPs) can work as a source of heat in response to the alternating magnetic field which is practically used in magnetic hyperthermia treatment. Additionally, MNPs can be affected by the application of the static magnetic field which is important for magnetic separation process. Finally, the MNPs can be also utilized as stabilizers of droplets and provide the magnetic properties to the droplet interface. This kind of emulsion is known as magnetic Pickering emulsion (MPE). One of the challenges on MPE development for biological and industrial applications is the control of the behaviour and the thickness of the particle shell and the size of droplets in MPE. Such a particle shell may affect the magnetic heating efficiency and heat transfer in MPE [1]. In this study, we present a novel result for characterizing the real structure of MPE by using ultrasound attenuation coefficient combined with ultrasound scattering theory. The core shell model was implemented for reproduce ultrasound attenuation coefficient with taking into account the contrast of physical parameters between three phases. The optical microscopy imaging shows in Fig. 1a the objects of aggregates in the range of micrometre size. Fig. 1b presents the comparison between the ultrasound experimental and theoretical results for magnetic Pickering emulsions. It indicates that nanoparticles do not form a single layer at the droplet interface but rather a layer of aggregates.

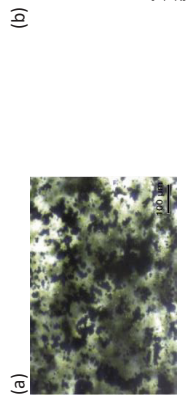


Fig. 1 (a) Optical microscopy image of the magnetic Pickering emulsion with the schematic illustration of magnetic Pickering droplet, and (b) The comparison of experimental and theoretical results of the ultrasound attenuation coefficient for Pickering emulsions.

### Reference

- [1] Bielaś, R., and Józefczak, A.: 'The Effect of Particle Shell on Cooling Rates in Oil-in-Oil Magnetic Pickering Emulsions', Materials, 2020, 13, (21), pp. 4783  
Acknowledgments  
This work was supported by the project no. 2019/35/O/ST3/00503 (PRELUDIUM Bis) of the Polish National Science Centre.

## Negative differential capacitance (NDC) and hysteresis achieved in DNA added cobalt ferrite Magnetic Nanoparticles

Arpita Das<sup>1</sup>, Debarati De<sup>1</sup>, Madhuri Mandal Goswami<sup>2</sup>, Kamik Palodhi<sup>1</sup>

<sup>1</sup> CRNN, University of Calcutta, Kolkata, 700098, India

<sup>2</sup> S.N Bose National Centre for Basic Science, Kolkata 700098, India

E-Mail address (corresponding author): [arpitadas16@gmail.com](mailto:arpitadas16@gmail.com)

The wet chemical co-precipitation method has been commonly applied for synthesizing different types of iron oxide nanoparticles. In a recent study, it can be seen that these nanoparticles, if functionalized with DNA, do not agglomerate in normal conditions and this can potentially enhance the memory effect as it shows the hysteresis effect [1]. For characterization of the size of the nanoparticles, standard FESEM is used and it shows that the size of the particles is around 20 nm as shown in Figure 1. Raman spectroscopy was also performed to establish the confirmation of the conjugation with the DNA.

In this work, cobalt ferrite magnetic nanoparticles have been synthesized for probable application in energy storage technologies. For electrical characterization, these particles have been developed into a simple structure such as a synthesized nanoparticles pellet and dots of platinum, upon it. During electrical characterization, the comparisons among capacitive response relative to the voltage at different frequencies of these batches have been studied with 4200 SCS Kathley particle analyzer as shown in Figure 2. From these comparison graphs, we can see a clear presence of negative differential capacitance (NDC). This particular phenomenon occurred due to the presence of DNA with cobalt ferrite as it was not observed for samples containing only cobalt ferrite (without DNA) as shown in Figure 3. In addition to NDC, we can also see hysteresis effects in the same sample as described earlier. The presence of both these phenomena in a single material makes this material hugely attractive for future applications in semiconductor industries etc.

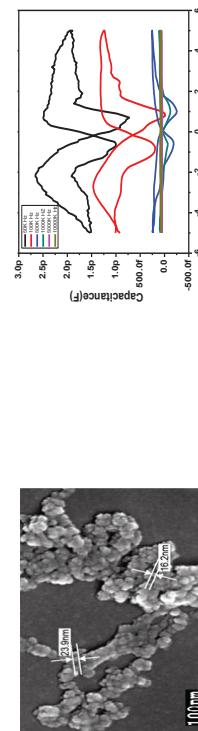


Figure 1: FESEM image of DNA added particle

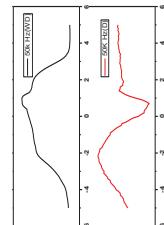


Figure 2: Capacitance Vs Voltage curve of DNA added particle

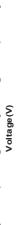


Figure 3: NDC phenomena comparison

Reference: 1. DNA Immobilized Co-Fe2O4 magnetic nanoparticles: a nature friendly material manifesting negative differential resistance (NDR) and hysteresis effect A Das, et. al. IEEE Transactions on Nanotechnology 20,386-391,1941-0085.

## Gold nanoshells with magnetic cores for multimodal imaging and sensing

Ondřej Kaman<sup>1</sup>, Duong Thuy Bui<sup>1,2</sup>, Lenka Kubíčková<sup>1</sup>, Jarmila Kulíčková<sup>1</sup>, Pavel Řezanka<sup>2</sup>, and Vít Herynek<sup>3</sup>

<sup>1</sup> Institute of Physics, Czech Academy of Sciences, Čukrovarnická 10, 162 00 Praha 6, Czech Republic

<sup>2</sup> University of Chemistry and Technology, Prague, Technická 5, 166 28 Praha 6, Czech Republic

<sup>3</sup> First Faculty of Medicine, Charles University, Salomonka 3, 120 00 Praha 2, Czech Republic

\*E-mail: [kamano@seznam.cz](mailto:kamano@seznam.cz)

Complex nanoparticles combining multimodal imaging with local sensing can provide a breakthrough in biomedical research, but reports demonstrating the contrast effect of a single nanosized probe in several imaging modalities together with its sensing performance are scarce. Gold nanoshells with magnetic cores and specific organic functionalization enable the development of such smart contrast agents. The present contribution describes complex gold nanoshells, whose surface functionalization is designed for pH sensing by means of surface-enhanced Raman spectroscopy (SERS) and which, at the same time, can be used as a multimodal contrast agent for MRI, fluorescence techniques and photoacoustic imaging (PAI). In addition, the potential of gold nanoshells as a platform for analytical applications is demonstrated in a case study on the functionalization of the gold surface with a urea-based receptor for sensing of fluoride anions.

Gold nanoshells with silica-coated Mn-Zn ferrite cores were obtained by a multistep procedure: (1) hydrothermal synthesis of Mn<sub>0.7</sub>Zn<sub>0.3</sub>Fe<sub>2</sub>O<sub>4</sub> nanoparticles with the mean crystallite size of 12 nm, (2) encapsulation into silica by the Stober process, (3) electrostatic self-assembly of polyelectrolyte multilayer that alters the negative zeta potential of silica to positive values, (4) adsorption of negatively charged  $\approx$ 3 nm gold seeds, (5) growth of the gold seeds to coalescence by reduction of a soluble Au(II) precursor. For the construction of a multimodal contrast agent capable of pH sensing, the gold surface was co-functionalized with 4-mercaptopbenzoic acid (MBA) as a SERS-active pH sensor and 7-mercaptop-4-methylcoumarin (MMC) as a fluorescent tag. <sup>1</sup>H NMR relaxometry revealed a very high transverse relaxation ( $r_2 \approx 900 \text{ s}^{-1} \text{ mmol}^{-1} \text{ L}$ , per formula unit of the ferrite), demonstrating its suitability for MRI, while a proof-of-concept PAI study evidenced a strong contrast effect with the maximum photoacoustic signal at  $\approx$ 700 nm, which corresponded to the maximum of surface plasmon resonance in the UV-Vis spectrum. Importantly, the SERS study evidenced a pH-dependent spectral response (Fig. 2a).

In the case study on the use of gold nanoshells for sensing of fluoride anions, the nanoshells were co-functionalized with the molecular sensor N-(4-nitrophenyl)-N'-(4-nitrophenyl)urea, synthesized directly on the gold surface, and the internal standard 4-nitrothiophenol (NTP). The SERS study in acetonitrile solutions of tetrabutylammonium fluoride (NBu<sub>4</sub>F) showed that the spectral response of the urea sensor was dependent on the concentration of the fluoride in the range of  $[10^5 - 10^1 \text{ mol L}^{-1}]$ .

Fig. 2. SERS studies of gold nanoshells for sensing applications: (a) pH-dependent intensity of the MBA band at  $1077 \text{ cm}^{-1}$  in the spectra of nanoshells functionalized with MBA and MMC. (b) dependence of the intensity (in the 2<sup>nd</sup> derivative) of the urea band at  $1080 \text{ cm}^{-1}$  on the fluoride concentration in an acetonitrile suspension of nanoshells functionalized with the urea receptor and NTP. Normalization of the spectra was carried out by using selected bands of MMC and NTP in (a) and (b), respectively.

## Development of multimodal phantoms for Magnetic Resonance Imaging and Magnetic Particle Imaging

Maria Alejandra Ardila Arenas<sup>1,2</sup>, Dirk Gutkovich<sup>1</sup>, Olaf Kosch<sup>1</sup>, Frank Wiekhorst<sup>1</sup>, Norbert Löwa<sup>1\*</sup>

<sup>1</sup> Physikalisch-Technische Bundesanstalt, 8.23 Metrology for Magnetic Nanoparticles, Germany,

<sup>2</sup> Institución Universitaria ITM, Departamento de Ciencias Aplicadas, Colombia.

\* Email: norbert.loewa@ptb.de

Magnetic particle imaging (MPI) is an emerging quantitative imaging technology visualizing the 3D distribution of MNP used as tracers, *in vivo*. However, since the signal is generated only by the MNP, the surrounding biological tissue cannot be imaged directly. Therefore, another imaging technique, such as magnetic resonance imaging (MRI), is usually used to provide anatomical information. For experiment planning, quality assurance, as well as validation, multimodal phantoms are required that serve both imaging modalities simultaneously. MPI phantoms are usually solid bodies with cavities of different sizes and geometries filled with different concentrations of MPI tracer. Biomimetic phantoms with cavities corresponding to anatomical geometries are used to simulate the uptake of MPI tracer in a given organ. Whereas MRI phantoms mostly consist of a gel (e.g., agar) to achieve the imaging properties of human tissue. These types of phantoms are usually produced by conventional processing techniques, such as molding and casting. In these existing forms, neither MPI nor MRI phantoms are compatible for imaging with the other modality. Due to the constraints of conventional manufacturing techniques, geometric freedom in the production of phantoms is limited.

In this work, we present the development of a multimodal phantom using additive manufacturing (AM) and address the challenges in selecting appropriate materials for the fabrication of MPI/MRI phantoms. Physical parameters of five commercially available materials for AM were evaluated, including absorption (of MPI-tracer), Shore hardness, aging, and printing accuracy. Time-domain Nuclear Magnetic Resonance (1D-NMR) was used to analyse the MRI performance of these materials. The materials were checked for potential magnetic contaminations and unwanted MPI tracer absorption by magnetic particle spectroscopy (MPS, i.e., 0-dimensional MPS). Of all investigated materials, silicone (Dreve, Biotez) exhibited the best properties (see Fig.) with a sufficient material signal ( $T_2=26$  ms,  $T_1=397$  ms) and the lowest absorption of MPI-tracer at the interface of AM materials (900 ng(Fe)/cm<sup>3</sup>).

From this, a phantom consisting of MR-visible silicon material (BioTec, Dreve) was designed and fabricated by AM (3D+, Rapidshape) that contained a cavities filled with an MPI-visible tracer (Synonag, Micromod Partikeltechnologie GmbH). The multimodal phantom was successfully imaged with MPI (preclinical MRI scanner, Bruker) and MRI (1T ICON, Bruker).

Additive manufacturing of silicone components that are MRI visible and compatible with MPI tracers enable flexible fabrication of MPI/MRI phantoms. In the future, composites made of silicone with embedded MNP will be developed that can be processed in multi-material AM systems. This would enable the fabrication of multimodal silicone phantoms with controllable magnetic properties within one single AM system.

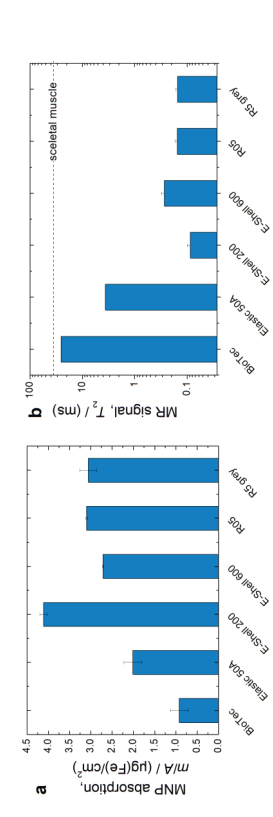


Figure. (a) MNP absorption in different AM materials quantified by MPS. (b) MR signal ( $T_2$  relaxation time) of AM materials measured by TD-NMR.

### Acknowledgement:

This project was funded by the Deutsche Forschungsgemeinschaft (DFG) within the research grants "Matrix in Vision" (SFB 1340/1 2018, no. 372486779, project A02), "cellMPI" (455706279), FOR917, 39748333/SFB 759 TFR 23/9/1, and DAAD (57177123). We further thank the B-smart Lab of PTB for the support with additive manufacturing.

[1] Uebel R, Schilher D. *Nat. Rev. Microbiol.* 2016; 14: 621

[2] Mickoleit F., et al. *Small* 2020; 16, 1906922

[3] Mittmann E., Mickoleit F., et al. submitted to ACS Appl. Mater. Interfaces

## Generation of reusable nano-biocatalysts by genetic engineering and functionalization of bacterial magnetic nanoparticles

Frank Mickoleit<sup>1</sup>, Esther Mittmann<sup>2</sup>, Clarissa Lanzloth<sup>1</sup>, Denis S. Maier<sup>1</sup>, Christof M. Niemeyer<sup>2</sup>,

Kersten S. Rabé<sup>2</sup>, Dirk Schilher<sup>1</sup>

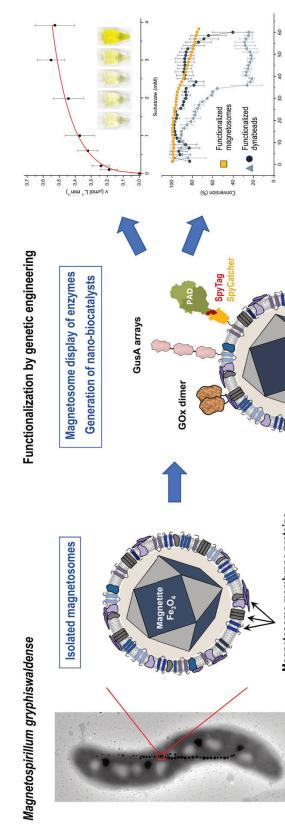
<sup>1</sup> Dept. Microbiology, University of Bayreuth, Universitätsstraße 30, D-95447 Bayreuth, Germany

<sup>2</sup> Institute for Biological Interfaces 1, Karlsruhe Institute of Technology (KIT), Hermann-von-Helmholtz-Platz 1, D-76344 Eggenstein-Leopoldshafen, Germany

E-mail: frank.mickoleit@uni-bayreuth.de

Magnetosomes are biogenic magnetic nanoparticles biosynthesized by magnetotactic bacteria. In the alphaproteobacterium *Magnetospirillum gryphiswaldense* they consist of a mono-crystalline core of chemically pure magnetite ( $\text{Fe}_3\text{O}_4$ ) that is surrounded by a biological membrane. Subtle control on each step of biomagnetization generates nanoparticles with unique characteristics such as high crystallinity, strong magnetization and a narrow particle size distribution. In addition, the enveloping membrane is accessible to genetic engineering and provides sites for covalent attachment of foreign protein "cargo".<sup>[1]</sup> Using optimized expression cassettes that enable the highly selective and controllable magnetosome display of functional moieties at distinct stoichiometries, a "set" of model particles was generated that feature one or several catalytically active enzyme proteins on the surface. Using the examples of the reporter enzyme glucose oxidase (GOx) and the biotechnologically more relevant glucose oxidase (GOx), we could demonstrate that even multimeric and cofactor-dependent enzymes can be stably expressed on the magnetosome surface. Kinetic parameters suggest the successful oligomerization of single monomers into functional units, which might be facilitated and stabilized by immobilization on the magnetic carrier "material".<sup>[2]</sup>

In order to further enhance the flexibility of the magnetosome display system, we investigated the expression of versatile coupling groups, thereby turning the particle surface into a multimodal platform for the immobilization of complementary-tagged protein cargo. Utilizing the Spy Tag-SpyCatcher biocoujugate system, we coupled a SpyTag-equipped version of a phenolic acid decarboxylase (PAD) to SpyCatcher-displaying magnetosomes.<sup>[3]</sup> The functionalized magnetosomes outperformed similarly functionalized commercial particles by exhibiting high catalytic activities and stable substrate conversion. Moreover, they could be efficiently utilized as reusable bio-nanocatalysis in flow processes, thereby significantly expanding the genetic toolbox for particle surface functionalization.



*In vivo* functionalization of bacterial magnetosomes. Foreign protein cargo is displayed on the magnetosome surface by genetic engineering, thereby generating nano-biocatalysts that provide stable substrate conversion and high enzymatic activities.

## Structural and magnetic characterization of citrate-coated superparamagnetic iron oxide nanoparticles for magnetically controlled immune therapy

<sup>1,2</sup> Amal Nasser<sup>1</sup>, Artem Feotystov<sup>1</sup>, Oleg Petracic<sup>3</sup>, Harald Unterweger<sup>4</sup>, Rainer Tietze<sup>4</sup>, Xiao Sun<sup>5</sup>,

Asmaa Qdemat<sup>1</sup>, Thomas Brückel<sup>3</sup>

<sup>1</sup> Forschungszentrum Jülich GmbH, Jülich Centre for Neutron Science ICNS at Heinz Maier-Leibnitz Zentrum MLZ, Garching, Germany

<sup>2</sup> Department of Physics, Technical University Munich (TUM), Garching, Germany

<sup>3</sup> Forschungszentrum Jülich GmbH, Jülich Centre for Neutron Science JCNS-2 and Peter Grünberg Institute PGI-4, Jülich, Germany

<sup>4</sup> Department of Otorhinolaryngology, Head and Neck Surgery, Section of Experimental Oncology and Nanomedicine (SEON), Else Kröner Fresenius-Stiftung-Professorship, University Hospital Erlangen, Erlangen, Germany

<sup>5</sup> Deutsches Elektronen-Synchrotron DESY, Hamburg, Germany

Superparamagnetic iron oxide nanoparticles (SPIONs) are promising for biomedical applications such as drug delivery, imaging, and magnetic hyperthermia. In our work, we used water-based SPIONs coated with citrate molecules (SPION<sup>Citrate</sup>) to obtain highly cytocompatible and stable particles in blood. In the magnetically controlled immune therapy the T cells, which are part of the immune system, are loaded with such SPIONs and are guided into a certain region of the body using a magnetic field gradient. The aggregation behavior of SPIONs is crucial for proper utilization and this is determined by their interface properties. Thus, a detailed knowledge of the inter-particle structural organization and their resulting magnetic properties is of great importance to avoid thromboembolic effects caused by agglomeration of released particles during future *in vivo* application and optimize the nanoparticle response to the applied magnetic field.

SPION<sup>Citrate</sup> was synthesized and stored in dry form. To obtain the properties of interest described above, the dry particles were dissolved in water and immobilized in an amorphous matrix of poly(ethylene glycol) crosslinked with DMPA (2-Dimethoxy-2-phenylacetophenone). The morphology of the particles in water and in solid matrix was determined by small angle x-ray scattering (SAXS) and transmission electron cryomicroscopy (Cryo-TEM). The TEM and SAXS results indicated a formation of large particle aggregates with an average size of 60 nm. However, the magnetometry data on the immobilized SPION<sup>Citrate</sup> (crosslinked in polymer matrix) points to the classical superparamagnetic behavior of single particles with a small size distribution. The obtained blocking temperature of 154 K corresponds rather to a particle diameter of 10-15 nm.

As a future plan, small-angle neutron scattering (SANS) experiment combined with contrast variation will be performed to obtain information about the internal structure of the particle aggregation. Additionally, SANS in magnetic field will be performed to directly determine the ensemble's magnetic size and clarify this surprising magnetic behavior.

## TiO<sub>2</sub> magnetic nanotubes for RNA isolation from complex biological samples

Denisa Smela<sup>1\*</sup>, Jan M. Macák<sup>2,3</sup>, Zuzana Bilková<sup>1</sup>

<sup>1</sup> Department of Biological and Biochemical Sciences, Faculty of Chemical Technology, University of Pardubice, Pardubice, Czech Republic

<sup>2</sup> Center of Materials and Nanotechnologies, Faculty of Chemical Technology, University of Pardubice, Pardubice, Czech Republic

<sup>3</sup> Central European Institute of Technology, Brno University of Technology, Brno, Czech Republic  
\* Email: Denisa.Smela@upce.cz

Commonly used methods for RNA isolation from biological samples are based on liquid-liquid extraction or solid-phase extraction. Very often, the commercial kits and methods for RNA isolation use chemicals such as phenol and chloroform, which are hazardous to work with and can also cause contamination of the final product. We wanted to develop a new method of RNA isolation from cells or from biological fluids that would be safer to perform and possibly more affordable as well. It was previously described, that materials based on TiO<sub>2</sub> have an affinity to nucleic acids thanks to their strong interactions with phosphate backbone. Nucleic acids are negatively charged and the charge of TiO<sub>2</sub> under acidic conditions is strongly positive. In addition, it was suggested that the adsorption of DNA on TiO<sub>2</sub> is caused by interaction between DNA and hydroxyl groups on the surface of TiO<sub>2</sub> [1]. Similar principles apply for TiO<sub>2</sub> interactions with RNA. In our work, we tested different materials based on TiO<sub>2</sub> to determine their applicability for RNA isolation. Among other materials, we used newly developed TiO<sub>2</sub> nanotubes coated with Fe<sub>3</sub>O<sub>4</sub> (TiO<sub>2</sub>NTs@Fe<sub>3</sub>O<sub>4</sub>NPs, CEMNAT). Magnetic properties of this material offered advantage in higher affinity towards RNA as well as an easier and faster performance of the protocol. This material was also successfully used for SARS-CoV-2 viral RNA isolation.

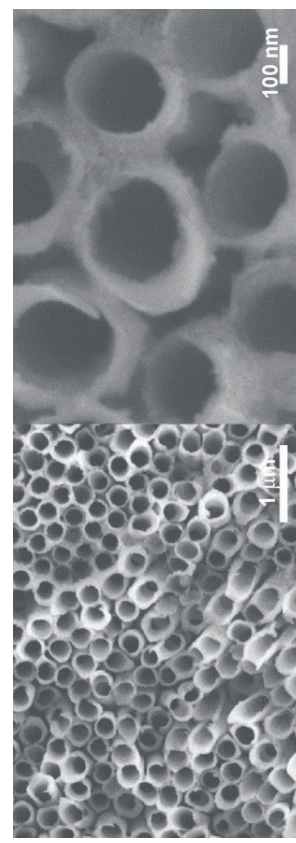


Figure 1: Structure of TiO<sub>2</sub> magnetic nanotubes, captured by SEM.

This work was supported by OP RDE project 'Strengthening interdisciplinary cooperation in research of nanomaterials and their effects on living organisms' [CZ.02.1.01/0.0/0.0/17\_048/0007421].

[1] Amano T., Toyooka T., Ibuki Y., *Science of The Total Environment* **2009**, 408(3), 480-5.

## Combining iron oxide nanoparticles and fluorescent protein for selective magnetic nanoheating studies

Illaria Armenia<sup>1\*</sup>, Jesús G. Ovejero<sup>2</sup>, David Serantes<sup>3</sup>, Nicoll Zaballos<sup>4</sup>, Fernando López-Gallego<sup>4</sup>, Jesús Martínez de la Fuente<sup>1,5</sup>, María del Puerto Morales<sup>2</sup>, Valeria Grazi<sup>1,5</sup>

<sup>1</sup>BioNanoSurf Group, Aragon Nanoscience and Materials Institute (INMA-CSIC-UNIZAR), Edificio I-D, 50018 Zaragoza, Spain.

<sup>2</sup>ManBio Group, Instituto de Ciencia de Materiales de Madrid (ICMM/CSIC), Calle Serrano Inés de la Cruz, 3, 28049, Madrid, Spain

<sup>3</sup>Applied Physics Department and Instituto de Investigación Tecnológicas, Universidad de Santiago de Compostela, 15782 Santiago de Compostela, Spain

<sup>4</sup>HeBioCat Group, CIC biomaGUNE, Miranón Pasealekua, 182, 20014 Donostia, Gipuzkoa, Spain.

<sup>5</sup>Centro de Investigación Biomédica en Red de Bioingeniería, Biomaterias y Nanomedicina (CIBER-BBN), Avenida Monforte de Lemos, 3-5, 28029 Madrid, Spain

\*E-mail: illaria.armenia@unizar.es

The heating properties of the magnetic nanoparticles (MNPs) have been extensively applied in medicine for thermal treatments of tumours, by taking advantage of the capability of the MNPs to absorb magnetic energy and dissipate it as heat when exposed to an alternating magnetic field (AMF). Only recently, this property has been explored for the regulation of enzymatic processes, where an extreme control of the local temperature is needed to obtain a fine tuning of the enzyme activity. This tuning can be reached by modulating the properties of the magnetic nanoparticles, such as composition, size, shape and aggregation state, or the frequency and field intensity of the AMF. A crucial point in finding the best activation conditions is the correct measurement of the local temperature reached during AMF activation at the active position of the enzyme. Commonly used systems, such as fluorophores or lanthanides, are not suitable for simulating the behaviour of a protein due to their small size and low complexity of their structure. Here, we report the use of fluorescent proteins, the Green Fluorescent Protein (GFP) or the Red Fluorescent Protein (RFP), as molecular thermometers immobilized to the magnetic nanoparticles, to simulate the one-pot activation of two proteins under AMF. These proteins possess, indeed, a temperature dependence decay of their fluorescence that can be easily monitored, furthermore, their emission spectra are compatible for a one-pot detection. We demonstrate the possibility to selectively activate the MNPs by adjusting the AMF conditions. Moreover, the differences in local heating observed among the different MNP systems under the same or different AMF settings support the feasibility to achieve simultaneously or sequentially different local temperatures in a one-pot scheme, paving the path for the implementation of a selective regulation of multi-enzymatic reactions.

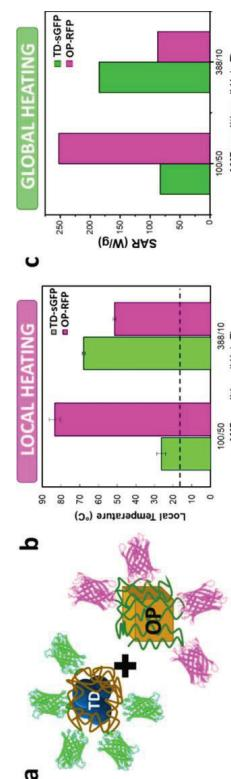


Figure 1. (a) OP-RFP and TD-sGFP complexes scheme (b) Estimated local temperature ( $T_{loc}$ ) registered from sGFP and RFP fluorescence in the mixture colloid after 5 min of exposure to AMF<sub>1</sub> = 100 kHz to 50 mT and AMF<sub>2</sub> = 388 kHz to 10 mT. Black dash line indicates the global temperature registered in the medium. (c) SAR registered for individual concentrated colloids (1 mg/mL) of OP-RFP and TD-sGFP at AMF<sub>1</sub> and AMF<sub>2</sub>.

### Acknowledgements

The research for this work has received funding from the European Union (EU) project HOTZYMEs (grant agreement n° 829162) under EU's Horizon 2020 Programme Research and Innovation actions H2020-FETOPEN-2018-2019-2020-01. Authors also thank Spanish MINECO project BIO2017-84246-C2-1-R and DGA and Fondos Feder (Bionanosurf E15\_17R).

## Magnetic Nanoparticle transformations and the effect on their heating properties

Yilian Fernández-Afonso<sup>1,2</sup>, Laura Asín<sup>1,3</sup>, Lilianne Beota<sup>1</sup>, Raluca M. Fratilă<sup>1,3,4</sup>, Lucía Gutiérrez<sup>1,2,3</sup>

<sup>1</sup>Institute of Nanoscience and Materials of Aragon (INMA-CSIC/University of Zaragoza), 50018 Zaragoza, Spain.

<sup>2</sup>Departamento de Química Analítica, Universidad de Zaragoza, Zaragoza, Spain. <sup>3</sup>Centro de Investigación Biomédica en Red de Bioingeniería, Biomaterias y Nanomedicina (CIBER-BBN), 50018 Spain. <sup>4</sup>Organic Chemistry Department, Universidad de Zaragoza, Zaragoza, Spain.

E-mail: yfaezarsonso@gmail.com  
In the Magnetic Hyperthermia (MH) and Photothermal Therapy (PTT) applications, magnetic nanoparticles (MNPs) are used as an "antenna" able to capture energy (either from an alternating magnetic field (AMF) or a near infrared (NIR) light) and transform it into local heat. In the frame of this therapy design, it is fundamental to know how possible particle transformation would affect its performance over time.

In this work, we used MNPs with two different coatings (dimercaptosuccinic acid - DMAA-NP<sub>s</sub> and poly(maleic anhydride-alt-1-octadecene) - PMAO-NP<sub>s</sub>) but with same magnetic core ( $\approx$ 13.5 nm) (Figure 1A). We evaluated how the MNP coating affects their degradation profile using a medium that simulates the lysosomal conditions and how this degradation affects their heating performance in the frame of both magnetic hyperthermia and photothermal treatments. The faster degradation of DMAA-NPs in comparison with PMAO-NPs was verified by transmission electron microscopy (TEM), magnetic and colorimetric measurements (Figure 1B).

To track how the transformations suffered by the particles along their degradation process affected their heating properties, magnetic hyperthermia and photothermal measurements were performed (Figure 1C). In both cases, the degradation process resulted in a decrease of the heating capacity of both types of materials. As a result of the faster degradation of DMAA-NPs, the reduction of the heating properties along time was increased for this material when compared to PMAO-NPs.

Thus, the less prone to degradation nanoparticles (PMAO-NPs) were selected for the *in vivo* analysis, to evaluate the degradation speed of this material in tumor tissues. In this study, although the number of particles decreased in the tumors along time after their administration, no transformations in the average particle size of particles occurred (Figure 1D).

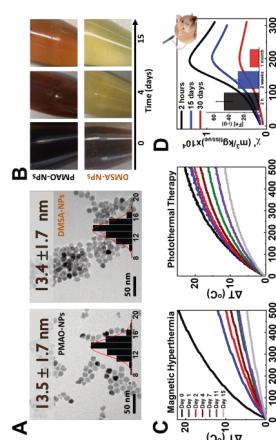


Figure 1. A) TEM images and particle size distribution of the nanoparticles used. B) Photos of the nanoparticle suspensions at different times during the degradation process. C) Magnetic Hyperthermia and photothermal measurements of the AC magnetic susceptibility profiles of the particles in the tumor calculated from the out-of-phase susceptibility data.

## Reversible chain formation during magnetic hyperthermia experiments

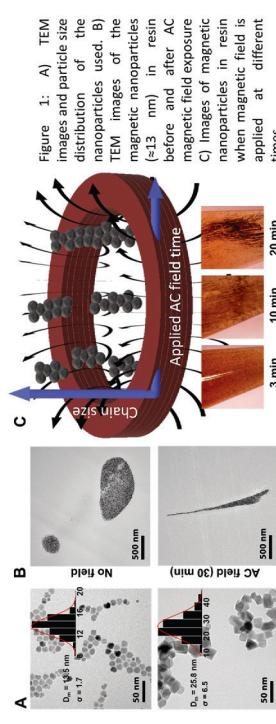
Ylian Fernández-Afonso<sup>1</sup>, David Serantes<sup>2</sup>, Sergiu Ruta<sup>3</sup>, Samuel E. Rannala<sup>4</sup>, Raluca M. Fratila<sup>5</sup>, Sabino Veintemillas-Verdaguera<sup>6</sup>, M. Puerto Morales<sup>6</sup>, Roy W Chantrell<sup>4</sup>, Lucía Gutiérrez<sup>1</sup>

<sup>1</sup> Department of Analytical Chemistry, Universidad de Zaragoza, Spain, <sup>2</sup> Applied Physics Department, Universidad de Santiago de Compostela, Spain, <sup>3</sup> College of Business, Technology and Engineering, Sheffield Hallam University, UK, <sup>4</sup> Department of Physics, University of York, UK, <sup>5</sup> Organic Chemistry Department, Universidad de Zaragoza, Zaragoza, Spain, <sup>6</sup> Materials Science Institute of Madrid (ICMM/CSCIC), Spain  
email: yldezafonso@gmail.com

In addition to the AC field conditions or the particle average size, others factors, often neglected, may play a fundamental role on the heating capacity of magnetic nanoparticles during magnetic hyperthermia treatments. In particular, the organization of particles into assemblies, such as chains, as a consequence of the AC field exposure has been poorly studied. Previous theoretical works had shown the impact of chaining on the heating properties of magnetic nanoparticles [1] and very recently the formation of chains or columns along the magnetic field direction during hyperthermia experiments has been demonstrated experimentally [2].

In this work, we have used two types of particles ( $\approx 13$  nm spherical and  $\approx 26$  nm octahedral) (Figure 1A) and several experimental set-ups to evaluate the chain formation over time during magnetic hyperthermia experiments. First, the particles were dispersed in a resin and this suspension was placed in a magnetic hyperthermia device with a closed coil. The alternating magnetic field was applied during 30 min. After, the sample exposed to the AC field and the control suspension was placed to a thermomixer at 60°C so that the resin fully polymerized. For small particles, long chains were observed by TEM in the sample exposed to the AC field but not in the sample not exposed to the AC field (Figure 1B). In contrast, for bigger particles, macroscopic chains were observed in the sample exposed to the AC field only. The effect of chain formation is investigating using computation model.

The dynamics of chain formation at different applied field times were studied using the 26 nm octahedral nanoparticles. An increase of the chain length over time under the exposure to the AC magnetic field was observed (Figure 1C). Once the magnetic field was removed, chains started to break down. This chain formation during the magnetic hyperthermia measurements may be a critical parameter to consider in the study of the heating properties of magnetic nanoparticles in the frame of magnetic hyperthermia.



- (1) Balakrishnan, P. B.; Silvestri, N.; Fernández-Cabada, T.; Marinato, F.; Fernandes, S.; Fiorito, S.; Miscuglio, M.; Serantes, D.; Ruta, S.; Livesey, K., et al. *Advanced Materials* **2020**, *32*, 2003712.  
(2) Mille, N.; De Masi, D.; Faure, S.; Asensio, J.; Chaudret, B.; Carrey, J. *Applied Physics Letters* **2021**, *119*, 022407.

## Cell membrane hyperfluidization with localized magnetic and optical hyperthermia

Javier Idiago-López<sup>1,2</sup>, Ylian Fernández-Afonso<sup>1</sup>, Eduardo Moreno-Antolín<sup>1</sup>, Valeria Gražul<sup>1,2</sup>, Lucía Gutiérrez<sup>1,2</sup>, Jesús Martínez de la Fuente<sup>1,2</sup> and Raluca M. Fratila<sup>1,2,3</sup>  
<sup>1</sup> Institute of Nanoscience and Materials of Aragon (INMA-CSIC)/University of Zaragoza, Zaragoza, Spain, <sup>2</sup> Centro de Investigación Biomédica en Red en Bioingeniería, Biomateriales y Nanomedicina (CIBER-BBN), Zaragoza, Spain, <sup>3</sup> Universidad de Zaragoza, Organic Chemistry Department  
Email: rfratila@unizar.es

One of the most interesting features of magnetic nanoparticles (MNPs) is their ability of producing heat when exposed to an alternating magnetic field (AMF) or to near-infrared (NIR) light. These processes are known as magnetic hyperthermia (MH) or optical hyperthermia (OH), respectively, and have been exploited mostly as co-adjuvant oncological therapies. In this work, we report our preliminary results regarding the disruptive use of MNP-based hyperthermia as a tool for modulating the biophysical properties of the cell plasma membrane. Our hypothesis was that MNPs bound to the cell membrane could act as nanohanders and lead to localized heating areas on the surface of living cells ("hotspots") upon exposure to a NIR laser or an AMF.

To immobilize MNPs on living cell membranes, we used the strain-promoted [3+2] azide-alkyne cycloaddition (SPAAC). The advantage of using a covalent reaction for the MNP immobilization is that it avoids their rapid internalization, which usually takes place when employing ligand-receptor binding. To this end, we installed artificial azide reporters on the surface of human colorectal carcinoma cells (HTCT116) and we functionalized iron oxide MNPs with a dibenzocyclooctyne (DBCO) derivative. The successful immobilization of the MNPs on the cell membrane was confirmed with electron microscopy, flow cytometry and elemental mass analysis. We then demonstrated that these MNPs can generate a localized heating of the cell membrane and lead to transient changes in cell membrane fluidity and permeability. We monitored the internalization of a cell-impermeant fluorescent probe (YOPRO-1), promoted by the application of an AMF or a NIR laser during 30 min. Interestingly, cell viability studies indicated the absence of apoptotic effects, reactive oxygen species (ROS) generation and alterations of the cell cycle after the thermal stimulus. All these results are encouraging for the development of a new method for intracellular delivery of exogenous molecules based on localized heating, without compromising cell viability.

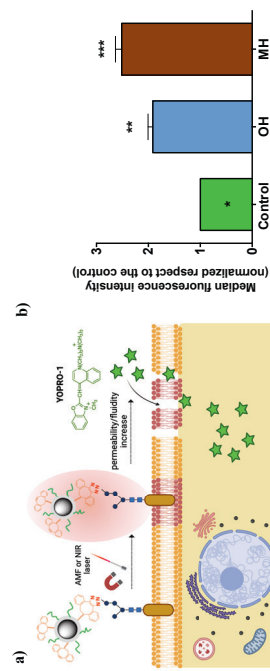


Figure 1. a) Scheme of cell membrane hyperfluidization with localized hyperthermia. b) Flow cytometry analysis of YOPO-1 internalization in HCT116 cells promoted by cell membrane hyperfluidization.

## PICKERING EMULSIONS STABILIZED BY MAGNETITE PARTICLES IN A ROTATING MAGNETIC FIELD

Rafał Bielaś, Bassam Jameel, Andrzej Skumiel and Arkadiusz Józefczak\*

Chair of Acoustics, Faculty of Physics, Adam Mickiewicz University in Poznań  
Uniwersytetu Poznańskiego 2, 61-614 Poznań, Poland

\* e-mail: arkadiusz.jozefczak@amu.edu.pl

A Pickering emulsion is an emulsion stabilized by solid particles that accumulate at the surface of droplets. Depending on the application, different types of particles can be utilized as stabilizers including magnetic particles that become a heat source when exposed to alternating magnetic fields. The magnetic field-induced temperature increase of the emulsion system was recently shown, among others, to form colloidal capsules from Pickering droplets precursors [1]. While most researchers use an oscillating magnetic field because it is relatively easy to generate, there has been another approach, namely the use of rotating magnetic fields (RMF) which could yield a higher heat output. Our study presents the results of the calorimetric measurements in oil-in-oil emulsion stabilized by magnetic nano- and microparticles under the influence of RMF. In our system, such a field is produced by four separate magnetic fluxes shifted in phase and space by 90° (Fig. 1a). The promising results show that RMF can be used for efficient heating of Pickering emulsion stabilized by magnetic particles (Fig. 1b).

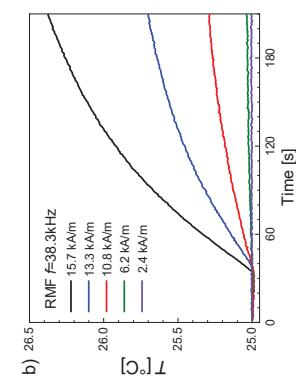
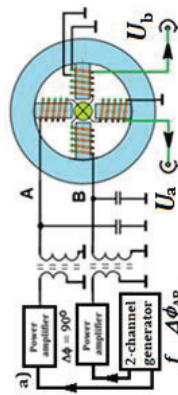


Fig. 1 a) Experimental setup used for generating a rotating magnetic field. b) Temperature increase measured in magnetic Pickering emulsions under the rotating magnetic field (RMF).

[1] R. Bielaś, D. Surekko, K. Kaczmara, A. Józefczak, The potential of magnetic heating for fabricating Pickering-emulsion-based capsules, *Colloids Surf. B* 192 (2020) 111070.

### Acknowledgments

This work was supported by the project no. 2019/35/O/ST3/00503 (PRELUDIUM BIS) of the Polish National Science Centre.

## Temperature-controlled drug release from magnetic PLGA nanospheres enabling efficient treatment of pancreatic cancer cells

Oliver Reisen<sup>1</sup>, Benedikt Mues<sup>1</sup>, Eva M. Buhl<sup>2</sup>, Ajali A. Röth<sup>3</sup>, Ioana Slabu<sup>1\*</sup>

<sup>1</sup>Institute of Applied Medical Engineering, Helmholtz Institute, Medical Faculty, RWTH Aachen University, Pauwelsstr. 20, 52074 Aachen, Germany

<sup>2</sup>Institute of Pathology, Electron Microscopy Facility, RWTH University Hospital Aachen, Pauwelsstr. 30, 52074 Aachen, Germany

<sup>3</sup>Department of General, Visceral and Transplant Surgery, RWTH University Hospital Aachen, Pauwelsstr. 30, 52074 Aachen, Germany

E-mail: reisen@ame.rwth-aachen.de | \*slabu@ame.rwth-aachen.de

For tumors like pancreatic cancer with high risk of early metastasis, conventional cancer therapies are mainly limited to systemic chemotherapy treatment causing severe side effects and having low therapeutic success. To reduce whole body exposition to the drug and raise the local drug concentration, controlled drug guidance and release is necessary. Such therapeutic approach can be enabled by magnetic nanoparticles (MNP). For this, MNP and cytostatic drugs are loaded inside biodegradable thermo-responsive poly-(lactide-co-glycolide) acid (PLGA) nanospheres. By application of a combination of static and alternating magnetic fields, the PLGA nanospheres can be accumulated at the tumor site and then heated inducing hyperthermia ( $>43^{\circ}\text{C}$ ) and temperature-controlled local drug release. The MNP-induced hyperthermia boosts the therapeutic efficiency of cytostatic drugs leading to a highly efficient tumor treatment.

In this work, the combined therapy of hyperthermia and drug release is tested with pancreatic tumor cells. For this, thermo-responsive magnetic PLGA nanospheres (Figure 1A) were synthesized. The PLGA nanospheres were loaded with cytostatics and MNP yielding a therapeutically relevant range and incubated for 24 h with MIA PaCa-2 cells. The internalization kinetics of the magnetic PLGA nanosphere into pancreatic cancer cells was tracked and determined *in vitro* via TEM. The cells were exposed to an alternating magnetic field for different time intervals  $t = (0, 30, 90)$  min and reached hyperthermic conditions of ca.  $43.6^{\circ}\text{C}$ . The effect on the MIA PaCa-2 cell viability was determined 24 h after treatment. Comparing the effects of either cytostatics or hyperthermia monotherapy and the combinational therapy for different treatment durations, the combined therapy shows significantly lower cell viability values (Figure 1B). The combined therapy was successfully demonstrated.

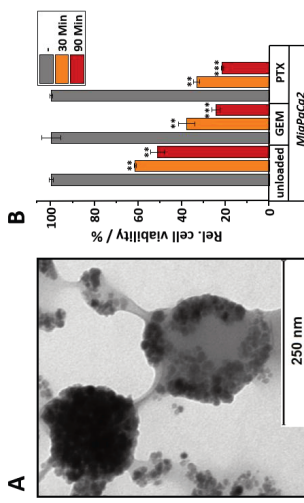


Figure 1: A) TEM image of Paclitaxel-loaded PLGA-MNP with an average diameter of 234 nm. B) Cell viability after three different treatment combinations of hyperthermia and cytostatics release for a pancreatic cancer cell line.

## Photothermal therapy for *in vitro* multimodal treatment of peritoneal carcinomatosis

Claudia Lozano-Pedraza<sup>1\*</sup>, Francisco Sanz-Rodríguez<sup>2,3</sup>, and Francisco J. Teran<sup>1,4</sup>

<sup>1</sup> Aldea Nanociencia, Campus Universitaria de Cantoblanco, 28049 Madrid, Spain

<sup>2</sup> Fluorescence Imaging Group, Dpto Biología, Universidad Autónoma de Madrid 28049 Madrid, Spain

<sup>3</sup> Nanobiology Group, Instituto Ramón y Cajal de Investigación Sanitaria, Hospital Universitario Ramón y Cajal, 28034 Madrid, Spain

<sup>4</sup>Nanobiotecnología (InMed-Nanociencia), Unidad Asociada al CNB (CSIC), 28049 Madrid, Spain.

\*Email: claudia.lozano@imdea.org

Iron oxide nanoparticles (IONPs) are one of the most employed nanomaterials for biomedical purposes such as hyperthermia due to their high biocompatibility and their ability to release heat in response to different stimuli. Nanoparticle-mediated hyperthermia can be classified as magnetic hyperthermia (MHT) or photothermal therapy (PTT) depending on the activation mechanism: alternating magnetic fields (AMF) or near infrared radiation (NIR), respectively. Recent studies have shown that, in contrast to magnetic losses, optical losses remain invariable inside live cells. This PTT efficiency preservation represents a major advantage with respect to MHT. At the same time, heating mediated by IONPs is of particular interest to address therapeutics in some types of cancer requiring minimally invasive and efficient approaches. This is the case of peritoneal carcinomatosis, an aggressive spread of a primary tumour in the peritoneal cavity.

In this work, we have assessed the *in vitro* efficacy of combining PTT and mitomycin C (MMC) on peritoneal carcinomatosis in HCT-116 cell line. Initially, we have determined the average heat dose per cell released in order to perform dose ranging study. We have also studied the effects of the combination of PTT with MMC, a widely used chemotherapeutic agent. PTT was performed irradiating IONP-loaded cells with an 808 nm laser at 1.2 W/cm<sup>2</sup> for 30 minutes. Cell viability and cell morphology were evaluated 24 hours after treatment. The multimodal treatment was performed in cells loaded with both IONPs and MMC at different experimental conditions, varying the MMC concentration and the irradiation power. The intracellular average heat dose per cell was estimated by calorimetry under non-adiabatic conditions in IONP suspensions at the same irradiation conditions and iron concentration than the ones in IONP loaded cells. Cytotoxicity assays and cell morphology analysis indicates that PTT is able to reduce cell viability to 80% when temperature reaches 42°C. Similarly, MMC by itself is able to reduce cell viability from 80% to 10% depending on MMC concentration and incubation time. However, multimodal treatment shows a stronger cytotoxic effect even using moderate heat and MMC doses. When we analyze the type of cell death produced by these treatments with Hoechst-33342, both apoptotic and necrotic cell death are found. The origin of the synergy between PTT and MMC is studied in deep. However, the combinational treatment using both approaches shows an appealing potential for cancer therapy which could allow for reducing chemotherapy dose and consequently, its undesired side effects.

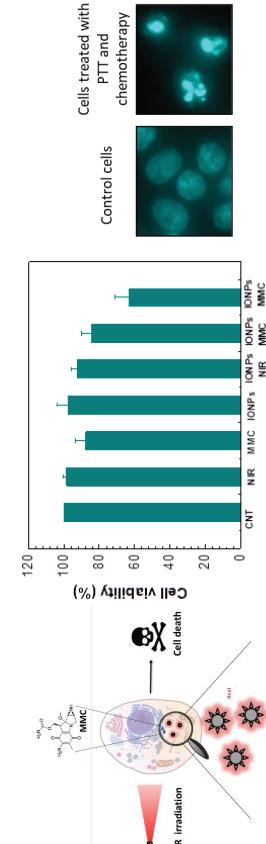


**Fig 1. HCT 116 cells treated with multimodal treatment using PTT and MMC.** A) Schematic representation of multimodal treatment. B) Cell viability of HCT-116 cells after 24 hours of multimodal treatment (10 mM MMC, 50 µg/mL Fe, 1.5 W/cm<sup>2</sup>). C) HCT-116 cells stained with Hoechst-33342 24 hours after multimodal treatment (40 mM MMCF65, 50 µg/mL Fe, 1.5 W/cm<sup>2</sup>).

## Tuning the Dynamics in $\text{Fe}_3\text{O}_4$ nanoparticles for Hyperthermia Optimization

Hao Chen<sup>1</sup>, David Billington<sup>2</sup>, Edward Riordan<sup>2</sup>, Jakob Blomgren<sup>3</sup>, Sean R. Giblin<sup>3</sup>, Christer Johansson<sup>2</sup>, Sara A. Majetich<sup>1,\*</sup>

<sup>1</sup> Department of Physics, Carnegie Mellon University, Pittsburgh, PA 15213, USA

<sup>2</sup> Department of Physics and Astronomy, Cardiff University, Cardiff CF24 3AA, UK

<sup>3</sup> Department of Smart Hardware, RISE Research Institutes of Sweden, Göteborg SE-411 33, Sweden

\*Corresponding author: sara@cmu.edu

Clinical magnetic hyperthermia uses a single excitation frequency, and the efficiency of heating depends on the overlap with the spectrum of relaxation frequencies for the magnetic nanoparticles. In addition to a particle size distribution ( $10.7 \pm 1.2$  nm), magnetostatic interactions among clustered particles also lead to a distribution of Néel relaxation rates. We used a model system of  $\text{Fe}_3\text{O}_4$  nanoparticles to study how magnetostatic interactions impact the real and imaginary parts of the AC magnetic susceptibility, measured over a wide range of excitation frequencies (10 kHz – 4 MHz) at different temperatures (100 K – 150 K). We find that both the relaxation peak frequency and amplitude can be tuned by the addition of a small DC field. This approach could be applied to match the magnetic hyperthermia excitation frequency and optimize heat delivery. The real ( $\chi'$ ) and imaginary ( $\chi''$ ) parts of the AC susceptibility reveal the distribution of relaxation frequencies (Fig. 1).

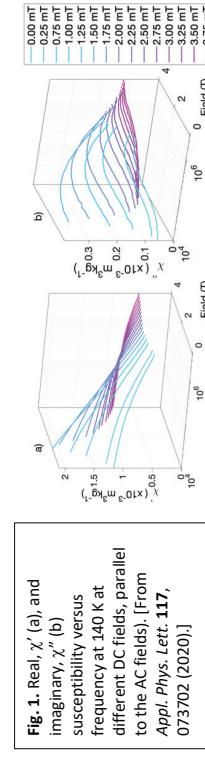


**Fig. 1. Real,  $\chi'$  (a), and imaginary,  $\chi''$  (b), susceptibility versus frequency at 140 K at different DC fields, parallel to the AC fields. [From Appl. Phys. Lett. 117, 073702 (2020).]**

The AC susceptibility as a function of a DC magnetic field provides insight about the blocking frequency distributions. Cole-Cole analysis of  $\chi''$  versus  $\chi'$  at fixed temperature revealed the average relaxation time  $\tau$  and relaxation time distribution as a function of  $H_{dc}$ . Large DC magnetic fields lock the spins in place, so that they respond minimally to a low amplitude AC driving field, and both  $\chi'$  and  $\chi''$  are very small across the entire frequency range. However, for smaller DC fields, surprisingly non-monotonic behavior is observed. The average  $\tau$  is sharply peaked, and is nearly 20 times larger at 1.25 mT than at  $H = 0$ , as shown in Figure 2. The dissipation at 100 kHz increases by a factor of 3.8 between 0 and 1.25 mT, which is very close to the  $H_{inc}$  estimated for with the Vogel-Fulcher scaling ( $\sim 1.5$  mT).

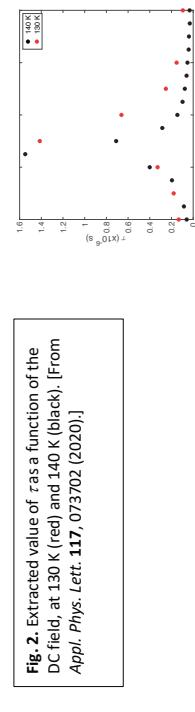


**Fig. 2. Extracted value of  $\tau$  as a function of the DC field, at 130 K (red) and 140 K (black). [From Appl. Phys. Lett. 117, 073702 (2020).]**

## The Impact of Alternating and Rotating Regimes on the Heating Characteristics of Magnetic Colloids and Dense Cellulose Structures.

Matus Molcan<sup>1,\*</sup>, Peter Kopancsik<sup>1</sup>, Milan Timko<sup>1</sup>, Kristina Zolochovska<sup>1</sup>, Ivo Safarik<sup>2,3</sup>, Andrzej Skunie<sup>1</sup>

<sup>1</sup> Institute of Experimental Physics, Slovak Academy of Sciences, Watsonova 47, Kosice, 04001, Slovakia

<sup>2</sup> Department of Nanobiotechnology, Biology Centre, ISB, CAS, Na Sádkach 7, 370 05 Ceske Budějovice, Czech Republic

<sup>3</sup> Regional Centre of Advanced Technologies and Materials, Czech Advanced Technology and Research Institute, Palacky University, Slechtitelu 27, 783 71 Olomouc, Czech Republic

<sup>4</sup> Faculty of Physics, Adam Mickiewicz University, Uniwersytetu Poznańskiego 2, 61-614, Poznań, Poland

\*Email: molcan@saske.sk

Magnetic hyperthermia is one of the established scientific fields in nanomedicine. Thanks to the huge number of possibilities how to influence the hyperthermic indicators, this area always offers new and interesting research stimuli.

The hyperthermia efficiency itself and the heating effect, is determined not only by the material properties but also by the technical-application factors. For this reason, we subjected our experimental materials to experiments in an alternating magnetic field (AMF) as well as in a rotating magnetic field (RMF). In general, according to known numerical models as well as comparative experiments, a higher efficiency is assumed in the case of the applied RMF.

As is shown in Figure 1, for the experimental Dextran FF sample, the  $dT/dt$  values are

significantly different when compared in RMF and AMF. Such tendency can be changed in the systems of higher density. This affects the particles' freedom of movement during field application, and thus there is a block of rotation. To research this, bacterial cellulose was magnetized in contact with magnetic fluid. By magnetic modification of bacterial cellulose, another range of potential applications is opened up including hyperthermia. Preliminary temperature evolution data of magnetized cellulose sample in RMF and AMF indicate a different behavior than in the case of a magnetic fluid.

Bacterial cellulose can be modified with a well-controlled amount of magnetic nanoparticles and can be potentially surgically located at the treated site. Such a system is promising for the synthesis of potential implants for multiple applications of an external magnetic field and repeated heating of cancer tissues. However, in the case of bacterial cellulose, it is necessary to consider the significant fixation of the particles in the cellulose structure.

The main goal of this study is to provide an analysis of various magnetic systems in the form of colloids and dense structures in conditions of rotating and oscillating magnetic fields.

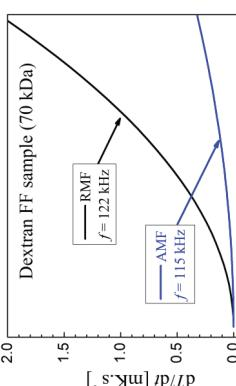


Figure 1 Comparison of the  $dT/dt$  dependence on the amplitude of the intensity  $H$  measured in RMF and AMF magnetic field in the Dextran FF sample.

## SAR determination from temperature measurement using repeated heating-cooling cycles

Sergiu Ruta<sup>1</sup>, Yilian F. Afonso<sup>2</sup>, Samuel E. Rannala<sup>3</sup>, Sabino Veintemillas-Verdaguer<sup>4</sup>, M. Puerto Morales<sup>4</sup>, David Serantes<sup>5</sup>, Lucia Gutierrez<sup>2</sup>, Roy W Chantrell<sup>3</sup>

<sup>1</sup> College of Business, Technology and Engineering, Sheffield Hallam University, UK

<sup>2</sup> Department of Analytical Chemistry, Universidad de Zaragoza, Spain

<sup>3</sup> Department of Physics, University of York, United Kingdom

<sup>4</sup> Materials Science Institute of Madrid (ICMM-CSIC), Spain

<sup>5</sup> Applied Physics Department, Universidade de Santiago de Compostela, Spain

In recent years magnetic hyperthermia has been proposed to help a range of biomedical applications such as a non-invasive alternative for cancer treatment. Accurate knowledge of the heating performance of magnetic nanoparticles (MNPs) under AC fields is critical for the development of hyperthermia-mediated applications. Usually, the heating efficiency reported in terms of the specific absorption rate (SAR) is obtained from the temperature variation ( $\Delta T$ ) vs. time ( $t$ ) curve (fig. 1a). Most estimates are based on simplified temperature dynamics such as adiabaticity (initial slope) or assuming Newton's law of cooling where the temperature evolution is defined as:

$$\frac{dT}{dt} = -a(T - T_{env}) + S_0, \quad (1)$$

where  $a$  stands for a characteristic relaxation time of the system, and  $S_0$  is defines the heating source ( $\sim$  SAR) and  $T_{env}$  is the environmental temperature. Such estimates are subjected to huge uncertainty due to dynamic changes in the sample or even from the measurement device/environment. For example, large variations in the heating efficiency of a given batch of particles have been reported when measured in different laboratories [1], under *a priori* the same experimental conditions.

In general, to have a correct description of the temperature evolution during hyperthermia protocol we need a detailed temperature profile both in time and space. This requires solving the full heat diffusion equation or the bioheat equation if the magnetic nanoparticles are in a biological environment [2]. We show, based on simulated heat diffusion, that for general magnetic hyperthermia conditions the heat profile is not uniform inside the sample. As a consequence the determination of SAR as described above leads to larger errors (figure 1c).

In this work, we present a novel protocol,

in which simple temperature measurements combined with eq. 1 can be used to obtain a more reliable SAR value, independent of environmental conditions (e.g. the device/laboratory). The proposed protocol is based on a set of repeated heating-cooling cycles as illustrated in figure 1b. To validate the protocol test cases are generated by numerically solving the heat diffusion equation considering the liquid, sample holder and surrounding environment (air). Although the temperature profile is not uniform, during a single heating-cooling cycle, there is a minimum variation in the spatial temperature profile between the final heating and the initial cooling processes. This allows for eq. 1 to be used at the transition from heating to cooling, leading to a more precise SAR determination. Examples of the error in determining SAR using a single (1c) or repeated heating-cooling cycles (1d) are shown in figure 1. The protocol has been successfully applied to experimental data of magnetic particles in liquid samples.

The proposed protocol will enable more accurate comparison of the SAR data generated by different laboratories. Also the new protocol can detect any time variation of SAR as for example during cluster formation during hyperthermia procedure, or variation of particle properties over time.

Figure 1: Diagram showing the single heat/cooling cycle (a) and the new protocol of repeated heating-cooling cycles (1b). Examples of error in SAR determination based on equation 1 for two test cases using the single heat/cooling cycle (c) and repeated heating-cooling cycles (d).

(1) Wells, J.; Ortega, D.; Steinhoff, U.; Dutz, S.; Garaio, E.; Sandre, O.; Natividad, E.; Cruz, M. M.; Brero, F.; Southern, P., et al. *Int J Hyperthermia* **2021**, *38*, 447–460.

(2) Pennes, H. H. *Journal of applied physiology* **1948**, *1*, 93–122.

# Magnetic heating of superparamagnetic KFeO<sub>2</sub> nanoparticles

## On the effective uniaxial anisotropy of magnetite nanoparticles

David Serantes<sup>1</sup>, Daniel Falilde<sup>1</sup>, Sergiu Ruta<sup>2</sup>, Ylian Fernández-Afonso<sup>3</sup>, Lucía Gutiérrez<sup>2</sup>, Roy Chantrell<sup>4</sup>

<sup>1</sup>Applied Physics Department, Universidade de Santiago de Compostela, Spain.

<sup>2</sup>College of Business, Technology and Engineering, Sheffield Hallam University, UK.

<sup>3</sup>Department of Analytical Chemistry, Universidad de Zaragoza, Spain.

<sup>4</sup>Department of Physics, University of York, UK.

Due to their good biocompatibility, magnetite nanoparticles are widely investigated as magnetic nanorobots for a variety of biomedical applications, ranging from imaging to drug release or hyperthermia cancer treatment. Often, delivering the required stimulus depends on the accurate knowledge of the particle anisotropy, as the effective parameter linking the spin to the lattice, for example to convert absorbed electromagnetic energy into heat, or generate a torque.

The issue is that, despite magnetite possesses a cubic (negative) magnetocrystalline anisotropy, it is generally described in terms of an effective uniaxial anisotropy. While such assumption may be reasonable for highly anisotropic magnetic nanoparticles, it clearly cannot be applied to more symmetrical particles. In this work we show, combining theory and experiment, how the assumption of an effective uniaxial anisotropy may, in fact be correlated with some degree of asymmetry in particle shape on top of the cubic contribution.

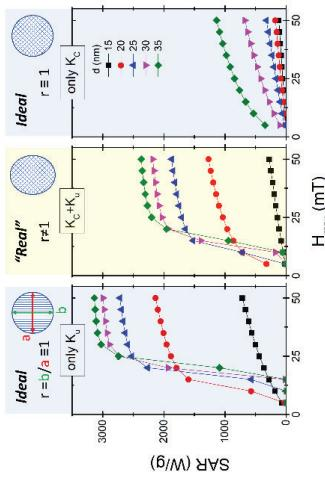


Diagram indicating the role of either cubic, uniaxial, or the combination of both anisotropies, on the hyperthermia performance.

## On the effective uniaxial anisotropy of magnetite nanoparticles

Sarbjit Singh

Department of Physics, Montgomery Public School, Punjab - 144602, INDIA

\*Corresponding author :Email Id: sarbjitsinghdavu@gmail.com, sarbjitphysics1989@gmail.com

## ABSTRACT

Hyperthermia is a therapeutic treatment in which malignant cancer cells/ tumors are destroyed or killed by increasing the temperature in a range of 42–46 °C under applied alternating field. Superparamagnetic nanoparticles has attracted huge attention in cancer treatment due to the selective heating of cancer cells via targeting cancer cells under the application of alternating magnetic field. The hysteresis loss generation from single domain superparamagnetic KFeO<sub>2</sub> nanoparticles is zero due to its zero coercive and remanence field. In early theoretical approaches Neel and Brown calculated the switching probability under the assumption of coherent rotation, i.e., at any time — even during the reversal — the magnetic moments of the entire particle remain magnetized in the same direction, behaving like a single giant spin (superparamagnet). Under these requirements the switching rate is described by the so-called Neel-Brown law. In addition to above, it have been reported so far that superparamagnetic nanoparticles may loss there heat energy due to Brownian and Neel's relaxation mechanisms.

**Keywords:** KFeO<sub>2</sub>, Superparamagnetic, Neel relaxation, Brownian, magnetic susceptibility..

## Reference:

1. S. Singh, A. Tovstolytkin, G.S. Lotey, J. Magn. Mater. 458 (2018) 62–65.
2. S. M. Hoque, M. S. Hossain, S. Choudhury, S. Akhter, F. Hyder, Materials letters, 162, 60-63,(2016).
3. A. K. Tangra, S. Singh, N. X. Sun, G. S. Lotey, Journal of Alloys and Compounds, 778, 47-52, (2019).

## Magnetic properties of iron oxide $\text{FeO}/\text{Fe}_3\text{O}_4$ core-shell nanocubes tuned by the preparation method

Tereza Šolíková,<sup>a,c</sup> František Zažímal,<sup>a</sup> Sahitya Kumar Avugadda,<sup>b</sup> Alessandro Di Girolamo,<sup>b</sup> Nisarg Rohithbhai Soni,<sup>b</sup> Giusy Maria Rita Rizzo,<sup>b</sup> Nathalie Milbrandt,<sup>d</sup> Yu Hsin Tsai,<sup>d</sup> Ivo Kuběna,<sup>a</sup> Anna Cristina Samra,<sup>d</sup> Roman Grigorčík,<sup>a</sup> and Teresa Pellegrino<sup>b</sup>

<sup>a</sup>Institute of Physics of Materials, Czech Academy of Sciences, Žižkovova 22, 616 00 Brno, Czech Republic

\*email: [solkova@ipm.cz](mailto:solkova@ipm.cz)

<sup>b</sup>Central European Institute of Technology, Brno University of Technology, Purkyňova 123, 612 00 Brno, Czech Republic  
<sup>c</sup>Department of Chemistry, Case Western Reserve University, Cleveland, Ohio 44106, United States  
<sup>d</sup>Department of Biology, Hacettepe University, 06800, Ankara, Turkey

\*email: [solkova@ipm.cz](mailto:solkova@ipm.cz)

Anisotropically-shaped magnetic nanoparticles have attracted great attention in the past few years especially with regard to magnetic hyperthermia (MH) and magnetic particle imaging (MPI) applications. The preference for using magnetite- and magnetite-based NPs in vivo follows from their excellent biocompatibility, magnetic properties, and chemical stability at room temperature. The shape, size, monodispersity, and the surface character are controlled by the preparation method.

In this work, we have prepared iron oxide  $\text{FeO}/\text{Fe}_3\text{O}_4$  core-shell nanocubes in the diameters from 16 to 23 nm by the thermal decomposition method. As-prepared nanocubes were annealed in organic and aqueous environments and their resulting magnetic properties were compared. We have also investigated the influence of nanoparticle sizes on their magnetic properties, such as specific absorption rate (SAR), saturation magnetization, magnetic particle imaging properties, T1/T2 relaxation times, and heating efficiency in viscous media. The size distribution, polydispersity index and stability in water were measured by dynamical light scattering. Detailed studies of their crystal structures were made by transmission electron microscopy. The compositions of these nanoparticles were characterised by powder X-ray diffraction and by Mössbauer spectroscopy. Their magnetic properties were characterized by PPMs, MPI, MRI, and T1/T2 relaxometry. The SAR was measured by AC magnetometry in viscous environments and the calorimetric SAR measurements were performed in water.

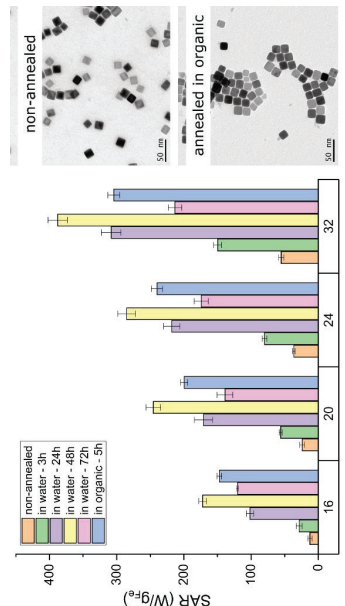


Figure 1: Comparison of SAR values of 16 nm core-shell nanocubes with respect to type and time of thermal treatment (left part) and the TEM pictures of non-annealed and annealed 16 nm sample (right part).

## DMSA-Coated Cubic Iron Oxide Nanoparticles as Potential Therapeutic Agents

Senem Cioğlu<sup>1</sup>, Özlem Duyar Coşkun<sup>2</sup>, Le Duc Tung<sup>3,4</sup>, Mehmet Ali Onur<sup>5</sup>, Nguyen Thi Kim Thanh<sup>3,\*</sup>

<sup>1</sup>Department of Nanotechnology and Nanomedicine, Hacettepe University, 06800, Ankara, Turkey.

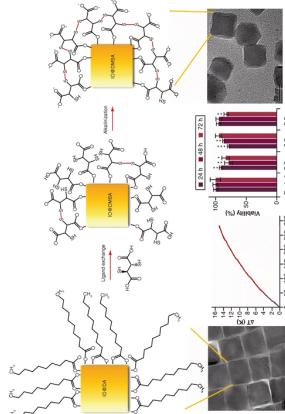
<sup>2</sup>Department of Physics Engineering, Hacettepe University, 06800, Ankara, Turkey.  
<sup>3</sup>UCL Healthcare Biomagnetic and Nanomaterials Laboratories, The Royal Institution of Great Britain, London W1S 4BS, UK.

<sup>4</sup>Biophysics Group, Department of Physics and Astronomy, University College London, Gower Street, London WC1E 6BT, UK.

<sup>5</sup>Department of Biology, Hacettepe University, 06800, Ankara, Turkey.

\*Email: ntk.thanh@ucl.ac.uk, <http://www.ntk-thanh.co.uk>

Superparamagnetic cubic iron oxide nanoparticles (IONPs) have shown great promise in cancer diagnosis and treatment due to their superior properties compared to the spherical ones of the similar size, such as higher magnetization, higher specific absorption rate (SAR) values<sup>1</sup>, better T<sub>2</sub>-relaxivity<sup>2</sup> and higher cellular uptake<sup>3</sup>. Our aim was to synthesize functionalized superparamagnetic cubic IONPs with impressive magnetic and magneto-thermal properties and low cytotoxicity as a potential agent for cancer treatment. In this study, monodisperse cubic IONPs with a high value of saturation magnetization were synthesized by thermal decomposition method and functionalized with meso-2,3-dimercaptosuccinic acid (DMSA) via ligand exchange reaction, and their cytotoxic effects on HeLa cells were investigated. DMSA functionalized cubic IONPs with an edge length of  $24.5 \pm 1.9$  nm had a specific absorption rate value of  $19.7 \text{ W/g}_{\text{Fe}}$  ( $15.95 \text{ kA/m}$  and  $488 \text{ kHz}$ ) and showed slight cytotoxicity on HeLa cells when incubated with  $3.3 \times 10^{10}$ ,  $6.6 \times 10^{10}$  and  $9.9 \times 10^{10}$  NPs/mL for 24, 48 and 72 h. The results show a promising potential on the use of the cubic IONPs functionalized with DMSA for biomedical applications. To the best of our knowledge, this is the first study to investigate both the cytotoxic effects of DMSA-coated cubic IONPs on HeLa cells and hyperthermia performance of these nanoparticles.<sup>4</sup>



### Acknowledgements

This work was funded by The Scientific and Technological Research Council of Turkey - Directorate of Science Fellowships and Grant Programmes (TUBITAK - BIDEB) with 2211-C National PhD Scholarship within the frame work of priority areas, and by Hacettepe University Scientific Research Project (BAP) Coordination Unit, Turkey (Project No: FHD-2018-16742). The authors acknowledge the National Nanotechnology Research Center (UNAM), TR and Hacettepe University Advanced Technologies Application and Research Center (HÜNTEK), TR and thanks EPSRC (EP/M015157/1 and EP/M018016/1); AOARD (FA2386-17-1-4042 award).

### References

1. Martinez-Bouhet, C., Simeonidis, K., Makridis, A., et al., Learning from Nature to Improve the Heat Generation of Iron-Oxide Nanoparticles for Magnetic Hyperthermia Applications, *Scientific Reports*, 3(1), 2013.
2. Zhou, G., Muir, B. W., Morat, B., et al., Comparative Study of the Magnetic Behavior of Spherical and Cubic Superparamagnetic Iron Oxide Nanoparticles, *115*, 327–334, 2011.
3. Salait, S., Maleki Dizaj, S., & Yari Khosraviani, A., Effect of the surface modification, size, and shape on cellular uptake of nanoparticles, *Cell Biology International*, 39(8), 881–890, 2015.
4. Cioğlu, S., Coşkun, Ö.D., Tung, L.D., Onur, M.A., and Thanh N.T. K., (2021) DMSA-coated cubic iron oxide nanoparticles as potential therapeutic agents, *Nanomedicine*, 16(11), 925-941.

## Synergistic effect of the doxorubicin loaded thermal and pH-sensitive nanocarriers on the different cell lines

Lilin Wang,<sup>a,b</sup> Aziz Hervault,<sup>ab</sup> Paul Southern,<sup>bc</sup> Olivier Sandre,<sup>d</sup> Franck Coulaud<sup>e</sup> and Nguyen Thi Kim Thanh<sup>a,b</sup>

<sup>a</sup>Biophysics Group, Department of Physics & Astronomy, University College London, Gower Street, London, WC1E 6BT, UK

<sup>b</sup>UCL Healthcare Bionangetic and Nanomaterials Laboratories, 21 Albemarle Street, London, W1S 4BS, UK

<sup>c</sup>Department of Medical Physics and Biomedical Engineering, University College London, Gower Street, London, WC1E 6BT, UK

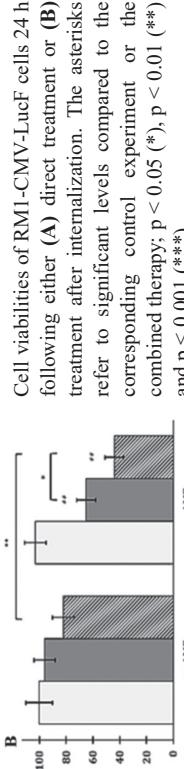
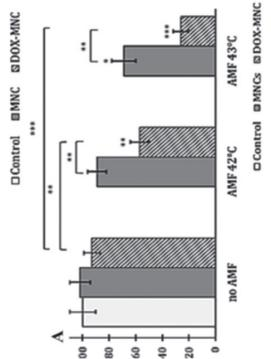
<sup>d</sup>Laboratoire de Chimie des Polymères Organiques (LCPO), Univ. Bordeaux, CNRS, Bordeaux INP, UMR 5629, 33600 Pessac, France

<sup>e</sup>Molecular Imaging and Innovative Therapies (IMOTION), Univ. Bordeaux, EA7435, Bordeaux, 33300, France  
E-mail: ntk.thanh@ucl.ac.uk, http://www.ucl-thanh.org.uk

Hyperthermia has been considered as a promising therapy for cancer since the last century. However, currently, only a few of them are translated into the clinical stage indicating a ‘medically underexplored nanoparticles’ situation, which encourages their comprehensive biomedical exploration.

The magnetic iron oxide cores were synthesized by the microwave method and conjugated with DOX via pH-cleavable imine bonds by a thermo-responsive copolymer. This study presents, for the first time, (i) a comprehensive biological evaluation of our previously well-developed dual pH and thermo-responsive polymer-coated magnetic doxorubicin nanocarrier (MNC-DOX) and (ii) multidirectional assessments on the thermally induced synergistic effects of intracellular/extracellular hyperthermia with the same type of DOX loaded magnetic nanocarrier in different cancer cell lines.

More specifically, this dual response system limited the cellular and systemic cytotoxicity compared to free DOX without AMF stimulation, enabling the lower side-effect when the therapy is applied *in vivo*. The thermo-chemotherapy treatment implemented with our system presented a much more potent and synergistic effect than either chemotherapy or magnetic hyperthermia alone, for multi-modal cancer therapy in nearly every studied condition.



Cell viabilities of RM1-CMV-LucF cells 24 h following either (A) direct treatment or (B) treatment after internalization. The asterisks refer to significant levels compared to the corresponding control experiment or the combined therapy;  $p < 0.05$  (\*),  $p < 0.01$  (\*\*), and  $p < 0.001$  (\*\*\*)�.

### Reference:

J. Mater. Chem. B, 2020, 8, 10527-10539. https://doi.org/10.1039/D0TB01983F

[1] W. Fan *et al*, Chem. Rev. **17** (2017) 13566  
[2] Y. Liu *et al*, ACS Appl. Mater. Interfaces **11** (2019) 31649  
[3] A. Bienia *et al*, Pharmaceutics **13** (2021) 1147  
[4] C. Dai *et al*, Biomaterials **219** (2019) 119374  
[5] S. Dong *et al*, Adv. Funct. Mater. (2019) 1907071  
Poster #24

## Determining the key parameters to reach synergistic effects between magnetic hyperthermia and ROS production in Zn<sub>x</sub>Fe<sub>3-x</sub>O<sub>4</sub> magnetic Nanoparticles.

Teobaldo E. Torres<sup>1,2</sup>, Adriela A. de Almeida<sup>1</sup>, Ana C. Moreno-Maldonado<sup>3</sup>, Manuel R. Ibarra<sup>3,4</sup>, Gerardo F. Goya<sup>3</sup>, Myriam Aguirre<sup>3,4</sup>, Elin L. Winkler<sup>1,2</sup>, Roberto D. Zysler<sup>1,2</sup> and Enio Lima Jr.<sup>1</sup>

<sup>1</sup> Instituto de Nanociencia y Nanotecnología, CNEA-CONICET, RS4024GP, Av. Bustillo 0500, Bariloche, Argentina.

<sup>2</sup> Instituto Balseiro, Universidad Nacional de Cuyo, RS4024GP, Av. Bustillo 9500, Bariloche, Argentina.

<sup>3</sup> Departamento de Física de la Matemática Condensada, Instituto de Nanociencia y Materiales de Aragón, Universidad de Zaragoza, 50018, C/Mariano Esquillor s/n, Zaragoza, Spain.

<sup>4</sup> Laboratorio de Microscopias Avanzadas (LMA), Universidad de Zaragoza, 50018, C/Mariano Esquillor s/n, Zaragoza, Spain.

\* Email: teobaldo@resmolina@gmail.com

Current challenges in the field of cancer research have gradually shifted their focus from monotherapy to combination therapy for enhanced treatment effectiveness [1]. In this way, the fast evolution in the field of nanoyzomes has led to the promising combination between nanocatalytic or chemodynamic therapy (CDT) with other kinds of therapies such as photothermal therapy (PTT) [2], photodynamic therapy (PDT) [3] and Magnetic Fluid Hyperthermia (MFH) [4] to improve their therapeutic results.

When talking about nanocatalytic therapies, the main idea is to use of the hydroxyl radical ( $\cdot\text{OH}$ ), the most toxic of the reactive oxygen species (ROS), to induce initial oxidative damage to the cell membrane, improving the permeability of the cell membrane and making it more sensitive to heat. This radical is produced by the disintegration of hydrogen peroxide ( $\text{H}_2\text{O}_2$ ) through a Fenton reaction with a metal ion. In this way, great therapeutic effects have been reported to threaten breast cancer and osteosarcoma cell lines [4, 5]. However, it is imperative to study how the intrinsic parameters of magnetic nanoparticles (MNPs) used as nanoyzomes affect the ROS production and heat release, to find the best relationship between them and improve the synergy between the therapies. In this work, a series of  $\text{Zn}_{x}\text{Fe}_{3-x}\text{O}_4$  MNPs with mean diameters  $<\text{d}>$  between 11-32 nm were studied. A detailed characterization study, including Proton-Induced X-ray emission (PIXE), Transmission Electron Microscopy (TEM), SQUID Magnetometry, Ferromagnetic Resonance (FMR), Electron Paramagnetic Resonance (EPR) and Specific Loss Power (SLP) was performed, unravelling a compromise between the heating efficiency of the MNPs and their ROS production. Values of SLP up to 1440 W/g and concentration up to 1000 nM of hydroxyl radical ( $\cdot\text{OH}$ ) were obtained, (see Figure). The optimal size of the MNPs for the combination therapy is in the range of 20-25 nm.

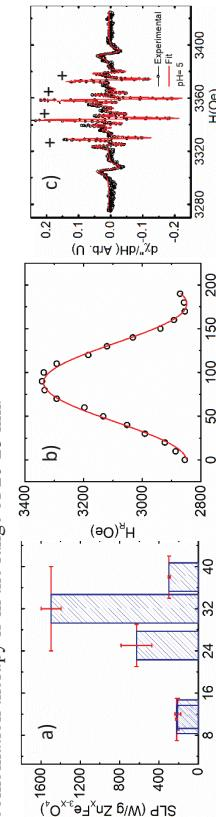


Figure. a) SLP in function of  $<\text{d}>$  for samples dispersed in toluene b) Angular dependence of  $H_{\text{R}}$  for sample with  $<\text{d}> 25$  nm. c) EPR spectrum and the corresponding fitting obtained. A) Sample AM12, B) Sample AM28, measurement 10 min after addition of  $\text{H}_2\text{O}_2$  at room temperature in pH 5. (+) indicate the characteristic peaks of  $\cdot\text{OH}$ .

## Untangling the influence of particle-intrinsic parameters and experimental conditions in magnetic fluid hyperthermia

Daniela P. Valdés<sup>1,2\*</sup>, Enio Lima Jr.<sup>1</sup>, Roberto D. Zysler<sup>1,2</sup>, Gerardo F. Goya<sup>3</sup>, Emilio De Biasi<sup>1,2</sup>

<sup>1</sup> Instituto de Nanociencia y Nanotecnología, CNEA-CONICET, R8402AGP Av. Bustillo 9500, Bariloche, Argentina.

<sup>2</sup> Instituto Balseiro, Universidad Nacional de Cuyo, R8402AGP Av. Bustillo 9500, Bariloche, Argentina.

<sup>3</sup> Departamento de Física de la Materia Condensada, Instituto de Nanociencia y Materiales de Aragón, Universidad de Zaragoza, 50018, C/Mariáns Esquillor s/n, Zaragoza, Spain.

\*Email: danielavaldes@ib.edu.ar

Optimization of the specific power absorption (SPA) of magnetic nanoparticles (MNPs) for magnetic fluid hyperthermia (MFH) applications is currently focused on designing MNPs with certain properties and finding favourable experimental conditions for each system. However, the role of relevant parameters in the relaxation is still under discussion. Moreover, *in vitro* and *in vivo* experiments generally lead to interacting MNP systems due to agglomeration in the cellular environment. In the particular case of linear aggregates, the impact of dipolar interactions on the SPA of the system is still an open discussion: there are reports of both beneficial [1] and detrimental [2] effects on the SPA.

Through a nonlinear model [1-5] for the magnetic relaxation of single-domain MNPs with uniaxial effective anisotropy, we simulated systems with different particle-intrinsic parameters (size, anisotropy) and experimental conditions (frequency, interactions). We determined four regions (I-IV) of magnetic behaviour as a function of relative anisotropy (anisotropy field with respect to the amplitude of the ac field), that dictate the SPA in MFH experiments through the area enclosed by hysteresis loops (see Figure [4]).

The boundaries between regions change with all of these parameters. We analyzed linear MNP arrangements and found out that, for the low relative anisotropy range, dipolar interactions increase the SPA while they are detrimental for the range of high relative anisotropy. This resolves the seemingly contradictory results of interaction effects in this kind of aggregates reported in the literature [1,2]. For low relative anisotropy regions, we also explained how the enhancement of the SPA by dipolar interactions (reflected by an increase in coercivity) is actually caused by the shift between the local and the applied magnetic field [5].

We also provide a simple, analytical tool aimed at the design of MNPs and the choice of the experimental conditions for optimal heating. Through the thermal interpretation of its validity range, we conclude that systems with low-thermal-fluctuation influence are the best candidates for MFH due to their high SPA values.

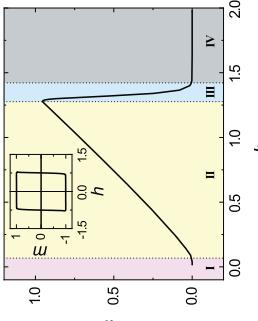


Figure 1. AC hysteresis loops measured with magneto-optical methods. (a) magnetic nanoparticles with core size of 8.5 nm under 129 kHz field. (b) magnetic nanoparticles with core size of 17.4 nm under 129 kHz. (c) magnetite nanoparticles with core size of 10.5 nm under 129 kHz. (d) the same as (a) but under 508 kHz field. Different loops on each plot show four different AC magnetic field amplitudes used.

[1] Carey, J., Mehdoui, B., & Respaud, M. Simple models for dynamic hysteresis loop calculations of magnetic single-domain nanoparticles: Application to magnetic hyperthermia optimization. *J. Appl. Phys.* **109**, 083921 (2011).

## Investigation of AC hysteresis from magnetic nanoparticle suspensions using magneto-optical methods

Xuyiling Wang<sup>1</sup>, Ying Yang<sup>1</sup> and Neil Telling<sup>1</sup>

<sup>1</sup>School of Pharmacy and Biengineering, Keele University, ST5 5BG, UK

\*Email: x.wang3@keele.ac.uk

Magnetic nanoparticles (MNPs) exposed to high frequency alternating magnetic fields, can generate localized heat and induce death of cancer cells; an effect termed magnetic hyperthermia (MH). AC magnetometry measurements of MNPs can quantify the heating effect, eliminating multiple systematic errors confronted by conventional calorimetric methods [1]. A new microscope was used here based on magneto-optical methods using Faraday rotation to determine the AC magnetisation of samples instead of conventional inductive pick-up coils. This increased the highest frequency at which measurements can be performed compared to coil-based magnetometry. The microscope could also measure AC magnetisation with spatial resolution of  $\sim 0.5 \mu\text{m}$ , and simultaneous probe the fluorescence lifetime, which is advantageous for simultaneous biological structural and functional imaging.

In this work, AC hysteresis loops of magnetic and magnetite nanoparticle suspensions with different sizes were measured at different frequencies using the microscope (Figure 1). For all samples, with increased field amplitudes, AC hysteresis evolves from minor to major loops. Nanoparticle size has a dominant effect on the width of AC hysteresis loops as shown from Figure 1(a) to (c), regardless of whether the nanoparticle cores were composed of magnetic (Figure 1a, b) or magnetite (Figure 1c). Comparing AC loops measured under the same field amplitudes but different frequencies (Figs. 1a and 1d), reveals a slight increase in width at the highest frequency (508 kHz), consistent with AC susceptibility measurements where the imaginary component was found to be higher at 508 kHz due to the dominance of Néel relaxation in this sample. Further results measured across different nanoparticle samples and different frequencies will be discussed in the context of their magnetisation dynamics and magnetisation relaxation properties.

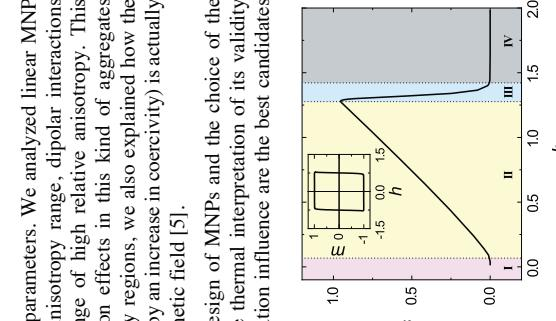


Figure. Normalized area  $a$  as a function of relative anisotropy field  $h_K$  (area curve) of a noninteracting MNP system with diameter 60 nm and anisotropy axes parallel to the external field for a frequency  $f = 100$  kHz. Regions I to IV are indicated by coloured zones. *Inset:* Loop corresponding to the maximum of the area curve.

- [1] B. Mehdoui *et al.*, *Phys. Rev. B* **87** 174419 (2013)  
 [2] L.C. Brancinho *et al.*, *Sci. Rep.* **3** 2887 (2013)  
 [3] E. De Biasi *et al.*, *J. Magn. Magn. Mater.* **320** 312 (2008)  
 [4] D.P. Valdés *et al.*, *Phys. Rev. Appl.* **15** 044005 (2021)  
 [5] D.P. Valdés *et al.*, *Phys. Rev. Appl.* **14** 014023 (2020)

## Multifrequency hyperthermia characterisation by calorimetry and dynamic magnetisation

James Wells<sup>1</sup>, Olaf Kosch<sup>1</sup> and Frank Wiekhorst<sup>1\*</sup>

<sup>1</sup>Physikalisch-Technische Bundesanstalt (PTB), Abbestraße 2, 10587 Berlin  
\*Email: frank.wiekhorst@ptb.de

Magnetic field hyperthermia (MFH) therapy is a promising and novel approach to cancer treatment. First, magnetic nanoparticles (MNP) are injected into the patient so that they accumulate within the tumour tissue. High-frequency time-varying magnetic fields are then applied. The magnetic field causes the MNP to dissipate heat into their immediate surroundings. This localised heating is used to inflict damage to the cancer cells, leaving the surrounding healthy tissues intact. MFH therapy has already shown great promise in clinical trials. The synthesis of new MNP types engineered to maximise their heating performance and biocompatibility has been the subject of many recent studies. Measurements of the MFH heating performance of nanoparticles are often reported in the literature. A major interlaboratory study recently highlighted the lack of consistency between MFH characterisation measurements conducted at different laboratories using different calorimetry apparatus and analysis<sup>1</sup>. In addition to differences in the sophistication of the measurement and analysis methods, this study also highlighted that the limited range of frequencies employed at many laboratories contributed to an incomplete picture of the overall MFH behaviour of MNP. The study highlighted the need for improved accuracy and standardisation in MFH characterisation measurements to support MFH therapy in reaching higher technology readiness levels.

To address this need, we present a comparative study between MFH characterisation measurements performed using two distinct methodologies. An AC magnetometer (Nanotech Solutions, Spain)) measures the dynamic hysteresis of MNP (Drive fields: 10–100 kHz, 8 kA/m–32 kA/m), with the specific loss power (SLP) heating characteristic calculated via the area enclosed by this loop. A homemade calorimeter system (Drive fields: 23 kHz–177 kHz, 2 kA/m–10 kA/m) was used to measure heating curves for the same MNP samples, with the SLP calculated via the corrected slope technique<sup>2</sup>. Data sets spanning a broad range of drive-field frequencies and amplitudes were measured using both techniques for commercial nanoparticle systems (Fenuecarbotran (Meito Sangyo, Japan), RCL-01 (Resonant Circuits, UK) and Synomag (Micromod, Germany)). The SLP datasets spanning multiple drive-field parameters were analysed and used to calculate the intrinsic loss power (ILP) for each MNP system<sup>1</sup>. A detailed analysis of the measurement results indicates significant agreement between the multifrequency characterisations made using the two techniques demonstrating the benefits of multi-frequency characterizations made using multiple complementary techniques.



a) Photographs of calorimetry system coil and electronics. b) Photograph of AC Hysteresis system. c) Table showing ILP values calculated based on analysis of datasets of SLP values measured at varying frequencies and intensities of drive-fields.

### References

- [1] J. Wells et al, Int. J. Hyp. 38, 01, 447–460 (2021)
- [2] J. Wells et al, Nanoscale, 35, (2020)

## Theoretical three-dimensional predictions for spatial focusing of magnetic hyperthermia using field-free point/line concept

Than-Anh Le<sup>1</sup>, Yaser Hadadian<sup>1</sup>, Hoheyon Kim<sup>1</sup> and Jungwon Yoon<sup>1</sup>

<sup>1</sup> School of Integrated Technology, Gwangju Institute of Science and Technology, Gwangju, Republic of Korea

\* Email: jyoon@gist.ac.kr. Mobile: 82-10-2402-6904

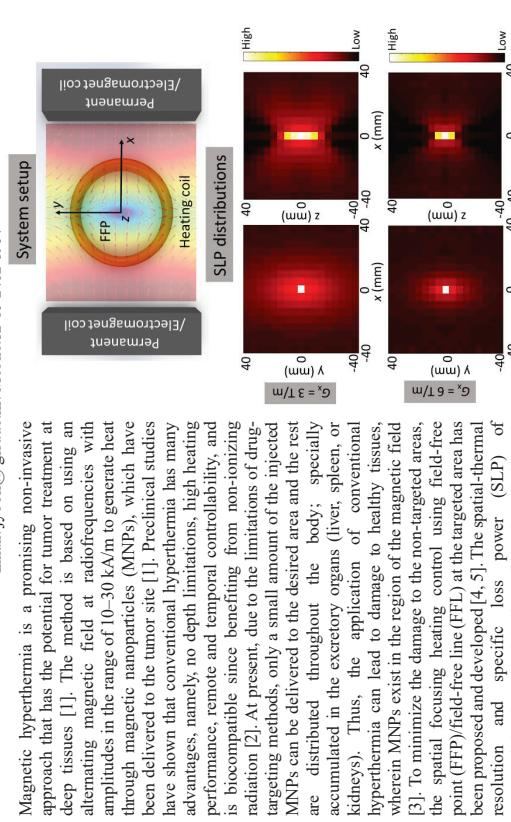


Fig. 1. The 3D SLP distribution of nanoparticles (core diameter of 25  $\mu\text{m}$  and hydrodynamical diameter of 50  $\mu\text{m}$ ) at 30 mT, 100 kHz heating field with different magnetic gradients. The application of conventional hyperthermia can lead to damage to healthy tissues, wherein MNPs exist in the region of the magnetic field [3]. To minimize the damage to the non-targeted areas, the spatial focusing heating control using field-free point (FFP)/field-free line (FFL) at the targeted area has been proposed and developed [4, 5]. The spatial-thermal resolution and specific loss power (SLP) of nanoparticles have mainly been investigated through experiments [4, 5]. To optimize the treatment protocols as well as invasive temperature monitoring during the treatment, a model to predict the spatial-thermal resolution and SLP of MNPs is required. Although a one-dimensional model for spatial focusing using FFP and without considering the magnetic field direction for predicting the spatial-thermal resolution and SLP was introduced [6], the model may not provide enough information for the prediction necessary before applying it in practice. In addition, as far as we know a model for the spatial focusing using FFL (two-dimensional) has not yet been considered. Thus, a multi-dimensional model to predict the spatial-thermal distribution and SLP using FFP/FFL should be considered. In this paper, by using the Shliomis (MRSH) equation, the temperature/SLP distribution in three dimensions for nanoparticles is investigated. One example for the temperature/SLP distribution in Fig. 1 from the distribution of SLP in three-dimensions, the bio-heat equation, and COMSOL Multiphysics software, the temperatures distributions of nanoparticles in a human brain are also investigated. This model will be tested through experiment in future works.

- [1] E. A. Perigo, G. Henrery, O. Sardie et al., "Fundamentals and advances in magnetic hyperthermia," *Applied Physics Reviews*, vol. 2, no. 4, pp. 041302, 2015.
- [2] S.-h. Noh, S. H. Moon, T.-H. Shin et al., "Recent advances of magnetic-thermal capabilities of nanoparticles: From design principles to biomedical applications," *Nano Today*, vol. 13, pp. 61–76, 2017.
- [3] C. Kuo, Y. Zhang, M. Hedayati et al., "Preliminary study of injury from heating systematically delivered, nonangled dextran-superparamagnetic ion oxide nanoparticles in mice," *Nanomedicine*, vol. 7, no. 11, pp. 1697–1711, 2012.
- [4] E. Moyrodi, N. Maniots, T. Sumanas et al., "Spatial focusing of magnetic particle hyperthermia," *Nanoscience and nanotechnology*, vol. 2, no. 1, pp. 408–416, 2020.
- [5] Z. W. Tay, P. Chandrasekhan, A. Choi-Lam et al., "Magnetic particle imaging-guided heating in vivo using gradient fields for arbitrary localization of magnetic hyperthermia therapy," *ACS nano*, vol. 12, no. 4, pp. 3698–3713, 2018.
- [6] R. Dhavalikar, and C. Rasaldi, "Theoretical predictions for spatially-focused heating of magnetic nanoparticles guided by magnetic particle imaging field gradients," *Journal of magnetism and magnetic materials*, vol. 419, pp. 267–273, 2016.

## Capturing magnetic nanoparticles with external magnetic fields in the fluidic flow

S. Ajomandii<sup>1,2</sup>, I. Dirba<sup>1\*</sup>, S. Ener<sup>1</sup>, A. Filatova<sup>3</sup>, U. Nuber<sup>3</sup>, and O. Gutfleisch<sup>1</sup>

<sup>1</sup> Functional Materials, Department of Material Science, Technical University of Darmstadt, Darmstadt, 64287, Germany

<sup>2</sup> Materials Engineering and Nanotechnology Department, Politecnico di Milano, Milan, 20133, Italy

<sup>3</sup> Biology, Stem Cell and Developmental Biology, Technical University of Darmstadt, 64287 Darmstadt, Germany

\*Email: sarah.ajomandii@gmail.com

Magnetic nanoparticles (MNPs) have recently attracted a lot of attention in biomedical applications due to their exceptional qualities such as low toxicity, biocompatibility, and large surface to volume ratios. One of the most important applications of MNPs is magnetic field-based bio separation systems, which are gaining popularity due to their vast applications in biomedical research, clinical diagnostics, and biotechnology. Moreover, MNPs can be used as controllable carriers of medical agents and flow through the bloodstream. Targeted application of magnetic field can be applied to capture the MNPs at a target spot.

The effectiveness of magnetic bio separation and/or targeting is determined by the interaction of numerous parameters, including the flow velocity of the fluid containing magnetic nanoparticles, the size of the nanoparticles, and the strength of the external magnetic field. In order to build an efficient microfluidic bio separation device, it is necessary to understand the particle behaviour in the fluidic flow, as well as the ideal range of velocity, nanoparticle diameter, and magnetic field strength.

In this study, we investigated the capturing behaviour of MNPs in phosphate buffered saline solution upon application of external magnetic field. For this purpose, a modified optical microscope setup is used which is equipped with light polarization options and an AC/DC external magnetic field generator up to 500 mT. The external magnetic field was applied perpendicular to the flow direction to observe capturing phenomena. Effect of three parameters on capturing was studied: i) the velocity of the fluid containing the magnetic nanoparticles, ii) the diameter of the magnetic nanoparticles, and iii) the strength of the magnetic field. The magnetic flux density necessary and sufficient to capture the MNPs for a short time period (blue data in Fig. 1) and to long-term capture the MNPs (red data in Fig. 1) were measured at different constant flow rates and shows linear increase. Furthermore, a mathematical model will be developed to combine these findings and aid in the design and development of innovative micro fluidic bio separation system.

## Visible Light-Driven Amide Synthesis from Thiocacid and Amine with CdSe QDs-Coated Magnetic PMMA nanocomposites in an Aqueous Solution

Chonnavee Maiupinnee<sup>1</sup>, and Numporn Insin<sup>1</sup>\*

<sup>1</sup> Department of Chemistry, Faculty of Science, Chulalongkorn University, Bangkok, 10330, Thailand

\*Email: numporn.ach@chula.ac.th

Amide bond formation is one of the most basic important reactions in organic synthesis of numerous organic molecules such as peptides, natural products, synthetic polymer and pharmaceutical agents. To obtain higher yield and produce less organic waste, CdSe semiconductor quantum dots (CdSe QDs) are the one promising photocatalysts for the synthesis of amide from thiocacids and simple amines in water at room temperature by visible light irradiation. However, the toxicity of cadmium leads to the requirement of efficient separation and recovery of the QDs out of the reaction mixture for avoidance of Cd contamination in the system. Moreover, the reported separation approaches need intensive labor and high energy consumption and could lead to the loss of the catalysts.

From properties of magnetic nanoparticles (MNPs), the attachment of MNPs to the catalyst could provide superparamagnetic character on the catalyst with colloidal stability and easy removal using magnet. Nonetheless, MNPs are semiconductor with small bandgap. The direct contact of CdSe QDs and MNPs could lead to fast photogenerated electron-hole recombination and photodissolution of MNPs, which could reduce photocatalytic activity of CdSe QDs. To maintain photocatalytic activity, facile insertion of PMMA as insulator to prevent electron-hole transfer between the photocatalyst and MNPs are required. In this work, novel composites of MNPs embedded biocompatible polymer PMMA and CdSe quantum dots were fabricated and investigated as photocatalyst for synthesis of amide bonds from thiocacids and simple amines in water solvent at room temperature under visible light irradiation with ease of separation and reusable, high activity, mild and safe conditions.

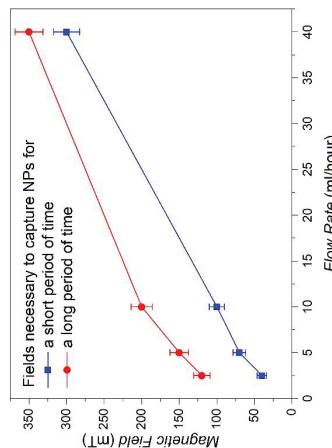
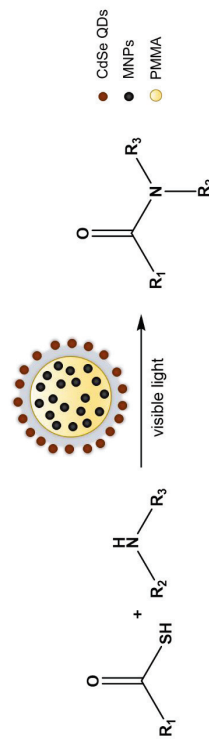


Figure 1: Magnetic field necessary to capture MNPs for a short time period (blue) and to long-term capture (red).

## Highly selective separation of magnetic nanoparticles using dynamic magnetic fields: a novel approach for MPI tracer purification

Norbert Löwa<sup>1\*</sup>, Bernhard Gleich<sup>2</sup>, Andreas Ide<sup>3</sup>, Sandro Eberbeck<sup>1</sup>, Dietmar Eberbeck<sup>1</sup>,

Gunnar Schütz<sup>2</sup>, Jörn Borgert<sup>2</sup>, Frank Wiekhorst<sup>1</sup>

<sup>1</sup> Physikalisch-Technische Bundesanstalt, 8.23 Metrology for Magnetic Nanoparticles, Berlin, Germany,

<sup>2</sup> Philips GmbH Innovative Technologies, Research Laboratories, Hamburg, Germany,

<sup>3</sup> MR and CT Contrast Media Research, Bayer AG, Berlin, Germany.

\* Email: norbert.loewa@ptb.de

Magnetic nanoparticles (MNP) intended for biomedical applications such as site-specific imaging, in vivo, cancer detection, or cancer therapy must exhibit a specific magnetic behavior resulting from a combination of crystal structure, shape, size, and size distribution. To exploit the full potential of the applications ensuring their safety and treatment success, the MNP properties must be tuned very precisely. Therefore, it is often challenging to find a synthesis route that provides sufficiently repeatable results, since many synthesis methods vary in both, MNP size and shape. Magnetic separation can be used to remove the low-forming components of a synthesis product and thus recover the valuable materials in high purity. Static magnetic separation is a versatile technique for sample quality enhancement by addressing the magnetic moments of MNP [1].

Here, we will present a novel dynamic magnetic separation approach for sample purification that exploits both, the magnetic moment and the anisotropy of MNP. A sophisticated separation system was modeled, designed, and manufactured for purification to improve the performance of Magnetic Particle Imaging (MPI) tracers. The system uses a special separation column filled with magnetic beads exposed to a high-frequency magnetic field ( $f=486\text{ kHz}$ ,  $\beta=10\text{ mT}$ ).

Our results show that purification of a high-performance MPI tracer using dynamic magnetic separation resulted in a further increase in MPI signal, such that the signal amplitude was 3.2-fold higher compared to the MPI gold standard Resovist®. This indicates the capability of the system to separate MNP according to their magnetic moment and anisotropy. In the future, this new separation approach could be used for purification and quality assurance of MPI tracers.

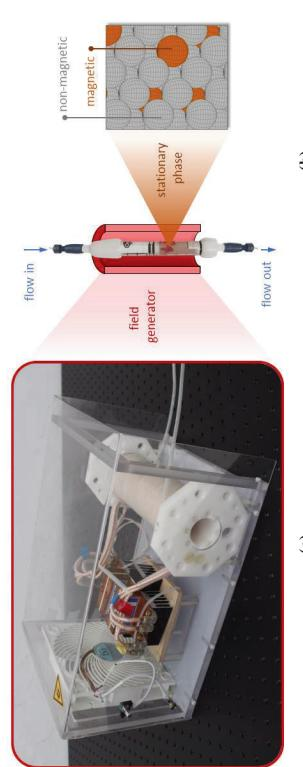


Figure. (a) Dynamic magnetic field generator; (b) Separation column filled with magnetic (orange) and non-magnetic beads (grey).

Acknowledgement:  
This project was funded by the Deutsche Forschungsgemeinschaft (DFG) within the research grant "cellMPI" (455706279) and the German Ministry of Education and Research under Grant MapIT (13N11092).

References:

- [1] Löwa N, Knappo F, Wiekhorst F, Eberbeck D, Thünenmann Alf, Trahms L. Hydrodynamic and magnetic fractionation of superparamagnetic nanoparticles for magnetic particle imaging. *J Magn Magn Mater* 2015;380:266–70. <https://doi.org/10.1016/j.jmmm.2014.08.057>.

## Magnetic anisotropy in polymeric magnetic hybrid material induced by vat photopolymerization additive manufacturing

Norbert Löwa<sup>1\*</sup>, Maria Alejandra Ardila Arenas<sup>1,2</sup>, Dirk Gulkelch<sup>1</sup>, Olaf Kosch<sup>1</sup>, Frank Wiekhorst<sup>1</sup>

<sup>1</sup> Physikalisch-Technische Bundesanstalt, 8.23 Metrology for Magnetic Nanoparticles, Berlin, Germany,

<sup>2</sup> Institut Universitario ITM, Departamento de Ciencias Aplicadas, Colombia.

\* Email: Norbert.loewa@ptb.de

Additive manufacturing (AM) is characterized by a high degree of design freedom and individualization and thus, ideally suited for the production of specimens for biomedical research. A fast and cost-effective AM variant for producing medical specimens is Digital Light Processing (DLP), in which the specimen is created layer by layer from light-curing photopolymer. This process can be used to fabricate parts from a wide range of materials with high detail and precision. In addition, the mechanical, electrical, magnetic, or optical properties of the photopolymers can be influenced by incorporating additives [1–3], e.g., materials that are dissolved or dispersed in small quantities into the photopolymer to induce and adjust desired material properties.

Different magnetic composites of liquid photopolymer and homogeneously distributed magnetic nanoparticles (MNP) as a magnetic additive were prepared using a special synthesis reactor. From this cylindrical standard specimen (diameter 5.2 mm, height 5.2 mm, height 5.2 mm) were printed. For process and quality control, established magnetic measurement methods were used (linear and non-linear dynamic susceptibility together with static magnetization measurements). A homogeneity demonstrator was developed composed of ten standard specimens stacked in building direction. Magnetic analysis of the individual standard hybrid material specimens showed that no sedimentation of the MNP occurred during the manufacturing process (duration 8 h, height 10 cm) for any of the fabricated magnetic composites. However, the investigation of the magnetic properties revealed an unexpected easy-plane (perpendicular to the building z-axis) anisotropy in the standard sample bodies (see Fig.). This indicates that the MNP prefer to align their magnetic moments within the printing plane. Results show that the formation of magnetic easy plane anisotropy in the AM process is influenced by the MNP type and concentration used. Due to this special behavior of the manufactured bodies, the orientation of these could be visualized using multicoil or magnetic particle imaging (MPI) in a preclinical MPI scanner (Bruker).

The AM of materials with anisotropic magnetic behavior might find broad application in magnetic labelling, such as Magnetic Particle Imaging-guided endovascular devices.

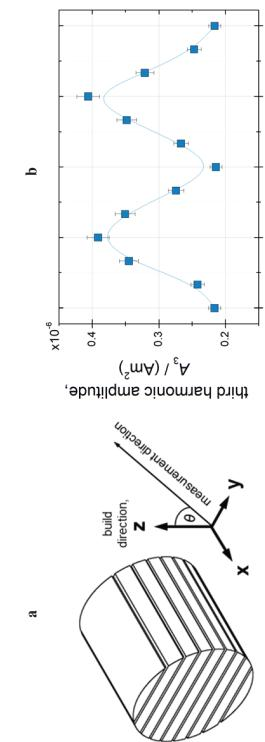


Figure. (a) Cylinder made of polymeric magnetic hybrid material additively manufactured in building-direction z. (b) Magnetic measurement (magnetic particle spectroscopy) of the cylinder made of magnetic composite at different angles  $\theta$  with respect to the building-direction z.

Acknowledgement:

This project was funded by the Federal Ministry for Economic Affairs and Climate Action within the TransMeT project "NANORM". We further thank the B-smart Lab of PTB for the support with additive manufacturing.

References:

- [1] A. Ruiz; S. Garg; S. Streeter; M.K. Giallorenzi; E. LaRochelle; K. Samko; B.W. Pogue *Sci. Rep.* **2021**; 11:17135.
- [2] M. C.-Gonzalez; A. D.-Alfaro; N. L.-Lanera; N. Alegre; D. Mecerreyes *ACS Appl. Polym. Mater.* **2021**, 3, 266–53.
- [3] N. Löwa; J.M. Fabert; D. Gulkelch; H. Paysen; O. Kosch; F. Wiekhorst *J. Magn. Magn. Mater.* **2019**, 469, 456–60.

## Improved Magneto-Microfluidic Separation of Nanoparticles through Formation of the $\beta$ -Cyclodextrin–Curcumin Inclusion Complex

J. Queiroz Campos<sup>1</sup>, M. Boulares<sup>2</sup>, M. Raboisson-Michell<sup>1,3</sup>, G. Verger-Dubois<sup>3</sup>, J. M. García Fernández<sup>4</sup>, G. Godeau<sup>1</sup> and P. Kuzhir<sup>1\*</sup>

<sup>1</sup> University Côte d'Azur, CNRS UMR 7010 Institute of Physics of Nice (INPHYNI) - Parc Valrose 06108 Nice, France

<sup>2</sup> University of Carthage, Faculty of Sciences of Bizerte, Centre des Recherches et des Technologies des Eaux (CERTE) Technopole de Borj-Cathia, Route touristique de Solliman BPn°273 Solliman 8020 Tunisia

<sup>3</sup> Adephos Biomedical - 1<sup>er</sup> Avenue 5th Street, 06570 Carros, France

<sup>4</sup> Instituto de Investigaciones Químicas, CSIC y Universidad de Sevilla, Av. Américo Vespucio 49, Isla de la Cartuja, 41092 Sevilla (Spain)

Email: Jordy.Quijano-Campos@univ-cotedazur.fr

Molecular adsorption to the nanoparticle surface may switch the colloidal interactions from repulsive to attractive and promote nanoparticle agglomeration. If the nanoparticles are magnetic, then their agglomerates exhibit a much stronger response to external magnetic fields than individual nanoparticles. Coupling between adsorption, agglomeration, and magnetism allows a synergy between the high specific area of nanoparticles ( $\sim 100 \text{ m}^2/\text{g}$ ) and their easy guidance or separation by magnetic fields. This yet poorly explored concept is believed to overcome severe restrictions for several biomedical applications of magnetic nanoparticles related to their poor magnetic remote control. In this presentation, we test this concept using curcumin (CUR) binding (adsorption to  $\beta$ -cyclodextrin ( $\beta$ CD)-coated iron oxide nanoparticles (IONP). CUR adsorption is governed by host-guest hydrophobic interactions with  $\beta$ CD through the formation of 1:1 and, possibly, 2:1  $\beta$ CD-CUR inclusion complexes on the IONP surface. A 2:1 stoichiometry is supposed to promote IONP primary agglomeration, facilitating the formation of the secondary needle-like agglomerates under external magnetic fields and their magneto-microfluidic separation. The efficiency of these field-induced processes increases with CUR concentration and  $\beta$ CD surface density, while their relatively short timescale ( $< 5 \text{ min}$ ) is compatible with magnetic drug delivery application.

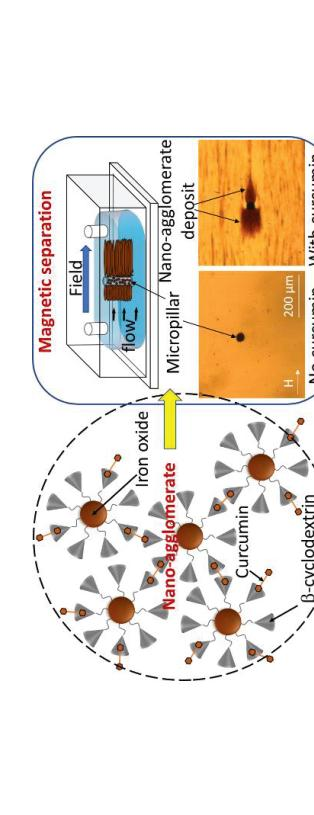


Fig. Mechanism of primary agglomeration of  $\beta$ CD-coated IONP through the formation of a 2:1  $\beta$ CD:CUR inclusion complex. The addition of CUR to the nanoparticle solution is expected to promote both 1:1 and 2:1  $\beta$ CD:CUR inclusion complexes on the IONP surface with sketch and results of the experimental setup with microfluidic channel (represented in an enlarged scale) with a micropillar used for the magnetic separation when the field-induced aggregates accumulate around the magnetized micropillar and are separated from the suspending liquid under flow.

## A Scalable Magnetic Control Strategy to Suppress Off-Target Nanoparticle Transport

Nima Mirkhani<sup>1</sup>, Michael Christiansen<sup>1</sup>, and Simone Schuerle<sup>\*</sup>

<sup>1</sup> Department of Health Sciences and Technology, ETH Zürich, CH-8092 Zürich, Switzerland.  
E-mail: simone.schuerle@hest.ethz.ch

Advances in nanomedicine have enabled delivery of therapeutics with reduced off-target effects. However, passive and active targeting strategies employed thus far fail to meet the expectations for enhanced, selective transport of drugs, particularly in hard-to-access tissues such as deep-seated solid tumors. Two approaches proposed to overcome such limitations are the use of external forces and harnessing biological agents to improve the drug transport. Magnetotactic bacteria (MTB) that biomimic iron-rich nanocrystals merge the benefits of both strategies [1]. Common techniques for magnetically-assisted delivery of nanoscale drug carriers suffer from lack of scalability and selectivity for deep targets. Recently, we reported on the capability of MTB to act as flow mediators due to their optimal magnetic and hydrodynamic properties under RMF. Here, we augment the scalable magnetic actuation scheme by rendering it selective through addition of a magnetostatic field.

By superimposing a magnetostatic gating field onto a uniform rotating magnetic field (RMF) and using MTB as a unique flow mediator, we transport nanoparticles (NPs) as model drug carriers in locations far from the source of the magnetic field. A microfluidic chip consisting of a central chamber as the model target tissue, surrounded by four off-target tissue chambers was fabricated. Such a design allows comparing different size of magnets placed at varying distances from the center. The magnetostatic field distribution, calculated through finite element modeling using COMSOL Multiphysics, indicates the ability to adjust the resolution of the zero-point in the central chamber (Fig. 1A). PV analysis of the torque-driven translational velocity of MTB in the wells containing only the bacterial suspension demonstrates complete suppression of motion in off-target chambers while MTB still generated flow in the target chamber (Fig. 1B).

Contact pinning lines centrally incorporated inside each well confined collagen in the center of each chamber, while an MTB-NP mixture was added around the tissue-minimicking compartment. RMF was generated by an electromagnetic setup composed of eight electromagnets. Two different actuation schemes were applied for 1 h: i) RMF alone and ii) selection field which is RMF superimposed with magnetostatic field from NdFeB magnets. Patterning was confirmed using labelled collagen type I and fluorescent NPs. (Fig. 1C). NP transport into the collagen was quantified in Fiji where integrated signals were normalized to the zero time point. Transport of NPs was reduced to the diffusion level in off-target areas when exposed to the selection field (Fig. 1D), while more than 40% of the magnetically enhanced transport was maintained in the target area. An even higher percentage is expected to be achieved in larger setups at animal or human scale. Here, a tradeoff between suppression and enhancement is attributed to field gradients acting against the transport to the target due to its proximity to the coils. This actuation scheme has the potential to pave the way for scalable and selective magnetic manipulation for drug delivery applications in combination with MTB or synthetic analogues as locally controlled flow mediators.

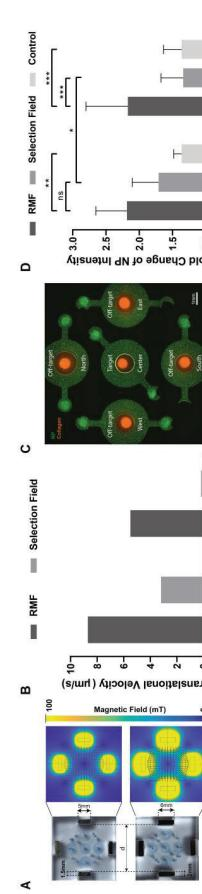


Figure 1. (A) Microfluidic chip consisting of five chambers and MTB-NP suspension. (B) NP transport under RMF and selection field. (C) Compartmentalized collagen and MTB-NP suspension. (D) NP transport under RMF and selection field.

[1] S. Schuerle et al., Science Advances, vol. 5, no. 4, p. eaav4803, 2019.

[2] N. Mirkhani et al., Advanced Functional Materials, vol. 30, no. 40, p. 2003912, 2020

## Red blood cell magnetophoresis as a function of oxygen partial pressure.

Lee R. Moore<sup>1</sup>, Nina A. Smith<sup>1</sup>, Mitchell Weigand<sup>2</sup>, Jenifer Gomez-Pastora<sup>2</sup>, Andre F. Palmer<sup>2</sup>, Jeffrey J. Chalmers<sup>2</sup>, Maciej Zborowski<sup>1\*</sup> (corresponding author: [zborown@ccf.org](mailto:zborown@ccf.org))

<sup>1</sup>Cleveland Clinic, Cleveland, Ohio and <sup>2</sup>The Ohio State University, Columbus, Ohio, U.S.A.

Red blood cell (RBC) magnetophoresis is the magnetic field-induced cell motion in viscous media such as blood plasma or physiologic saline solutions. We studied it as a function of the concentration of dissolved oxygen in normal RBCs using a cell tracking velocimetry (CTV, Fig. 1A) [1]. The hemoglobin (Hb) magnetic susceptibility changes from diamagnetic (when fully oxygenated, oxyHb) to paramagnetic (when fully deoxygenated, deoxyHb) resulting in a small shift in the RBC diamagnetic susceptibility from lower than that of water ( $-9.05 \times 10^{-6}$ ) to a higher than that of water, respectively. We systematically measured the resulting changes in the RBC magnetophoresis as a function of incremental changes in the solution O<sub>2</sub> concentration (measured by the O<sub>2</sub> partial pressure, pO<sub>2</sub>) and compared them with the O<sub>2</sub> equilibrium curve (OEC, by Hemox Analyzer and Blood Oxygen Binding System, BOBS™).

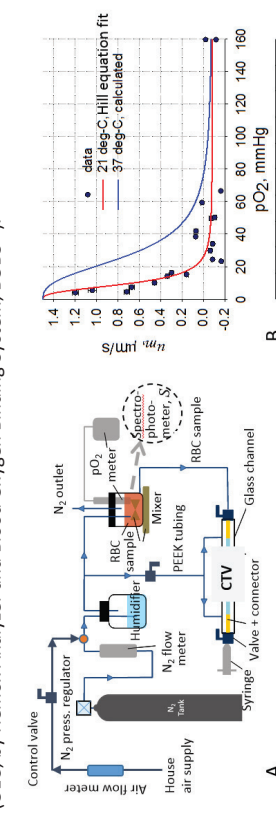


Figure 1. **A**: Experimental layout of the integrated CTV with in-line deoxygenation and pO<sub>2</sub> control system. **B**: RBC magnetophoresis vs. pO<sub>2</sub> data from a single normal blood sample,  $N=200$  data points,  $\sim 200$  RBC tracks per point. Red line is Hill equation fit for  $n=2.86$ ,  $p50=9.57$  mmHg at 21°C (CTV conditions), blue line is extrapolation to  $n=2.76$ ,  $p50=26.9$  mmHg at 37°C (BOBS conditions) characteristic of normal blood parameters.

The de-identified, normal blood samples were procured from the Cleveland Clinic Pathology discarded tissue repository with the approval of the institutional ethics committee. The resulting dependence of the RBC magnetophoretic velocity,  $u_m$  (in  $\mu\text{m}/\text{s}$ ) on  $\text{pO}_2$  (in millimeters mercury, mmHg) resembled an inverted, sigmoidal shape characteristic of the OEC curve (Fig. 1B) indicating that the intracellular Hb magnetic moment changes according to the kinetics of the cooperative Hb-O<sub>2</sub> binding. Understanding the detailed mechanism of RBC magnetophoresis may provide additional means to diagnose and treat hematological diseases. [1] Xie, W., Moore, L. R., Nakano, N., Chalmers, J. J., and Zborowski, M. (2019) Single cell magnetometry by magnetophoresis vs. bulk cell suspension by SQUID-MPMs: - A comparison. *JMM/M* **474**: 152-160. doi: 10.1016/j.jmm.2018.10.108

## Magnetic bio-hybrid microrobots for targeted stem cell delivery

Kiana Abolfathi<sup>1</sup>, Ralf M. Zwack<sup>2</sup>, Andrea Mohr<sup>2</sup>, Ali K. Hoshnai<sup>1\*</sup>

<sup>1</sup>School of Computer Science and Electronic Engineering, University of Essex, Colchester CO4 3SQ, UK

<sup>2</sup>School of Life Sciences, Protein Structure and Mechanism of Disease Group, Cancer and Stem Cell Biology Laboratory, University of Essex, Colchester CO4 3SQ, UK

amohr@essex.ac.uk, akafahhoshnai@essex.ac.uk

Small-scale (micro/nano) robots emerged as a revolutionary tool for minimally invasive and non-invasive interventions. One of the major applications of these robots is targeted drug/stem cell delivery for cancer treatment. The primary goal in this approach is to improve a drug/stem cell delivery to a desired location to provide an optimal concentration of the therapeutic agent.

We fabricated bio-hybrid microrobots (Fig. 1 (a)) by labelling mesenchymal stem cells (MSCs) with magnet particles. These can be magnetically guided under a rotating magnetic field (Fig. 1 (b)). In this study, first, the effective forces on the microrobot are introduced and the rotating magnetic field is studied. To identify the effects of fabrication parameters on the bio-hybrid microrobots cyocompatibility and magnetic responsiveness are experimentally studied using a magnetic microrobotics system (Fig. 1 (b)).

The image processing techniques (Fig. 1 (c and d)) are used to extract information including the microrobots size, the velocity under different magnetic field conditions and velocity under different fabrication parameters. The most influential parameters are identified using the resulting experimental data.



Fig. 1. **(a)** The bio-hybrid microrobot consist of MSCs loaded with nanoparticles, **(b)** MFG100 magnetic microrobotics system to study rotating magnetic field, **(c and d)** image process of the microrobots for characterization

## Magnetoresponsive nanocomposite aggregation during magnetic targeting

Sandor I. BERNAD<sup>1,\*</sup>, Vlad SOCOLIUC<sup>1</sup>, Daniela SUSAN-RESIGA<sup>2</sup>, Izabell CRACIUNESCU<sup>3</sup>, Rodica TURCU<sup>3</sup>, Elena S. BERNAD<sup>4</sup>, Maria IONICA<sup>5</sup>, Ladislau VEKAS<sup>1</sup>

<sup>1</sup> Centre for Fundamental and Advanced Technical Research, Romanian Academy - Timisoara Branch

<sup>2</sup> West University of Timisoara, Faculty of Physics, Timisoara, Romania

<sup>3</sup> National Institute for Research and Development of Isotopic and Molecular Technologies (INCDTIM),

<sup>4</sup> University of Medicine and Pharmacy "Victor Babes" Timisoara, Timisoara, Romania  
Cluj-Napoca, Romania

<sup>5</sup> Politehnica University of Timisoara, Department of Mechanical Machines, Equipment and Transportation, Timisoara, Romania

E-mail: \*sandor.bernad@upt.ro

The polymer, polyethylene glycol (PEG), is a stable, biocompatible, hydrophilic polymer, which has been extensively studied for applications to drug delivery. Moreover, PEG reduces the response of the immune system to nanoparticles. To reduce the clearance of the nanoparticles from the circulation, thereby allowing a longer circulation time and more nanoparticle accumulation at the target site. MNPs are prone to aggregation due to magnetic dipole-dipole interactions or Van der Waals forces which lead to their detection and clearance from the human mononuclear phagocytic system (MPS2) before they can reach their target sites, thus, limiting their biomedical applications. To generate the magnetic field, we used a Neodymium 50 type magnet (NdFeB50) with a maximum energy product ( $B_{\text{H}}$ ) of 50 MGOe. During magnetic particle targeting, 20 ml of the model suspensions are injected by the syringe pump in the mean flow into the artery model. In the present experiment, the MC\_PEG delivery at the targeted site is achieved by flow-mediated particle transport. The evolution of the functionalized magnetoresponsive clusters build-up is acquired at a frame rate of 30 frames/s. The MP's deposition and the magnetically induced chain length are investigated at the end of the injections (after 30 s).

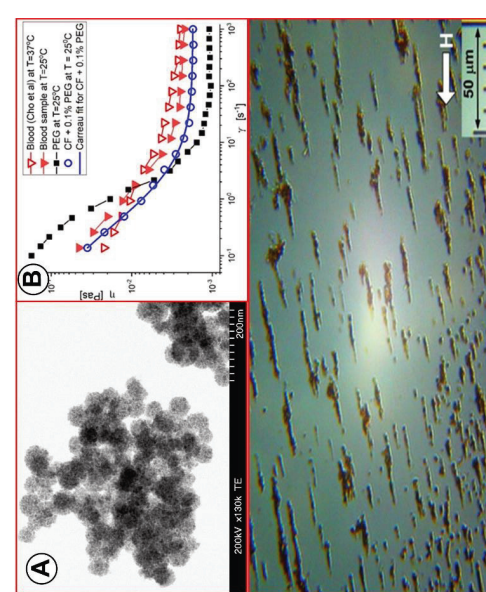


Figure: (A) TEM image of the magnetic nanoclusters coated with PEG. (B) Viscosity curves for blood (values from literature and healthy volunteer), PEG-coated function alised nanocomposite (MC\_PEG), and model suspension fluid (carrier fluid + 0.1% MC\_PEG). (C) Aggregation of the MC\_PEG coated nanocomposite in carrier fluid under the action of the magnetic field.

## The effect of SPIONs modified by aluminium nanoparticles on the growth of *S. aureus* and *E. coli*

Tomas Grondzak<sup>\*</sup>, Jakub Petrus<sup>1</sup>, Jana Meissnerova<sup>1</sup>, Bozena Hosnedlova<sup>2</sup>, Eva Klapkova<sup>1</sup>, Vedha Hari B Narayanan<sup>3</sup>, Jana Cepova<sup>1</sup>, Richard Prusa<sup>1</sup> and Rene Kizek<sup>1</sup>

<sup>1</sup> Department of Medical Chemistry and Clinical Biochemistry, Second Faculty of Medicine, Charles University in Prague and Motol University Hospital, V Uvalu 44, 150 06 Prague 5, Czechia

<sup>2</sup> BIOCEV, First Faculty of Medicine, Charles University, Praha 2, 130 00 Prague 2, Czechia

<sup>3</sup> Pharmaceutical Technology Lab, School of Chemical & Biotechnology, SASTRA Deemed University, Thanjavur-613401, India

\*Email: tomasgrondzak@gmail.com

Understanding the importance of methodology in traditional medicine could provide us with additional knowledge about the development of new drugs for serious diseases. Antibiotic resistance poses a significant threat in the treatment of bacterial infections. Ethnobotany provides us with a lot of information about plants with remarkable antibacterial effects, such as neem (*Azadirachta indica*). Furthermore, nanomedicine brings additional possibilities, thanks to different types and variations of nanoparticles. In this work, we focused on a new type of aluminum nanoparticles (AlNPs) which were synthesized by the green method from the leaves of *Azadirachta indica* (AlNPSN). SPIONs ( $\text{Fe}_3\text{O}_4$ ) were prepared according to standard procedure and then purified on a magnet. All nanoparticles were lyophilized (48 h, -80 °C) and then converted to a solution (60 min, 40 W). For testing, SPIONs were modified with chitosan (300 rpm, 25 °C), then purified on a magnet. SPIONs/Chitosan subsequently modified with AlNPSN (300 rpm, 25 °C, 6 h). Afterwards, the particles (SPIONs/Chitosan/AlNPSN) were washed with phosphate buffer (pH 7) and their properties were studied on bacterial cultures (*S. aureus* (MSSA) and *E. coli*), which were grown reproducibly in a pure medium (the areas under the growth curves (AUCs) were considered as a baseline). The antibacterial activity of particles was observed on bacterial growth curves, which were measured at 450 nm/540 nm for 24 hours at 25 °C, 300 rpm at 0.01 OD in LB medium, repeatedly in four cycles. AlNPSN alone were added to the bacteria at concentrations of 300–1600 µg/ml. The results were evaluated as AUCs. Following the addition of AlNPSN, the minimum inhibitory concentrations (MICs) and the minimum bactericidal concentrations (MBCs) were observed to be lower for *E. coli* (MIC = 310 µg/mL, MBC = 630 µg/mL) than for *S. aureus* (MSSA (MIC = 470 µg/mL, MBC = 1380 µg/mL), MRSa (MIC = 480 µg/mL, MBC = 1560 µg/mL),  $\text{Al}^{3+}$  alone were more effective for *E. coli* (MIC = 6 µg/mL, MBC = 22 µg/mL) than for *S. aureus* (MSSA (MIC = 9 µg/mL, MBC = 25 µg/mL), MRSa (MIC = 7 µg/mL, MBC = 23 µg/mL)). The study provided initial information on the effect of newly synthesized nanoparticles on *S. aureus* and *E. coli*.

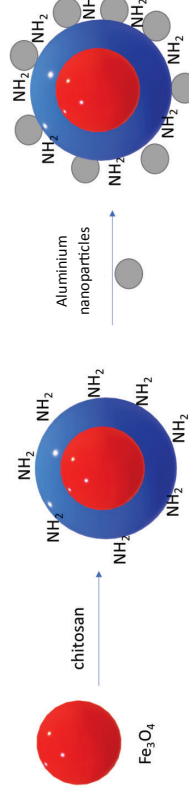


Figure: SPIONs modified with chitosan and subsequently with aluminum nanoparticles for antimicrobial activity monitoring and potentially further targeting the infection site.  
Acknowledgements. The project is being implemented under the grant project MZ ČR – RV0, FN in Motol 00064203.

## The effect of SPIONs modified by silver nanoparticles and vancomycin on the growth of *S. aureus* and *E. coli*

Jana Cepová<sup>1</sup>, Tomáš Grondzák<sup>1\*</sup>, Jakub Petrus<sup>1</sup>, Bozena Hosnedlova<sup>2</sup>, Eva Klapkova<sup>1</sup>, Vedha Hari B Narayanan<sup>3</sup>, Hoai Viet Nguyen<sup>4</sup>, Richard Prusa<sup>1</sup> and Rene Kizek<sup>1</sup>

<sup>1</sup>Department of Medical Chemistry and Clinical Biochemistry, Second Faculty of Medicine, Charles University in Prague and Motol University Hospital, V Úvalu 84, 150 06 Prague 5, Czechia

<sup>2</sup>BIOCEV, First Faculty of Medicine, Charles University, Prunovská 595, 252 50 Vesteč, Czechia

<sup>3</sup>Pharmaceutical Technology I Lab, School of Chemical & Biotechnology, SASTRA Deemed University, Thanjavur-613401, India

<sup>4</sup>Research Center for Environmental Monitoring and Modeling, University of Science, Vietnam National University, 334 Nguyen Trai Street, 100000 Hanoi, Vietnam  
\*Email: tomagrondzak@gmail.com

Multi-resistant bacterial strains pose a serious threat in the hospital environment. Management of such nosocomial infections requires completely new approaches. Vancomycin is known to be an antibiotic for the management of serious infections, among others caused by MRSA strains. Thanks to the use of nanotechnology, nanomedicine brings new possibilities, including targeting the use of surface modification of nanoparticles. In addition, green synthesis makes it possible to take advantage of the known medicinal properties of plants in traditional medicine. Sage (*Salvia officinalis*) has been known for its antibacterial and antiviral effects for a long time. Silver nanoparticles synthesized from sage extracts show significant antibacterial properties. They showed a 20 to 40% higher inhibitory activity than the control. Based on IC<sub>50</sub> calculation, MICs were determined to be 150 µg/mL AgNPsSS were prepared (24 h, 300 rpm, 25 °C), then centrifuged and lyophilized (48 h, -80 °C). SPIONs were prepared according to standard procedures, then purified on a magnet and lyophilized (48 h, -80 °C.) The nanoparticles were then resuspended by ultrasound (60 min, 40 W). For the purpose of this study, SPIONs were modified with chitosan (300 rpm, 25 °C) and then purified on a magnet. SPIONs/Chito were subsequently modified with AgNPsSS (300 rpm, 25 °C, 6 h). The particles were washed with phosphate buffer (pH7) and then modified with vancomycin (100 µg/mL). SPIONs/Chito/AgNPsSS/VANCO. The stability of SPIONs/Chito/AgNPsSS/VANCO prepared nanoparticles was verified in PBS (pH 7) by vancomycin analysis using HPLC. Subsequently, antibacterial activity was monitored by growth curves (*S. aureus* (MSSA, MRSA) and *E. coli*) which were measured at 450 nm/540 nm for 24 hours at 25 °C, 300 rpm at 0.01 OD in LB medium, repeated in four cycles. The results were evaluated as AUC growth curves. Bacterial cultures were grown reproducibly in a pure medium (AUCs were considered baseline). The study provided initial information on the effect of newly prepared species of nanoparticles on *S. aureus* and *E. coli*.

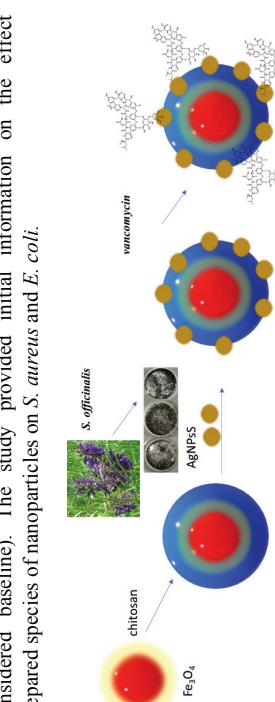


Figure: SPIONs modified with chitosan followed by AgNPsSS and vancomycin to monitor their antimicrobial activity with an aim to establish their potential for further targeting of the infection site.

Acknowledgements: The project is being implemented under the grant project MZ ČR – RVO, FN in Motol 00064203.

## Biodegradable PLGA-Based Magnetic Nanocomposites for Magnetic Target Retention and Sustained Release of Triamcinolone Acetonide from Detachable Microneedles

Chonnaeve Manupunt<sup>1</sup>, and Numporn Insin<sup>1</sup>

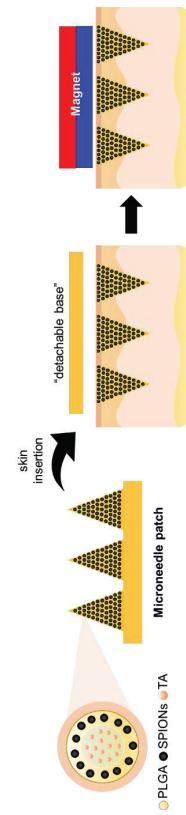
<sup>1</sup>Department of Chemistry, Faculty of Science, Chulalongkorn University, Bangkok, 10330, Thailand

\*Email: numporn@chula.ac.th

Triamcinolone acetonide (TA) is a well-known synthetic corticosteroid used as anti-inflammatory drug to treat some autoimmune diseases such as psoriasis, psoriatic arthritis, and alopecia areata. Furthermore, TA is commonly used to treat allergic rhinitis, acne, and aphthous stomatitis. Although TA has been applied to cure many diseases, it has rapid clearance from blood circulation for intravenous injection. To overcome the problems, intralesional injection of 10 to 40 mg/mL of TA is usually used for the treatment to provide sustained therapeutic level. The use of large drug dose can cause many side effects including skin atrophy, angioedema, women's menstrual disorders, rupture in the injection sites and adrenal suppression. To prolong therapeutic level without use of large drug dose, encapsulation of TA in slow biodegradable polymer or poly(lactic-co-glycolic acid) (PLGA) is necessary.

Dissolving microneedle treatment is one type of transcutaneous drug delivery approaches. This treatment use arrays of biodegradable polymer microneedles to provide controlled drug release into a cutaneous tissue. Compared to hypodermic injection, this route is non-invasive, rapid, pain-free, and possible for self-administration. Moreover, the microneedles may reduce the spread of disease from needle-reuse and needle-based injury.

Dissolving microneedles with detachable design have been extensively studied because of their controlled and sustained drug release ability of the polymers. Nonetheless, the polymers generally have very weak mechanical properties. Magnetic nanoparticles (MNPs) are interesting materials when forming composites with polymer particles due to their high mechanical properties. Furthermore, existing of magnetic properties from MNPs show good potential to provide high retention and good localization of polymer particles to improve prolong drug release profile and minimize side effect from drug. In this work, the microneedles made from composites of MNPs and TA loaded PLGA particles will be investigated. The microneedles with 50 mg MNPs loaded composites could improve mechanical strength of the needles up to 44% (2.3N at compression displacement 200 µm). Furthermore, the composites with 25 mg MNPs loaded composites show slower *in vitro* TA release profile when apply magnet about 71% cumulative release on 20 days (compared to 90% cumulative release of without magnet applying condition). The MNPs loading into these composites show good potential to fabricate a new microneedle drug delivery system with improved mechanical properties, magnetic target retention and sustained drug release.



## The magnetic field generated by single or multiple magnets for the magnetic drug targeting process

Maria-Cristina IONICA<sup>1,\*</sup>, Sandor I. BERNAD<sup>2</sup>, Daniela SUSAN-RESIGA<sup>3</sup>, Vlad SOCOLIU<sup>2</sup>, Izabell CRACIUNESCU<sup>4</sup>, Rodica TURCU<sup>4</sup>, Elena S. BERNAD<sup>5</sup>, Ladislau VEKAS<sup>2</sup>

<sup>1</sup> Politehnica University of Timisoara, Department of Mechanical Machines, Equipment and Transportation, Timisoara, Romania

<sup>2</sup> Centre for Fundamental and Advanced Technical Research, Romanian Academy - Timisoara Branch, Laboratory of Hydrodynamics and Cavitation

<sup>3</sup> West University of Timisoara, Faculty of Physics, Timisoara, Romania

<sup>4</sup> National Institute for Research and Development of Isotopic and Molecular Technologies (INCDTMI), Cluj-Napoca, Romania

E-mail: \*maria.ionica@student.upb.ro  
E-mail: maria.ionica@studnet.upb.ro

**Single** or multiple magnets configurations can be used to conduct the drug targeting process. A permanent magnet assembly consists of two or more magnets in an integrated magnet system designed to obtain an increased magnetic field. The main challenge for magnetic drug targeting (MDT) is that the magnetic gradients drop off fast when the distance from the magnet's source increases. Using multiple magnet combinations, we wanted to investigate the differences and advantages of their magnetic fields compared to the ones generated by single magnets. This paper aims to investigate (both numerically and experimentally) the magnetic fields generated by several single neodymium permanent magnets (NdFeB) and multiple magnet combinations used in magnetic drug targeting. The heights at which the magnetic fields were measured are closely related to the fact that most organs are not at a distance more prominent than 4 centimetres from the skin's surface. The obtained magnetic field values were used to analyse a series of magneto-rheological fluids (MRFs). The model suspension of magnetic carriers used in experiments was obtained, mixing blood analogous carrier fluid (CF) with PEG\_CMC (sizes in the range 80–150 nm), dispersed in distilled water, with 0.1% mass concentration, silver particles (sizes in the range 8–10  $\mu\text{m}$ ), and iron particles with two different dimensions (range 4–6  $\mu\text{m}$  and range 8–10  $\mu\text{m}$ , Carl Roth GmbH, Karlsruhe, Germany). Magneto-viscous characteristics were measured using a rotational rheometer (MCR 300, Physica, Stuttgart, Germany).

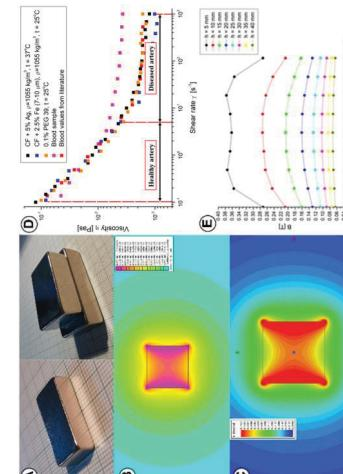


**Figure:** (A) Single and superimposed neodymium magnets used for experimental measurements. (B) Numerical simulation of the magnetic field used during the experimental investigation (via the free Finite Element Method of Magnetism (FEMM) software). (C) Numerical magnetic field simulation for the same permanent magnet using the commercial software Ansys Maxwell. (D) Comparison between the viscosity curves of the different model suspension fluid and blood. Blood viscosity curves were compared with the literature values and values measured from the healthy volunteer. (E) A magnetic field generated by the permanent magnet was used in the experimental investigation (measurements were done for several distances from the magnet surface). Experimental measurement was done using an F.W. Bell Gausmeter, model 5080.

## Molecular Insights of the Oxidation Process of Copper-Zinc Ferrites Nanoparticles Coated by a Polymer Layer

Dorota Lachowicz<sup>1\*</sup>, Angelika Knita<sup>1</sup>, Elżbieta Trynkiewicz<sup>1</sup>, Marta Gajewska<sup>1</sup>, Marcin Sikora<sup>1</sup>, Jan Żukowski<sup>1</sup>, Joanna Stępień<sup>1</sup>, Andrzej Bernasiak<sup>1,2</sup>

<sup>1</sup> AGH University of Science and Technology, Academic Centre for Materials and Nanotechnology,

al. A. Mickiewicza 30, 30-059 Krakow, Poland

<sup>2</sup> AGH University of Science and Technology, Faculty of Physics and Applied Computer Science, al. A. Mickiewicza 30, 30-059 Krakow, Poland  
email:dorota.bielinska@agh.edu.pl

The clinical use of MRI has been continuously developed since 1973, when Paul C. Lauterbur<sup>1</sup> collected the first MRI images, later enhanced in quality upon the introduction of gradient field selectors by Peter Mansfield. Lauterbur and Mansfield were awarded the 2003 Nobel Prize for their work. Meantime, two revolutionary ideas were introduced, namely functional MRI and the use of magnetic contrast agents. The first commercial MRI contrast agent, Magnevist® (Gd-DTPA) was presented in 1988. Unfortunately, there are several reports on the nephrotoxicity of gadolinium chelates as well as a concentration-dependent deposition of Gd in the brain revealed as high signal intensities in the globus pallidus and dentate nucleus on unenhanced T1-weighted images<sup>2</sup>. This is why iron oxides and ferrite nanoparticles have been intensively researched as alternative MRI contrast agents<sup>3</sup>. However, the biomedical application of ferrite and iron oxide nanoparticles is limited by the aggregation phenomenon<sup>4</sup>. The use of polymer coatings can prevent this negative phenomenon<sup>5,6</sup>. We showed that the coatings based on ionic derivatives of chitosan<sup>7,8</sup> ensured the stability and biocompatibility of the SPIONs aqueous suspension<sup>9</sup>. Importantly, the applied derivatives can form durable metal-polymer connections by chelating relevant metal ions. Moreover, such coating enables further functionalization of the nanoparticles by applying oppositely charged polymers in the so-called "layer-by-layer" approach<sup>5,6</sup>. However, there are reports that the attachment of ligands via anchor groups to nanoparticles may cause changes on the particle surface, such as oxidation or surface degradation<sup>10</sup>. Oxidation processes reduce the saturation magnetization of iron nanoparticles<sup>11</sup>. Although the appropriate ligands can reduce spin slanting in the surface region, Salafraza and coauthors<sup>12</sup> showed that a higher surface density of capping molecules improves the magnetic properties of iron oxide nanoparticles.

The main goal of the project was to investigate the influence of the polymer layer (a cationic derivative of chitosan and dextran, PEG) on the magnetic structure of copper-zinc ferrite nanoparticles. For the application of copper-zinc ferrite nanoparticles as contrast agents in magnetic resonance imaging (MRI) or in magnetic hyperthermia, their surface has to be coated by a polymer or surfactant layer. This modification can influence the surface oxidation state and the magnetic properties of the particles. In this project, the effect of the layer of three polymers, cationic chitosan, cationic dextran, and polyethylene glycol on copper-zinc ferrite nanoparticles was evaluated. For this purpose, X-ray absorption spectroscopy (XAS) and X-ray magnetic circular dichroism (XMCD) measurements were used, thanks to which the local magnetic and electronic properties of the particles' surface area were examined with and without surface modification. The local structures around the Cu, Zn, Fe, and O sites were investigated as reflected by K-edge X-ray Absorption Spectra. Based on a multivariate analysis supported by  $^{57}\text{Fe}$  Mössbauer and ICP-OES data, the nanoparticle composition was determined. To further explore the structure of all obtained nanoparticle systems, XPS spectra of all polymer shells were analyzed to determine the chemical states.

Reference: 1. Nature, 1973 (242), 190–191.

2. Front. Mol. Neurosci., 2018 (11), 1–12.

3. Monitor. Sci. Rep., 2019 (9).

4. Adv. Coll. Interface Sci., 2019 (265), 29–44.

5. J. Nanoparticle Res., 2014 (16), 1–11.

6. Coll. Surf. B, 2017 (150), 402–407.

7. J. Mater. Chem. B, 2019 (7), 2962–2973.

8. Soft Matter, 2009 (5), 4726–4732.

9. Nanomedicine, 2018 (14), 131–140.

10. Zeitschrift für Phys. Chemie, 2018 (232), 819–844.

11. J. Phys. Chem. C, 2015 (119), 19404–19414.

12. Nano Lett., 2012 (12), 2499–2503.

## NP-cellular hitchhiking system for targeted combination therapy and diagnosis of glioblastoma

Xanthippi Koutsoumpou<sup>1</sup>, Steven De Vleeschouwer<sup>2</sup>, Jeff Rozenski<sup>4</sup>, Teresa Pellegrino<sup>5</sup>, Stefaan J. Soenens<sup>1</sup>, Bella B. Manshian<sup>1,3</sup>

1. NanoHealth and Optical Imaging Group, Department of Imaging and Pathology, KU Leuven, Leuven, Belgium.
2. Department of Neurosurgery, University Hospitals Leuven, Leuven, Belgium.
3. Translational Cell and Tissue Research Unit, Department of Imaging and Pathology, KU Leuven, Leuven, Belgium.
4. Rega Institute for Medical Research, Department of Pharmaceutical and Pharmacological Sciences, KU Leuven, B3000 Leuven, Belgium.
5. Nanomaterials for Biomedical Applications, Istituto Italiano di Tecnologia, Via Morego 30, 16163 Genova, Italy.

Email: bella.manshian@kuleuven.be

Glioblastoma (GBM) remains an incurable tumor and there is a paramount need for more effective therapeutic approaches, taking into consideration the Blood Brain Barrier impediment. In this project, we propose a novel nanoparticle (NP) cellular hitchhiking system (NPCHS) for GBM treatment. Here, monocytes were conjugated with PLGA NPs packed with the drug paclitaxel (PTX) and Super Paramagnetic Iron Oxide nanocubes (SPIONs) which will bestow the system with MRI contrast, magnetic targeting and hyperthermia treatment while monocytes will provide a direct targeting to GBM by natural chemotaxis. For this end, fluorescently labelled plain and PTX-loaded PLGA NPs were synthesised using the nanoprecipitation method, and fully characterised for their physicochemical properties and drug loading efficiency using DLS, Zeta potential, TEM, HPLC and ICP-MS. The NPs were screened for toxic effects in relevant human and mouse cell lines, namely, monocytes, endothelial cells and glioma cells, using high content screening and image based flow cytometry systems. The optimal ratio of NP-cell conjugation was determined. Next, SPION nanocubes, approximately 20 nm in size were loaded into the PLGA NPs, MRI measurements of SPION loaded PLGA NPs or U87 cells incubated with SPION-loaded NPs revealed the increase of  $r_2$  relaxation rates with increasing Fe concentrations. *In vivo* chemotaxis was investigated using optical imaging with the IVIS Spectrum and via intravital microscopy, in subcutaneous and orthotopic glioma tumors following intravenous injection of NP conjugated monocytes. Tissue slices from tumors and major organs were investigated for targeting and therapeutics using H&E staining and immunohistochemistry. In general, formulation showed homing ability towards GBM tumors, *in vivo*, promising a potential for targeted GBM treatment.

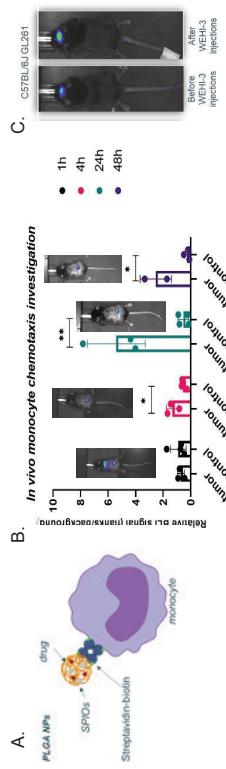


Figure 1) A) Representative sketch of the proposed NP-cell formulation. B) *In vivo* homing of NPCHS in subcutaneous glioma tumors. C) *In vivo* homing of NPCHS in orthotopic glioma tumors.

## Trifunctional Fluorescent Cobalt Ferrite Nanoparticles for Hyperthermia Therapy, Cell Probing and Drug Delivery

Madhuri Mandal Goswami,<sup>1,2,3\*</sup> Arpita Das<sup>3</sup>, Damodar Prasad Goswami<sup>1</sup>

<sup>1</sup>Centre for Biomedical Research,, Bharat Sevasharam Sangha Hospital, Diamond Harbour Road, Joka, Kolkata – 700104, India

<sup>2</sup>School of Material Sciences, Indian Association for the Cultivation of Sciences, 2A & 2B Raja S C Mullick Road, Jadavpur, Kolkata 700032, India

<sup>3</sup>CRNN, Calcutta University, Block-ID, Sector III/2, Salt Lake, Kolkata-700106, India

\*Email: madhuri.snbose@gmail.com

Here we have reported a new protocol for drug delivery from hollow sphere cobalt ferrite nanoparticles (HCF NPs). The structure and crystallite size of HCF NPs are analyzed by XRD measurement and the morphological information is obtained from FESEM & TEM analysis. Here the HCF NPs are properly designed for delivery of dopamine (DA) as anticancer drug to cancer site. The DA polymerizes to its giant molecule polydopamine (PDA) inside hollow HCF in presence of TRIS buffer at higher pH 9 and a composite, HCF-PDA is formed. Being giant molecule polydopamine remain stable inside the hollow particles, but when these HCF-PDA come in contact of low pH i.e.pH 5 (cancer cells pH), free DA start to be released. The DA release studies are monitored by UV-visible spectroscopy with progress of time at two different pH and temperatures. At hyperthermic temperature (45 °C) release enhances compared to physiological temperature (37 °C). It has been observed that HCF-PDA has a fluorescent property whereas DA has no such effect. So, tagging of HCF-PDA with cancer cells can also be monitored by fluorescence imaging. Hence, we have successfully synthesized trifunctional HCF-PDA composite which can serve three purposes like cancer cell probing, hyperthermia therapy and drug delivery.

## Hybrid iron oxide core@mesoporous silica shell nanoparticles for magnetic hyperthermia, phototherapy and drug delivery

Alexandre Adam<sup>1</sup>, Joëlle Bizeau<sup>1</sup>, Francis Perton<sup>1</sup>, Sébastien Harlepp<sup>2</sup>, Florent Meyer<sup>3</sup>, Mariana Tasso<sup>4</sup>, Sylvie Beguin-Collin<sup>1</sup>, Damien Mertz<sup>1</sup>

<sup>1</sup>IPCMS-CNRS UMR 7504, Univ. of Strasbourg, <sup>2</sup>INSERM U1109, Univ. of Strasbourg, <sup>3</sup>INSERM U1121, Univ. of Strasbourg, <sup>4</sup>Univ La Plata, Argentina.

E-mail : [damien.mertz@ipcms.unistra.fr](mailto:damien.mertz@ipcms.unistra.fr)

Designing nanoparticle platforms responding to external fields such as radiofrequency magnetic field and light has become a great challenge for the development of new treatments for nanomedicine. Iron oxide nanomaterials appear as suitable remotely wave-responsive materials respectively for magnetic hyperthermia and phototherapy applications while mesoporous silica (MS) are suitable shell coatings given their biocompatibility, easy surface modification and high drug delivery capability. In this talk, we will present various iron oxide@MS core shell controlled nanostructures designed and functionalized as various nanoplateforms that may serve as : multimodal theranostics probes for fluorescence/MRI imaging coupled with magnetic hyperthermia,<sup>[1-3]</sup> hybrid fluorescent nanoplateforms assessed *in vivo* models<sup>[4]</sup> or drug release coupled with NIR light-induced phototherapy applications<sup>[5]</sup>.

- [1] F. Perton, M. Tasso, G. A. Muñoz Medina, M. Ménard, C. Blanco-Andujar, E. Portiansky, M. B. F. van Raap, D. Beguin, F. Meyer, S. Beguin-Collin, D. Mertz, *Applied Materials Today* **2019**, *16*, 301.
- [2] M. Ménard, F. Meyer, C. Affolter-Zbaraszczuk, M. Rabineau, A. Adam, P. D. Ramirez, S. Beguin-Collin, D. Mertz, *Nanotechnology* **2019**, *30*, 174001.
- [3] A. Adam, K. Parkhomenko, P. Dueñas-Ramirez, C. Nadal, G. Cotin, P.-E. Zorn, P. Choquet, S. Beguin-Collin, D. Mertz, *Molecules* **2021**, *26*, 971.
- [4] F. Perton, S. Harlepp, G. Follain, K. Parkhomenko, J. G. Goetz, S. Beguin-Collin, D. Mertz, *Journal of Colloid and Interface Science* **2019**, *542*, 469.
- [5] A. Adam, S. Harlepp, F. Ghilini, G. Cotin, B. Freis, J. Goetz, S. Beguin, M. Tasso, D. Mertz, *Colloids and Surfaces A: Physicochemical and Engineering Aspects* **2022**, *640*, 128407.

## LC-MS/MS as a Study Method of the Release Kinetics of Remdesivir from Magnetic Nanoparticles

Jakub Petrus<sup>1</sup>, Tomas Grondzak<sup>1</sup>, Katerina Dunovska<sup>1</sup>, Bozena Hosnedlova<sup>2</sup>, Eva Klapkova<sup>1</sup>, Carlos Fernandez<sup>3</sup>, Jana Cepova<sup>1</sup>, Richard Prusat<sup>1</sup> and Rene Kizek<sup>1</sup>

<sup>1</sup> Department of Medical Chemistry and Clinical Biochemistry, Second Faculty of Medicine, Charles University in Prague and Motol University Hospital, V. Úvalu 841/150/06 Prague 5, Czechia

<sup>2</sup> BIOCEV, First Faculty of Medicine, Charles University, 252/50 Vesce, Czechia

<sup>3</sup> School of Pharmacy and Life Sciences, Robert Gordon University, Garthdee Road, Aberdeen AB10 7QB, Aberdeen, United Kingdom

\*Email: [jakubpet@gmail.com](mailto:jakubpet@gmail.com)

Originally targeted against Ebola and Marburg viruses, antiviral drug remdesivir (RDV) has shown clinically relevant effects against SARS-CoV-2 virus. RDV is metabolised into its triphosphate form which acts as an inhibitor of viral replication by being an ATP analogue and stalling viral RNA polymerase. In blood, 93% of RDV is bound to proteins and its half-life is around one hour. Because of its concentration declining quite rapidly, it might be beneficial to develop a magnetic nanocarrier with the ability to release RDV over time. Firstly, we aimed to develop a LC-MS/MS method to detect RDV in blood plasma/serum. Secondly, we prepared magnetic nanoparticles (MNPs) to which we bound RDV. Then, the release kinetics of RDV in blood plasma/serum/buffers was studied at different pH. Finally, we compared the stability of free RDV with RDV bound to MNPs in blood plasma/serum in order to determine whether the attachment increases RDV half-life. LC-MS/MS method for the detection of RDV was developed - mobile phase A (100% water + 0.1 % HCOOH), mobile phase B (95% ACN + 5 % water + 0.1 % HCOOH), colon Zorbax C18, RT 1.88 min, 603.2 m/z → 200 m/z. In buffer solution, the RDV signal-concentration relation was linear ( $r = 0.9996$ ), LOD 0.3 ng/ml, LOQ 5 ng/ml. In plasma/serum, the relation was linear, too ( $r = 0.9960$ , 9996%), LOD 1.9 ng/ml, LOQ 6.5 ng/ml. RDV was bound to the prepared MNPs primarily by electrostatic interaction (24 h, 25°C, 400 rpm). Subsequently, the dynamics of RDV release into the media was studied over 24 h. RDV was successfully eluted from the magnetic carrier and detected by LC-MS/MS. For the potential biomedical use of nanoparticles, it is necessary to study the effects of selected molecules that modify the surface in a significant way by the formation of a protein corona. The protein corona can affect the behavior of the nanotransporter, both positively and negatively.

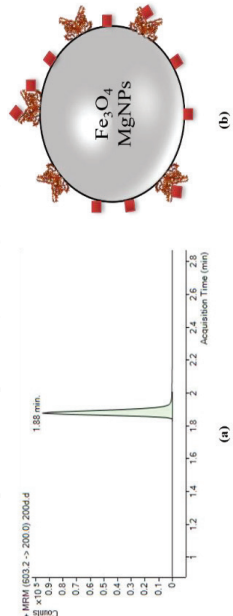


Figure. (a) LC-MS/MS peak of RDV with RT 1.88 min. (b) structure of MNPs with bound RDV (red squares) and protein corona made primarily of albumine.

Acknowledgements: The project is being implemented under the grant project MZ ČR – RVO, FN in Motol 00064203 and PortASAP CA COST Action CA16215.

## Functionalization of primary T cells with magnetic Nanoparticles for guided immunotherapy

Felix Pfister<sup>1</sup>, Philipp Boosz<sup>1</sup>, Rene Stein<sup>1</sup>, Bernhard Friedrich<sup>1</sup>, Lars Fester<sup>2</sup>, Diana Dudziak<sup>2</sup>, Christoph Alexiou<sup>1</sup> and Christina Jank<sup>1</sup>

<sup>1</sup> Department of Otorhinolaryngology, Section of Experimental Oncology and Nanomedicine (SEON), Else Kröner Fresenius-Stiftung-Professorship, Universitätsklinikum Erlangen, Germany; <sup>2</sup> Institute of Anatomy and Cell Biology, Friedrich-Alexander-Universität Erlangen-Nürnberg (FAU); <sup>3</sup> Laboratory of Dendritic Cell Biology, Department of Dermatology, Universitätsklinikum Erlangen, 91054 Erlangen, Germany

\*E-mail: felix.pfister@uk-erlangen.de

Adoptive T cell therapies are an emerging part of immunotherapies targeting cancer. While these forms of treatment can significantly improve patient survival and reduce disease burden, they can also cause severe adverse side effect. Furthermore, the positive results of T cell therapy against blood cancers cannot yet be reproduced on solid tumors. This might be due to the immunosuppressive microenvironment of solid cancers, limiting T cell functionality and infiltration. Therefore, it is of interest to improve the efficacy of T cell therapies against solid tumors by increasing the number of tumor infiltrating T cells. However, a systemic escalation of administered T cell numbers is not advisable due to the aforementioned risk of serious side effects. To accumulate T cells in the tumor region, adoptive T cells will be loaded with superparamagnetic iron oxide nanoparticles (SPIONs) and re-administered administered into the vascular supply of the respective cancer tissue. Due to the magnetic properties of SPIONs, T cells are guidable by an external magnetic field, allowing the local enrichment in the tumor, which should increase anti-tumor activity and a reduction of systemic side effects.

Prior experiments resulted in the development of a suitable particle system with citrate-coated SPIONs, which we improved to enhance SPION stability in the medium, SPION uptake and T cell viability. We were also able to enrich these nanoparticle-loaded T cells magnetically in a dynamic flow system. Additionally, we investigated the impact of SPION loading on the immune response of primary human T cells. No difference in the production of cytokines such as IFNγ, TNFα or IL-2 after polyclonal stimulation was detected (Figure A). Additionally, we found that the SPIONs were located either intracellularly or were stably attached to the plasma membranes, without spilling over to non-loaded cells (Figure B). Therefore, we have shown a particle system suited for the local magnetic enrichment of T cells for possible future therapeutic approaches.

**Acknowledgments:** This research was funded by the Else Kröner Fresenius Stiftung, Bad Homburg v.d.H., Germany (2018\_A88) to C.J. and Deutsche Forschungsgemeinschaft (DFG)-SFB TRR 305-B05, DU5485-1 to D.D. as well as intramurally by the Emerging Fields Initiative EFL-BIG-Thera and the Staedler-Stiftung to D.D. and C.A.

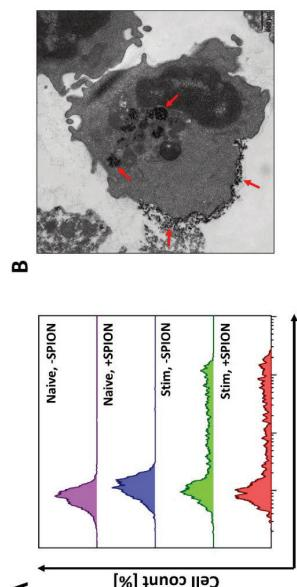


**Figure. Activation of SPION-loaded T cells and cellular SPION localization.** Primary human CD3+ T cells were isolated from peripheral blood and loaded with SPIONs overnight. A) After loading, T cells were polyclonally stimulated with anti-CD3/CD28/CD2 antibodies and rhIL-2 (Stim) or not (Naive) for 24 h and analyzed for cytokine expression. B) Transmission electron microscopy picture of a T cell after SPION-loading. Intracellular SPIONs and SPIONs attached to the plasma membrane are marked via red arrows (from Boosz et al., *Cancers* 2021).

## Magnetic nanoparticle focusing system on the blood vessel using an array of permanent magnets

Boyoung Son and Jungwon Yoon

School of Integrated Engineering, Gwangju Institute of Science and Technology, Gwangju 61005, Republic of Korea.  
Email: Sonbyoung@gm.gist.ac.kr Mobile: 82-10-4071-4616

Magnetic nanoparticles (MNPs) are a core research topic in medical nanotechnology because they are nano-scale particles that can be manipulated in the human body. Targeted drug delivery (TDD) and Magnetic Hyperthermia are the latest medical technologies using MNPs, which are being researched as a representative. What these two technologies need in common is to focus the injected MNPs into a single point. So, we studied how to focus MNPs injected into the blood vessel into a single point within the blood vessel.

As per Earnshaw's theorem, a static magnetic field cannot focus a magnetic particle to a point in a 3D environment. Therefore, existing studies utilize a coil system to focus particles with a dynamic magnetic field. However, these systems have problems with heat generation due to the operation of the coil, the size and weight of equipment becoming large and heavy, and it is difficult to concentrate particles immediately. This study proposes a method that utilizes an array of permanent magnets to instantly focus magnetic particles on the vessel wall through a compact and lightweight system. Taking advantage of the specificity of blood vessels, we use a static magnetic field to target MNPs to a point on the vessel wall rather than a point in space. This system is simple and small, so it can be used together with TDD and Magnetic Hyperthermia systems.

The permanent magnet arrangement of the system is simulated in Figure (a). In this system, two axes out of three axes in space apply a collecting force based on the center point, and the other axis gives a pushing force. In Figure (b), we experiment with focusing MNPs in a static fluid environment. The size of the MNPs is 1 μl (Resovist, 55.85 Fe-mg/ml), and the size of the working space is 3cm. In the figure (c), the MNPs focusing experiment in dynamic flow is conducted by constructing a blood vessel model. The core size of MNPs is 60nm (Resovist, 55.85 Fe-mg/ml) and the fluid is 60% aqueous glycerol solution. The fluid velocity is 5mm/s. The radius of the tube is 3.5mm. Through these experiments, we show that the MNPs focusing system can be implemented using a simple permanent magnet system.

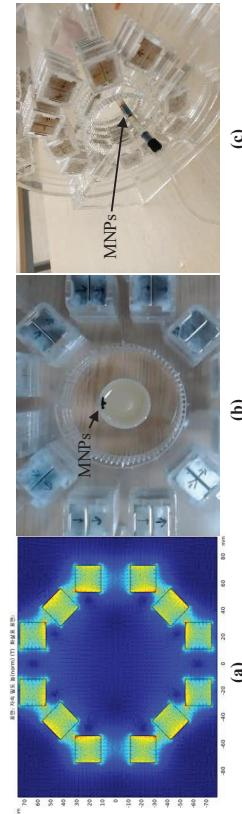


**Figure. (a)** COMSOL simulation of permanent magnet arrangement. The direction of the arrow indicates the direction of the force received by the MNPs. **(b)** An experiment in which MNPs were injected in a static flow. Tested in oil environment. **(c)** A system that tested the focusing performance of MNPs in dynamic flow. After flowing the fluid at a constant rate using a cylinder pump, 10μl of particles are injected through a syringe, and the amount of MNPs collected at the target location is measured.

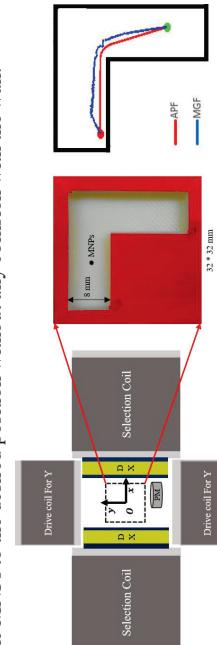
## A Novel Guidance Scheme for Magnetic Particles Inspired by the Artificial Potential Field

**Yonggyu Kim<sup>1</sup>, Minh Phu Bui<sup>1</sup>, Myungjin Park<sup>1</sup>, Hosu Lee<sup>1</sup> and Jungwon yoon<sup>1\*</sup>**

<sup>1</sup>School of Integrated Technology, Gwangju Institute of Science and Technology, Gwangju 61005, South Korea.  
\*Email: jyoon@gist.ac.kr

Magnetic nanoparticles (MNPs) can be controlled using a magnetic field for magnetic drug targeting (MDT), and they can also be used as a contrast agent for imaging devices using technologies such as Magnetic Particle Imaging (MPI). Magnetic actuation has the benefits of safety and depth of penetration into organic tissue, however accurate control and monitoring of the MNPs is difficult. To enhance the targeting efficiency of MDT, a MNPs guidance system that integrates actuation and imaging feedback needs to include the application of a path-planning algorithm for the MNPs. Furthermore, an effective actuation method capable of driving the MNPs according to the planned path must also be considered. In this research, we propose a system for guiding the MNPs along a desired path generated using an Artificial Potential Field algorithm. In this system, the attractive and repulsive fields are generated using a permanent magnet and electromagnetic coils, respectively. This method can contribute to the path-planning required to increase the targeting ratio of MNPs by manipulating the magnetic gradient field using a method inspired by the artificial potential field method that is usually used for robot navigation.

The coil configuration used in this experiment is shown in figure (a). The PM shown in this figure is a permanent magnet, while  $D_x$  denotes the drive coils for the x-axis. The coil configuration used in this system consists of one Maxwell coil (Selection coil) and two Helmholtz coils (Drive coils for the x- and y-axis). The operation of these coils is controlled using a C-RIO (National Instruments, USA) controller and interface device. Figure (b) shows the experimental model and the result of the experiment carried out with the developed apparatus. The model size is  $32 \times 32$  mm and BNF-Dextran MNPs are used in this experiment. To detect the MNPs, a camera (Logitech Brio UHD PRO, Korea) is used. The result of the experiment, presented on the right side of figure (b), shows that the actuation system was able to move the MNPs to the desired position without any collision with the wall.



Coaxial drive coils are connected in series.  
 $X$ -axis and  $Y$ -axis respectively.

Figure. (a) Coil configuration for the proposed actuation system. (b) Experimental model and results. The red line (APF) is the result of the Artificial Potential Field simulation and the blue line (MGF) is the experimental result with the developed apparatus. The MNPs are injected at the starting point (red dot) and moved to the target point (green dot) by the permanent magnet (PM) shown in (a). If the MNPs come close to the model wall during the experiment, the coil system generates a magnetic field and forces them away from the wall.

## Quantitative measurements of the influence of polymer brush length on magnetic nanoparticle interactions and signal enhancement during linear aggregation via magnetic particle spectroscopy

A.R. Hunter<sup>1</sup>; O.T. Mefford<sup>1</sup>

<sup>1</sup>Department of Materials Science and Engineering, Clemson University, Clemson, SC

The design of magnetic nanoparticles for functional polymer nanocomposite materials is an expanding field with recent interest in therapeutic techniques like magnetic hyperthermia for biomedical applications, sequestration of transuranics for environmental remediation, and functional catalytic materials utilizing inductive heating.

The interest of this study is to measure the influence of magnetic dipole-dipole interactions on hysteresis curves, signal intensity and the corresponding harmonic spectra which elucidates physical and structural properties of the particle and bound analytes valuable to the design and application of magnetic bioassays. A recently proposed solution to controlling cluster formation is the surface modification of the particles with stabilizing hydrophilic polymers which has shown to be a promising method for controlling colloidal arrangement.<sup>1</sup> Rinaldi et al. recently demonstrated by theoretical modeling that magnetic dipole-dipole interactions between chains formed by aggregation under an applied field enhances the MPI signal.<sup>2</sup> This suggests that the intensity of the signal and the higher odd harmonic frequencies emitted by the particles can be tuned by surface modification. Herein, this study aims to experimentally demonstrate this prediction by evaluating the influence of steric repulsion on chain formation via MPS. In this work, we have synthesized and characterized nitroDOPA terminated poly(ethylene oxide) coated iron oxide nanoparticles of molecular weights 2,000, 5,000, and 10,000 g/mol. MPS measurements of each sample will be conducted to measure the hysteresis curves and relaxation behavior. The postulated results of this study include demonstration of the tunability of particle signal strength under surface modifications and further evaluation of the interactions between chains and clusters of particles under applied field. The implications of this are improved synthesis techniques that can generate higher contrast images for MPI applications and a deepened understanding of the parameters that modulate variations in theoretical particle behavior.

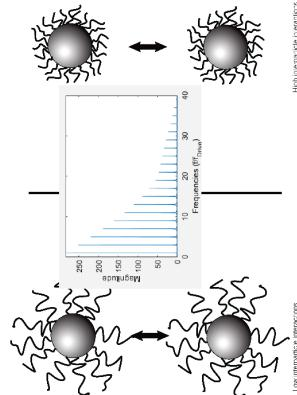


Figure: Demonstration of interparticle interactions and predicted MPS measurement data

### References:

1. Saville et al. *J. Colloid Interface Sci.* **2014**, *424*, 141-151.
2. Zhao, Z.; Rinaldi, C. *C. Phys. Med. Biol.* **2020**, *65*, 185013.

## Temperature imaging with a single harmonic magnetic particle imaging approach

Khas-Julian Jansen<sup>\*</sup>, Jing Zhong<sup>2</sup>, Thilo Vierect<sup>1</sup>, Meinhard Schilling<sup>1</sup> and Frank Ludwig<sup>1</sup>

<sup>1</sup>Institute for Electrical Measurement Science and Fundamental Electrical Engineering, TU Braunschweig

<sup>2</sup>School of Instrumentation and Optoelectronic Engineering, Beihang University

\*Email: k.janssen@tu-bs.de

Magnetic Particle Imaging (MPI) is a very promising imaging modality for disease theranostics. Thereby, magnetic nanoparticles (MNPs) are used as tracers for imaging by utilizing their non-linear response signal to an alternating magnetic field to image their spatial distribution. In addition, the particles can also be functionalised to store drugs in their shell and release them by remote heating for targeted drug delivery and release. Another application is magnetic hyperthermia, where the particles are heated by a high frequency external magnetic field. One application for this can be found in cancer research, to induce apoptosis of cancer cells. For both applications the knowledge of the particle's temperature and the environmental temperature is of great interest.

In this study we employ our single harmonic MPI approach for temperature imaging with the signal of the  $3f_0$  harmonic of the particles. A spot sample of synomag D-70 particles ( $c(\text{Fe}) = 10 \text{ mg/ml}$ ) is measured at different temperatures to obtain a calibration curve of the signal change of the particles. Afterwards, we measured a line phantom with a size of  $4 \times 1.5 \text{ mm}$  filled with the same particles also at different temperatures. A reconstruction of the measured images was performed at the  $3f_0$  harmonic of the particles with an algebraic reconstruction technique (ART). Furthermore, the  $3f_0$  harmonic signal was used to estimate the temperature of the particle's environment, via a change of the phase of the particles signal. In the figure below, you can see the results of the temperature estimation (Fig. 1) and the reconstruction of a line phantom (Fig. 2, left). Fig. 2 also shows a temperature difference of  $\Delta T \leq 1^\circ\text{C}$ , compared between the measured temperature with a fibroptic sensor and the estimation from the particles.

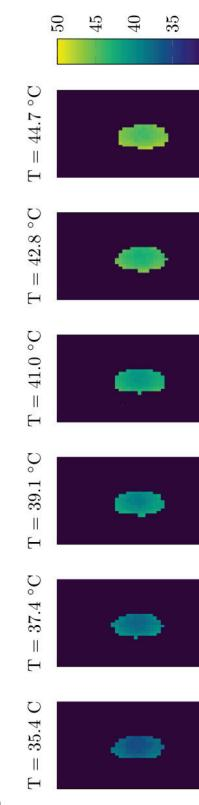


Fig. 1: Temperature image of the line phantom at different temperatures, calculated by the calibration function

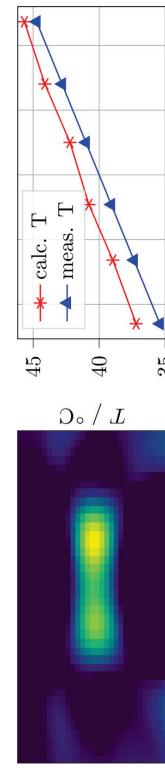


Fig. 2: Reconstruction based on the  $3f_0$  harmonic of a line phantom (left). Measured temperature with a fibrooptic thermometer (right, blue) and the calculated temperature (right, red)

## Human-Head-Sized Magnetorelaxometry Imaging of Magnetic Nanoparticles using Optically Pumped Magnetometers

Aaron Jaufenthaler<sup>1</sup>, Peter Schier<sup>1</sup>, Tillmann Sander-Thömmes<sup>2</sup>, Maik Liebl<sup>2</sup>, Frank Wielhorst<sup>1</sup>,

and Daniel Baumgarten<sup>1</sup>

<sup>1</sup>Private University for Health Sc., Medical Informatics and Technology (UMIT-Tirol), Hall in Tirol, Austria

<sup>2</sup>Physikalisch-Technische Bundesanstalt (PTB), Berlin, Germany

\*Email: aaron.jaufenthaler@umit-tirol.at

Exciting biomedical applications of magnetic nanoparticles (MNP), e.g. magnetic hyperthermia require quantitative imaging of MNP distributions for treatment planning and monitoring. MNP can be quantified by magnetorelaxometry (MRx), where the MNP's relaxation after previous magnetization is measured. Spatial information can be obtained by repeating the MRx procedure with different inhomogeneous magnetization fields and solving an ill-posed inverse problem. This approach, called magnetorelaxometry imaging (MRxi), has been successfully demonstrated with superconducting magnetometers (SQUID)[1] and optically pumped magnetometers (OPM) [2]. In contrast to magnetic particle imaging (MPI), MRxi potentially offers covering large, e.g. human head sized regions of interest, at the cost of a much lower temporal resolution. However, the promoted upscaling of MRxi has not been demonstrated experimentally yet.

In this work, we theoretically and experimentally investigate the feasibility of a human head sized MRxi imaging setup for quantitative imaging of MNP. We exploit the possibility of flexible OPM sensor positioning and the combination of small and large magnetization coils for targeted magnetization of surface resp. deep regions containing MNP. Our setup (Figure 1 left) is composed of a 3D-printed helmet, which was generated based on MRI data. The helmet houses 25 dual-axis OPM from QuSpin LLC, 64 small magnetization coils and eight large magnetization coils. The phantom houses Berlin MNP ( $c(\text{Fe})=3.7 \text{ mg/cm}^3$ , 1.2 mm cubes). The setup was operated within a moderately shielded room (Ak3b) at the PTB Berlin.

Like expected from our simulations, the large coils generate high SNR signals, allowing for a coarse reconstruction of the MNP distribution. The relaxation signals obtained when activating the small coils are sparse and improve the reconstruction results for surface regions containing MNP. A preliminary reconstruction result is shown in Figure 1 (right). In our (poster) presentation we will especially discuss the challenges of building a head sized OPM-MRxi setup, current limitations and possible improvements.

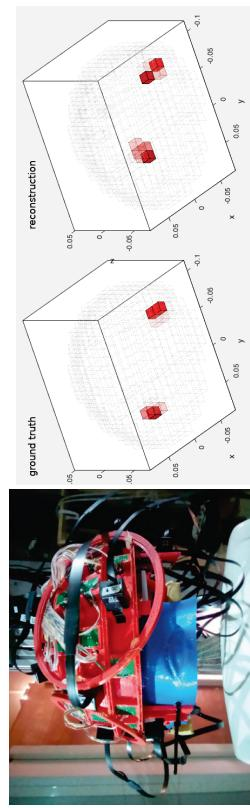


Figure 1. **Left:** experimental OPM-MRxi setup, composed of 3D-printed helmet (red), 25 OPM (black), 64 small coils (green) and 8 large coils (red, glued to the helmet). The head phantom (blue) is carrying cubes of immobilized MNP. **Right:** Ground truth and reconstructed MNP distribution.

### Acknowledgements

Financial support by the Austrian Science Fund (FWF, grant I 4357-B) and the German Research Foundation (grant WI 4230/4-1) is gratefully acknowledged.

### References

- [1] M. Liebl et al., *Biomedical Engineering/Biomedizinische Technik*, 60(5):427–443, 2015.
- [2] A. Jaufenthaler et al., *Sensors*, 20(3):753, 2020.

## Tracer comparison including MPI scanner characteristics by 2-voxel-analysis

Olaf Kosch\*, Amani Remmo, James Wells, Frank Wiekhorst  
Physikalisch-Technische Bundesanstalt, Berlin, Germany,  
\*Email: olaf.kosch@ptb.de

Magnetic particle imaging (MPI) is an emerging tomographic imaging technique capable of quantitatively determining the 3D distribution of a magnetic nanoparticle (MNP) based tracer material. MPI technology is still under development and requires the characterisation of available tracers for imaging performance at a dedicated MPI scanner. For this purpose, we developed an MPI performance quantification called 2-voxel-analysis simulating different arrangements of two MNP accumulations from the measured system function (SF) required in Lissajous scanning MPI. The SF is a calibration measurement required for image reconstruction that is recorded with a point-like reference sample for a tracer in a grid-like manner at different selected positions of the field of view.

For our 2-voxel-analysis, we measured the SFs of six commercial and 5 non-commercial tracer systems using a preclinical MPI system (MPI 25/20 FF, Bruker Biospin, GER). For the SF recording, a tracer volume of  $V_{ref} = 2 \times 2 \times 1 \text{ mm}^3$  at an iron concentration of 45 mmol/L was used. Each SF had a size of 25x25x13 voxels of volume  $V_{voxel} = 1 \text{ mm}^3$ . The SF  $\mathbf{S}$  contains for all voxel positions the individual measurements with the reference, including positions like  $i$  and  $j$  stored in the columns  $\mathbf{s}_i$  and  $\mathbf{s}_j$ . To simulate an arrangement of two distinct MNP sources as shown in Fig. 1a, the corresponding data are extracted from SF and superimposed including additionally the noise data of a blank scanner measurement  $\bar{\mathbf{u}}_{empty}$  giving the total signal  $\bar{\mathbf{u}}$

$$\bar{\mathbf{u}} = \mathbf{s}_i + \mathbf{s}_j + \bar{\mathbf{u}}_{empty} \quad (1)$$

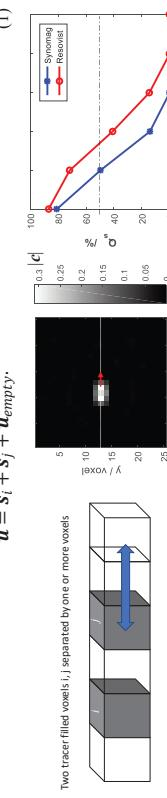


**Figure 1:** **a)** Voxels  $i$  and  $j$  filled with MNP (grey) separated by one or more voxels without MNP (white); **b)** The plane containing voxels  $i$  and  $j$  of the reconstructed MNP distribution for the case of one separating distance voxel; **c)** separation quality  $Q_s$  as a function of distance (number of empty voxels) between  $i$  and  $j$  exemplified for the two commercial MNP systems Synnomaq (Micromod, GER) and Resovist (Bayer Healthcare, GER).

By inversion of  $\bar{\mathbf{S}} \cdot \mathbf{c} = \bar{\mathbf{u}}$ , the resulting image  $\mathbf{c}$  of the MNP distribution is calculated, see Fig. 1b for the case of two voxels separated by one empty voxel. By repeating the procedure while stepwise increasing the number of empty (distance) voxels, the quality of the separation  $Q_s$  of the voxel arrangement is assessed by the factor  $Q_s$  (ratio between minimum reconstructed MNP content and maximum at voxel positions  $i, j$ ). Fig. 1c shows  $Q_s$  as a function of the distance between the two voxels for two different tracer types resolving the different resolution and performance under real scanner conditions.

Our 2-voxel-analysis is a powerful procedure to quantify the image quality of a tracer directly from a SF measurement, without the need for additional MPI measurements to estimate resolution and detection limit. This allows us to compare the imaging properties of different tracers, incorporating constant scanner and reconstruction parameters. In contrast, this becomes much more difficult when using measurements with real 1-mm cubes as a phantom. With these, for example, only a very small displacement of the cube determines whether this cube is distributed either over 1 voxel or up to 8 voxels. In addition, there are other parameters that can vary in real phantom measurements, which leads to greater uncertainties when comparing tracers. These uncertainties are significantly reduced by the 2-voxel-analysis.

## Probing Relaxation Characteristics of Magnetic Nanoparticles by a Home-made Magnetic Particle Spectroscopy Setup

Lenka Kubíčková<sup>1,2\*</sup>, Jaroslav Kohout<sup>2</sup>, Denisa Kubániová<sup>1,2</sup>, Pavel Veverka<sup>1</sup>, Tomáš Knížek<sup>1,2</sup>, Miroslav Veverka<sup>2</sup>, Zdeněk Jirák<sup>1</sup>, Vít Herynek<sup>3</sup>, and Ondřej Kaman<sup>1</sup>

<sup>1</sup> Institute of Physics, Czech Academy of Sciences, Na Slovance 199/2, 182 21 Praha 8, Czech Republic

<sup>2</sup> Faculty of Mathematics and Physics, Charles University, V Holešovičkách 747/2, 180 00 Praha 8, Czech Republic

<sup>3</sup> First Faculty of Medicine, Charles University, Salinovská 3, Praha 2, Czech Republic

\* Email: kubikol@fzu.cz, tel.: +420 205 18 418

Magnetic particle spectroscopy (MPS), sometimes called zero-dimensional magnetic particle imaging (MPI), represents a versatile method enabling not only assessment of tracers for MPI, but also studying processes that modulate the magnetic response of a particle suspension to an AC magnetic field, such as Néel relaxation and Brownian rotation. In MPS, a sinusoidal magnetic field is applied to a suspension of magnetic nanoparticles (MNPs), and the dynamic magnetic response of the suspension, which is in essence non-linear, is collected by pick-up coils. The Fourier transform of the time-dependent signal provides an MPS spectrum that consists of odd higher harmonics of the drive-field frequency.

In our laboratory, we have built a single-drive-field MPS setup with five excitation coils that are impedance-matched to frequencies of  $\sim 10$ ,  $15$ ,  $25$ ,  $35$ , and  $50$  kHz, with magnetic induction of up to 20 mT. The signal is collected by an oscilloscope and Fourier transformed, see Fig. 1 for an illustrative MPS spectrum of Resovist. The analyzed parameters comprise the amplitudes normalized to the concentration of the 3<sup>rd</sup> (3f) and 5<sup>th</sup> (5f) harmonics. The amplitude of the 1<sup>st</sup> harmonic may contain a contribution of the drive field, and therefore it is not used, its signal is suppressed by the two pick-up coils and a high-pass filter. The selected drive-field frequencies roughly correspond to the Bruker PreClinical MPI scanner (available at Charles University, Prague) with the drive-field frequency of  $\sim 25$  kHz and an actual induction of up to 14 mT.

In this contribution, we compare MPS parameters of suspensions of MNPs prepared by two different methods, solvothermal synthesis and thermal decomposition. First, superparamagnetic Zn-doped magnetic/maghemitic nanoparticles with Zn:Fe ratio of  $\sim 0.1$  and size of  $\sim 8-12$  nm were prepared by a solvothermal method (metal acetylacetones in benzyl alcohol). The particles were stabilized by citrate, which forms a monomolecular surface layer, or coated with  $\sim 4$  nm silica by the Stöber process (Fig. 2a), which led to coated clusters. Second, the thermal decomposition in presence of surfactants was employed to prepare doped magnetic nanoparticles of (i)  $\text{Co}_{0.6}\text{Fe}_{3.1}\text{O}_4$  with high magnetic anisotropy and size of  $\sim 16$  nm, and (ii)  $\text{Zn}_{0.37}\text{Fe}_{2.63}\text{O}_4$  with size of  $\sim 15$  nm, which are superparamagnetic at room temperature. The particles were coated with silica of various thicknesses by the reverse microemulsion method, which produced individually coated crystallites (Fig. 2b). Apart from the results on these samples with different Néel relaxation times, we will also present data on suspensions in water/glycerol mixtures with modified Brown relaxation.

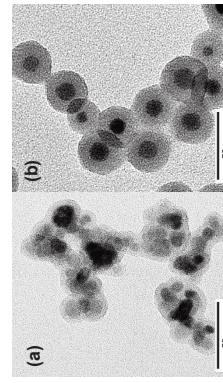


**Fig. 2. TEM of silica-coated Zn-doped iron oxide particles with cores prepared by the (a) solvothermal synthesis, and (b) thermal decomposition**

## Core-shell structured MNPs: coating effect on the $^1\text{H-NMR}$ relaxation properties

Margherita Porru<sup>1,\*</sup>, Francesca Brero<sup>1</sup>, Davide Cicilaro<sup>1</sup>, Martin Albino<sup>2</sup>, Francesco Orsi<sup>3</sup>, Claudio Sanggorio<sup>1</sup>, Claudia Innocenti<sup>2</sup>, Manuel Mariani<sup>1</sup>, Paolo Arosio<sup>1</sup>, Alessandro Lascialfari<sup>1</sup>

<sup>1</sup> Department of Physics, INFN and INSTM, University of Pavia, Pavia 27100, Italy.

<sup>2</sup> Department of Chemistry, ICCOM-CNR and INSTM, University of Florence, Sesto Fiorentino 50019, Italy.

<sup>3</sup> Department of Physics, INFN and INSTM, University of Milan, Milan 20133, Italy.

\*Email: margherita.porru01@universitadipavia.it; Mobile: +39 340 8761831

The Magnetic Resonance Imaging (MRI) is a diagnostic technique based on the nuclear relaxation times (spin-lattice  $T_1$  and spin-spin  $T_2$ ) of the hydrogen nuclei composing the tissues of the investigated region. The MRI contrast is ruled by the modification of the relaxation rates of the nearby nuclei, carried out by the contrast agents (CAs) that perturb the local magnetic field at the nuclear sites. Thus, the MRI contrast is enhanced according to the distribution of the CA in the biological structures, where the signal can be locally increased or decreased depending on the kind of injected system (paramagnetic/superparamagnetic). The CAs efficiency is quantified by the relaxivity  $r_1$  ( $i = 1,2$ ), defined as the change of relaxation rate normalized to 1 mM of CA concentration. In this framework, iron oxide magnetic nanoparticles (MNPs) are widely studied because of their high magnetization that generates sizeable inhomogeneities in the local magnetic field. The organic coatings of the MNPs are of considerable importance for biocompatibility and biodistribution of these systems and have been recently suggested to influence the magnetic properties at a certain extent, depending on the core size. The present work focuses on the effects of the coatings on the longitudinal and transverse relaxivities. In detail, we studied two sets of colloidal solutions of spherical superparamagnetic iron oxide nanoparticles (SPIONs) with different magnetic core sizes. The first set presents a core with mean diameter  $d_{11} = (8.86 \pm 0.90)$  nm, coated with 3-Aminopropylphosphonic acid (APPA) or meso-2,3-Dimercaptosuccinic acid (DMSA). The core diameter of the second set is  $d_{22} = (4.4 \pm 0.7)$  nm, coated with Polyacrylic acid (PAA) or Benzene-1,3,5-tricarboxylic acid (TMA) or DMSA. The samples were structurally and morpho-dimensionally characterized by means of X-Ray Diffraction (XRD) and Transmission Electron Microscopy (TEM). The magnetic properties of the samples have been investigated by measuring the zero-field cooled/field cooled (ZFC/FC) curves and the hysteresis curves. The Nuclear Magnetic Relaxation Dispersion (NMRD) profiles of the longitudinal ( $r_1$ ) and transverse ( $r_2$ ) relaxativity have been determined at room temperature, ranging from 10 kHz to 86 MHz. The physical mechanisms that influence the Nuclear Magnetic Resonance (NMR) relaxation rates of SPIONs are often well modelled by a heuristic model, hence the experimental data were fitted with the Roch-Müller-Gill model, and it emerged that for frequencies approximately below 1 MHz, the nuclear relaxation rate enhancement is led by the Néel correlation time, while at higher frequencies the Curie relaxation mechanism is dominant. Furthermore, as predictable, magnetic cores that differ in size present distinct NMRD profiles (Fig. a). In the second set of samples, for distinct organic coatings, a different frequency behaviour of the NMRD profiles is singled out (Fig. b). This occurrence is tentatively attributed to the effect of the diverse polymeric shells on the surface spins dynamics and topology, with a subsequent influence on the fundamental magnetic properties. We suggest that the polymeric coating could help in finely tuning the relaxometric properties of small dimension systems *i.e.*, few nanometres.

Figure. (a) Longitudinal NMRD profile ( $r_1$ ) of two samples of MNPs presenting different core size and same polymeric coating (DMSA). (b) Longitudinal NMRD profile ( $r_1$ ) of two samples of MNPs presenting the same core and different polymeric coating (DMSA, PAA).

## Magnetic Particle Imaging for cell tracking: Establishing quality and effectiveness in magnetic cell labeling

Amani Remmou<sup>\*</sup>, Norbert Löwa<sup>1</sup>, Antje Ludwig<sup>2</sup>, Olaf Kosch<sup>1</sup>, Cordula Grüttner<sup>3</sup>, Frank Wiekhorst<sup>1</sup>

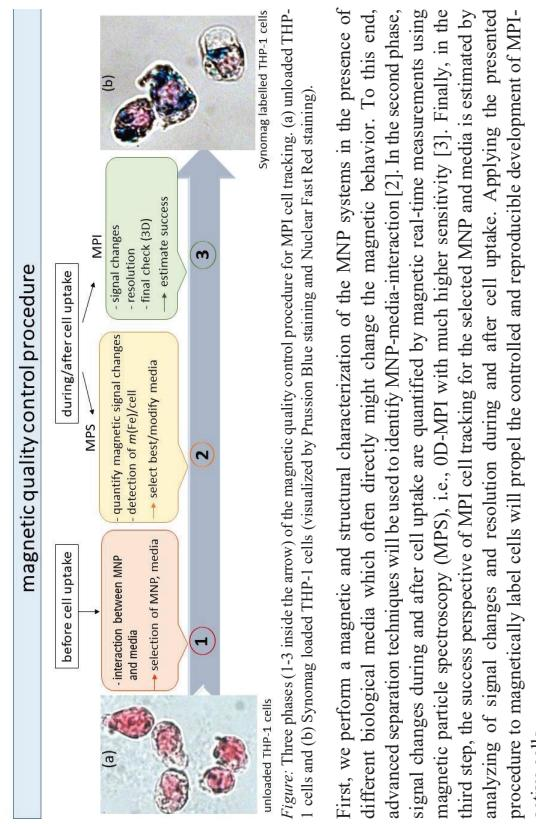
<sup>1</sup> Physikalisch-Technische Bundesanstalt, Abbestr. 2-12, 10587 Berlin

<sup>2</sup> Charité-Universitätsmedizin Berlin, Hessische Str. 3-4, 10115 Berlin

<sup>3</sup> Micronord Partikeltechnologie GmbH, Schillingallee 68, 18057 Rostock

\* Corresponding author, email: amani.remmou@ptb.de

Magnetic nanoparticles (MNP) are of great interest in biomedicine as they offer numerous promising therapeutic and diagnostic applications each using specific magnetic properties of the MNP. An emerging method for visualizing the spatial distribution of MNP in biological objects for preclinical research studies is magnetic particle imaging (MPI). In addition, the capability of MPI cell tracking, e.g., monitoring living cells labeled with MNP by MPI, has successfully been shown [1]. Nevertheless, the signal quality of MNP often decreases due to cell uptake and subsequent degradation processes, which diminishes the effectiveness and quality of MPI cell tracking. Thereby, the cell uptake is impacted by the selection of the MNP system (coating, size, zeta potential) and the type of biological medium. Presently, there is no magnetic quality control of cell labeling available including these aspects. Here, we will present a magnetic quality control procedure of MPI cell labeling for the examples of THP-1 cells labelled by two MNP systems Synomag and Permag (*Micromod, GER*). This consist of three phases (see Fig.).



- [1] Payser, H., Löwa, N., Stach, A., et al. Cellular uptake of magnetic nanoparticles imaged and quantified by magnetic particle imaging. *Sci Rep* 10, 1922 (2020).  
 [2] Remmou, A., Löwa, N., Peter, J., and Wiekhorst, F. "Physical characterization of biomedical magnetic nanoparticles using multi-detector centrifugal field-flow fractionation" Current Directions in Biomedical Engineering, vol. 7, no. 2, 2021, pp. 327-330.  
 [3] Löwa, N., Patricia R., Dirk G., Rinaldo A., and Frank W.. 2015. "Hyphenation of Field-Flow Fractionation and Magnetic Particle Spectroscopy" *Chromatography* 2, no. 4: 655-668.

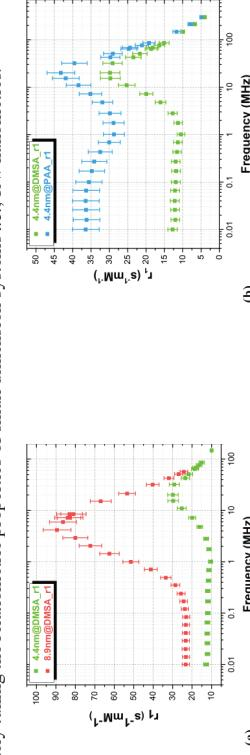


Figure. (a) Longitudinal NMRD profile ( $r_1$ ) of two samples of MNPs presenting different core size and same polymeric coating (DMSA). (b) Longitudinal NMRD profile ( $r_1$ ) of two samples of MNPs presenting the same core and different polymeric coating (DMSA, PAA).

## Optimising excitation field frequency for handheld detections of magnetic nanoparticles

S. Salamzadeh, B. ten Haken, L. Allic

Magnetic Detection & Imaging Group, Technical Medical Centre,  
University of Twente, Enschede, The Netherlands.

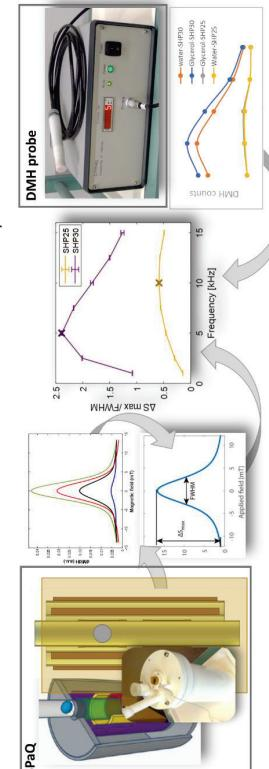
Magnetic nanoparticles (MNPs) are used in many biomedical applications, including sentinel lymph node biopsy (SLNB) and magnetic particle imaging (MPI). Recently, several handheld probes (based upon nonlinear detection principles) have been developed for SLNB with MNPs. These methods use an excitation coil to activate the MNPs, and a detection coil to acquire the consequent magnetization of the MNPs. In this paper, we investigate a method to optimize tracer-detector sensing for a nonlinear handheld detection during SLNB procedure.

We use superparamagnetic quantifier (SPaQ) to predict handheld detection by acquiring the consequent magnetization curve of MNPs in a homogeneous magnetic field. SPaQ is oil-cooled, custom-built system (University of Twente) and uses an AC excitation field ( $|HAC| = 1.33 \text{ mT}$ ) and a DC offset field ( $|HDC| \leq 13.3 \text{ mT}$ ). The consequent magnetization of the sample induces a voltage in a pair of gradiometric detection coils. A digital phase-sensitive detection algorithm is applied to sense the amplitude of the acquired signal.

The handheld detections are acquired using in-house build DiffMag system based upon a patented nonlinear principle (differential magnetometry). The DMH system is (at the same time) sensitive to small amounts of MNP and oblivious to strong first-order responses (e.g. like the human body would generate). The system consists of a DMH probe, a base unit, an isolation transformer, and a laptop. The DMH probe utilises a combination of AC and DC magnetic fields generated by an excitation coil. Consequently to excitation magnetic field, a sample will generate a magnetization acquired as a RF signal at a gradiometric coil setup in the DMH probe. A DMH count was generated as a difference between the excitation by a DC magnetic field and a field at a AC offset.

Two single-core iron-oxide particles (SHP, Ocean Nanotech, USA) with core sizes 25 and 30 nm were diluted with water and Glycerol (to enhance sample viscosity observable in clinical situation); total sample volume of 150  $\mu\text{l}$  consisting of 100  $\mu\text{l}$  pure MNP and 50  $\mu\text{l}$  added water or Glycerol. Both SPaQ and DMH data was acquired at a room temperature (21 °C) and at various AC frequencies (i.e. 2.5, 5, 7.5, 10 and 12.5). To compare magnetic properties of MNPs using SPaQ data, two features were extracted from the measured curve, i.e. the maximum signal difference ( $MS_{\text{Max}}$ ) and the full width at half maximum (FWHM). The DMH data was directly compared by DMH counts.

Figure illustrates the both systems (SPaQ and DMH probe) including derivative of the magnetization curve and features extracted. SHP-30 produces a significantly higher DMH counts at a excitation frequency of 5 kHz. Derivative of magnetization curve is decreased by increasing the viscosity of particles. However SHP-25 was less sensitive to an increase of viscosity.



## Estimation Accuracy Improvement of Magnetic Nanoparticle Tomography by Combining Inverse Solution Methods

Teruyoshi Sasayama\*, Naoki Okamura\*, Koha Higashino\*, and Tatsushi Yoshida<sup>†</sup>

\*Email: sasayama@se.kyushu-u.ac.jp Mobile: +81-92-802-3830  
<sup>†</sup> Department of Electrical and Electronic Engineering, Kyushu University, Fukuoka 819-0395, Japan.

A magnetic nanoparticle (MNP) imaging method is expected to become a new *in vivo* diagnostic technique for detecting MNPs accumulated in a cancer. An MNP imaging method using a magnetic sensor array, namely magnetic nanoparticle tomography (MNT), has been proposed [1]. A high sensitivity and spatial resolution were achieved using the nonnegative least-squares (NNLS) inverse solution in MNT. However, owing to the presence of measurement noise, certain MNPs were estimated inaccurately, i.e., artifacts were generated.

To suppress the artifacts, a method was proposed to apply a minimum-variance spatial filter (MV-SF), which is a widely used spatial filter in magnetoencephalography (MEG), instead of the NNLS method [2]. The results indicate that the signal was more clearly represented and artifacts were successfully eliminated. However, the performance of MV-SF worsens in the presence of a correlated signal.

To overcome these issues, a method is proposed that combines the inverse solution, spatial filter, and NNLS methods to compensate for their individual weaknesses. First, a spatial filter method is applied to estimate the position of MNPs approximately, and the analysis region is restricted. Second, the NNLS method is applied to estimate the amount and positions of MNPs in the restricted region. In this study, standardized low resolution brain electromagnetic tomography (sLORETA), which is also used in MEG studies, is chosen as the spatial filter. sLORETA has a lower spatial resolution compared with MV-SF; however, it can detect correlated signals, such as several clusters of MNPs.

The developed MNT system has one excitation coil and 16 detection coils. The excitation coil magnetizes the MNPs, and the third-harmonic magnetic field from MNPs is detected using the detection coils. The inverse problem is solved using the detected third harmonics to estimate the amount and positions of the MNPs. The estimation result, shown in Fig. 1, demonstrates that the proposed method successfully suppresses the artifacts and adequately estimates the amount and positions of MNPs.

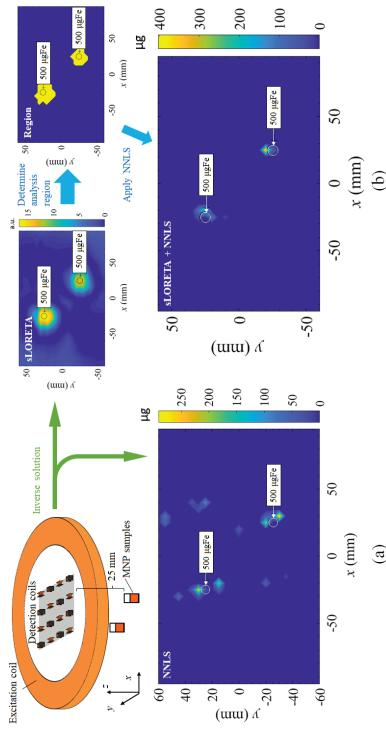


Fig. 1. Results of inverse solutions of MNT using (a) NNLS method and (b) combined method (sLORETA plus NNLS).

## Acknowledgments

This study was supported by the Japan Society for the Promotion of Science (JSPS) KAKENHI (Grant Number JP21H01342).

[1] T. Sasayama, T. Yoshida, and K. Enpuku, *J. Magn. Magn. Mater.*, Vol. 505, 2020, Art. no. 166765.

[2] N. Okamura, T. Sasayama, and T. Yoshida, *IEEE Trans. Magn.*, Vol. 56, No. 2, 2022, Art. no. 6500305.  
Poster #62

## The Impact of MNP Agglomerations inside Magnetic Fibers on MRI, MPI and Hyperthermia Performance

Max Schoenen<sup>1</sup>, Benedict Mues<sup>1</sup>, Benedict Bauer<sup>2</sup>, Thomas Gries<sup>2</sup>, Thomas Schmitz-Rode<sup>1</sup> and Ioana Slabu<sup>1\*</sup>

<sup>1</sup>Institute of Applied Medical Engineering, Helmholtz Institute, Medical Faculty, RWTH Aachen University, Pauwelsstr. 20, 52074 Aachen, Germany

<sup>2</sup>Institut für Textiltechnik, RWTH Aachen University, Otto-Blumenthal-Str. 1, 52074 Aachen, Germany

E-mail: schoenen@ame.rwth-aachen.de | \*slabu@ame.rwth-aachen.de

Magnetic nanoparticles (MNP) are of high interest as additives for the production of magnetic scaffolds, as they promise to enable the control and monitoring of therapies in nanomedicine. For example, using MNP magnetic hyperthermia and thermo-sensitive drug release from the scaffolds can be achieved by controlled heating in an alternating magnetic fields (AMF). Scaffold visualization is enabled via magnetic particle imaging (MPI) and magnetic resonance imaging (MRI). Recently, it was reported that MNP interactions inside agglomerations significantly affect their magnetic response. In this work, we investigate this impact on MPI, MRI and hyperthermia performance with a focus on the influence of the MNP agglomerate orientation inside hybrid fibers relative to the direction of the applied magnetic field. For this, hybrid fibers consisting of polypropylene and MNP were produced [1] and characterized with the above-mentioned techniques. Figure 1 shows the MNP agglomerate orientation inside fibers and the MPI system matrix models used for the reconstruction of the image for differently oriented fiber snippets. From the reconstructed images it can be concluded that MPI signal quality significantly depends on the orientation of the MNP agglomerates in the hybrid fibers. Similarly, the hyperthermia investigations showed different heating outputs for different orientations of MNP agglomerates. The results were consistent with simulation data. These effects are attributed to magnetic interactions of MNP in agglomerates which cause a collective relaxation behavior and a preferential orientation of the easy axes and the magnetic moments of the MNP in elongated agglomerates. In comparison to MPI and MFH, the MRI signal did not show such clear dependency. In conclusion, MNP agglomerate orientation and thus fiber orientation plays a significant role for their MPI and hyperthermia performance. For an optimized application of magnetic scaffolds, such effects must be considered as the orientation of the agglomerations strongly depends on the type and position of the scaffold.

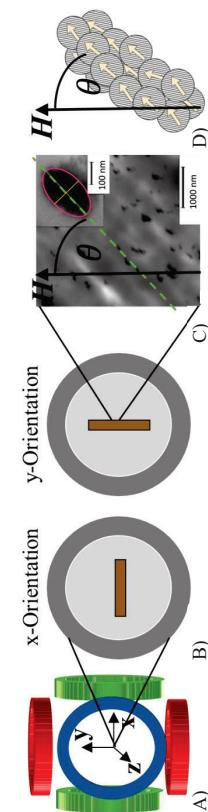


Figure 1: A) Sketch of a MPI setup. B) TEM image of the fiber (adapted from [1]). The inset shows an elongated MNP agglomerate.  $\theta$  is the angle between the major axis orientation of the agglomerates and the magnetic field. D) Sketch of the simulated MNP agglomerates.

[1] Mues et al. Nanomagnetic Actuation of Hybrid Stents for Hyperthermia Treatment of Hollow Organ Tumors *Nanomaterials* 2021, 11(3), 618

## Small Iron Oxide Nanoparticles as MRI T<sub>1</sub> Contrast Agent

Maximilian O. Besenhard,<sup>a</sup> Luca Panariello,<sup>a</sup> Céline Kiefer,<sup>b</sup> Alec P. LaGrow,<sup>c</sup> Liudmyla Storožuk,<sup>d</sup> Francis Peron,<sup>b</sup> Sylvie Begin,<sup>b</sup> Damien Mertz,<sup>b</sup> Nguen Thi Kim Thanh,<sup>a,\*</sup> Asterios Gavrilidis<sup>a</sup>

<sup>a</sup>Department of Chemical Engineering, University College London, London, WC1E 6BT, U.K.

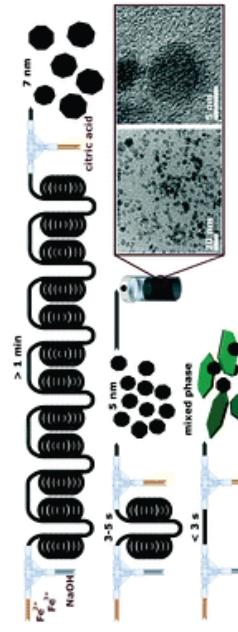
<sup>b</sup>Institut de Physique en Chimie des Matériaux de Strasbourg, BP 43-67034, Strasbourg, France

<sup>c</sup>International Iberian Nanotechnology Laboratory, Braga 4715-330, Portugal

<sup>d</sup>BioPhysics group, Department of Physics and Astronomy, University College London, London, WC1E 6BT, U.K.

The most common aqueous synthetic methods, i.e., the co-precipitation, are rather simple from an experimental point of view, as they use relatively cheap and non-toxic chemicals, temperatures  $< 100^\circ\text{C}$ , and require solely a pH increase of a precursor solution containing ferrous and/or ferric ions. However, particles produced by co-precipitation are often polydisperse, and of a restricted size range, i.e., larger than 7 nm and therefore too large for clinical use as T<sub>1</sub> MRI contrast agents. To obtain a reproducible, and scalable production of IONPs in water, which are preferred when targeting biomedical applications is non-trivial.

In our original research we demonstrated that IONPs of  $\sim 5$  nm can be produced via the co-precipitation method, when quenching the growth of IONPs by adding an acidic solution (e.g. citric acid) rapidly after the initiation of co-precipitation. Furthermore, this continuous synthesis enables the low-cost ( $<\text{£}10$  per g) and large-scale production of highly stable small IONPs without the use of toxic reagents. The flow-synthesised small IONPs showed high T<sub>1</sub> contrast enhancement, with transversal relaxivity (r<sub>2</sub>) reduced to  $20.5 \text{ mM}^{-1} \text{ s}^{-1}$  and longitudinal relaxivity (r<sub>1</sub>) higher than  $10 \text{ mM}^{-1} \text{ s}^{-1}$ , which is among the highest values reported for water-based IONP synthesis.



Schematic of precisely-timed quenching of particle growth at different times after the initiation of the co-precipitation.

### Acknowledgement:

EPSRC (EP/M015157/1), EPSRC IAA D2U (KE12020-01).

### Reference:

Besenhard M. O., Panariello, L., Kiefer, C., LaGrow, A. P., Storožuk, L., Peron F., Begin, S., Damien Mertz, D., Thanh, N. T. K.\* and Gavrilidis, A. (2021) Small Iron Oxide Nanoparticles as MRI T<sub>1</sub> Contrast Agent: Scalable Inexpensive Water-Based Synthesis Using a Flow Reactor. *Nanoscale*, 13: 8795-8805. <https://doi.org/10.1039/DINR00877C>

## Low Frequency AC Susceptometry with Optically Pumped Magnetometers

O. Baffa<sup>1</sup>, R. H. Matsuda<sup>1</sup>, J. R. A. Miranda<sup>2</sup> R. T. Wakai<sup>3</sup> and F. Wiekhorst<sup>4</sup>

<sup>1</sup>Departamento de Física, FFCLRP, USP, Ribeirão Preto, SP, Brazil. <sup>2</sup>Departamento de Biofísica e Farmacologia, Instituto de Biociências, UNEESP, Botucatu, SP, Brazil and <sup>3</sup>Department of Medical Physics, University of Wisconsin-Madison, Madison, WI, USA.

<sup>4</sup>Physikalisch-Technische Bundesanstalt, Berlin, Germany  
e-mail: baffa@usp.br.

Due to their sensitivity, small size and flexibility, Optically Pumped Magnetometers (OPMs) have become attractive as sensors in many applications. In magnetencephalography [1] and magnetoangiography [2] complex arrangement of OPM-arrays are used whereas single detectors have been employed for detecting magnetic properties [3-4]. Another promising application we are investigating is online monitoring of magnetic properties during synthesis of magnetic nanoparticles (MNP). One synthesis route to produce MNP of high quality is microfluidics. In this process, the reaction mixture passes through capillary tubes, which compose the chemical reactor at a certain temperature. Transit time and temperature, among other factors, determine the physical properties (size, magnetization, etc.) of the produced NMPs. We suggest here OPM measurement of the magnetic susceptibility as an online method to detect magnetic properties during MNP synthesis. The susceptometer is composed of a gradient coil arrangement with an anti-Helmholtz circular coil (10 turns, 13.5 mm radius) with one OPM (QuSpin Inc., Louisville, Colorado, USA) at its center (null field point). The setup is operated in a small magnetically shielded chamber (three-layer mu metal ZG-206, Magnetic Shield Corporation, Bensenville, IL, USA) with an open end to facilitate accessing and sample handling. Emulating a micro reactor, we used a plastic silicone micro tube with 3.5 mm outer diameter and 2 mm inner diameter passing near the coils. MNP with an effective volume of 100  $\mu\text{L}$  conducted through one of the coils produce a change in the signal detected by the OPM. By using a multturn potentiometer, the current through the coils (balancing the field) can be adjusted so that a common mode rejection up to  $10^{-4}$  can be achieved. The presence of MNPs in one coil produces a magnetic field imbalance that is detected by the OPM and the field intensity can be used to calculate the magnetic susceptibility. Finally, the frequency of operation is below 100 Hz, typically at about 10 Hz, which makes this susceptometer unique to study low frequency magnetic phenomena of MNP.

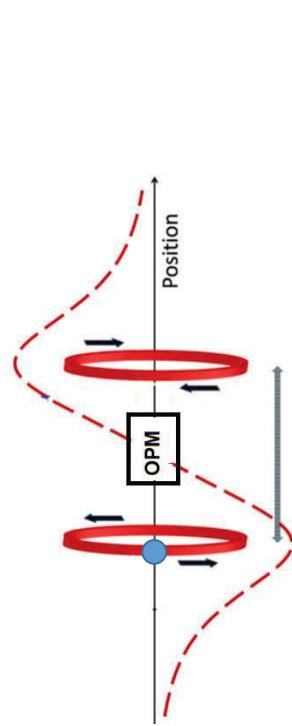


Figure 1: Schematics of the experimental set up to measure the magnetic susceptibility of a small sample place (blue sphere) at the center of one of the coils.

**Acknowledgements:** Partial financial support: FAPESP (2013/07699-0), CAPES-PROBRAL (88887.19874/2018-00), CNPq, DAAD proj ID 57446914

### References:

- 1- E. Boto, et al., Nature, vol. 555, no. 7698, pp. 657–661, 2018
- 2- S. Strand, et al., Journal of the American Heart Association, 8: e013436, 2019
- 3- L. Bougas, et al., Scientific Reports, vol. 8, no. 1, p. 3491, 2018
- 4- O. Baffa, et al., Journal of Magnetism and Magnetic Materials, Volume 475, , Pages 533-538, 2019

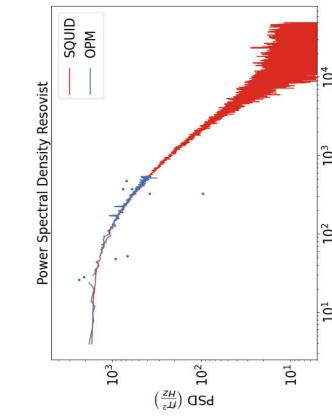
## Tabletop setup for Thermal Noise Magnetometry of magnetic nanoparticles based on Optically Pumped Magnetometers

K. Everaert<sup>1,2</sup>, T. Sandner<sup>1</sup>, R. Kürber<sup>1</sup>, B. Van Waeyenberghe<sup>2</sup>, J. Lelijaert<sup>2</sup>, F. Wiekhorst<sup>1</sup>  
<sup>1</sup>Physikalisch-Technische Bundesanstalt, Abbestraße 2-12, D-10587 Berlin, Germany  
<sup>2</sup>Department of Solid State Sciences, Ghent University, 9000 Ghent, Belgium  
katrijn.everaert@ptb.de / katrijn.everaert@ugent.be

Magnetic nanoparticles are very useful in biomedical applications, where they are employed in both diagnosis (contrast agent in Magnetic Resonance Imaging, tracer in Magnetic Particle Imaging) and therapy (heat generator in magnetic hyperthermia, carrier in magnetic drug targeting). To improve the performance of these applications, the particle properties need to be precisely characterized, for which numerous magnetic measurement techniques are employed. All methods have the disadvantage that they require the application of an external field to measure the magnetic response of the particles, which may change the magnetic state of the particles. To overcome this limitation, the method of Thermal Noise Magnetometry (TNM) has been developed to characterize magnetic nanoparticle ensembles without any use of an external magnetic excitation [1].

Thermal energy in the system causes the magnetic moment of the particles to change direction, which results in fluctuations of the magnetic signal of the ensemble detected in TNM. The total switching rate of these fluctuations depend on the physical and chemical properties of the particles and their state in the suspension. The characteristics of the nanoparticle ensemble thus greatly influences the magnetization dynamics of the sample, which can be mapped by measuring its thermal noise. Such measurements have been proven to be feasible, and complementary to other characterization techniques due to its diminutive impact on the sample [2].

Until now, TNM measurements have been performed with SQUID sensors because of the small signals in the fT ( $10^{-15}$  T) range [3]. Optically Pumped Magnetometers (OPMs) offer an alternative sensor system attractive for TNM. In this contribution, we present a tabletop TNM setup working with commercially available OPMs (QuSpin Gen-2 Zero-Field Magnetometers) in a laboratory magnetic shielding (Twinleaf MS-2).



Since our spectral measure is phase insensitive, we are able to use the OPMs above their bandwidth specified by the manufacturer by compensating for their frequency response profile in the power spectrum. As an example, in the figure we compare the TNM spectrum of a Resovist sample measured in the OPM based setup with that measured in an in-house developed SQUID system and find a very good agreement. The OPM setup with high accessibility complements the SQUID setup with high sensitivity and bandwidth, thereby expanding the field of TNM to possible other magnetic noise related applications.

- [1] J. Lelijaert et al. Appl. Phys. Lett., 107(22):222401, 2015.
- [2] J. Lelijaert et al. J. Phys. D: Appl. Phys., 50(8):085004, 2017.
- [3] K. Everaert et al. IEEE Access, 9:11105, 2021.

## Characterising magnetic nanoparticles using data-driven methods

Ondrej Hovorka<sup>1\*</sup>, Srinandan Dasmahapatra<sup>1</sup>, Simon Cox<sup>1</sup>

<sup>1</sup>Faculty of Engineering and Physical Sciences, University of Southampton, Southampton, UK

\*Email: o.hovorka@soton.ac.uk

Achieving industrial-scale manufacturing of reproducible and standardised magnetic nanoparticles (MNP) has been among the key challenges in developing diagnostic and therapeutic applications for healthcare. New progress requires devising advanced characterisation techniques to allow precise and efficient determination of intrinsic properties of MNPs [1]. Properties of MNPs are often inferred based on a variety of measurement techniques frequently available only at different laboratories. Data analysis is commonly based on fits to models founded on linear response theory, which is often only truly applicable far from operational conditions in applications. In addition, the presence of magnetic interactions in MNP aggregates also severely complicates data interpretation in most sizing measurement methods. It is therefore clear that accurate MNP characterisation is essential not only to guide our understanding of the behaviour of MNPs in various application scenarios but also for laboratory measurement consistency checking and MNP standardisation.

We will discuss our efforts to develop a machine learning-based MNP characterisation tool utilising standard magnetometry data, such as magnetisation vs magnetic field hysteresis loops or ZFC-FC data, for example (Fig. 1). The approach is data-driven and combines datasets from experiments and large-scale computational modelling. We will discuss the achievable accuracy of the parameter estimation and various challenges encountered in the design and training of machine-learning algorithms. We will also address the prospects for using the technique for guiding the real-time production of standardised MNPs for healthcare and other applications.

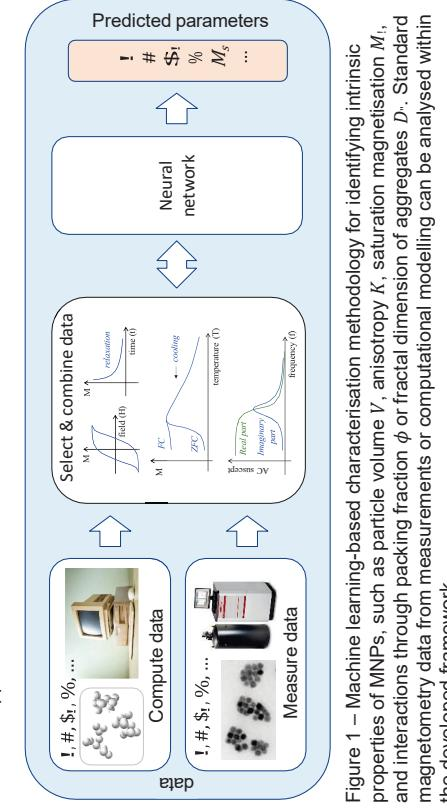


Figure 1 – Machine learning-based characterisation methodology for identifying intrinsic properties of MNPs, such as particle volume  $V$ , anisotropy  $K$ , saturation magnetisation  $M_s$ , and interactions through packing fraction  $\phi$  or fractal dimension of aggregates  $D$ . Standard magnetometry data from measurements or computational modelling can be analysed within the developed framework.

### References:

- [1] J. Wells, ‘Standardisation of Magnetic Nanoparticles in Liquid Suspension’. *Journal of Physics D: Applied Physics* 50, no. 38 383003 (2017).
- [2] Tay, Zhi Wei et al. ‘Pulsed Excitation in Magnetic Particle Imaging.’ *IEEE transactions on medical imaging* vol. 38,10 (2019) 2389-2399.

## Construction of a broadband 3D magnetic particle spectrometer

Justin Ackers<sup>1\*</sup>, David Conrad<sup>1</sup>, Thorsten M. Buzug<sup>1,2</sup>, Matthias Graeser<sup>1,2,\*</sup>

<sup>1</sup> Fraunhofer Research Institution for Individualized and Cell-Based Medical Engineering IMTE, Lübeck, Germany

\*E-Mail: (justin.ackers, matthias.graeser)@imte.fraunhofer.de

Magnetic particle spectroscopy (MPS) is an important method to analyze the properties of magnetic particles. Especially for Magnetic Particle Imaging (MPI) the measuring of the dynamic magnetization response at sinusoidal excitation frequencies around 25 kHz is a standard process in nanoparticle characterization [1]. While most spectrometers are only able to transmit a single frequency, the use of different frequencies or waveforms like rectangular pulses gained more interest in the field of MPI due to better resolution performance with specific tracer material [2]. We therefore designed and built a 3D field generator which is capable of creating arbitrary field waveforms. The device is extremely flexible in the characterization of magnetic nanoparticles and will be capable of diverse applications such as AC susceptibility measurements, hysteresis curves or measurement of MPI system matrices for arbitrary trajectories.

The field generator of the presented system consists of three orthogonal transmit and receive coils each, with the whole oil assembly being just 23 mm in size. The transmit coils are wound from litz wire and held in shape with epoxy. They can be driven with arbitrary current waveforms due to the absence of any impedance matching circuits present in existing spectrometers which would limit the excitation waveforms to a small frequency range. Due to the small inductances of the excitation coils they can be directly driven by a power amplifier (AETechnon 7224). Currently, the bandwidth of the system is limited by the frequency bandwidth of the amplifier. First experiments show a bandwidth of 1.27 kHz, 68 kHz, and 50 kHz (12 mT sinusoidal current wave) for x,y,z coil respectively. To achieve the small size of the coil assembly the y- and z-receive coils were manufactured on a flexible PCB. Feedthrough suppression is handled by a cancellation approach with a second set of transmit and receive coils which can be geometrically adjusted to fine tune the coupling between the transmit and receive paths.

First measurements show the capability of the system for the evaluation of different excitation schemes in 2D for MPI, with a successful triangular excitation with a base frequency of around 2.5 kHz. With further optimization of the power amplifiers the transmit bandwidth will be increased allowing higher frequencies or more challenging waveforms like rectangular pulses. The setup will enable sequence studies for optimizing resolution and sensitivity for specific nanoparticle systems by allowing the superposition of low frequency and high frequency fields in one broadband setup.

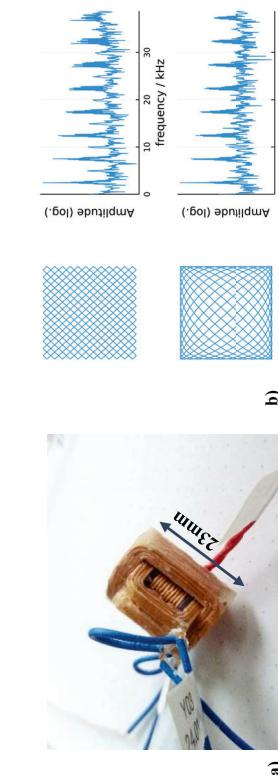


Figure. (a) Constructed excitation coil assembly with three orthogonal channels optimized for low inductance. (b) Recorded spectrum of Lissajous trajectories, with triangular and sinusoidal excitation waveforms of around 2.5 kHz (trajectories have been thinned for visualization).

## Resolving ambiguities in core size determination of magnetic nanoparticles from magnetic frequency mixing data

Ali Mohammad Pourshahidi<sup>1,2</sup>, Ulrich M. Engelmann<sup>3</sup>, Andreas Offenbässer<sup>1,2</sup>, and Hans-Joachim Krause<sup>1,4,\*</sup>  
<sup>1</sup>Institute of Biological Information Processing, Bioelectronics (IBI-3), Forschungszentrum Jülich, Germany,  
<sup>2</sup>Faculty of Mathematics, Computer Science and Natural Sciences, RWTH Aachen University, 52062 Aachen, Germany,  
<sup>3</sup>Medical Engineering and Applied Mathematics, FHI Aachen University of Applied Sciences, 52428 Jülich, Germany,  
<sup>4</sup>Institute of Nano- and Biotechnologies (INB), FHI Aachen University of Applied Sciences, 52428 Jülich, Germany  
\*c-mail: [h.j.krause@fz-juelich.de](mailto:h.j.krause@fz-juelich.de)

Frequency mixing magnetic detection (FMMMD) has been widely utilized as a measurement technique in magnetic immunoassays. It can also be used for characterization [1] and distinction [2] (also known as “colorization”) of different types of magnetic nanoparticles according to their core sizes. It is well known that the large particles contribute most of the FMMMD signal. Typically, 90% of the signal stems from the largest 10% of the particles [1]. This leads to ambiguities in core size fitting since the contribution of the small sized particles is almost undetectable among the strong responses from the large ones. In this work, we report on how this ambiguity can be overcome.

Magnetic nanoparticle samples from Micromod (Rostock, Germany) were prepared in liquid and filter-bound state. Their FMMMD response at mixing frequencies  $f_1 \pm f_2$  to magnetic excitation  $H(t) = H_0 + H_1 \sin(2\pi f_1 t) + H_2 \sin(2\pi f_2 t)$ , with  $H_1 = 1.3 \text{ mT} \mu_0$  at  $f_1 = 40.5 \text{ kHz}$  and  $H_2 = 16 \text{ mT} \mu_0$  at  $f_2 = 63 \text{ Hz}$ , was measured as a function of offset field strength  $H_0 = (0, \dots, 24) \text{ mT} \mu_0$ . The signal calculated from Langevin model in thermodynamic equilibrium [1] with a lognormal core size distribution  $f_1(d, d_0, \sigma, A) = A \exp(-\ln^2(d/d_0)/(2\sigma^2)) (d/\sigma(2\pi)^{1/2})$  was fitted to the experimental data. For each choice of median diameter  $d_0$ , pairs of parameters  $(\sigma, A)$  are found which yield excellent fit results with  $R^2 > 0.99$ . All the lognormal core size distributions shown in Figure (a) are compatible with the measurements because their large-size tails are almost equal. However, all distributions have different number of particles and different total iron content. We determined the samples’ total iron mass with inductively coupled plasma optical emission spectrometry (ICP-OES) and, out of all possible lognormal distributions, determined the one with the same amount of iron. With this additional externally measured parameter, we resolved the ambiguity in core size distribution and determined the parameters  $(d_0, \sigma, A)$ .

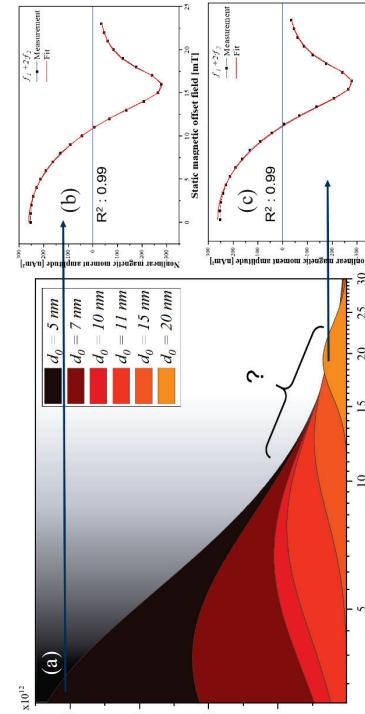


Figure. (a) Lognormal core size distributions with different fixed  $d_0$ , fitted width  $\sigma$  and amplitude  $A$  that all yield excellent agreement with measured FMMMD data, with  $R^2 > 0.99$ . Exemplarily, measured and fitted FMMMD mixing component  $f_1 + 2f_2$  data are shown for (b)  $d_0 = 5 \text{ nm}$  and (c)  $d_0 = 10 \text{ nm}$ . Both fits are barely distinguishable.

- [1] U.M. Engelmann, A. Shalaby, C. Shasha, K.M. Krishnan, H.-J. Krause, Comparative modeling of frequency mixing measurements of magnetic nanoparticles using micromagnetic simulations and Langevin theory, *Nanomaterials* **11**, 1257 (2021).
- [2] A.M. Pourshahidi, S. Achtschnicht, M.M. Nambiarpeache, A. Offenbässer, H.-J. Krause, Multiplex detection of magnetic beads using field dependent frequency mixing magnetic detection, *Sensors* **21**, 5859 (2021).

## Monte Carlo and Experimental Study of the Magnetic Behaviour of Superparamagnetic Nanoparticles

Éléonore Martin<sup>1</sup>, Yves Gossuin<sup>1</sup>, Sara Bais<sup>2</sup>, Safiyye Kavak<sup>2</sup>, Quoc Lam Vuong<sup>1</sup>

1. Biomedical Physics Unit, UMONS, Bâtiment 6, Avenue Maistriau, 7000 Mons, Belgium  
2. Electron Microscopy for Materials Science (EMAT) and NANOLab Center of Excellence, University of Antwerp, B-2020 Antwerp, Belgium

email: [eleonore.martin@umons.ac.be](mailto:eleonore.martin@umons.ac.be)

Superparamagnetic Iron Oxide Nanoparticles (SPION) are nanosize crystals of magnetite or maghemite. Their peculiar magnetic properties makes them particularly suited for a variety of biomedical applications, ranging from cellular imaging to cancer treatment by hyperthermia [1]. The usual theory used to describe their magnetic behaviour is that developed by Paul Langevin [2], which only applies to idealized (isotropic, monodisperse in size and non-interacting) nanoparticles at high temperatures. Reality however always deviates from that theoretical framework: real samples exhibit polydispersity in sizes, particles usually have at least one anisotropy axis, and, particularly in biological media, they tend to aggregate, leading to locally high particle volumic fractions and therefore interaction between their magnetic moments [3]. All those phenomena impact the magnetization of particle ensembles in a non-trivial way and are impossible to model simultaneously theoretically.

In this work, these deviations from the Langevin law are studied numerically, at thermodynamic equilibrium and at 300K, using a Metropolis algorithm, and compared with experimental data obtained using a Vibrating Sample Magnetometer for real SPION, whose size distribution was evaluated by transmission electron microscopy. Thorough tests are led on the simulations to ensure convergence of the magnetization. The effect of each parameter on the field-dependent magnetization curves is then studied.

Figure 1 shows an example of the impact of one of those parameters: inhibiting rotation of the particles (i.e. the Brown relaxation process). As can be seen, it leads to a slower saturation of the magnetization in samples with a high size dispersion parameter ( $\sigma_z = 0.5$ ). Likewise, the presence of dipolar interaction between particles also leads to slower saturation in such samples, as does drying samples under a magnetic field perpendicular to the measurement field (as opposed to drying them under a field parallel to the measurement field, which yields the opposite effect). These various modifications of the curves result in erroneous size dispersion parameters when fitting them to an integrated Langevin equation. The simulations compare well with experimental results, as can be seen on figure 2. In future work, the simulations could be improved by changing the anisotropy model from uniaxial to a more realistic cubic anisotropy.

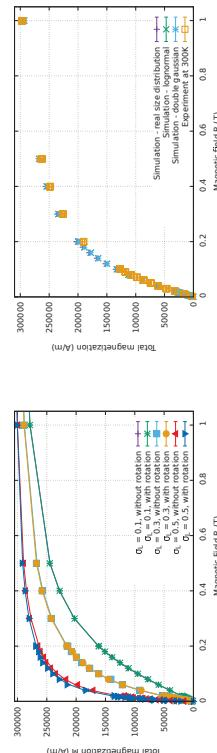


Figure. 2 Comparison between experimental results (in orange) obtained on HO Nano 6nm maghemite nanoparticles and three simulations differing in the particle size distribution.

## References

- [1] A. Ito, M. Shinkai, et al., *J. Bioscience and Bioengineering*, 2005, **100**(1), 1-11.
- [2] P. Langevin, *J. Phys. Theor. Appl.*, 1905, **4**(1), 678
- [3] M. Lévy, C. Wilhelm, et al., *Nanoscale*, 2011, **3**, 4402

## Nanorheology monitoring using magnetic nanoparticles and AC susceptometry

Sobhan Sephrin<sup>1\*</sup>, Johanna Andersson<sup>1</sup>, Vincent Schaller<sup>1</sup>, Cordula Grüttner<sup>2</sup>,

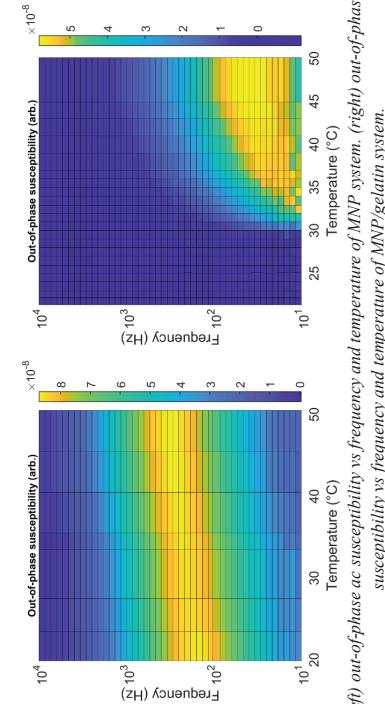
Mats Stading<sup>1</sup>, and Christer Johansson<sup>1</sup>

<sup>1</sup>RISE Research Institutes of Sweden, Göteborg, Sweden.

<sup>2</sup>micromod Partikelchirologie GmbH, Rostock, Germany.

\*Email: sobhan.sephrin@ri.se

We have developed a nanorheological characterization method to extract frequency and temperature dependent rheological properties of soft materials. The measurement system consists of two differentially connected detection coils centered coaxially with the excitation coil aligned in the middle of the detection coils. A lock-in amplifier is used to both generating the excitation ac magnetic field and measuring the voltage from the detection coils. To investigate the effect of temperature on the sample, the sample is placed inside a water jacketed flask which is connected to a temperature-controlled circulating water bath. The flask is located directly above one of the two detection coils. By measuring the dynamic magnetization of magnetic nanoparticles blended in the matrix material, the viscosity and storage module can be determined in the matrix material [1-3]. Commercially available iron-oxide multicore nanoparticles (MNP) of 100 nm (micromod, BNF Starch) are used as tracer in the excitation frequency range of 1 Hz-10 kHz. As an example, we show the result of mixing 2% gelatin to the MNP tracer. The out-of-phase ac susceptibility vs frequency and temperature for both MNP systems with and without gelatin can be seen below. The frequency and temperature dependent dynamic magnetic properties are affected by the mechanical interaction with the gelatin-matrix. The rheological properties of the matrix can be estimated using theoretical models [1,2]. The remote magnetic sensing of the MNP tracers and the estimation of the rheological properties allows rheological monitoring of food matrices under oral processing.



[1] Ludwig, Frank, and Hilke Remmer. "Rotational dynamics of magnetic nanoparticles in different matrix systems." Physical Sciences Reviews (2020).  
[2] Sriviriyakul, Thana, et al. "Nanorheological studies of xanthan/water solutions using magnetic nanoparticles." Journal of Magnetism and Magnetic Materials 473 (2019): 268-271.  
[3] Stading, Mats, et al. "Nano-rheometry for food oral processing." Trans. Nordic Rheol. Soc 27 (2019): 117-120.

## Novel methodologies to determine the magnetic anisotropy of iron oxide nanoparticles in colloidal suspensions

David Cabrera<sup>1,2</sup>, Takanori Yoshida<sup>3</sup>, J.L.F. Cunado<sup>4</sup>, Gorka Salas<sup>5</sup>, Alberto Bollero<sup>1</sup>, María del Puerto Morales<sup>6</sup>, Julio Camarero<sup>1,4</sup>, and Francisco J. Teran<sup>1,5</sup>

<sup>1</sup>iMdea Nanociencia, Campus Universitario de Cantoblanco 28049 Madrid, Spain.

<sup>2</sup>School of Pharmacy and Bioengineering, Keele University, Guy Hilton Research Centre, Thumbarrow Drive, ST4 7QB, Stoke on Trent, UK.

<sup>3</sup>Dpt. of Electrical Engineering, Kyushu University, Fukuoka 819-0385, Japan.

<sup>4</sup>Dpto Física de la Materia Condensada & Instituto Nicolás Cabrera, Universidad Autónoma de Madrid, 28049 Madrid, Spain.

<sup>5</sup>Nanobiotecnología (iMdea Nanociencia), Unidad Asociada al CNB-CSIC, Cantoblanco, 28049 Madrid, Spain

<sup>6</sup>Instituto de Ciencia de Materiales de Madrid-CSIC, Cantoblanco, 28049 Madrid, Spain

\*Email: franciscoteran@imdea.org

The potential of magnetic nanoparticles for acting as active agents in catalysis, magnetic particle imaging or magnetic hyperthermia grounds on their superparamagnetic behaviour under alternating magnetic fields (AMF). In spite of the application potential of this magnetic phenomenon, the identification of fingerprints specifically related to the transition from unblocked to blocked states at room temperature under alternating magnetic fields remains a challenge to provide easy access tools for characterising magnetic properties of nanomaterials.

Here, we report an experimental and theoretical study to determine the effective magnetic anisotropy from iron oxide nanoparticles (IONPs) in colloidal suspensions at room temperature. The experimental methodology is based on magneto-optical measurements of IONP suspensions based on Faraday effect under alternating magnetic fields in a six decades frequency range from hundreds of mHz to kHz with field intensities up to 40 kA/m. Our measurements demonstrate a room temperature transition from unblocked to blocked magnetic states in magnetic suspensions under alternating magnetic fields. The transition is characterized by AC anhysteretic (unblocked magnetic state) magnetization cycles at low frequencies and AC hysteretic (magnetically blocked state) magnetization cycles beyond an onset frequency ( $f_{onset}$ ) value which depends on nanoparticle size (see Figure). Thus,  $f_{onset}$  values vary from 13 kHz for 12 nm IONPs to 30 Hz for 22 nm IONPs. Our experimental observations that explains the experimental results in terms of the magnitude of the effective magnetic anisotropy barrier ( $\beta E_{eff} = K_{eff}^{-1}$ ). Thus, an empirical expression is proposed to determine the effective magnetic anisotropy ( $K_{eff}$ ) from  $f_{onset}$ :

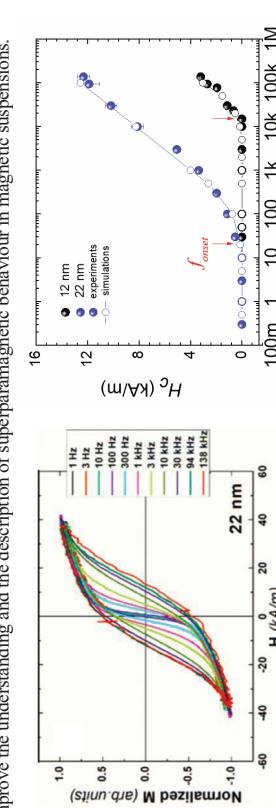


Figure: Left) Frequency dependence of AC magnetization cycles of 22 nm IONP suspension at 0.4 g<sub>e</sub>/L. Right) Experimental (filled dots) and theoretical (empty dots) frequency dependence of coercivity obtained for 12 nm (black dots) and 22 nm (blue dots) IONP sizes ( $H=40$  kA/m),  $f_{onset}$  values for 12 and 22 nm IONPs are highlighted with red arrows.

## Portable MPS device for radical innovation in medical point-of-care diagnostics

Bernhard Friedrich<sup>2</sup>, Rainer Tieze<sup>2</sup>, Stefan Lyer<sup>2</sup>, Martin A. Rückert<sup>1</sup>, Thomas Kampf<sup>1,5</sup>, Thomas Hennig<sup>4</sup>, Lars Dolken<sup>3,4</sup>, Volker C. Behr<sup>1</sup>, Christoph Alexiou<sup>2</sup>, Patrick Vogel<sup>1</sup>

<sup>1</sup>: Department of Experimental Physics 5 (Biophysics), Julius-Maximilians-University Würzburg, Germany. <sup>2</sup>: Department of Otorhinolaryngology, Head and Neck Surgery, Section of Experimental Oncology and Nanomedicine (SEON), Else Kröner Fresenius-Stiftung-Professorship, University Hospital Erlangen, Department of Example Science, Germany. <sup>3</sup>: Helmholtz Institute for RNA-based Infection Research, Helmholtz-Center for Infection Research, Würzburg, Germany. <sup>4</sup>: Institute for Virology and Immunobiology, Julius-Maximilians-University Würzburg, Germany. <sup>5</sup>: Department of Diagnostic and Interventional Neuroradiology, University Hospital Würzburg, Germany.

E-mail: patrick.vogel@physik.uni-wuerzburg.de

By controlled engineering of a specific surface properties (functionalization), magnetic nanoparticles (MNPs) become special features for desired applications, e.g., bioassays for detection of binding compartments, e.g., antibodies.

The characterization as well as a measurement of such binding states is of high interest and limited to highly specific techniques such as ELISA (Enzyme-linked Immunosorbent Assay) which are inflexible, expensive and time-consuming. Established as well as novel upcoming methods, such as ACS (AC susceptibility) or MPS (Magnetic Particle Spectroscopy), exploit the magnetization response of functionalized MNP ensembles to assess specific information about the MNP mobility within their environment as well as the conjugations of chemical or biological compounds on their surface. Both methods have shown promising results in the past but cannot reach the sensitivity of above-mentioned techniques. We used a novel method based on modified MPS method, that is sensitive to minimal changes in the diameter of MNPs, e.g., resulting from SARS-CoV-2 antibodies binding to the S1 antigen on the surface of functionalized MNPs. With a validated sensitivity of more than 50 ng/mL SARS-CoV-2-S1 antibodies (Figure 1), the proposed technique is competitive with the sensitivity of commonly used ELISA methods but provides more flexibility, robustness and a rapid measurement times of milliseconds. Our method thus paves the way for deep insights into complex and rapid binding dynamics of functionalization chemistry and will revolutionize not only the point-of-care diagnostics but also impacts other fields in research and industries.

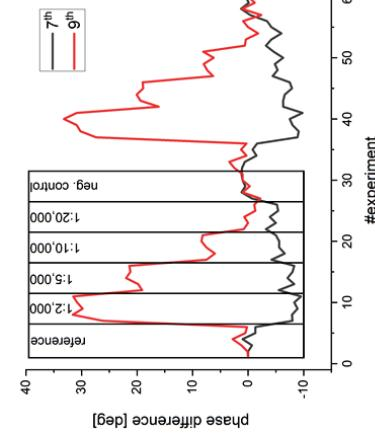


Figure 1: Results of the MPS experiments.

The single experiments of the measuring sequence (ref. 1:2,000, 1:5,000, 1:10,000, 1:20,000 (equalling 50 ng/ml), neg. control) show a clear trend in phase difference of the 7th and 9th higher harmonics. Each sample was measured 5 times without any averaging (acquisition time 10 ms each).

Acknowledgements: The work was supported by the German Research Council (DFG) (grant numbers: VO-22288/1-1, VO-2288/3-1, BE 5293/1-2), the Manfred Roth Stiftung, Fürth, Germany and the "Forschungssstiftung Medizin am Universitätsklinikum Erlangen", Erlangen, Germany.

## Characterization of physical properties of commercial nanoparticle for biomedical application

Hohyon Kim<sup>1</sup>, Yaser Hadadian<sup>1</sup>, Myungjin Park<sup>1</sup>, Bui Minh Phu<sup>1</sup>, Tuan-Anh Le<sup>1</sup>, and Jungwon Yoon<sup>1,\*</sup>  
<sup>1</sup> School of Integrated Technology, Gwangju Institute of Science and Technology, Gwangju 61005, Republic of Korea;  
\*Email: jyoon@gist.ac.kr Mobile: +82-10-2402-6904

Superparamagnetic iron oxide nanoparticles have received a substantial attention during the past two decades in biomedical applications due to their unique magnetic properties and high biocompatibility. Saturation magnetization, magnetic anisotropy, magnetic susceptibility, and colloidal stability are of the most relevant properties determining their use for different application in biomedical research area. Magnetic nanoparticles with higher susceptibilities (reaching values close to their saturation magnetization at lower applied magnetic field) can be suitable candidate for magnetic particle imaging (MPI). Higher saturation magnetization with moderate effective magnetic anisotropy are key features for magnetic nanoparticles to be used in magnetic hyperthermia. A larger magnetic moment in the particles is a desirable property for magnetic navigation systems for targeted delivery using the gradient field. Although tremendous research has been devoted to development of biocompatible iron oxide nanoparticles with tailored physical and chemical properties to requirements of each application, not many have been approved for preclinical or clinical use. In addition, despite the fact that some commercially available particles for research and preclinical purposes have shown high performance in different applications such as magnetic resonance imaging (MRI), MPI, and magnetic hyperthermia, their intrinsic properties have not been fully provided by the producer company. Moreover, no quantitative data regarding their performance in biomedical application has been presented by the provider. In recent years, some research groups have reported on characterization and examination of the performance of some commercially available nanoparticles; however, most of these works either have studied particles from small number of companies or they lack the study of the performance of the particles in conditions where the particles are immobilized. The latter is of crucial importance as for *in vivo* application the particles are immobilized in tissue and because of suppressing the Brownian relaxation mechanism, their performance may differ from the condition in colloidal condition substantially. Therefore, a comprehensive characterization of various commercially available iron oxide nanoparticles investigating their performance in colloid condition and using tissue mimicking gelatin phantom have been investigated.

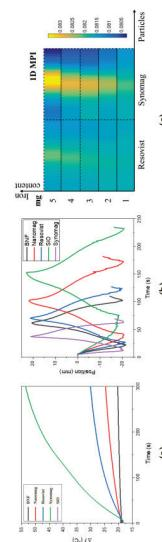


Figure. (a) Temperature increase of each particle for hyperthermia. (b) particle movement control under gradient field. (c) MPI image comparison at different concentration.

# Studies aggregation mechanism of magnetic nanoparticles under possible scenarios during magnetic drug targeting

Myungjin park<sup>1</sup>, Tuan-Anh Le<sup>1</sup> and Jungwon Yoon<sup>1,\*</sup>

<sup>1</sup>School of integrated technology, Gwangju Institute of Science and Technology, chemdan-gwagiro 123,  
Republic of Korea

\*Email: jyoon@gist.ac.kr

Magnetic drug targeting (MDT) is a method by which magnetic drug carriers in the body are manipulated by external magnetic fields to reach the target area. This method is potentially promising in applications for treatment of diseases like cancers, nervous system diseases, sudden sensorineural hearing loss, and so on, due to the advantages in that it can improve efficacy, reduce drug dosage and side effects. Therefore, it has received extensive attention in recent years. However, there are restrictions for using individual magnetic nanoparticles for MDT due to lack of imaging devices and small magnetic actuation forces.

Recently, aggregation phenomena of magnetic nanoparticles under the magnetic field has been considered as one of the great mechanism to overcome lack of actuation force problems and imaging resolution problems. However, it is significant problems that aggregation could occur clogging or sticking inside the blood vessel during MDT. Therefore, aggregation phenomena during MDT should be considered carefully for improving targeting efficiency and safety especially in case for navigating magnetic nanoparticles inside the blood vessel under dynamic magnetic field. Although magnetic nanoparticles were aggregated as magnetic chains and these magnetic chains reach equilibrium state (no grows) after few milliseconds under the static magnetic field (uniform magnetic field), in case of using dynamic magnetic field, the relations (distance or angle) between magnetic chains are continuously changed. Therefore, magnetic chains may not reach equilibrium state. In this paper, we have analyzed aggregation mechanism (dipole force, time, velocity, trajectories) of magnetic chains about possible two scenarios during MDT; using uniform magnetic field, using magnetic gradient field. Furthermore, the length of aggregated magnetic nanoparticles is different under the magnetic field so that we set length of aggregated magnetic nanoparticles as a variable. The photo-graphs have been taken during the motion with respect to time (Figure). It can be seen that given the initial relative position and initial angle, time required for magnetic chains to aggregate with each other increased as length of magnetic chain increased under the uniform magnetic field. Furthermore, it affects to trajectory of both magnetic chains. Whereas, under the magnetic gradient, aggregation can be hinder. These simulation results show that length of magnetic chain and presence or absence of magnetic field can affect to overall aggregation mechanisms.

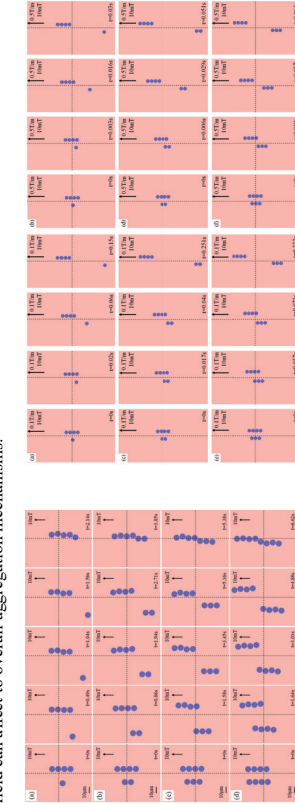


Figure. (a)-(d) Photographs of magnetic chains in the same relative position, initial angle and uniform magnetic field vs. time with the length of magnetic chain 1 (a)  $k=1$ , (b)  $k=2$ , (c)  $k=3$  and (d)  $k=5$ . (e)-(f) Photographs of magnetic chains in the same relative position, initial angle and magnetic gradient vs. time with the length of magnetic chain 1 (a)  $k=1$  and  $0.1\text{T}/\text{m}$ , (b)  $k=1$  and  $0.5\text{T}/\text{m}$ , (c)  $k=2$  and  $0.1\text{T}/\text{m}$ , (d)  $k=2$  and  $0.5\text{T}/\text{m}$ , (e)  $k=3$  and (f)  $k=5$ .

## Iron-cementite nanoparticles in carbon matrix: Synthesis, features and biomedical perspectives

A. Makridis<sup>a</sup>, K. Kontou<sup>b</sup>, D. Karfaridis<sup>b</sup>, F. Pinakidou<sup>b</sup>, M. Katsikini<sup>b</sup>, M. Tsompanoglou<sup>a</sup>, M. Angelakeris<sup>a,b</sup>

N. Sisakyan<sup>c</sup>, H. Gyulasyan<sup>c</sup>, G. Chilengaryan<sup>c</sup>, A. Manukyan<sup>c</sup>

E. Papadopoulou<sup>d</sup>, M. Spasova<sup>d</sup>, M. Farle<sup>d</sup>

<sup>a</sup>*Magnetic Nanostructure Characterization, Technology and Applications (Magnacharta) Center for Interdisciplinary Research and Innovation (CIRI-AUTH) 57001 Thessaloniki, Greece*

<sup>b</sup>*School of Physics, Aristotle University of Thessaloniki, Greece*

<sup>c</sup>*Institute for Physical Research of National Academy of Sciences, Armenia  
<sup>d</sup>*Faculty of Physics and Center of Nanointegration (CENIDE), University of Duisburg-Essen, Germany**

Iron carbides, especially cementite ( $\text{Fe}_3\text{C}$ ), are well known for their hardness and chemical resistance. They also attract much interest due to their tunable magnetic properties. Iron/iron Carbide nanoparticles are also good candidates for preparing multifunctional electrocatalysts for oxygen catalysis. In this work, we study the structural and magnetic properties of carbon coated  $\text{Fe}@\text{Fe}_3\text{C}$  "core-shell" nanoparticles, to examine their perspectives as biomedical heating carriers possessing high losses of magnetic energy under AC field, i.e. magnetic particle hyperthermia cancer modalities. To start with, carbon encapsulated iron-cementite ( $\text{Fe}-\text{Fe}_3\text{C}$ ) nanoparticles with "core-shell" architecture, were synthesized by a single-step solid-state pyrolysis at variable temperatures (700, 800, 850, 900, 950, 1100°C) and duration (5, 15, 30 min). X-ray diffraction outlined the tunable crystallinity with respect to synthesis parameters. Dimensional and morphological features have been investigated using high resolution transmission and scanning transmission electron microscope (HRTEM, STEM) showing  $\text{Fe}-\text{Fe}_3\text{C}$  nanoparticles with an average diameter less than 10 nm embedded in carbon matrix. Mössbauer spectroscopy, XANES, EXAFS combined with Reactive Force-Field Molecular Dynamics simulations confirm the evidence of "core-shell" architecture, which is further supported by the magnetic features exhibited in low (10 K) and high (300 K) temperatures. The biomedical applicability is examined by magnetic particle hyperthermia experiments (375, 765 kHz and 30–60 mT) where the structural features directly reflected to superior magnetic features also conclude to enhanced heating efficiency.

This work was supported by European Union's Horizon 2020 research and innovation programme under grant agreement No 857502 (MaNaCa).

## Mind the Solvent Impurity and Never Give Up on Catechol Anchor: 3D Nano-Assembly and Aqueous Dispersion of Cobalt-Ferrites

Mohammad Suman Chowdhury<sup>1,2</sup>, Enja Laureen Rösch<sup>1,2</sup>, Markus Etzkorn<sup>2,3</sup>, Meinhard Schilling<sup>1</sup>, Aidin Lak<sup>1</sup>

<sup>1</sup>Institute for Electrical Measurement Science and Fundamental Electrical Engineering, Hans-Sommer-Str. 66, Braunschweig, 38106, Germany

<sup>2</sup>Laboratory for Emerging Nanometrology (LENA), TU Braunschweig, Langer Kamp 6a/b, 38106 Braunschweig, Germany

<sup>3</sup>Institute of Applied Physics, TU Braunschweig, Mendeissohnstraße 2, 38106 Braunschweig, Germany

Email: m.chowdhury@tu-bs.de

Magnetic nanoparticles (MNPs) offer a wide variety of applications including therapeutics and diagnostics probes in biology and biomedicine. However, to meet the application needs, designing nanoparticles with a suitable size and shape often poses a challenge largely because of multi-parametric nature of the colloidal synthesis. In addition, when cobalt is employed as a second transition metal to generate magnetically blocked nanoparticles and enhance magnetic anisotropy, they are not open to surface modification with classical catechol-based ligands. Therefore, the use of MNPs-based platforms with diverse metal components for intracellular and bioanalytical research and diagnostics is still limited.

Here, we provide insights into designing highly monodisperse cobalt-ferrite (Co-Fe) magnetic nanocubes (NCs) with precise shapes by decoupling influence of solvent impurity in classical synthesis recipe. Additionally, we showcase how to assemble the nanocubes into a three-dimensional (3D) cubic nano-assembly by selectively choosing a series of solvent impurities. We then transfer these particles from an organic medium to aqueous medium using custom-designed catechol-based polyethylene glycol ligands. Combining high-resolution transmission electron microscopy (HRTEM), proton nuclear magnetic resonance spectroscopy, and ex-situ monitoring of the particle growth, we elucidate the formation mechanism of the 3D nano-assemblies. Their 3D formation is further validated by zero-field-cooled (ZFC) and field-cooled (FC) magnetic susceptibility measurements, where 3D nano-assemblies show an initial magnetic transition that resembles single nanocubes, suggesting the existence of multiple nanocubes within the nano-assemblies of Co-Fe. We will furthermore unravel the effect of solvent impurities on the formation mechanism of the 3D assemblies using X-ray photoelectron spectroscopy.

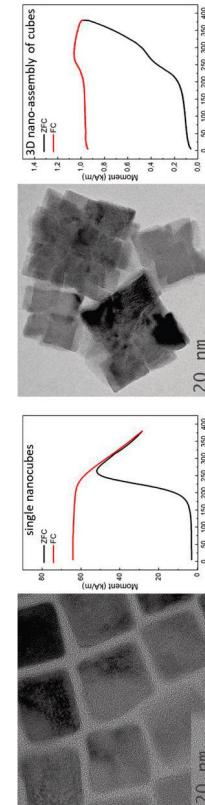


**Figure 1.** HRTEM and respective magnetic susceptibility of mixed NCs: Co<sub>0.85</sub>Fe<sub>2.15</sub>O<sub>4</sub> (left panel) and Co<sub>1.33</sub>Fe<sub>1.67</sub>O<sub>4</sub> (right panel).

**Acknowledgement:**  
We acknowledge the financial support by DFG RTG 1952 "NanoMet" and Junior Research Group "Metrology4Life".

## Effects of Size, Shape and Defects of Iron Oxide Nanoparticles on Photothermal and Magnetothermal therapies

Barbara Freis<sup>1,2</sup>, Celine Kiefer<sup>1</sup>, Ali Abou-Hassan<sup>3</sup>, Emilia Benassai<sup>3</sup>, Cristian Iacovita<sup>4</sup>, Sébastien Harlepp<sup>5</sup>, Sophie Laurent<sup>2</sup>, Sylvie Beguin-Colin<sup>1\*</sup>

(1) Université de Strasbourg, CNRS, Institut de Physique et Chimie des Matériaux, UMR CNRS-UdS 7504, 23 Rue du Loess, BP 43, 67034 Strasbourg, France.

(2) Laboratoire de NMR et d'imagerie moléculaire, Université de Mons, Avenue Maistriau 19, B-7000 Mons, Belgium.

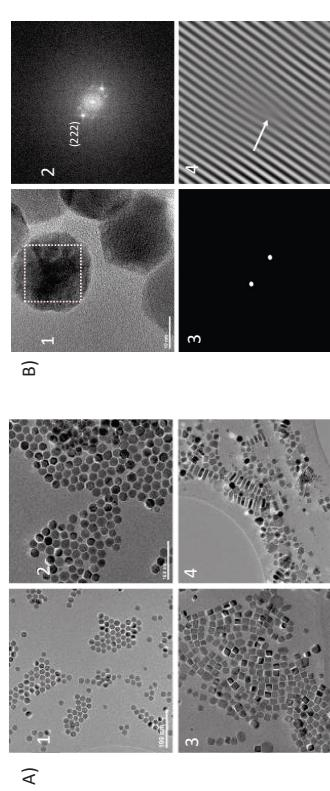
(3) Sorbonne Université, Campus Pierre et Marie Curie, Laboratoire PHENIX - UMR CNRS 8234, Tour 43-42 - 3e étage - CC 51, Place Jussieu, 75005 Paris.

(4) "Iuliu Hatieganu" University of Medicine and Pharmacy Victor Babes street 8, 400012, Cluj-Napoca, Romania.

(5) Inserm U1109, Centre de recherche en biomédecine de Strasbourg, 1 rue Eugène Boeckel, CS 60026, 67084 Strasbourg Cedex, France.

In nanomedicine, the goal is to develop multimodal nanoparticles (NPs) to speed up targeted diagnosis, to increase its sensitivity, reliability and specificity for a better management of the disease. Besides being excellent T2 contrast agents for MRI, iron oxide NPs are promising as therapeutic agents by magnetic hyperthermia when correctly designed (high magneto-crystalline anisotropy) and they also have an interest for photothermal treatment<sup>[1]</sup>. Recently, it has been reported that the defects in nanoparticles may have a strong influence on therapeutic efficiency of both treatments<sup>[2][3]</sup>. So, defect evaluation on different sized and shaped NPs is a crucial point to find the best NPs design for ensuring multimodal therapies.

We have thus optimized the reproducible synthesis of iron oxides NPs with different sizes (10 and 20 nm) and shapes (nanocubes and nanoplates) by the thermal decomposition approach by tuning synthesis parameters such as the reaction temperature, the heating rate and the nature of surfactant. Defects such as dislocation or antiphase boundaries were evaluated by XRD and FFT studies on HRTEM images; and by calculating band gap and Urbach energies. NPs behaviors towards the different kinds of therapies were investigated both in suspensions in water and viscous media and in cancerous cells allowing to establish the key role of defects and NPs design for multimodal therapy.



**A)** TEM images of various sized and shaped NPs: 1 - 12nm spherical NPs, 2 - 22nm spherical NPs, 3 - 15nm nanocubes, 4 - 30nm nanoplatelets.  
**B)** 1-HRTEM image of 22nm NPs, 2-FFT of the area of HRTEM image. 3-Mask of the FFT. 4-Zoom of inverse FFT showing defects in the plan (222)

### References:

- [1] Espinosa, A. *et al.* Magnetic (Hyper)Thermal or Phototherapy? Progressive Comparison of Iron Oxide and Gold Nanoparticles Heating in Water, in Cells, and in Vivo. *Adv. Funct. Mater.* **28**, 1802660 (2018).
- [2] Colin, G. *et al.* Unveiling the role of surface, size, shape and defects of iron oxide nanoparticles for therapeutic applications. *Nanoscale*, **13**, 1455 (2021).
- [3] Bertoli, E. *et al.* Structure-Property-Function relationships of iron Oxide Multicore nanoflowers in Magnetic Hyperthermal and Phototherapy. *ACS nano*, **16**, 271-284 (2022).

This project received funding from ANR (EURO-NANOMEDEV2020-121 - THERAGET) under the umbrella of the ERA-NET EuroNanoMed (GA N723770) of the EU Horizon 2020 Research and Innovation.

## Synthesis of Size-Controlled Iron Oxide Nanocubes for MPI-MFH Applications

S. Harvell-Smith<sup>1,2</sup> and N. T. K. Thanh<sup>1,2\*</sup>

<sup>1</sup> Biophysics Group, Department of Physics and Astronomy, University College London, London WC1E 6BT, UK  
<sup>2</sup> UCL Healthcare Biomaterials and Nanomaterials Laboratories, University College London, London W1S 4BS, UK  
\* Corresponding Author. Email: nt.k.thanh@ucl.ac.uk. http://www.ntk-thanh.co.uk

Magnetic particle imaging (MPI) is a newly developed tracer-based modality which has emerged as a promising tool for many potential therapeutic and diagnostic applications.<sup>1</sup> Standardly, the tracers employed by MPI are superparamagnetic iron oxide nanoparticles (SPIONs). MPI implements a gradient field with strong gradients and weak field strengths, and the non-linear magnetic response of these SPIONs to the gradient field is detected directly for image generation. Overall MPI performance and imaging quality is greatly influenced by the magnetic properties of the SPION implemented. By improving these properties of SPIONs through tailoring of their physical and chemical characteristics, including the iron oxide core size and shape, it is possible to significantly improve the sensitivity and imaging resolution properties of MPI. These particles can also be optimised for improved performance in specific MPI applications. The application of interest in this study is MPI in combination with magnetic fluid hyperthermia (MFH), known as MPI-MFH. This refers to MFH performed using the MPI gradient system which permits localised heat deposition to a desired region in biological tissue, mitigating some of the issues with standard MFH application paradigms.

In this work, the aim is to synthesise and optimise single-core superparamagnetic iron oxide nanocubes (IONCs) towards both MPI, and combination MPI-MFH application. Due to their lower spin disorder at the surface and smaller surface anisotropies, IONCs have a greater overall performance in terms of saturation magnetisation and magnetic susceptibility compared to equivalent spherical SPIONs.<sup>2</sup> However, IONCs have not been optimised yet for these mentioned applications, which is the focus of this study. The effect of changing the core size of spherical SPIONs on MPI performance and sensitivity is well-documented with monodisperse single-core SPIONs having an increasingly improved MPI performance up to a magnetic core diameter of  $\sim 25$  nm.<sup>3</sup> With this in mind, an array of IONCs with sizes smaller than 25 nm were synthesised in our study. For good MPI-MFH performance, the nanoparticle must demonstrate both impressive MPI spatial resolutions, so heat can be localised more specifically using the MPI gradient field system, and heating performance, individually.

Reaction parameters in a thermal decomposition process were altered to obtain decanoic acid-coated magnetite IONCs of different sizes. TEM images of the syntheses are shown in Fig. 1. In all syntheses, there is clear formation of majority cubic shapes with narrow size distributions. The MFH properties have been measured for the largest and smallest synthesised IONCs. The heating performance for the 7 nm IONCs (Fig. 1d) was poor, with an intrinsic loss parameter (ILP) value of just  $0.17 \text{ nrm}^2/\text{kg}$ . The ILP value was much larger for the 24 nm IONCs (Fig. 1a), at  $2.71 \text{ nrm}^2/\text{kg}$ . The 24 nm size of our IONCs is also close to the optimal size of  $\sim 25$  nm for MPI, indicating their potential application in MPI, and because of the good heating properties, MPI-MFH also.

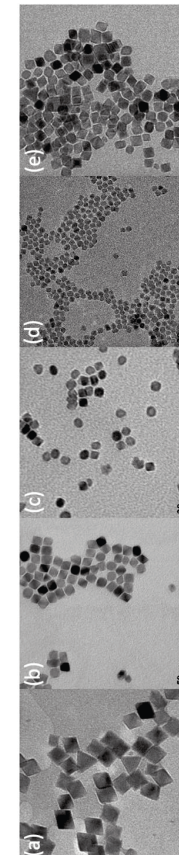


Fig. 1. TEM images of the IONCs synthesized under various conditions, with sizes of (a) 24 nm, (b) 18 nm, (c) 11 nm, (d) 7 nm, (e) 1 mm.

1. S. Harvell-Smith, L. D. Tung, and N. T. K. Thanh, *Nanoscale, Advance Article*, 2022.
2. L. M. Bauer, S. F. Situ, M. A. Griswold, and A. C. Samia, *Nanoscale*, 2016, **8**, 12162–12169.
3. Z. W. Tay, D. W. Hensley, E. C. Vreeeland, B. Zheng, and S. M. Connolly, *Biomed. Phys. Eng. Express*, 2017, **3**, 035003.

## A tunable acid-etching procedure for the preparation of partially hollow magnetic nanostructures

Sebastian Nemec<sup>1,2</sup> and Slavko Kralj<sup>1,2,3\*</sup>

<sup>1</sup> Department for Materials Synthesis, Jozef Stefan Institute, Jamova 39, 1000 Ljubljana, Slovenia,  
<sup>2</sup> Faculty of Pharmacy, University of Ljubljana, Askerceva cesta 7, 1000 Ljubljana, Slovenia,  
<sup>3</sup> Nanos SCI, Nanos Scientifica d.o.o., Teskova 30, 1000 Ljubljana, Slovenia

\*Email: slavko.kralj@ijs.si

Nanostructures with hollow core and outer shell are an exciting type of nanoparticles. The central void is a space available for the incorporation of various functional cargo(s), such as drugs and catalysts. However, a wider applicability of the hollow nanostructures is delayed due to scarce and challenging synthetic procedures needed to obtain such complex nanostructures. So far, various approaches have been utilised to prepare hollow nanostructures. The most widely used etching methods rely on the synthesis of nanoparticles that have a shell and a sacrificial core, which gets selectively removed while the shell is kept intact. If the removal of the sacrificial core is only partial, we obtain a partially hollow structure, commonly referred to as yolk-shell or rattle-type nanostructures. These partially hollow nanostructures are also attractive as they may offer combined functionalities of the shell and the residual core part. The procedures for the preparation of partially hollow nanostructures are generally more challenging than obtaining completely hollow nanostructures, as the core removal process needs to be precisely controlled and should offer the possibility for rapid termination of the core removal. An elegant way to control the core removal process is to utilise core-shell nanoparticles, where the shell and the sacrificial core are composed of chemically different materials. In such way we achieve a selective core removal and, moreover, the core removal rate can be nicely controlled by changing the thickness and morphology (porosity) of the shell.

In our work, we synthesized hollow and partially hollow magnetic silica nanostructures (Figure). These structures were prepared from silica-coated magnetic nanochains by using an acid etching method to partially dissolve iron oxide cores. The iron oxide cores were either completely or partially dissolved using hydrochloric acid. Iron oxide dissolves readily in the hydrochloric acid while the silica shell remains intact. The silica porosity affects the rate of the iron oxide dissolution. Moreover, the protective ability of silica shells with different thicknesses (ranging from  $\sim 3$  nm to  $\sim 60$  nm) and morphologies (low-porous and mesoporous) was systematically studied by using different durations of the etchings and different hydrochloric acid concentrations. We have figured out some differences in the protective ability of different silica shells towards the acid dissolution of iron oxide cores. Our findings can be further applied to efficiently adjust the preparation procedures for obtaining partially hollow magnetic nanostructures. Finally, we conducted preliminary drug-loading experiments to test the ability of such hollow silica nanostructures to be used as drug delivery system for the model drug ibuprofen.

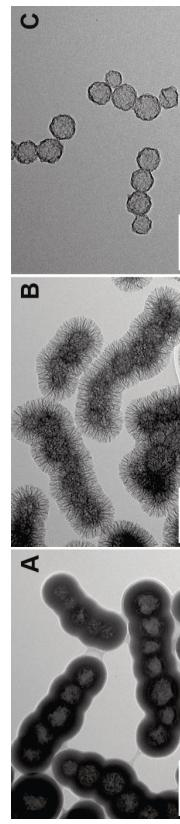


Figure. Transmission electron microscope micrographs of hollow silica nanostructures. (A)  $\sim 60$  nm thick low-porous silica shells, (B)  $\sim 70$  nm thin low-porous silica shells, and (C)  $\sim 3$  nm mesoporous silica shells. All scale bars are 500 nm.

## Synthesis and characterisation of $\text{BaTiO}_3 - \text{CoFe}_2\text{O}_4$ magnetostrictive nanoparticles for biomedical applications.

Samyog Adhikari, Le Duc Tung and Nguyen TK Thanh\*

\*[ntk-thanh@ucl.ac.uk](http://www.ntk-thanh.co.uk), <http://www.ntk-thanh.co.uk>

*BioPhysics Group, Department of Physics & Astronomy University College London, Gower Street, London WC1E 6BT, UK and UCL Healthcare Biomaterials and Nanomaterials Laboratories, 21 Albemarle Street, London W1S 4BS*

Magnetostrictive nanoparticles (MENP) have magnetic and electric properties coupled together.[1] Here, the significant coupling between the two properties will allow direct control of ferroelectricity and magnetism. MENP are of significant interest in biomedical applications as they exhibit new functionalities such as magnetic field control of electric polarisation used in on-demand drug release among others.[2] Although there are several ways of achieving the magnetostrictive (ME) effect, combining a magnetic material with a ferroelectric one in a core-shell structure has gained significant interest in recent years due to its large ME effects.[3] The magnetic phase used in this study will be cobalt ferrite (CF) due to its high magnetostrictive coefficient and the ferroelectric phase barium titanate (BT) due to its high piezoelectric coefficient.[4, 5]

First, we present an optimisation of the synthesis protocol for the ferroelectric and the ferrimagnetic phase to control morphology of the nanoparticles. The effect of morphology and size on the properties of MENP will be studied by using different characterisation techniques (TEM, SQUID, STM, XRD, Raman, DLS).

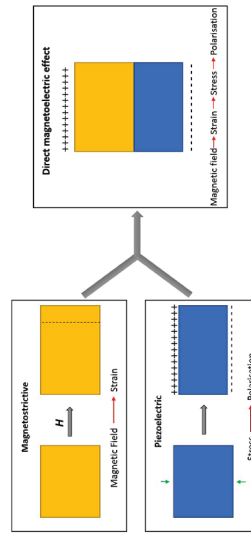


Figure 1: Schematic of magnetostrictive coupling causing the direct magnetoelectric effect.

When a magnetic field is applied on a MENP, CF undergoes magnetostriction which causes the material to strain and elongate. This mechanical energy is transferred to BT which then exhibits polarisation. This is called strain-mediated magnetostrictive coupling (figure 1). The shape and size of the core-shell nanostructure is controlled using synthetic parameters.

### References:

- Spaldin NA. Magnetic materials: fundamentals and applications. Cambridge university press; 2010 Aug 19.
- Kolishetti N, Vashist A, Arias AY, Atturi V, Dhar S, Nair M. Recent advances, status, and opportunities of magneto-electric nanocarriers for biomedical applications. Molecular aspects of medicine. 2021 Nov 4;101046.
- Wang P, Zhang E, Toledo D, Smith JT, Navarrete B, Furman N, Hernandez AF, Telusma M, McDaniel D, Liang P, Khizroev S. Colossal Magnetoelectric Effect in Core-Shell Magnetostrictive Nanoparticles. Nano Letters. 2020 Jul 8;20(8):5765-72.
- Pan Q, Xiong YA, Shao TT, You YM. Recent progress in the piezoelectricity of molecular ferroelectrics. Materials Chemistry Frontiers. 2021;5(1):44-59.
- Bozorth RM, Tilden EF, Williams AJ. Anisotropy and magnetostriction of some ferrites. Physical Review. 1955 Sep 15;99(6):1788.

## Synthesis of flower-like manganese ferrite nanostructures for enhancing chromium bio-reduction by *Shewanella oneidensis*

Diana S. Raie,<sup>a,b</sup> Stefanos Moudrikidis,<sup>a,b</sup> Antonis Makridis,<sup>c</sup> Lena Cricic,<sup>d</sup> Nguyen T. K. Thanh<sup>a,b,\*</sup>

<sup>a</sup>*BioPhysics Group, Department of Physics and Astronomy, University College London, Gower Street, London, WC1E 6BT, UK*

<sup>b</sup>*UCL Healthcare Biomaterials and Nanomaterials Laboratories, UCL, 21 Albemarle Street, London W1S 4BS, UK*

<sup>c</sup>*Department of Physics, Aristotle University of Thessaloniki, 54124 Thessaloniki, Greece*

<sup>d</sup>*Healthy Infrastructure Research Group, Department of Civil, Environmental and Geomatic Engineering, UCL, Gower Street, London WC1E 6BT*

\*Email: ntk.thanh@ucl.ac.uk, <http://www.ntk-thanh.co.uk>

Chromium is a common environmental pollutant deriving from several industries including plating, tanning and metal finishing. Human exposure to hexavalent chromium (Cr(VI)) can cause cancer and neurotoxicity. Leaking chrome from industrial sites into water can lead to soil and groundwater contamination which is a risk currently being considered in several industries. Integrating both adsorption and biological reduction of highly toxic Cr(VI) into the less toxic trivalent one (Cr(III)) together has been proposed as a promising strategy to tackle the aforementioned issue. In this context, nanoscale materials possess special features that make them promising candidates for such applications; nanoclusters have been gaining much attention due to their simple preparation, high surface to volume ratio, high stability and enhanced efficiency due to the complex interparticle interactions which depend on the single crystal particle size, orientation and spacing. Herein we report a simple route for the robust, single-step and scalable preparation of  $\text{Mn}_{x}\text{Fe}_{3-x}\text{O}_4$  nanoflowers ( $60 \pm 12$  nm diameters) that can adsorb 12 mg of Cr(VI). The effect of nanoflowers on the Cr(VI) reduction and tolerance by *Shewanella oneidensis* have been explored as a safe and integrated way with good performance in heavy metal removal from water.

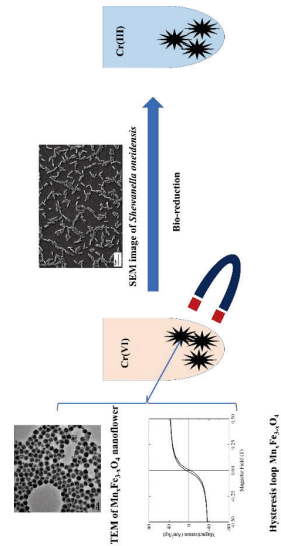


Figure 1. Representation of an integrated adsorption bio-reduction method for safe removal of hexavalent chromium

**Acknowledgements:** DSR thanked Newton Mosharfa for the PhD scholarship, UCL grand challenges and UCL small grant for doctoral school, EPSRC are thanks for financial support.

## Effect of Iron Oxide Nanoparticle Surface Chemistry on Magnetic Property and Cytotoxicity on Hela Cells

Senem Çitoglu<sup>1</sup>, Mehmet Ali Onur<sup>2\*</sup>, Özlem Duyar Coşkun<sup>3</sup>

<sup>1</sup>Department of Nanotechnology and Nanomedicine, Hacettepe University, 06800, Ankara, Turkey.

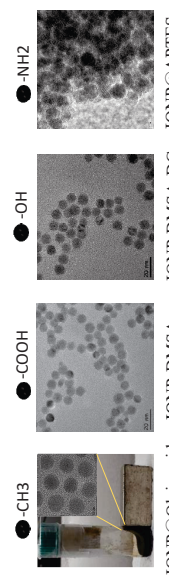
<sup>2</sup>Department of Biology, Hacettepe University, 06800, Ankara, Turkey,

<sup>3</sup>Department of Physics Engineering, Hacettepe University, 06800, Ankara, Turkey.

\*Email: malii@hacettepe.edu.tr

Superparamagnetic iron oxide nanoparticles (IONPs) with appropriate surface chemistry are in the field of great interest due to the high potential for a wide range of biomedical applications such as drug delivery, magnetic fluid hyperthermia, magnetic resonance imaging and stem cell therapy. Surface properties of nanoparticles (NPs) (i.e. surface chemistry, charge) provide them not only stability and biocompatibility but also conjugation capability for drug molecules and/or targeting ligands. Surface properties are also important to avoid or delay the interaction of NPs with the reticuloendothelial system, which might prolong their circulation half-life in the blood stream<sup>1</sup>. Optimization of surface properties of NPs allows to use these NPs not only in separate application but also in combined modalities.

The aim of this study is to synthesize superparamagnetic IONPs with different surface properties (i.e. carrying carboxyl, hydroxyl, and amine groups) convenient for biomedical applications and to investigate the effects of surface chemistry on magnetic properties and in vitro cytotoxicity on HeLa cells. For this purpose, three types of IONPs (IONP@DMSA, IONP@DMSA-DG, IONP@APTES) were prepared. First, 8.4±1.0 nm spherical oleic acid coated-IOPNs were synthesized by thermal decomposition method and then coated with meso-2,3-Dimercaptosuccinic acid (DMSA) or (3-Aminopropyl)triethoxysilane (APTES) via ligand exchange reaction. DMSA-coated IONPs were further conjugated with 2-deoxy-D-glucose (DG) by esterification reaction to impart functionality. Structural and magnetic properties of all IONPs were characterized by X-ray diffraction, transmission electron microscope, Fourier-transform infrared spectroscopy, zeta sizer, thermogravimetric analysis and vibrating sample magnetometer. Cytotoxicity of the IONPs with the three types of coatings was assessed through 3-(4,5-dimethylthiazol-2-yl)-2,5-diphenyltetrazolium bromide (MTT) assay. The results showed that all NPs exhibited a typical superparamagnetic property at room temperature. Surface modification with DMSA resulted in a magnetization increment of 22% while DG conjugation and APTES coating caused a reduction of magnetization (6.5% and 32%, respectively). HeLa cells remained more than 80% viable relative to the control group when incubated with all nanoparticle types with the nanoparticle concentrations of 2.5 µg ml<sup>-1</sup>, 5 µg ml<sup>-1</sup> and 10 µg ml<sup>-1</sup> for 24, 48, and 72 h. The results showed a promising potential for the use of IONP@DMSA and IONP@DMSA-DG NPs for biomedical applications. To the best of our knowledge, this is the first study to compare IONPs with these three types of surface coatings.



### Acknowledgements

This work was funded by The Scientific and Technological Research Council of Turkey - Directorate of Science Fellowships and Grant Programmes (TUBITAK - BIDEB) with 2211-C National PhD Scholarship within the frame work of priority areas, and by Hacettepe University Scientific Research Project (BAP) Coordination Unit, Turkey (Project No: FHD-2018-16742). The authors acknowledge the National Nanotechnology Research Center (UNAM), TR and Hacettepe University Advanced Technologies Application and Research Center (HÜNTEREK), TR.

Reference: Martinez-B Arribio, M., Fernández-Pacheco, R., Ibárra, M. R., & Santamaría, J. Magnetic nanoparticles for drug delivery, Nano Today, 2(3), 22–32, 2007.

## Competing Interactions, and magnetization dynamics in Doped Rare-earth Manganites nanostructural system

Wiqar Hussain Shah,  
Department of Physics, Faculty of Basic and Applied Sciences,  
Islamic International University, Islamabad, Pakistan

### Abstract:

The Structural, magnetic and transport behavior of  $\text{La}_{1-x}\text{Ca}_x\text{MnO}_{3+\delta}$  ( $x=0.48$ , 0.50, 0.52 and 0.55 and  $\delta=0.015$ ) compositions close to charge ordering, was studied through XRD, resistivity, DC magnetization and AC susceptibility measurements. With time and thermal cycling ( $T=300$  K) there is an *irreversible* transformation of the low-temperature phase from a partially ferromagnetic and metallic to one that is less ferromagnetic and highly resistive. For instance, an increase of resistivity can be observed by thermal cycling, where no effect is obtained for lower Ca concentration. The time changes in the magnetization are logarithmic in general and activation energies are consistent with those expected for electron transfer between Mn ions. The data suggest that oxygen non-stoichiometry results in mechanical strains in this two-phase system, leading to the development of *irreversible* metastable states, which relax towards the more stable charge-ordered and antiferromagnetic microdomains at the nano-meter size. This behavior is interpreted in terms of strains induced charge localization at the interface between FM/AFM domains in the antiferromagnetic matrix. Charge, orbital ordering and phase separation play a prominent role in the appearance of such properties, since they can be modified in a spectacular manner by external factor, making the different physical properties metastable. Here we describe two factors that deeply modify those properties, viz. the doping concentration and the thermal cycling. The metastable state is recovered by the high temperature annealing. We also measure the magnetic relaxation in the metastable state and also the revival of the metastable state (in a relaxed sample) due to high temperature (800 °C) thermal treatment.

wiqarhussain@yahoo.com  
[wiqar.hussain@iui.edu.pk](mailto:wiqar.hussain@iui.edu.pk)

## “Core-shell”-like $\text{Fe}_3\text{O}_4/\text{CeO}_2$ Nanocomposites for Perspective Application in Medicine: Synthesis, Physical-chemical Characterization and Bio-activity

**Yuliia Shlapa<sup>1\*</sup>, Illia Timashkov<sup>1</sup>, Katarina Siposova<sup>2</sup>, Ivana Garcarova<sup>2</sup>, Dagmar Sedlakova<sup>2</sup>,**

**Andrey Musatov<sup>2</sup>, Valentin-Adrian Maraloiu<sup>3</sup>, Anatolii Belous<sup>1</sup>**

<sup>1</sup> V. I Vernadsky Institute of General & Inorganic Chemistry of the NAS of Ukraine, Kyiv, Ukraine

<sup>2</sup> Institute of Experimental Physics SAS, Kosice, Slovakia

<sup>3</sup> National Institute of Materials Physics, Magurele, Romania

\*e-mail: yuliayushlapa@ukr.net; Mobile: +38 099 327 18 63

Multifunctional “core-shell”-like nanocomposites based on the magnetic  $\text{Fe}_3\text{O}_4$  nanoparticles (MNPs) and cerium dioxide ( $\text{CeO}_2$ ) attract significant scientific interest due to the possibility to combine the simultaneous ability of MNPs to heat up effectively in AC magnetic field with the antioxidant and anti-amyloid activities of  $\text{CeO}_2$ . Such composites can be promising for biomedical investigations, particularly, in the therapy of diseases caused by oxidative stress and amyloidogenesis. The aim of this study was the synthesis of “core-shell”-like nanocomposites based on  $\text{Fe}_3\text{O}_4/\text{CeO}_2$ , examination of their physical-chemical properties and morphology as well as evaluation of their antioxidant and anti-amyloid activity.

A set of  $\text{Fe}_3\text{O}_4/\text{CeO}_2$  “core/shell”-like nanocomposites with the theoretically calculated thickness of  $\text{CeO}_2$  “shell” of 3, 5, and 7-layers was fabricated by the precipitation of  $\text{CeO}_2$  NPs onto the surface of the  $\text{Fe}_3\text{O}_4$  MNPs. According to XRD data, signals of both  $\text{Fe}_3\text{O}_4$  and  $\text{CeO}_2$  were present in XRD patterns of the composites, but the intensity of the main peak of  $\text{Fe}_3\text{O}_4$  at 20° equal to ~35° reduced with the growth of  $\text{CeO}_2$  “shell” on the surface of MNPs. HR TEM and EELS studies revealed that  $\text{Fe}_3\text{O}_4/\text{CeO}_2$  nanocomposites consist of  $\text{Fe}_3\text{O}_4$  NPs core with an average size of ~3 nm are surrounded by  $\text{CeO}_2$  NPs with an average size of ~3 nm forming the “core-shell”-like structures. Increasing  $\text{CeO}_2$  “shell” thickness is manifested by the increased hydrodynamic diameter of NPs, in aqueous suspensions and better stability of nanocomposites in the suspensions expressed as zeta potential (DLS measurements).  $\text{Fe}_3\text{O}_4/\text{CeO}_2$  NPs with the 5- and 7-layers “shell” formed the highly-stable suspensions without any additional stabilizers ( $\zeta \geq +30$  mV) in opposite to  $\text{Fe}_3\text{O}_4$  NPs, which had zeta-potential values +17.7 mV. The thickness of the  $\text{CeO}_2$  “shell” affected also the heating efficiency of nanocomposites under applying of AC magnetic field ( $H=9.3$  kA/m,  $f=300$  kHz). The maximal heating temperature values were 40–50°C and decreased with increasing of the “shell” thickness. The specific loss power (SLP) values reduced from 33 W/g for  $\text{Fe}_3\text{O}_4/\text{CeO}_2$  NPs with the theoretically calculated “7-layers shell”.

Bioactivity of prepared nanocomposites expressed as the antioxidant and anti-amyloid effect has been examined. All tested NPs significantly inhibited the formation of insulin amyloid aggregates in vitro. The anti-amyloid activity was highly dependent on the thickness of  $\text{CeO}_2$  layers on the core of  $\text{Fe}_3\text{O}_4$ . The highest ability to inhibit the process of fibrils formation was observed for nanocomposites with the theoretically calculated “7-layers shell”. The antioxidant activity of  $\text{Fe}_3\text{O}_4$  and  $\text{Fe}_3\text{O}_4/\text{CeO}_2$  nanocomposites was evaluated by monitoring their catalase- and superoxide dismutase-like activity.

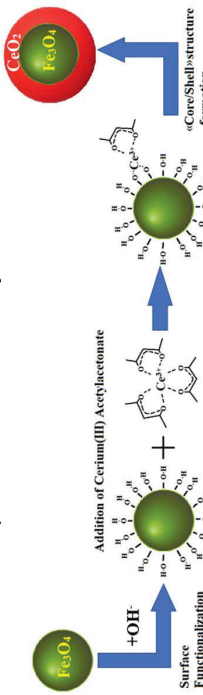


Fig. 1. Scheme of synthesis of  $\text{Fe}_3\text{O}_4/\text{CeO}_2$  ‘core/shell’-like structures

Acknowledgment: This work was supported by grants: grant No 0121U110363 in the framework of the Target Program of Scientific Researches of the National Academy of Sciences of Ukraine “Grants of the NAS of Ukraine to research laboratories/groups of young scientists of the NAS of Ukraine” (2021–2022); grant No 20207013 by CERIC-ERIC Consortium for access to experimental facilities, by the NATO Science for Peace and Security Programme under grant [G5683]; Slovak Grant Agency VEGA (No. 2/0094/21; 2/0034/22), Slovak Research and Development Agency (APVV-19-0324).

## Millifluidic two-phase system for the continuous automated manufacturing of MNP

Lennart Göpfert<sup>1</sup>, Eva Miriam Buhl<sup>2</sup>, Thomas Schmitz-Rode<sup>1</sup> and Ioana Slabu<sup>1\*</sup>

<sup>1</sup> Institute of Applied Medical Engineering, Helmholtz Institute, Medical Faculty, RWTH Aachen University, Pauwelsstr. 20, 52074 Aachen, Germany

<sup>2</sup> Institute of Pathology, Electron Microscopy Facility, RWTH University Hospital Aachen, Pauwelsstr. 30, 52074 Aachen, Germany

E-mail: goepfert@ame.rwth-aachen.de | \*slabu@ame.rwth-aachen.de

From a translational perspective, magnetic nanoparticles (MNPs) require manufacturing processes that can be performed reliably and at scale. Continuous and automated manufacturing processes are particularly well suited for this purpose compared to batch processes, which have high technical variability and low throughput production.

In this study, a continuous MNP manufacture approach based on oxidative precipitation is presented. For this, a setup was built consisting of a 10-meter-long coiled tube and a mixing element. Air (20.95 vol.-% oxygen) and a mixture of iron sulfate and ammonia solution were alternately pumped into the tube coil (Figure 1 A). Over the 10-minute continuous flow in the mixing element, superparamagnetic iron oxide nanoparticles (SPION) were then formed. The fluid exchange rate for the reaction was varied by changing the volume ratios between gas and liquid bubbles and by increasing the total number of bubbles per tube length. For different rates, SPION were synthesized and physico-chemically characterized (Figure 1 B). Transmission electron microscopy (TEM), dynamic light scattering (DLS), and iron concentration based on complexation of  $\text{Fe}^{3+}$  was determined. Exemplary results are depicted in Figure 1 B demonstrating the influence of oxidation on SPION formation. Tuning gas transfer into the liquid indicates that the diameter of the resulting SPOIN can be controlled. SPION with tunable properties are of high interest for many medical applications in imaging and therapy.

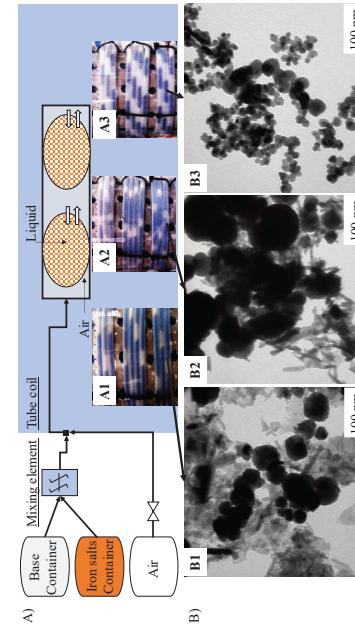


Figure 1: A) Sketch of the continuous MNP synthesis. Precise adjustment of the gas and liquid bubbles allows the reaction environment to be varied. A1: 1.4 cm<sup>3</sup> liquid and 0.5 cm<sup>3</sup> gas bubble (volume ratio: 0.27). A2: 1.4 cm<sup>3</sup> liquid and 0.65 cm<sup>3</sup> gas bubble (volume ratio: 0.46). A3: 1.0 cm<sup>3</sup> liquid and 0.75 cm<sup>3</sup> gas bubble (volume ratio: 0.75). B) Representative transmission electron microscopy (TEM) images of the settings A1 (TEM image B1), A2 (TEM image B2) and A3 (TEM image B3) without purification or coating. Images show different SPION morphologies.

## Synthesis and characterization of gold-coated superparamagnetic iron oxide nanoparticles for magnetic drug targeting treatment

René Stein<sup>1\*</sup>, Bernhard Friedrich<sup>1</sup>, Marina Mühlberger<sup>1</sup>, Harald Unterweger<sup>1</sup>, Rainer Tietze<sup>1</sup>, Aldo R. Boccaccini<sup>2</sup> and Christoph Alexiou<sup>1</sup>

<sup>1</sup>Department of Otorhinolaryngology - Head and Neck Surgery, Section of Experimental Oncology and Nanomedicine (SEON), Else Kröner Fresenius-Stiftung-Professorship, Universitätsklinikum Erlangen, Germany;

<sup>2</sup>Institute of Biomaterials, University of Erlangen-Nuremberg, Erlangen, Germany;  
\*E-mail: rene.stein@extern.uk-erlangen.de

Treating cancer is still a major challenge for modern medicine. Conventional therapies such as chemotherapy are accompanied by severe side effects on healthy tissue as well as ineffective drug accumulation in diseased tissue. The concept of magnetic drug targeting (MDT) provides the means to tackle the disadvantages of conventional chemotherapy while further enhancing the effectiveness of the treatment.

Surface functionalized gold-coated superparamagnetic iron oxide nanoparticles (Au-SPIONS) might offer the possibility of a strong covalent bond for actively transporting drugs towards diseased tissues by an external magnetic field. The gold-coating process increased the hydrodynamic size of pure citrate-stabilized SPIONS (Cit-SPIONS) from an average of 107 nm to 445 nm with a broadened size distribution and resulted in non-uniform particle aggregates. While magnetic properties could be maintained after the gold-coating, particle size control and stability against sedimentation of the particles were challenges. Thus, Au-SPIONS were surface stabilized with additional citrate to create Cit-Au-SPIONS. These synthesized particles were found to be controllable in size by the variation of the added citrate concentration accompanied by better long-term stability and moderate pH values of the dispersion as well as reproducible particle sizes of around 150 nm.

Investigating procedure parameters during the gold-coating process revealed a strong influence of the concentration of the used gold salt on the hydrodynamic particle size, pH value and reproducibility of the particle dispersions. With an increase in gold content, the particle size increased while the reproducibility decreased. After further characterization, a promising Cit-Au-SPION system was tested for cell toxicity.

No major toxic effects were found on the cell viability and proliferation of Jurkat T cell leukemia cells even after 48 h of exposure. Early functionalization of the gold surface with the thiol-containing amino acid cysteine demonstrated a 6-fold higher cysteine binding on Cit-Au-SPIONS in comparison to pure Cit-SPIONS. Binding a cysteine terminated peptide on 95 nm large Cit-Au-SPIONS still resulted in stable nanoparticles with a size of 114 nm bearing 45 nmol of peptide per mg of iron. Thus, gold-coating SPIONS might present a way to strongly bind thiolated molecules to their gold surface. These molecules or proteins could e.g. be specialized for carrying drugs for the usage in magnetic drug targeting treatments.

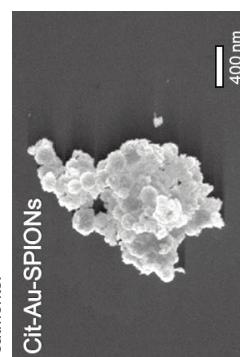


**Figure 1:** Scanning electron microscope image of citrate-stabilized gold-coated SPION aggregates. Cit-Au-SPIONS show no severe toxic effects on Jurkat T cell leukemia cells and a 6-fold higher cysteine binding when compared with pure citrate-stabilized SPIONS.

**Acknowledgements:** This project was funded by the Manfred-Roth-Stiftung Fürth and the Medizinische Forschungsgesellschaft am Universitätsklinikum Erlangen, Germany.

## Magnetic Microspheres: A Toolbox for Hyperthermia, Drug Delivery and Immunomagnetic Separation

Diana Zahn<sup>1\*</sup>, Svenja Jung<sup>1</sup>, Jan Dellith<sup>2</sup>, Katayoun Saatchi<sup>3</sup>, Urs O. Häfeli<sup>3</sup>, Silvio Dutz<sup>1</sup>

<sup>1</sup>Institut für Biomédizinische Technik und Informatik, Technische Universität Ilmenau, Ilmenau, Germany

<sup>2</sup>Leibniz Institute of Photonic Technology, Jena, Germany

<sup>3</sup>Faculty of Pharmaceutical Sciences, University of British Columbia, Vancouver, Canada

\*E-mail: diana.zahn@tu-ilmenau.de

Polymeric microspheres (MS) are of great interest for several medical and biotechnological applications. By incorporating drugs into the MS, they can be used for drug delivery, where diseased organs are targeted in a controlled manner by linking specific antibodies to the MS surface. Additionally, magnetic nanoparticles (MNP) can be embedded into the MS, leading to magnetic microspheres (MMS), that can be used for hyperthermia and to enhance the drug release out of the MMS. Antibody conjugated MMS can also be utilized for immunomagnetic separation and pathogens can be extracted out of a specimen. For all mentioned applications, a high concentration as well as a homogeneous distribution of the MNP inside the spheres is needed. Therefore, we are working on MS made of poly(lactic-co-glycolic acid) (PLGA) or poly(lactic acid) (PLA) with embedded oleic-acid coated MNP and antibodies linked to their surface. Microspheres were produced by an emulsion-evaporation method, where the polymer, MNP and a drug are suspended in an oil phase that is homogenized in an aqueous phase containing PVA. The oil droplets are allowed to harden and finally form the MS. The tunability of the MS size was studied by varying several synthesis parameters, using static light scattering for size measurements. To incorporate the MNP, a hydrophobic coating is needed, why we established an oleic-acid coating of the MNP, characterizing the resulting particles with VSM, DLS and TGA. The incorporation of oleic acid coated MNP into the MMS was investigated with SEM on focused ion beam cross sections and VSM. Last, antibody conjugation was evaluated using a click chemistry approach as well as the biotin-avidin adsorption mechanism. As a proof of principle, the release of an anticancer drug out of MMS by magnetic heating to 43 °C compared to 37 °C was investigated. We found that mainly the homogenization speed and method (mechanical or ultrasonic) and PVA concentration can be used to control the MS size, enabling the synthesis of MS between 0.5 and 6 µm. Coating the MNP with oleic acid enables monodisperse and stable particles in organic solvents with a mean diameter of 190 nm ( $\pm$ average), a PDI of 0.12 and approx. 8 wt% oleic acid relative to the overall particle weight. SEM images revealed a homogeneous distribution of MNP throughout the spheres while maintaining a perfect spherical shape (see figure) with concentrations of MNP up to 33 wt%. Antibodies were conjugated on PLA microspheres, confirmed by photometry (ELISA). Drug release was increased by 30% due to magnetic heating, compared to release at body temperature, confirming the use of magnetic particles to accelerate drug delivery mechanisms. Summarized, we developed a toolbox of MS that can be adapted to several applications by tuning their size, incorporating magnetic nanoparticles and conjugation of antibodies to their surface.

**Acknowledgements**  
This work was supported by the "Thüringer Innovationszentrum für Medizintechnik-Lösungen" (ThIMEDOP; FKZ IZN 2018 0002) and by the Freistaat Thüringen in the project "SARS-rapid" (contract 2020FGR0052). It is co-financed from the European Union in the frame of the "European Regional Development Fund (ERDF)". Funding was provided by the DFG core facility, grant number KO321/3 and grant number TR408/11 for the MPS quantification measurements.

## Ferrimagnetic iron oxide nanoparticles for heating applications: large single domain particles prepared by the green rust method

Diana Zahn<sup>1\*</sup>, Joachim Landers<sup>2</sup>, Julianne Buchwald<sup>1</sup>, Marco Diege<sup>3</sup>, Soma Salamon<sup>2</sup>, Robert Müller<sup>3</sup>, Moritz Köhler<sup>4</sup>, Germot Ecke<sup>5</sup>, Heiko Wende<sup>2</sup>, Silvio Dutz<sup>1</sup>

<sup>1</sup> Institute for biomedical engineering and informatics, Technische Universität Ilmenau, Ilmenau, Germany

<sup>2</sup> Faculty of Physics & CENIDE, University of Duisburg-Essen, Duisburg, Germany

<sup>3</sup> Leibniz Institute of Photonic Technology, Jena, Germany

<sup>4</sup> Jena Center for Soft Matter (JCSM), Friedrich Schiller University Jena, Jena, Germany

<sup>5</sup> Institute for Micro- and Nanoelectronics, Technische Universität Ilmenau, D-98693 Ilmenau, Germany

\*E-mail: diana.zahn@tu-ilmenau.de

Magnetic iron oxide nanoparticles are known to be used for intracorporeal hyperthermia treatments, but can also be used for extracorporeal heating applications, for example as a thermal marker on lateral flow assays instead of the common colorimetric markers. For thermal markers, applied magnetic fields don't need to match the restrictions for patient's safety and therefore particles with higher coercivities ( $H_c$ ) can be used.  $H_c$  can be increased by increasing the shape anisotropy (creating non-spherical particles) or doping the iron oxide with other metal atoms like cobalt or barium. Another method to increase  $H_c$  is to synthesize larger particles, since  $H_c$  increases with particle volume as long as only one magnetic domain is formed. Therefore, we investigated the synthesis and resulting characteristics of large single domain particles (LSDP) using the green rust method at various synthesis temperatures from 5 to 85 °C. Ferrous chloride solution was mixed with NaOH and NaNO<sub>3</sub> solutions under oxygen free conditions, leading to the precipitation of non-magnetic green rust particles, slowly oxidizing to a magnetic material in 24 hours. Particles were characterized using a variety of measurement methods: transmission electron microscopy (TEM), X-ray diffraction (XRD), Auger electron spectroscopy (AES), vibrating sample magnetometry (VSM), Mössbauer spectroscopy and calorimetric measurements for SAR evaluation. Particles show increasing mean sizes by XRD with increasing synthesis temperatures, ranging from 30 to 65 nm and at the same time increasing coercivity, resulting in values from 6 to 15 kA/m. Saturation magnetization Ms can be classified into three regions (see figure): synthesis temperature of 5 °C does not enable the complete transformation to magnetic material and therefore leads to an Ms of only 47 Am<sup>2</sup>/kg. For temperatures 15 to 35 °C, high magnetization values around 85 Am<sup>2</sup>/kg are obtained, whereas for temperatures above 45 °C, Ms decreases, indicating the formation of a non- or weak magnetic phase apart from magnetite/maghemite. This parasitic phase was also confirmed by Mössbauer spectroscopy, showing an additional subspectrum for those samples indicating an antiferromagnetic Fe<sup>3+</sup>-bearing material. AES measurements support this assumption by confirming Na in the 75 °C sample whereas only Fe and O was found in the 35 °C sample. SAR measurements ( $H = 55$  kA/m;  $f = 290$  kHz) of immobilized particles showed promising values up to 600 W/g, while exhibiting the same trend as Ms: samples synthesized above 45 °C show lower SAR values due to their diminished magnetic behaviour. Our LSDP are promising candidates for heating applications due to their high  $H_c$  and Ms for synthesis temperatures below 45 °C. In ongoing work, we are investigating the parasitic non-magnetic phase in more detail and evaluate strategies to prevent its formation.

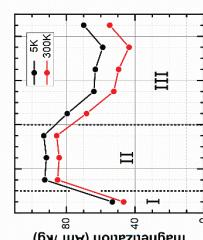


Figure: Ms for varying synthesis temperatures

saturation magnetization ( $H = 55$  kA/m;  $f = 290$  kHz) of immobilized particles showed promising values up to 600 W/g, while exhibiting the same trend as Ms: samples synthesized above 45 °C show lower SAR values due to their diminished magnetic behaviour. Our LSDP are promising candidates for heating applications due to their high  $H_c$  and Ms for synthesis temperatures below 45 °C. In ongoing work, we are investigating the parasitic non-magnetic phase in more detail and evaluate strategies to prevent its formation.

### Acknowledgements

This work was funded within the "Central Innovation Programme for small and medium-sized enterprises" by the Federal Ministry for Economic Affairs and Climate Action of Germany in the frame of project "NanoTherMag" (16KNO8133) and was supported by the "Thüringer Innovationszentrum für Medizintechnik-Lösungen (THIMEDOP; FKZ IZN 2018 0002)". Funding by the DFG via the CRC/TRR 247 (ID 388390466, Project B2) is acknowledged.

## COLLOIDAL MICROCAPSULES FABRICATED FROM PICKERING DROPLETS USING ALTERNATING MAGNETIC FIELDS

Rafał Bielski\*, Bassam Jamnejel and Arkadiusz Józefczak

Chair of Acoustics, Faculty of Physics, Adam Mickiewicz University in Poznań  
Uniwersytetu Poznańskiego 2, 61-614 Poznań, Poland

\*e-mail: rafal.bielski@amu.edu.pl

During recent decades, the ability of magnetic particles to generate heat when exposed to alternating magnetic fields has been studied intensively, primarily because of its potential use in magnetic hyperthermia therapy. The temperature elevation in a magnetic material is caused by the magnetic relaxation and hysteresis losses and depends on the size of particles, their mass concentration as well as the arrangement of particles. For instance, in Pickering droplets where magnetic particles are attached to the droplet surface, the heating efficiency was worse for a more dense particle shell [1]. By using proper particles it is possible to obtain a temperature high enough to partially sinter thermo-responsive particles (e.g., polymer particles) that makes the particle shell around the droplets more rigid. In this manner, the microcapsules are prepared from Pickering droplets (Fig. 1a). What is more, in this approach the capsules can be inherently responsive to the external magnetic fields which is crucial when it comes to their applications in targeted therapies.

Here, we will show the proof-of-concept results for fabricating microcapsules with polymer shells from oil-in-oil Pickering droplets used as precursors. The stable Pickering droplets were prepared via ultrasound homogenization and electrocoagulation. Then, such droplets were exposed to high-frequency alternating magnetic fields. The improved rigidity of the capsule shell after the exposition to high-temperature increase was tested under electric heating, the shells were much more resistant to the applied electric stress [2]. For the fabrication of capsules in bulk quantities more efficient techniques of controlling successful capsulation should be developed and one of the potential approaches is to use a non-destructive ultrasound testing.

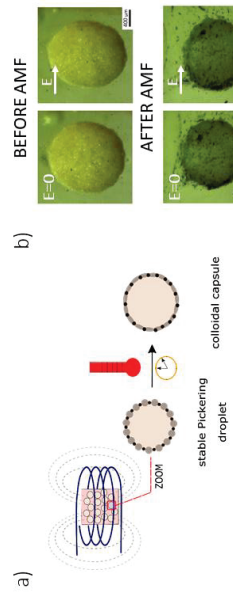


**FIG. 1 (a)** The scheme of the formation of magnetic colloidal capsules from Pickering droplets as templates.  
**(b)** The optical microscopy imaging of such capsules before and after the application of alternating magnetic field (AMF).

### References

- [1] R. Bielski, T. Horowski, K. Paulovičová, M. Raňák, A. Józefczak, The effect of magnetic particles covering the droplets on the heating rate of Pickering emulsions in the AC magnetic field, *Journal of Molecular Liquids*, 2020, 320, 114388.
- [2] R. Bielski, D. Surdeko, K. Kaczmarek, A. Józefczak, The potential of magnetic heating for fabricating Pickering-emulsion-based capsules, *Colloids and Surfaces B: Biointerfaces*, 2020, 192, 111070.

### Acknowledgments

This work was supported by the project no. 2019/35/N/ST5/00402 (PRELUDIUM) of the Polish National Science Centre.

## STEM cells carriers of Fe-Cr-Nb-B ferromagnetic particles for cancer cell destruction by magneto-mechanical actuation

H. Chiriac<sup>a\*</sup>, A. Minutu<sup>b,2</sup>, C. Stavila<sup>b,2</sup>, L. Labusca<sup>b</sup>, D.-D. Heraea<sup>b</sup>, N. Lupu<sup>b</sup>

<sup>a</sup> National Institute of Research and Development for Technical Physics, Iasi 700050, Romania

<sup>b</sup> Faculty of Physics, "Alexandru Ioan Cuza" University, Iasi 700056, Romania

\*E-mail: [leliniac@phys-fisi.ro](mailto:leliniac@phys-fisi.ro)

Magnetic particles (MPs) can be used in different cancer treatment applications, such as magnetic hyperthermia, magnetic controlled delivery and release of antitumoral drugs at the targeted site of a tumor, or through magneto-mechanical actuation.

Recently, we have introduced a new type of magnetic particles (MPs) for cancer treatment by magneto-mechanical actuation (MMA) [1]. The rectangular shapes of the milled MPs and superferromagnetism of the glassy ribbons of which they are made induce important magnetic shape anisotropies which, along with a large saturation magnetization, generate an improved torque in a rotating magnetic field, producing important damages on the cellular viability of tumor cells. In this work we studied the possibility of transporting Fe-Cr-Nb-B MPs to areas with cancer cells (human osteosarcoma - HOS), using adipose-derived stem cells (ADSC) as carriers, considering their tumor-targeting capacity [2], and the MPs-mediated magneto-mechanical effect on HOS viability.

The Fe-Cr-Nb-B MPs were used to obtain a ferrofluid which was added with cell culture media in the cell cultures. Then, HOS and ADSC cells were incubated for 24h with the MPs, and a specific cellular viability assay MTT was performed. No cytotoxic effect was observed while the MPs upload by HOS was confirmed using TEM. By using a "wound healing" model, the migration of ADSC, both loaded and unloaded with MPs, was recorded by time-lapse imaging. The recorded films showed that ADSC were able to easily target osteosarcoma cells. The traveled distance of MPs-loaded ADSC is twice the length of the MPs-free ADSC, due to the higher metabolism of the loaded cells induced by the presence of iron (Figure 1a). Magneto-mechanical actuation led to the destruction of ADSC and to the release of MPs on HOS cells, the latter incorporating the released MPs, further leading to the destruction of 80% of HOS cells (Figure 1b).

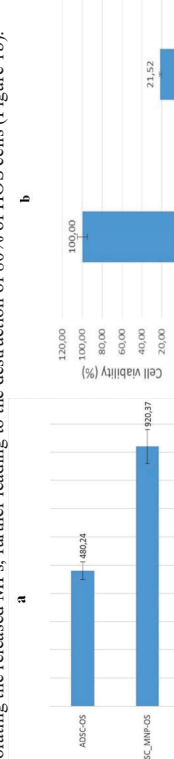


Figure 1. (a) *In vitro* cell migration of ADSC loaded and non-loaded, respectively, with MPs towards tumor cells. (b) Cell viability of HOS and ADSC cell, controls and cells with MPs after MM actuation.

In conclusion, after checking for the biocompatibility of Fe-Cr-Nb-B magnetic particles (MPs), we have shown that MPs were successfully incorporated by ADSC and HOS cells and MPs-loaded ADSCs displayed increased motility towards tumor cells, compared with their unloaded counterparts. The magneto-mechanical actuation led to the release of the MPs towards tumor cells, the latter being destroyed in high proportion (about 80%) by immediate application of MMA.

**Acknowledgements:** Work supported by UEFISCDI under contract no. PCE20/2021 (PN-II-RP4-ID-PCE-2020-2-381).

- [1] H. Chiriac et al., "Fe-Cr-Nb-B ferromagnetic particles with shape anisotropy for cancer cell destruction by magneto-mechanical actuation", *Sci. Rep.* 8 (2018) 11538.
- [2] M.G. Sciolari et al. "Adipose-derived stem cells in cancer progression: new perspectives and opportunities", *Int. J. Mol. Sci.* 20(13) (2019) 3296.

## Ferromagnetic drug loaded biodegradable nanocapsules for externally controlled and non-invasively monitored nanotherapies.

A. Lafuente<sup>a\*</sup>, Z. Li<sup>1</sup>, A. Fluckerman<sup>2</sup>, A.G. Roca<sup>1</sup>, J.Nogues<sup>1</sup>, O. Benny<sup>2</sup>, B Sepulveda<sup>3</sup>.

<sup>1</sup> Catalan Institute of Nanoscience and Nanotechnology (ICN2), Bellaterra, Spain

<sup>2</sup> Institute for Drug Research, The Hebrew University of Jerusalem, Jerusalem, Israel

<sup>3</sup> Institut de Microelectrònica de Barcelona (IMB-CNM, CSIC), Bellaterra, Spain

\*email: [artiz.lafuente@icn2.cat](mailto:artiz.lafuente@icn2.cat)

Cancer nanotherapies based on drug-loaded nanoparticles require new tools to locally enhance their efficacy. This critical need could be achieved by nanomaterials enabling external control of the accumulation and non-invasive visualization and detection of the therapeutic action. Here we present novel magnetoplasmonic drug loaded biodegradable nanocapsules based on metallic iron semishells (MAPSULES) merging highly efficient external actuation with magnetic fields and near infrared light to locally boost the therapeutic action[1,2].

The MAPSULES are engineered by a combination of bottom-up and top-down techniques. Briefly, monodisperse drug loaded poly-lactic-co-glycolic-acid (PLGA) cores of around 150 nm, fabricated by nanoprecipitation, are partially coated by Fe/X ( $X=SiO_2$ , Au, Ti) by combining colloidal self-assembly and physical vapour deposition. The outer layer can be tuned to exploit different effects such as X-ray imaging or enhanced photothermal efficiency.

The MAPSULES exhibit ferromagnetic vortex configuration (i.e., zero net magnetic moment at zero field), which allows high colloidal stability and strong magnetic manipulation. The magnetophoretic forces are ca. 1000-fold larger than in superparamagnetic iron oxide nanoparticles. The nanocapsules exhibit very intense  $I_2$  relaxivity (370 mM $\cdot$ s $^{-1}$ ) in magnetic resonance imaging, i.e., much higher than commercial iron oxide contrast agents. The metal Fe semishell exhibits highly damped plasmonic behavior with intense broadband absorbance in the near infrared (NIR), which allows excellent photothermal conversion efficiencies in the 1st and 2nd biological windows.

This combination of properties allows the nanocapsules to operate as nanothermometers and monitor the induced temperature increase by laser heating as well as follow the carrier degradation through optical spectroscopy or NMR imaging, enabling the external and non-invasive control of the therapy.

Remarkably, the MAPSULES show very low *in vitro* and *in vivo* toxicity and promising therapeutic effect even at low doses due to the combined magnetic accumulation, photothermal and chemotherapeutic effects.

## References

[1] Z. Li, et al. *Appl. Mater. Today* **12**, 430 (2018)

[2] Z. Li, et al. *Small* **14**, 1800868 (2018).

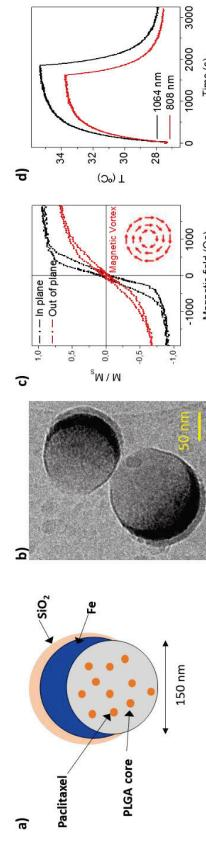


Figure 2. (a) Schematic of the drug loaded ferromagnetic nanocapsules components and their functionalities. (b) TEM images of the ferromagnetic nanocapsules. (c) In plane and out-of-plane magnetization loops showing the ferromagnetic behaviour, the magnetic anisotropy and the vortex magnetic structure (inset image shows a schematic magnetic vortex configuration). (d) Demonstration of the efficient optical heating in the first and second biological windows.

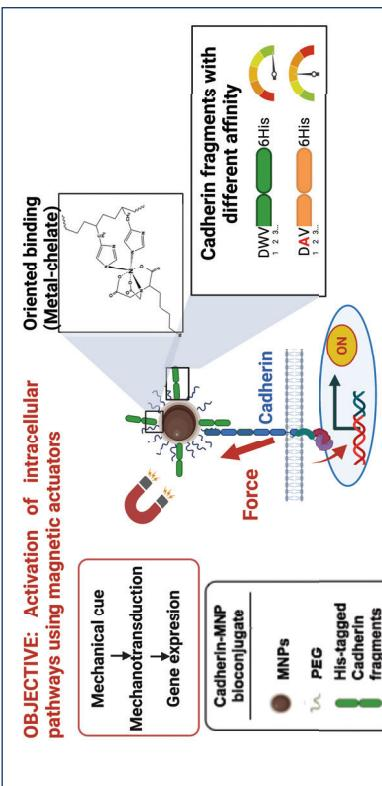
## Oriented immobilization of cadherin fragments on magnetic nanoparticles as a novel magneto-mechanical cell actuators

C. Castro-Hinojosa<sup>1</sup>, S. Del Sol-Fernández<sup>1</sup>, P. Martínez-Vicente<sup>1</sup>, P. Gomollón-Zueco<sup>1</sup>, Jesús G. Ovejero<sup>2</sup>, Jesús Martínez de la Fuente<sup>1,3</sup>, Raluca M. Fratila<sup>1,3</sup>, María Moros<sup>1,3</sup>  
<sup>1</sup>Instituto de Nanociencia y Materiales de Aragón (INMA), CSIC-Universidad de Zaragoza, Zaragoza, Spain, <sup>2</sup>Instituto de Ciencia de Materiales de Madrid (ICMM), Madrid, Spain, <sup>3</sup>Centro de Investigación Biomédica en Red de Bioingeniería, Biomateriales y Nanomedicina (CIBER-BBN), Spain  
manoros@unizar.es

Magnetic nanoparticles (MNPs) can be used in a multitude of applications in the field of nanomedicine due to their unique characteristics. Among them, their ability to generate heat or tensile forces when manipulated by external magnetic fields are highly interesting. The forces generated by the remote stimulation of the MNPs can be harnessed to convert the MNPs in mechanostimulation platforms, able to exert forces directly on the cell membranes. By targeting receptors that convert mechanical stimuli into biochemical signals (mechanotransduction), MNPs could be used to activate intracellular pathways in a controlled way.<sup>1</sup> In this context, mechanotransduction can take place in the adherent junctions, which relies on the role of E-cadherin. In fact, E-cadherin mechanotransduction is critical to mediate collective epithelial remodelling that takes place during tissue repair. Functionalizing MNPs with cadherins would allow to attach the nanomaterials to the cadherins on the cell membrane in an orientation-dependent manner, prior to an external magnetic stimulation that could be used to activate intracellular pathways implicated in regeneration processes.

In the present work we generated different fragments of E-cadherin, composed of the first two extracellular domains, which are enough to establish stable nonpolar interactions with the cadherins present on the cellular membrane. We used the *wild type* E-cadherin recombinant fragment, and two E-cadherin mutants generated by site directed mutagenesis, in order to control the binding affinity. The cadherin fragments were modified with a histidine tag (His-Tag) at the C-terminus to allow their oriented attachment via metal-chelate affinity to the MNPs. 15-nm iron oxide MNPs were grafted with polyethylene glycol (PEG) and functionalized with a nitrotriacetic acid derivative (NTA), a molecule able to chelate metal ions like  $\text{Ni}^{2+}$  or  $\text{Co}^{2+}$ . Then, His-tagged cadherin fragments were bound in an oriented fashion to the MNPs, controlling at the same time the number of proteins/MNP. In order to use the MNPs as potential cellular mechanostimulators, besides controlling the number and orientation of cadherins over the MNPs surface, the strength of the union protein-MNP surface is another crucial step. Thus, we stabilized these links to reach a higher union strength, through two different strategies.

Finally, we immobilized the E-cadherin-MNPs on membrane of living cells that express E-cadherin. The selective binding of the MNPs functionalized with the *wild type* fragment on cells was assessed, while MNPs functionalized with E-cadherin mutants did not bind to them. This is the first step towards the selective activation of intracellular pathways linked to cadherins using MNPs.



## Magnetic hyperthermia as a combinatorial tool to develop new therapies against cancer

Giulia Eugenia Paola Nucci<sup>1,2\*</sup>, Teresa Pellegrino<sup>1\*</sup>

<sup>1</sup> Nanomaterials for Biomedical Applications Department, Istituto Italiano di Tecnologia (IIT), via Morego 30, 16163 Genoa, Italy  
<sup>2</sup> Dipartimento di Chimica e Chimica Industriale, Università di Genova, Via Bodeganoso 31, 16146 Genoa, Italy  
\*Email: giulia.nucci@iit.it, teresa.pellegrino@iit.it

In the last decades, magnetic nanoparticles (MNPs) have been widely investigated in the field of cancer therapy. Among their several applications, MNPs have shown a great potential in magnetic hyperthermia treatment (MHT), an adjuvant tumor therapy now undergoing clinical trials. The therapeutic effects provided by MNPs in MHT are based on their ability to heat up at therapeutic relevant temperatures (40–45°C) at the tumor site when exposed to an alternating magnetic field (AMF). This leads to apoptotic and necrotic processes of cancer cells.<sup>1,2</sup> To improve the antitumor therapeutic effect of MNPs-based MHT, combinatorial strategies with drug delivery, immunotherapy, photothermal, and radiotherapy, are exploited.<sup>3,4</sup> In particular, MHT can trigger the release of chemotherapeutic drugs at the tumor site or boost immune system response against tumoral cells.

In this regard, here, we present two approaches. In a first strategy, an electrospun polycaprolactone (PCL) fiber mat was co-loaded with iron oxide nanoclusters (IONCs) and doxorubicin (DOXO), and the resulted platform was exploited as a scaffold to combine MHT with the heat-mediated delivery of the anti-cancer drug (Figure 1A).<sup>5</sup> Thanks to the outstanding heating properties of the scaffold, which allow to reach the therapeutic temperature (45°C) and to induce the subsequent DOXO release, we were able to use a lower dose of the drug than that administered intravenously. Moreover, this significant cytotoxic effect against the DOXO sensitive HeLa cell line was reached under clinical conditions for MHT. In the other strategy, MHT was used in combination with immunotherapy (Figure 1B). In our group, indeed, we have demonstrated that MHT at 43°C performed on Glioblastoma cancer cells (U87 cell line) can induce the upregulation of specific stress ligands on U87 cells, making them more susceptible to macrophages and NK cell killing.<sup>6</sup> This study suggests the possible use of MHT with MNPs as a tool to remotely switch on the immune response at the tumor by mild temperature increase, thus providing full-body coverage.

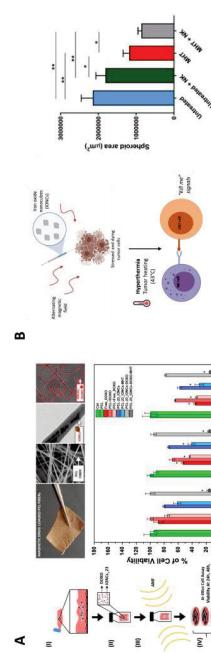


Figure 1: (A) MHT in combination with controlled drug release. The scheme of the experiment and the viability of HeLa cells after MHT combined with DOXO are shown. Stars show statistically significant differences compared with control, CTRL ( $N = 3$ ; \* $p < 0.05$ ; one-way ANOVA). (B) MHT in combination with immunotherapy. The sketch of the experimental procedure and the evaluation of the susceptibility of MHT-treated U87 cells to NK-cell-mediated killing are shown. Statistical analysis was performed using a one-way ANOVA test (\* $p < 0.01$ ; \*\* $p < 0.001$ ; \*\*\* $p < 0.0001$ ).

- References: 1-Del Sol-Fernández, S., et al. Magnetogenetics: remote activation of cellular functions triggered by magnetic switches. *Nanoscale*, 2021, 14, 2091–2118  
Funding: SIRocco has received funding from the European Research Council (ERC) under the European Union's Horizon 2020 research and innovation programme (grant agreement 853468)

## Dendronized Iron Oxide Nanoparticles used as theragnostic agents for breast cancer treatment

Maria de los Ángeles Ramírez<sup>1\*</sup>, Barbara Freis<sup>1</sup>, Thomas Gevaert<sup>2</sup>, Céline Henoumont<sup>2</sup>, Sophie Laurent<sup>2</sup>, Sophia Sarapaki<sup>3</sup>, Thodoris Karampelas<sup>3</sup>, Panagiotis Papadimitriou<sup>3</sup>, Sylvie Beguin Colin<sup>1</sup>

\* Email: maria.ramirez@ipoms.unistra.fr

<sup>1</sup> Université de Strasbourg, CNRS, Institut de Physique et Chimie des Matériaux de Strasbourg, UMR 7504, F-67000 Strasbourg, France

<sup>2</sup> University of Mons, General, Organic and Biomedical Chemistry Group, Mons, Belgium

<sup>3</sup> BIOMETECH, Athens, Greece

Among females, breast cancer is the most diagnosed cancer and the leading cause of cancer death<sup>1</sup>.

There is a strong need of new treatments without side effects<sup>2</sup>. In nanomedicine, the goal is to develop multimodal nanoparticles (NPs) to speed up targeted diagnosis, to increase its sensitivity, reliability and specificity for a better management of the disease (patient's care), and to treat the disease in a specific personalized manner in feedback mode. Combination of therapies to target individual cancer-specific vulnerabilities is a way to increase the efficacy of anticancer treatment. Therefore, besides precision diagnosis, challenges for personalized nanomedicine are to develop multifunctional theragnostic nanoplatforms to be able to target specifically tumoral cells, to test quickly different treatments and to follow-up the effect(s) of the treatment(s) of the disease by imaging. The selective accumulation of NPs in diseased organs to enable precise diagnosis and targeted therapy remains also an important issue. Most of developed NPs accumulate, after intravenous injection, in eliminating organs and only low amounts are seen accumulating in tumors. For a precise treatment, active targeting with affinity ligands to achieve tumor specificity is crucial. Among NPs developed for nanomedicine, superparamagnetic iron oxide nanoparticles (IONPs) are promising as they may be designed to respond to magnetic fields, to enable multimodal therapy. Indeed, besides being excellent T2 contrast agents for MRI, IONPs are promising as therapeutic agents by hyperthermia when suitably designed.

In that context, we developed IONPs coated with an original dendron molecule, which have been demonstrated in several *in vitro* and *in vivo* studies to display antifouling properties (no strong RES accumulation). With their favorable biodistribution and bioelimination profile, dendronized NPs (DNP<sup>s</sup>) are very well adapted for investigating affinity targeting. Thus, we have studied the targeting of breast cancer cells by coupling selected targeting ligands on DNP<sup>s</sup>' surface. We have chosen peptides with high affinity for specific membrane proteins overexpressed particularly in these cancer cell lines: MDA-MB-231 and MCF-7. The coupling method of targeting ligands and their grafting yield were important issues to face. We succeeded in establishing a reproducible method for the coupling of the targeting ligands and for the quantification of their amount at the surface of DNP<sup>s</sup>. These DNP<sup>s</sup> coupled with targeting ligands were shown to internalize in cell lines, when without targeting ligand the internalization amount was quite low. Additionally, we conjugated chelating agents (CA), with this approach an radioisotope was successfully loaded. We have thus followed their biodistribution *in vivo* by molecular imaging techniques like PET and SPECT.

**Acknowledgement:** The authors thank UCL-A\*STAR for the PhD studentship

### References:

- [1] S. Kumar, N. Sharma and S. V. Sahi, *Pharmaceutics*, 2021, **13**, 1174.
- [2] X. Liu, Y. Zhang, Y. Wang, W. Zhu, G. Li, X. Ma, Y. Zhang, S. Chen, S. Tiwari, K. Shi, S. Zhang, H. M. Fan, Y. X. Zhao and X.-J. Lian, *Theranostics*, 2020, **10**(9), 3793-3815.
- [3] C. Chen, L. Kuo, S. Lee, Y. Hwu, S. Chou, C. Chen, F. Chang, K. Lin, D. Tsai and Y. Chen, *Biomaterials*, 2013, **34**(4), 1128-1134.
- [4] A. López-Ortega, M. Estrader, G. Sáizar-Alvarez, A. Roca and J. Nogués, *Physics Reports*, 2015, **553**, 1-32.
- [5] G. Lerebaancic, *Lang. Sensors*, 2013, **13**(8), 1038-10369.
- [6] S. Chou, P. Wu, Y. Yang, D. Sheih and C. Chen, *J. Am. Chem. Soc.*, 2010, **132**, 13270-13278.
- [7] M. Chen, S. Yamamoto, D. Farrell and S. Majetich, *J. Appl. Phys.*, 2003, **93**, 7551-7553.
- [8] H. Gavilán, S. Avugadda, T. Fernández-Zabala, N. Soni, M. Cassani, B. Mai, R. Chantrell and T. Pellegrino, *Chem. Soc. Rev.*, 2021, **50**, 1161-4-11667.
- [9] B. Mehdaoui, A. Meffre, L. Lacroix, J. Carey, S. Lachaise, M. Goiguen, M. Repaud and B. Clauquet, *J. Magn. Magn. Mater.*, 2010, **322**(19), L49-L52.
- [10] S. Noh, W. Na, J. Jang, J. Lee, E. Lee, S. Moon, Y. Lim, J. Shin and J. Cheon, *Nano letters*, 2012, **12**(7), 3716-3721.



Figure 1: DNP: iron oxide nanoparticle with dendron on the surface and functionalized with Tl and CA  
This project received funding from ANR (EURO-NOME D20-121 - THERAGET) under the umbrella of the ERA-Net+ EuroNanoMed (GA N°773370 of the EU Horizon 2020 Research and Innovation).

- (1) Sung, H.; Ferlay, J.; Siegel, R. L.; Laversanne, M.; Soerjomataram, I.; Jemal, A.; Bray, F. Global Cancer Statistics 2020: GLOBOCAN Estimates of Incidence and Mortality Worldwide for 36 Cancers in 185 Countries. *Cancer Journal for Clinicians*, 2021, **71**(3), 1087-1107.
- (2) Alparaghali, H. G. J.; Kashanian, S.; Rafipour, R. A Review on Targeting Nanoparticles for Breast Cancer. *Curr Pharm Biotechnol*, 2019, **20**(13), 1087-1095.

## Using Magnetic Torques to Enhance Tumor Infiltration of Cargo-Carrying Magnetotactic Bacteria

Timotenda Gwisi,<sup>1</sup> Nima Mirkhani,<sup>1</sup> Michael G. Christiansen,<sup>1</sup> Thuy Trinh Nguyen,<sup>1</sup> Vincent Ling,<sup>2</sup>

Simone Schuerle<sup>1\*</sup>

<sup>1</sup>Department of Health Sciences and Technology Institute for Translational Medicine, ETH Zurich, CH-8092 Zurich, Switzerland

<sup>2</sup>Takeda Pharmaceuticals, 40 Lansdowne St., Cambridge MA 02139, USA.

Email: simone.schuerle@hest.ethz.ch

Tumor-targeting bacteria are appealing therapeutic vectors because of their capacity to produce or transport a wide range of payloads and their ability to modulate an intratumoral inflammatory response. Nevertheless, translation of this approach has been hindered by difficulties in achieving sufficient tumor colonization. Developing strategies to enhance accumulation at the target site is essential for facilitating robust colonization, while concurrently decreasing the required initial dose and associated toxicity.

Recently, magnetotactic bacteria (MTB), which biomineralize magnetite-based nanocrystals, have been manipulated with external magnetic fields as guidable drug carriers. Thus far, control strategies have either relied on poorly scalable magnetic field gradients that diminish rapidly with increasing distance from their source, or have employed directing magnetic fields with propulsive forces limited by the bacterial motor. Here, we employ a magnetic torque-driven actuation scheme based on rotating magnetic fields (RMF) to wirelessly control *Magnetospirillum magneticum* AMB-1 bearing versatile liposomal cargo.

By studying extravasation with computational models (Fig. 1A) and *in vitro* (Fig. 1B), we find that the main mechanism driving the enhancement of translocation is increased surface exploration resulting from torque-driven translational motion at the cell interface. We then assess the spatiotemporal characteristics of MTB infiltration and find that fluorescently labelled bacteria colonize core regions in 3D tumor models, with 9.9-fold higher signal in samples exposed to RMF (Fig. 1C). Finally, to better recapitulate *in vivo* conditions, we study magnetically-enhanced penetration of MTB in a microfluidic chip containing spheroids embedded in a collagen matrix (Fig. 1C). Overall, our findings suggest that scalable control strategies that harness magnetic torque-driven motion and autonomous taxis-based locomotion can be leveraged advantageously for improved targeting and colonization of living therapeutics in tumors.

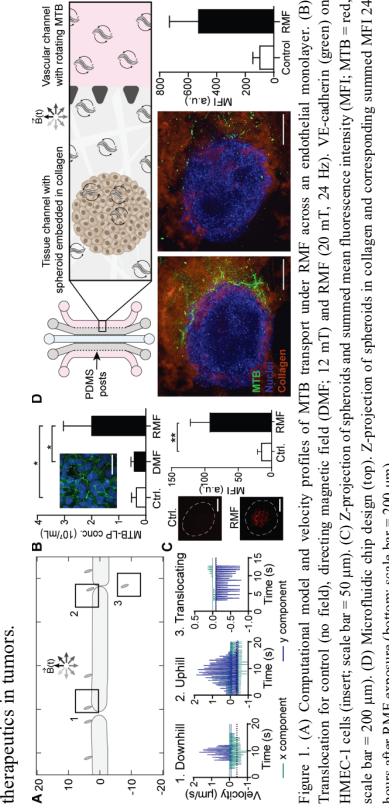


Figure 1: (A) Computational model and velocity profiles of MTB transport under RMF across an endothelial monolayer. (B) Translocation for control (no field), direct magnetic field (DMF; 12 mT) and RMF (20 mT, 24 Hz). (C) Z-projection of spheroids and summed mean fluorescence intensity (MFI; MTB = red). (D) Microfluidic chip design (top) Z-projection of spheroids in collagen and corresponding summed MFI 24 hours after RMF exposure (bottom; scale bar = 200  $\mu$ m).

## Poly-histidine functionalized $\gamma$ -Fe<sub>2</sub>O<sub>3</sub>@SiO<sub>2</sub> nanoparticles to access the cell cytoplasm

Mathilde Le Jeune, Mélody Perret, Jean-Michel Siaugue, Fabienne Burlina, Christine Ménager,  
Emilie Secret  
email : emilie.secret@is Sorbonne université.fr

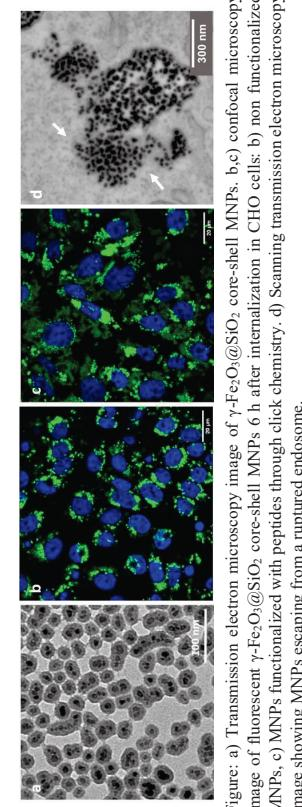
Physico-chimie des Électrolytes et Nanosystèmes Interfaciaux, PHENIX, Sorbonne Université, CNRS, F-

75005 Paris, France

Laboratoire des Biomolécules, LBM, Sorbonne Université, CNRS, F-75005 Paris, France

Magnetic nanoparticles (MNPs), as any other type of nanoparticles, are internalized by cells through endocytosis, and thus are trapped in intracellular vesicles called endosomes<sup>[1]</sup>. But for a number of bio-applications, such as cellular engineering or magnetic hyperthermia treatments, it can be of great interest to have particles able to reach the cell cytoplasm. This would allow to have less dipolar interactions between the MNPs, and hence increase their intracellular heating properties<sup>[2]</sup>. It would also enable the possible diffusion of the MNPs in the cytosol and the targeting of specific intracellular proteins of organelles, which would open the door to intracellular engineering with MNPs<sup>[3,4]</sup>.

In this study, we studied the effect of the functionalization of  $\gamma$ -Fe<sub>2</sub>O<sub>3</sub>@SiO<sub>2</sub> core-shell nanoparticles with poly-histidine moieties through two types of functionalization: a permanent bound made by strain-promoted azide-alkyne cycloaddition (SPAAC) or an intracellularly labile disulfide link. After careful characterization of the functionalized MNPs, we showed, by means of confocal microscopy and transmission electron microscopy, that the poly-histidine peptide promoted cytosol access to the MNPs probably through the proton sponge effect<sup>[5]</sup>. In the case of the disulfide bound, the peptide was cleaved from the surface of the MNPs thanks to intracellular glutathione, decreasing the possible interactions between the MNPs and the intracellular membranes.



References:

- [1] Conner and Schmidt, Nature (2003) 422, 692-7, 37-44, [2] Di Corato et al., Biomaterials (2014) 35, 6400-6411, [3] Schöneborn et al., Journal of Functional Biomaterials (2019) 10, 3, 32, [4] Raudzus et al., Scientific Reports (2020) 10, 1, [5] Le Jeune et al., ACS Applied Materials and Interfaces, accepted (2022), doi.org/10.1021/acsami.2c01346.

## Optimal particles for highly sensitive biosensing application in mixed frequency excitation: Insights from a fundamental simulative approach

Ulrich M. Engelmann<sup>1,\*</sup>, Ahmed Shalaby<sup>1</sup>, and Hans-Joachim Krause<sup>2,3</sup>

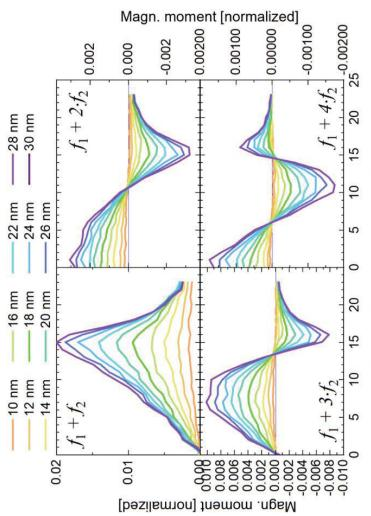
<sup>1</sup>Department of Medical Engineering and Applied Mathematics, FH Aachen University of Applied Sciences, Jülich, Germany  
<sup>2</sup>Institute of Biological Information Processing – Biocertronics (IBI-3), Forschungszentrum Jülich, Jülich, Germany  
<sup>3</sup>Institute of Nano- and Biotechnologies (INB), FH Aachen University of Applied Sciences, 52428 Jülich, Germany

\*Correspondence: [uegelmann@fh-aachen.de](mailto:uegelmann@fh-aachen.de) (U.M.E.)

Magnetic nanoparticles (MNP) are widely investigated for biomedical applications in diagnostics (e.g., imaging), therapeutics (e.g., hyperthermia) and general biosensing. For all these applications, the MNPs' unique magnetic relaxation mechanism in an alternating magnetic field (AFM) is stimulated to induce desired effects. Whereas magnetic fluid hyperthermia (MFH) and magnetic particle imaging (MPI) are the most prominent examples for biomedical application, we investigate the relatively new biosensing application of frequency mixing magnetic detection (FMMMD) from a fundamental perspective. Generally, we ask how specific MNP parameters (core size, magnetic anisotropy) influence the signal, specifically we predict the most effective MNP core size for signal generation.

In FMMMD, simultaneously two AFM are applied: a low-frequency magnetic driving field, driving MNP close to saturation, and a high-frequency excitation field that probes MNP susceptibility:  $H(t) = H_0 + H_1 \sin(2\pi f_1 t) + H_2 \sin(2\pi f_2 t)$ . Resulting from the nonlinear magnetization of the MNP, harmonics of both individual incident frequencies as well as intermodulation products of these frequencies are generated. In this work, we present numerical Monte-Carlo(MC)-based simulations of the MNP relaxation process, solving the Landau-Lifshitz-Gilbert (LLG) equation to predict FMMMD signals:  $\frac{d\mathbf{m}_p}{dt} = \frac{\mu_0 Y}{1+\alpha^2} \cdot (\mathbf{H}_{\text{eff}} \times \mathbf{m}_p + \alpha \mathbf{m}_p \times (\mathbf{H}_{\text{eff}} \times \mathbf{m}_p))$ . Details on the method can be found in [1].

As Figure 1 shows for the first four intermodulation signals  $f_1 + n \cdot f_2$ , with  $n = 1, 2, 3, 4$ , we can clearly see that larger core sizes generally increase the signal intensity. Same trend is predicted by a simple Langevin-function based thermal equilibrium model. Both predictions include a lognormal size distribution. The effect of core size distribution presumably dominates the effect of magnetic anisotropy. The findings are supported by comparison with experimental data and help to identify which MNP are best suited for magnetic biosensing applications using FMMMD.



Reference:  
[1] Eigelmann, U.M.; Shalaby, A.; Shasha, C.; Krishnan, K.M.; Krause, H.-J. Comparative Modeling of Frequency Mixing Particles of Magnetic Nanoparticles Using Micromagnetic Simulations and Langevin Theory. *Nanomaterials* 2021, 11, 1257. <https://doi.org/10.3390/nano11051257>

## Optimizing virus detection with magnetic nanoparticles

Tamara Kahmann<sup>1,\*</sup>, Aidin Lak<sup>1</sup>, Thilo Viereck<sup>1</sup>, Meinhard Schilling<sup>1</sup> and Frank Ludwig<sup>1</sup>

<sup>1</sup>Institute for Electrical Measurement Science and Fundamental Electrical Engineering and Laboratory for Emerging Nanometrology (LENA), TU Braunschweig, Braunschweig D-38106, Germany  
\*Email: tamara.kahmann@tu-bs.de

The COVID-19 pandemic highlighted the need for reliable virus detection methods. Homogenous immunoassays with magnetic nanoparticles (MNPs) as markers offer a highly sensitive, rapid, easy-to-use and quantitative detection concept in combination with magnetic particle spectroscopy (MPS) or ac susceptometry (ACS) measurements. Wu et al. [1] detected the spike and nucleocapsid protein of the SARS-CoV-2 virus in MPS measurements. Zhong et al. [2] proved the use of magnetic measurement techniques for the detection of the whole virus by mimicking the virus via streptavidin coated polystyrene beads surrounded with biotinylated spike proteins. In these studies, a limit of detection (LOD) around  $10^9 - 10^{10}$  viruses/ml (v/ml) [1,2] is achieved, but still not sensitive enough for infective persons with low virus load. Beyond the LOD, the binding rate between MNPs and virus defines the success of the detection scheme. For magnetic immunoassays to compete with other nanotechnology-based platforms, several critical parameters have to be identified and understood.

In this study, we systematically investigate the influence of parameters such as particle and antibody concentration, mono vs. polyclonal antibodies, incubation temperature, and mechanical agitation on the binding kinetics and efficiency. We focus on the detection of mimic virus with Protein A coated MNPs and antibody functionalization against the SARS-CoV-2 spike protein through MPS and ACS measurements. The binding of antibodies to the mimic virus increases the particle's hydrodynamic diameter, which changes the magnetization response to an alternating magnetic field. We observe a systematic broadening of the Brownian relaxation peak of the imaginary part of the complex susceptibility  $\chi''$  at low virus concentrations, indicating a successful binding. Adding more viruses leads to the emergence of a second relaxation peak shifting gradually from 10 Hz towards 1 Hz (Figure 1). We will discuss how to further improve the LOD by considering carefully the influence of all parameters.

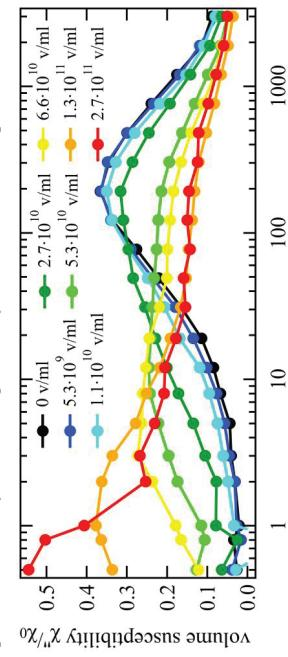


Figure 1: ACS spectrum of the normalized imaginary part of the magnetic susceptibility over frequency. Each color represents a different virus concentration (in viruses per ml). With increasing virus concentration, a broadening of the maximum of the imaginary part and a shift to lower frequencies is measured.  
[1] K. Wu, V. K. Chugh, V. D. Krishna, A. di Girolamo, Y. A. Wang, R. Saha, S. Liang, M. C.-J. Cheeरan and J.-P. Wang, ACS Appl. Mater. Interfaces 13, 37, 44136–44146 (2021)  
[2] J. Zhong, E. L. Rosch, T. Viereck, M. Schilling and F. Ludwig, ACS Sensors 6 (3), 976–984 (2021)

## Point-of-need detection of pathogen-specific nucleic acid targets using magnetic particle spectroscopy

Enja Laureen Rosch<sup>1</sup>, Jing Zhong<sup>1</sup>, Aidin Lak<sup>1</sup>, Zhe Liu<sup>2</sup>, Markus Etzkorn<sup>2</sup>, Meinhard Schilling<sup>1</sup>, Frank Ludwig<sup>1</sup>, Thilo Viereck<sup>1</sup> and Birka Lalkens<sup>3</sup>

<sup>1</sup>Institute for Electrical Measurement Science and Fundamental Electrical Engineering and Laboratory for Emerging Nanotechnology (LENA), TU Braunschweig, 38106 Braunschweig, Germany

<sup>2</sup>Institute of Semiconductor Technology and Laboratory for Emerging Nanometrology (LENA), TU Braunschweig, Langer Kamp 6a/b, 38106 Braunschweig, Germany

Email: enja.rosch@tu-brunschweig.de

The pandemic caused by severe acute respiratory syndrome coronavirus 2 (SARS-CoV-2) strongly demonstrates the need for a sensitive, fast and reliable pathogen diagnostics tool. While reverse-transcription polymerase chain reaction (RT-PCR) can detect down to single copies of virus DNA, this comes at high cost, several hours of preparation and evaluation time, need for qualified personnel, and well-equipped laboratories. Here, we present a rapid, easy-to-handle, and cost-efficient diagnostic assay for detection of pathogen-specific nucleic acids based on Magnetic Particle Spectroscopy (MPS). In MPS, magnetic nanoparticles (MNPs) are exposed to alternating magnetic fields. Upon binding to biological targets, the relaxation process of the MNPs changes, which is reflected in the higher harmonics of the MPS spectrum.

In this study, MNPs and polystyrene beads were functionalized with single-stranded (ss)DNA. By the addition of a specific target ssDNA sequence, the particles and beads are crosslinked, resulting in increased particle hydrodynamic size and retarded Brownian relaxation mechanism, causing a decrease of odd higher harmonics in the MPS spectrum (Fig. 1A). To exclude the effect of particle concentration,  $3^{rd}/1^{st}$  harmonics ratio is calculated (Fig. 1B). Our preliminary study shows that ssDNA can be detected in a concentration-dependent manner, providing the means to quantify the results, with a limit of detection of 280 pM (Fig. 1C). We show that not only synthetic DNA with an arbitrary sequence, but also RNA can be detected. In addition, SARS-CoV-2-specific DNA as well as saliva as a sample medium can be used for an accurate assay. Our proof-of-principle experiments demonstrate the potential of MPS-based assays for a reliable and fast diagnostic of pathogens like SARS-CoV-2 in a point-of-need fashion without the need of complex sample preparation.

Here, we present a rapid, easy-to-handle, and cost-efficient diagnostic assay for detection of pathogen-specific nucleic acids based on Magnetic Particle Spectroscopy (MPS). In MPS, magnetic nanoparticles (MNPs) are exposed to alternating magnetic fields. Upon binding to biological targets, the relaxation process of the MNPs changes, which is reflected in the higher harmonics of the MPS spectrum.

In this study, MNPs and polystyrene beads were functionalized with single-stranded (ss)DNA. By the addition of a specific target ssDNA sequence, the particles and beads are crosslinked, resulting in increased particle hydrodynamic size and retarded Brownian relaxation mechanism, causing a decrease of odd higher harmonics in the MPS spectrum (Fig. 1A). To exclude the effect of particle concentration,  $3^{rd}/1^{st}$  harmonics ratio is calculated (Fig. 1B). Our preliminary study shows that ssDNA can be detected in a concentration-dependent manner, providing the means to quantify the results, with a limit of detection of 280 pM (Fig. 1C). We show that not only synthetic DNA with an arbitrary sequence, but also RNA can be detected. In addition, SARS-CoV-2-specific DNA as well as saliva as a sample medium can be used for an accurate assay.

Our proof-of-principle experiments demonstrate the potential of MPS-based assays for a reliable and fast diagnostic of pathogens like SARS-CoV-2 in a point-of-need fashion without the need of complex sample preparation.

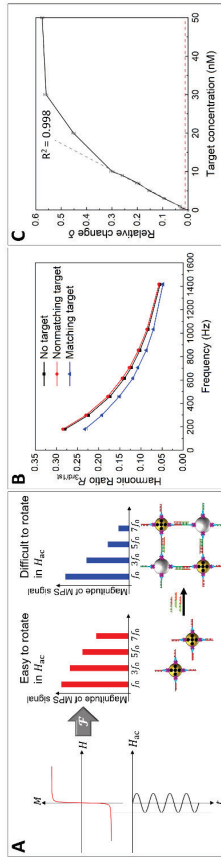


Figure 1 A) Measurement and assay principle of MPS. B) Exemplary result of the harmonic ratio. C) Target concentration dependence of the relative change  $\Delta$  (difference between the measured harmonic ratio with target present and the blank probe).

### Acknowledgement:

This work was supported by the Deutsche Forschungsgemeinschaft (DFG, German Research Foundation) under Germany's Excellence Strategy – EXC-2123 QuantumFrontiers – 390837967, the DFG Research Training Group 1952 Metrology for Complex NanoSystems, Zh 782/-1 and "Niedersächsisches Vorab" through "Quantum- and Nano-Metrology (QUANOMET)" initiative within the projects Nl-1(B1) and Np-2 (TV).

## Ultra-Flexible Giant Magnetoresistance Biosensors for Realtime Monitoring of Tumor Cells:

### Method for Future Lab-on-a-Needle Biosensors

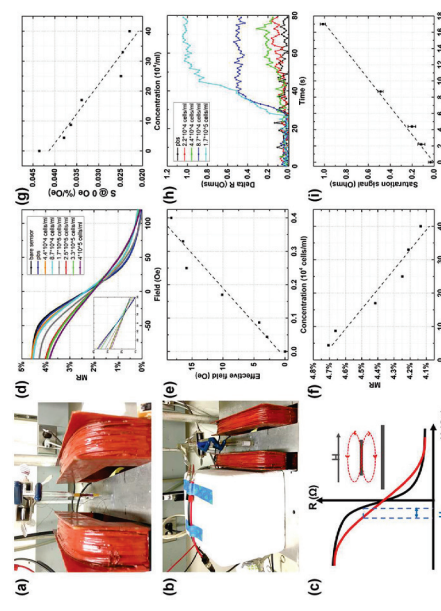
Diqing Su<sup>1</sup>, Kai Wu<sup>2</sup>, Zohreh Nemati<sup>2</sup>, Karthik Srinivasan<sup>2</sup>, Vinit Chugh<sup>2</sup>, Renata Saha<sup>2</sup>, Bethanie Stadler<sup>1,2</sup>, and Jian-Ping Wang<sup>1,2,\*</sup>

<sup>1</sup>Department of Chemical Engineering and Materials Science, University of Minnesota, Minneapolis, MN

<sup>2</sup>Department of Electrical and Computer Engineering, University of Minnesota, Minneapolis, MN

\*Presenter and corresponding author; E-mail: jpwang@umn.edu (J.-P. W.)

Flexible biosensors exhibit great potential for the detection of various biomarkers with the ability to adapt to different surface textures. Here, a lab-on-a-needle biosensing platform based on ultra-flexible giant magnetoresistance (GMR) biosensors is developed for the detection of osteosarcoma cells (OSCA-8) cells (see Fig. (a)-(c)). The fabricated flexible GMR sensors exhibit a MR ratio of 5.2% and a sensitivity of 0.13%/ $\text{o}$  in the linear region, which are comparable to their rigid counterparts. It is found that the magnetic properties of the flexible GMR sensors remain unchanged after 500 cycles of compressive and tensile stress, indicating strong robustness even when applied to a surface that's constantly in motion. The platform's capability in cell detection is validated through the detection of different concentrations of OSCA-8 cells with a LOD of 104 cells/ml, which corresponds to 200 cells in the sample, as shown in Fig. (d)-(i). The ability to perform real-time, sensitive cell detection based on the developed platform makes it possible to realize cell tracking in cell metastasis studies as well as onsite biopsies at potential tumor sites with proper cell recognition bioassays.



(a) Images of the detection setup for bare GMR sensors at 1 mm bending radius.  
 (b) Images of the detection setup for lab-on-a-needle detection within the reaction tube.  
 (c) Schematic illustration of the stray field from the MNWs near sensor surface and the RH loops before (black) and after (red) the addition of Ni-MNW cells.  
 (d) MR response curve of flexible GMR sensors under different cell concentrations. The inset exhibits the response curves within the linear region.  
 (e) Cell concentration dependence of effective field during full-loop measurement.  
 (f) Cell concentration dependence of MR during full-loop measurement.  
 (g) Cell concentration dependence of sensitivity during full-loop measurement.  
 (h) Real-time sensor signal under different concentrations.  
 (i) Calibration curve of the saturation signal at different cell concentrations.

# Understanding the dynamic susceptibility of magnetic nanoplatelet suspensions

M. Rosenberg<sup>1</sup>, S. S. Kantorovich<sup>1</sup>

<sup>1</sup>Computational and Soft Matter Physics Dept., University of Vienna, Austria

Following advances in synthesis techniques, magnetic soft matter research has expanded to increasingly investigate anisotropic and anisometric magnetic colloidal suspensions. The persistent interest in studying and refining anisotropic colloidal systems comes from the knowledge that colloidal anisometry can be used as an effective control parameter to tune both self-assembly scenarios and thermodynamic, rheological and phase behavior of dipolar (magnetic) soft matter[1]. Potential applications for such tailored suspensions include drug delivery[2] and magnetic hyperthermia[3].

One recently prominent example of such a suspension would be that of magnetic nanoplatelets with a dipole oriented perpendicular to the surface, which have recently drawn attention for their potential to form a ferromagnetic nematic phase[4]. This contribution will focus on the computational work to characterise properties such as the static and dynamic magnetic susceptibilities of polydisperse magnetic nanoplatelets, as well as the microstructure of such suspensions. While these properties are well-described by mean-field approaches in conventional moderately concentrated and interacting ferrofluids[5], we see that the interparticle interactions in polydisperse suspensions render the situation significantly more complex.

The influence of spatial crosslinker distribution on the rheological and magnetic properties of magnetic nanogels

Ivan Novikau\*, Sofia Kantorovich

March 28, 2022

It is unknown, how mechanical and rheological properties of micro- and nano-gels depend on their topology. The latter is usually controlled by the distribution of crosslinkers in the gels polymer matrix, by temperature or by quality of the solvent. For directional transport one of the most efficient ways to guide micro- or nanogels is to incorporate magnetic nanoparticles into the gel, creating so-called magnetic micro- or nano-gels(MNGs) and employ magnetic fields.

Using Molecular Dynamics computer simulations with implicit solvent to model coarse-grained representation of an MNG with random crosslinkers under a given spatial distribution we design and investigate four different topologies: uniform, with shifted centre of mass, with Gaussian distribution from the centre to periphery and reverse. In all four cases magnetic particles are distributed uniformly.

In this work we are particularly interested in the combined effects of magnetic field and shear flow mutual orientation and intensity on the MNG magnetorheology depending on their topology. This study allows us to pinpoint the most suitable configurations for drug delivery.  
[DRAFT\*] Example: movie of the simulation

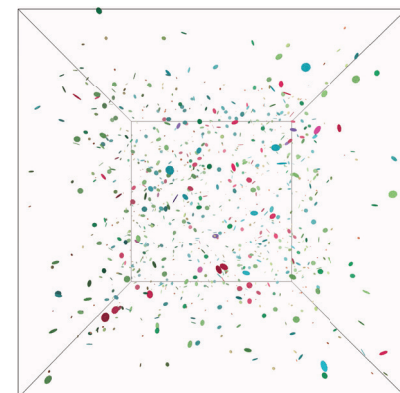


Figure 1: Simulation snapshot of a polydisperse magnetic nanoplatelet simulation.

- References
  - [1] P. Tiemo, Phys. Chem. Chem. Phys., 16, 23515-23528 (2014)
  - [2] K. Ulbrich et al., Chem Rev. 116 (9), 5338-5431 (2016)
  - [3] C. Yang et al., Nanoscale Research Lett. 13, 378 (2018)
  - [4] A. Mertelj, et al., Nature, 504, 237-241 (2013)
  - [5] J. Sindt, P. Camp, S. Kantorovich, et al., Physical Review E, 93 (2016)

## Safety and efficacy assessment of iron oxide nanoparticles intended for magnetic hyperthermia: a translational story

Gary Hannon<sup>1,2</sup>, Sarah Holmes<sup>1,2</sup>, Anna Bogdanska<sup>1,2</sup>, Felista L. Taus<sup>3</sup>, Ingrid Hilger<sup>3</sup>, Zamira V. Diaz Riascos<sup>4,5</sup>, Ibane Abusolo<sup>6,5</sup>, Paul Southern<sup>6,7</sup>, Quentin Pankhurst<sup>6,7</sup>, Nuria Lafuente-Gómez<sup>8</sup>, Yurena Luengo<sup>8</sup>, Gorka Salas<sup>8,9</sup>, Álvaro Somoza<sup>8,9</sup>, Adrielle Prina-Mello<sup>1,2,10</sup>

<sup>1</sup>Nanomedicine and Molecular Imaging Group, Department of Clinical Medicine, Trinity Translational Medicine Institute, Dublin, Ireland

<sup>2</sup>Laboratory of Biological Characterization of Advanced Materials (LBCAM), Trinity Translational Medicine Institute, Trinity College Dublin, Dublin, Ireland

<sup>3</sup>Dept. of Experimental Radiology, Institute of Diagnostic and Interventional Radiology, Jena University Hospital - Friedrich Schiller University Jena, Erlanger Allee 10, 07747 Jena, Germany

<sup>4</sup>Functional Validation & Preclinical Research, Drug Delivery & Targeting Group, Vall Hebron Institut of Research (VHIR), Universitat Autònoma de Barcelona (UAB), Barcelona, Spain

<sup>5</sup>Networking Research Center on Bioengineering, Biomaterials and Nanomedicine (CIBER-BBN), Instituto de Salud Carlos III, 28029 Madrid, Spain.

<sup>6</sup>Resonant Circuits Limited, London, UK

<sup>7</sup>Healthcare Biomagnetics Laboratory, University College London, London, UK

<sup>8</sup>Instituto Madrileño de Estudios Avanzados en Nanociencia (IMDEA Nanociencia), Faraday 9, 28049 Madrid, Spain

<sup>9</sup>Unidad Asociada al Centro Nacional de Biología Celular (CSIC), Darwin 3, 28049 Madrid, Spain

<sup>10</sup>Advanced Materials and Bioengineering Research (AMBERR) Centre, CRANN Institute, Trinity College Dublin, Dublin, Ireland

Pancreatic ductal adenocarcinoma (PDAC) carries a dismal five-year survival rate of less than 10%, and a median survival time of 10-12 months from diagnosis. At present, efforts to improve overall outcome in these patients have been minimally effective, with five-year survival statistics barely increasing in the last four decades (<4%). Clearly, novel approaches for treating this cancer are required to overcome the lack of success in recent times.

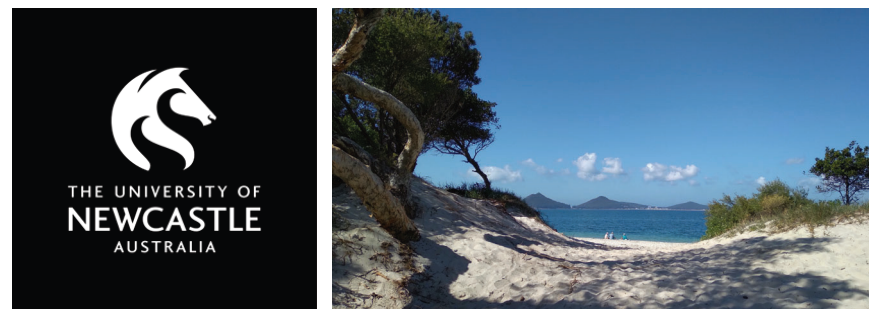
Magnetic hyperthermia is an innovative thermal treatment for cancer that utilizes tumour-residing superparamagnetic iron oxide nanoparticles (SPION) and externally-applied alternating magnetic fields (AMF). This treatment is clinically approved in Europe to treat glioblastoma and is currently undergoing clinical evaluation in prostate cancer in the United States. These are not the only potential indications, however, with many preclinical studies demonstrating efficacy in multiple solid malignancies.

Here we present highlights of the NoCanTher (Nanomedicine upscaling for early clinical phases of multimodal cancer therapy) and Safe-N-MedTech (Safety testing in the life cycle of nanotechnology-enabled medical technologies) projects where magnetic hyperthermia treatment - both SPION and AMF device - were successfully translated to a clinical study currently ongoing for locally-advanced PDAC. Work related to the early contamination screening, blood compatibility analysis, *in vitro* and *in vivo* safety and efficacy testing will be presented that resulted in the approval of a clinical study by the Spanish National Competent Authority in 2021.



# Basics of Magnetic Nanoparticles

Karen Livesey



13<sup>th</sup> Magnetic Carriers Meeting, London, 2022

 @KarenLlivesey

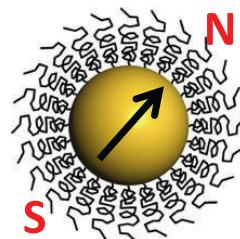
1

# Basics of Magnetic Nanoparticles

Karen Livesey

## Three tutorials

1. Basics and energies
2. Magnetic nanoparticle dynamics
3. Characterizing magnetic nanoparticles



2

# Basics of Magnetic Nanoparticles

Karen Livesey



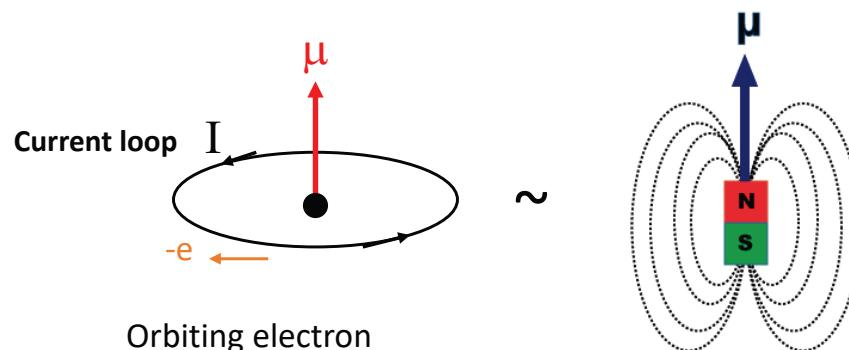
## Three tutorials

1. Basics and energies
2. Magnetic nanoparticle dynamics
3. Characterizing magnetic nanoparticles

3

## Magnetic materials

- Have atomic magnetic dipoles due to electrons
- Dipoles (left) are equivalent to mini bar magnets (right)

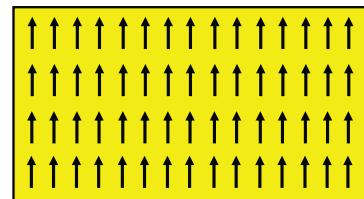


$\vec{\mu}$  = atomic magnetic dipole moment [A m<sup>2</sup>]      ie. Current X area

4

## FERROmagnetic materials

- All those dipoles tend to align



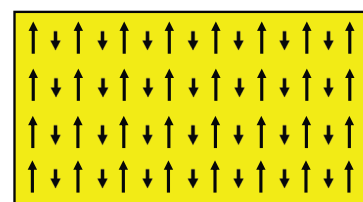
- We say there is a net **magnetization**, found by summing up dipole moments  $\vec{\mu}$  and dividing by the volume  $V$  they occupy

$$\bar{M} = \frac{\sum_i \vec{\mu}}{V} = \text{magnetization } [\text{A/m}]$$

5

## FERRImagnetic materials

- All the dipoles tend to **anti-align**, with different moments on each sublattice



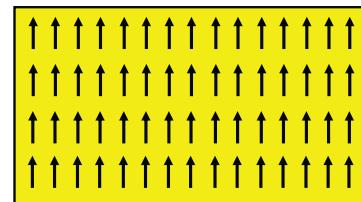
- Still a net **magnetization**, found by summing up dipole moments  $\vec{\mu}$

$$\bar{M} = \frac{\sum_i \vec{\mu}}{V} = \text{magnetization } [\text{A/m}]$$

6

## FERROmagnetic materials: exchange energy

- This is what most people mean by “a magnet”

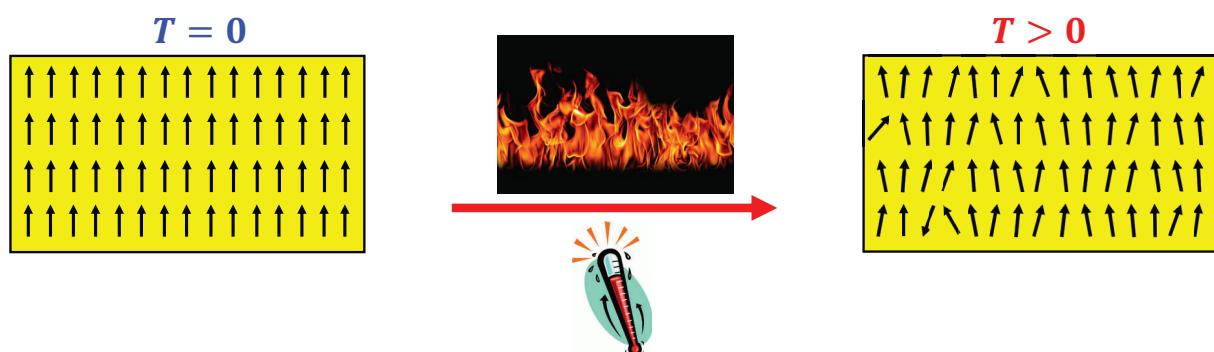


- Alignment is due to an interaction between neighbouring dipoles: the quantum “exchange” energy  $E_{ex}$

7

## Thermal energy

- Atomic-level **jiggle** affects all systems at finite temperature  $T$

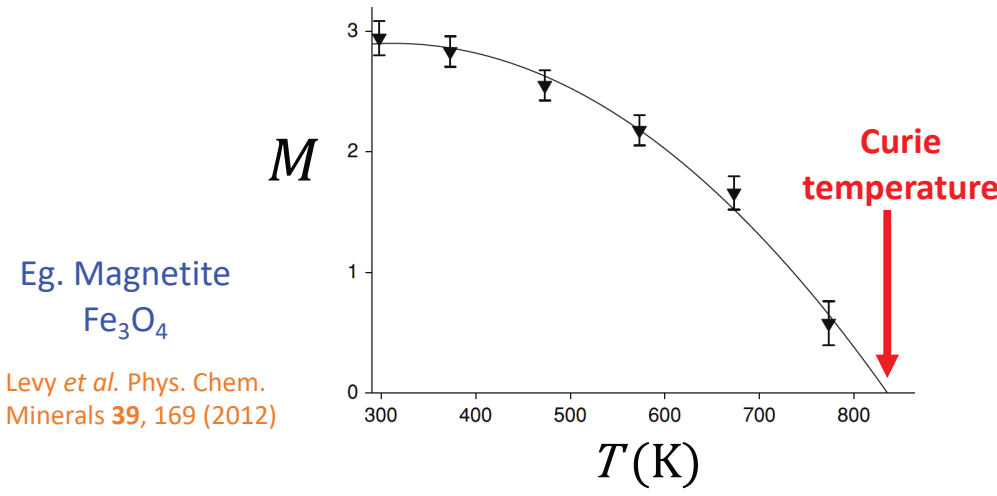


- Jiggle reduces the alignment → lower net magnetization  $\vec{M}$

8

## Magnetization versus temperature

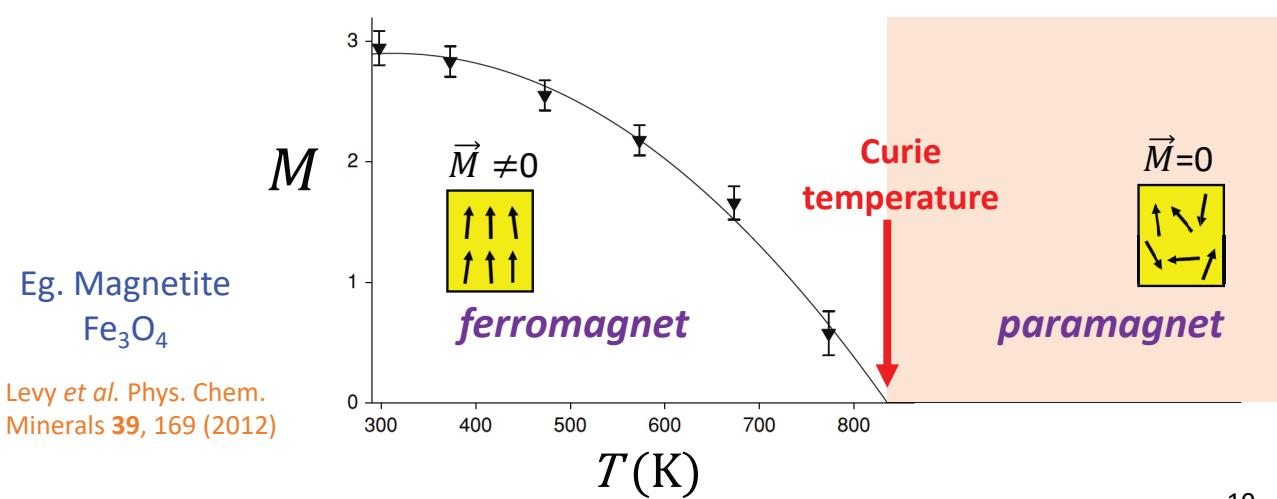
- For large temperatures, **thermal energy** dominates **exchange** and magnetization is lost! ( $\vec{M}=0$ )



9

## Ferromagnet and paramagnet

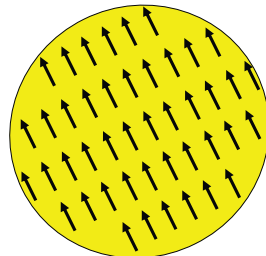
- Exchange energy in competition with thermal energy



10

## Now make it nano!

- Imagine a tiny ferromagnetic ball

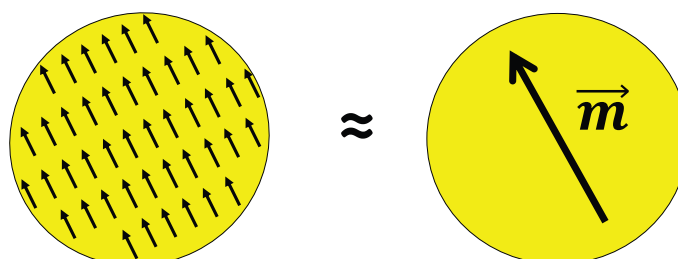


10 – 30 nanometer-wide core  
(40 – 120 atoms)

11

## Now make it nano!

- Imagine a tiny ferromagnetic ball



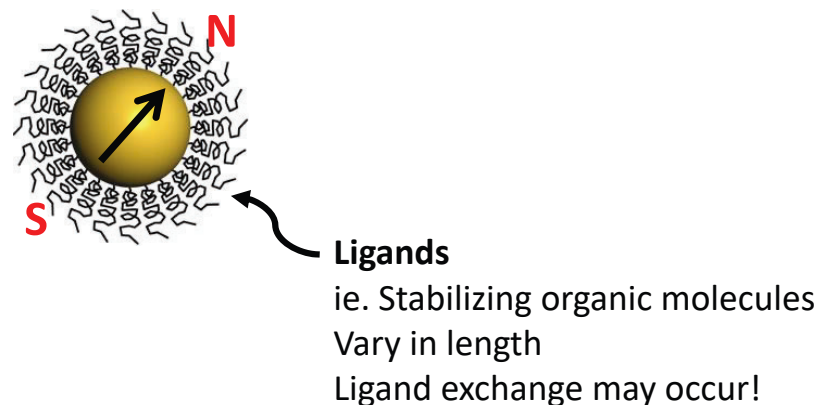
- Since the atomic dipoles are all aligned, replace with one “macrospin” magnetic moment

$$\vec{m} = V \overrightarrow{M} = \text{macrospin moment} \quad [\text{A m}^2]$$

12

## Now make it nano!

- Imagine a tiny **hairy** ferromagnetic ball

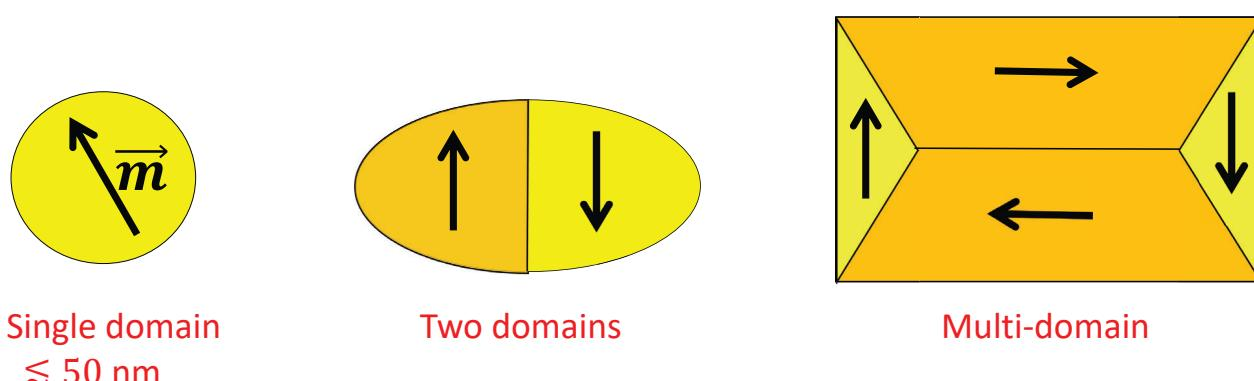


One slide for the chemists!

13

## Single domain particle

- If nanoparticles are too big, then the magnet splits into **regions of aligned magnetization**, ie. "domains"

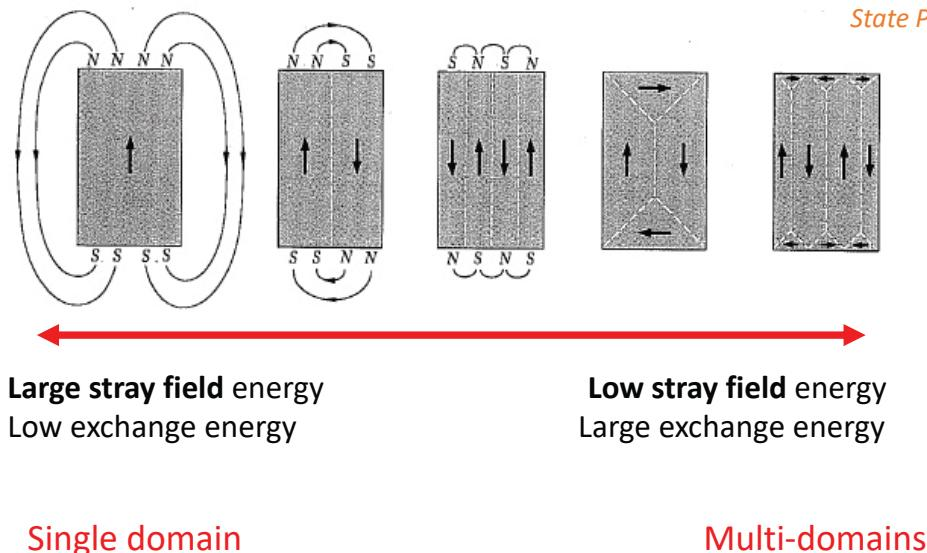


- Domains form to reduce stray magnetic field energy

14

## Stray field energy

Kittel, *Intro to Solid State Physics*.

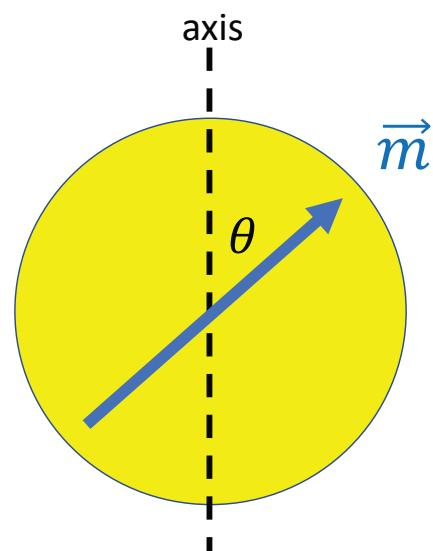


15

## Anisotropy energy

- There is a **preferred axis** for macrospin to point, due to underlying crystal structure
- Usually assume “uniaxial”
- Key to understanding thermal behaviour of magnetic nanoparticles!

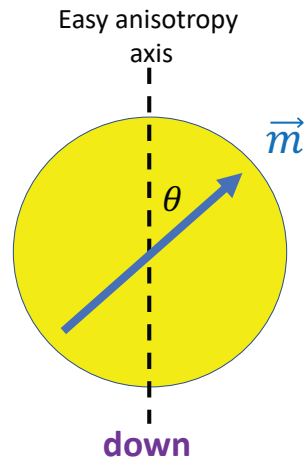
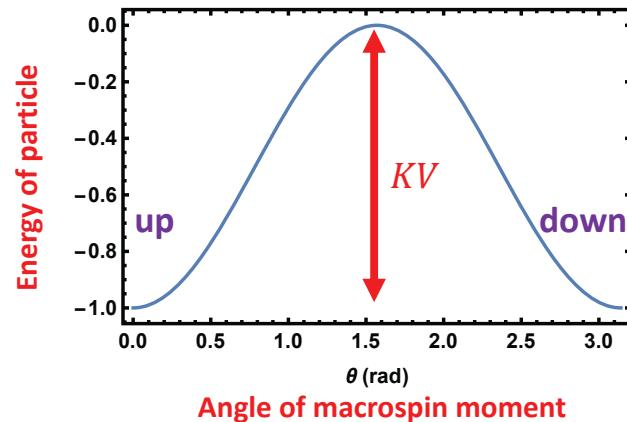
Easy anisotropy



16

## Anisotropy energy

- Two happy directions
- Energy barrier  $KV$  in between

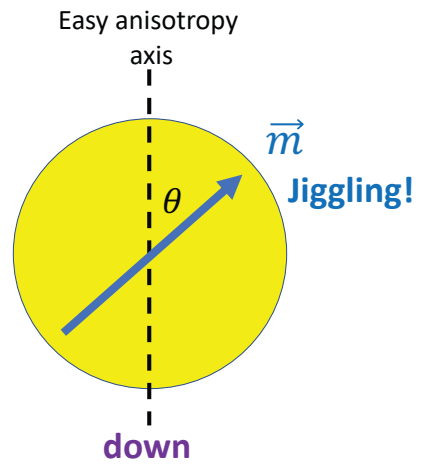
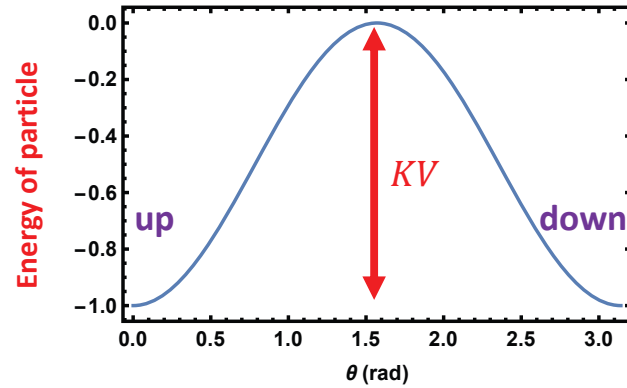


$K$  = anisotropy constant [J/m<sup>3</sup>]  
 $V$  = volume [m<sup>3</sup>]

17

## Anisotropy energy

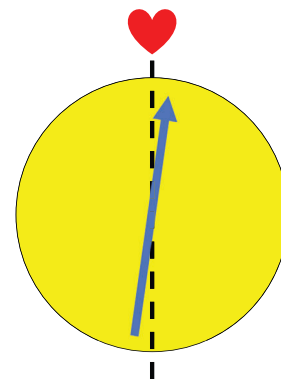
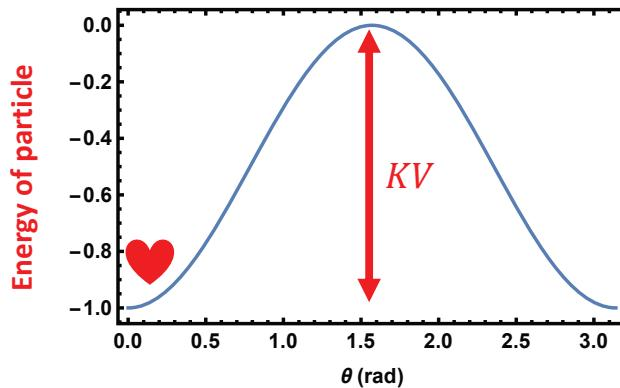
- Consider competition between **anisotropy energy** and **thermal energy**



18

## Low temperatures...

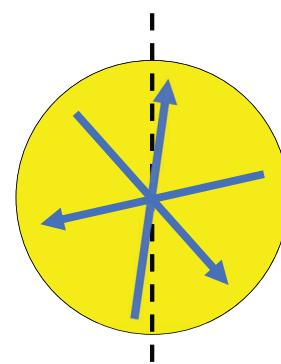
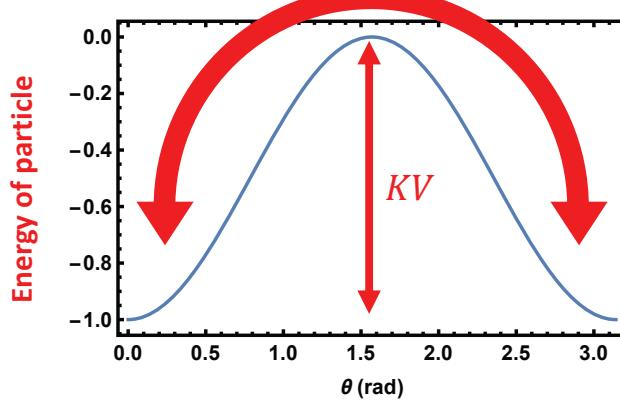
- Macrospin is stuck in an energy well
- Anisotropy dominates thermal energy
- **"Blocked" moment**



19

## High temperatures...

- Macrospin jumps over barrier easily.
- Average magnetization  $\vec{M} = 0$
- **"Superparamagnetic" behaviour**

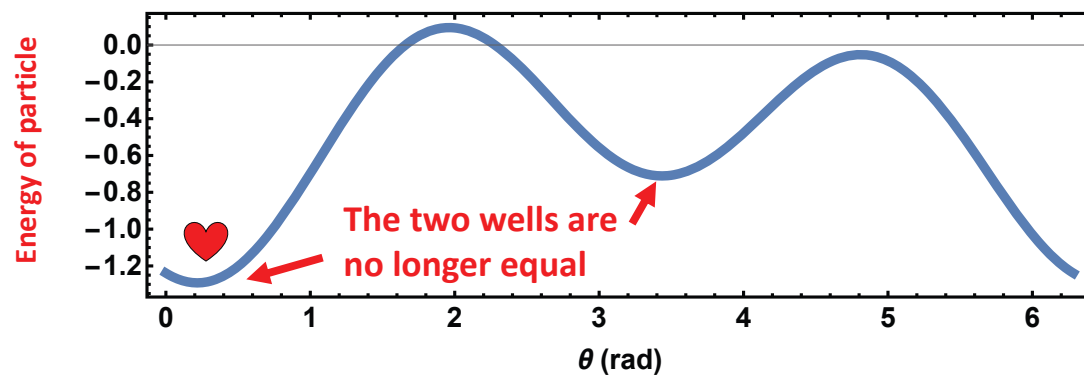
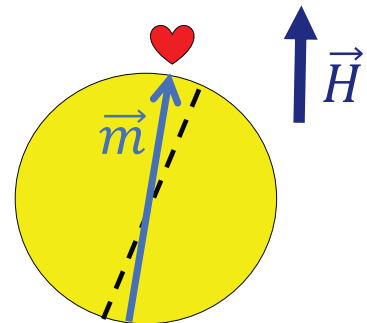


- Onset depends on size
- $\sim 25$  K for 5 nm radius magnetite

20

## Zeeman energy

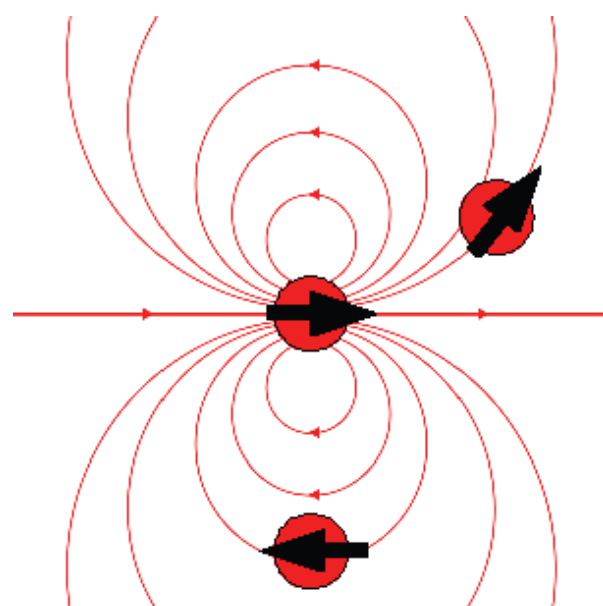
- Macrospin prefers to align with an applied magnetic field  $\vec{H}$



21

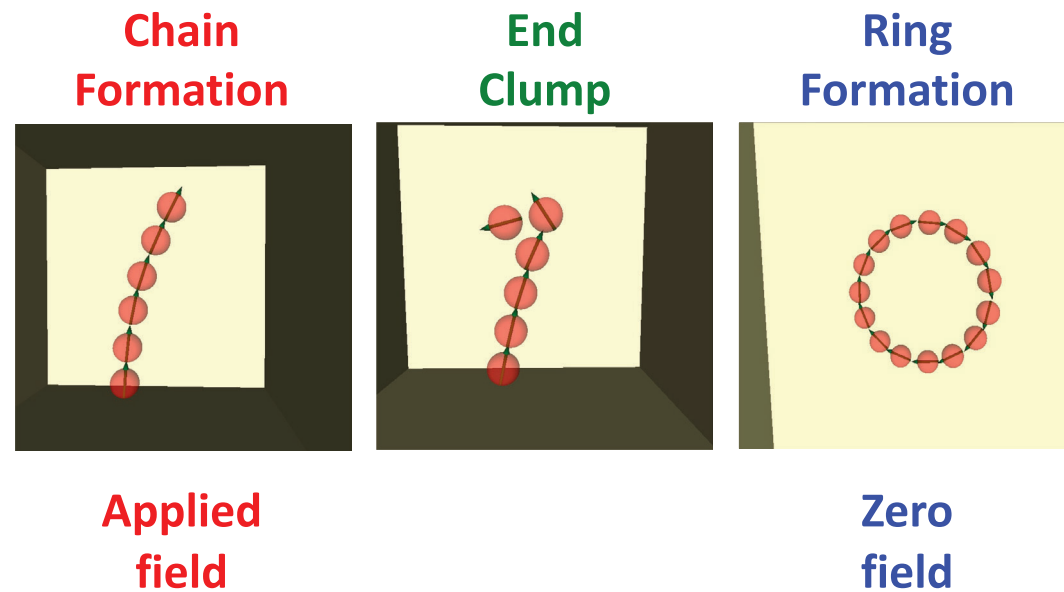
## Dipolar interaction energy

- Each macrospin produces a dipolar magnetic field
- Other macrospins want to align with that dipolar field
- Very complicated magnetic arrangements



22

## Dipolar interaction energy – in fluids



23

## Recap of energies

1. Exchange energy
2. Stray field energy
3. Anisotropy energy
4. Thermal energy
5. Zeeman energy
6. Dipolar interaction energy

These energies will be needed to understand dynamics... next time!

24

# Basics of Magnetic Nanoparticles

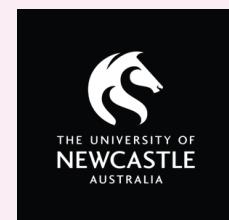
Karen Livesey

End of part 1

25

# Basics of Magnetic Nanoparticles

Karen Livesey



Three tutorials

1. Basics and energies
2. Magnetic nanoparticle dynamics
3. Characterizing magnetic nanoparticles

26

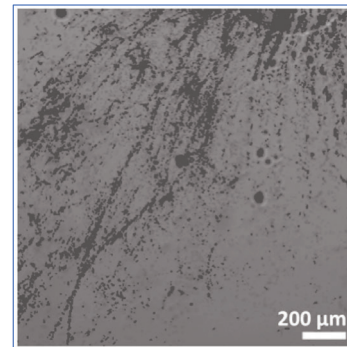
## Why study dynamics (changes with time)?

- Most applications of magnetic carriers rely on their **magnetic or physical response** to a stimulus **over time**

e.g. Drug delivery through mucus

30 nm magnetite particles in magnetic field gradient

Picture courtesy Profs Spendier & Celinski (UCCS)



27

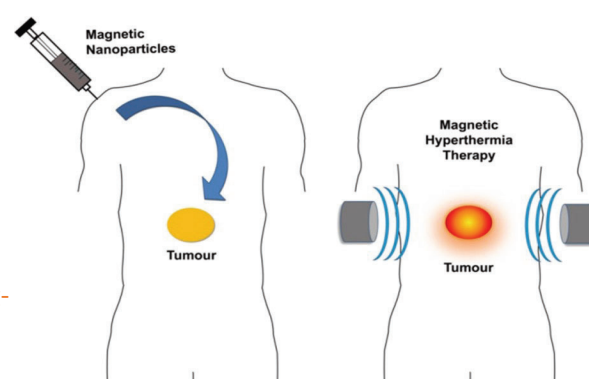
## Why study dynamics (changes with time)?

- Most applications of magnetic carriers rely on their **magnetic or physical response** to a stimulus **over time**

e.g. Hyperthermia

Oscillating field  
→ jiggling particles  
→ heat generated

A. Andrade et al., Biomedical Engineering-Frontiers and Challenges (2011)



28

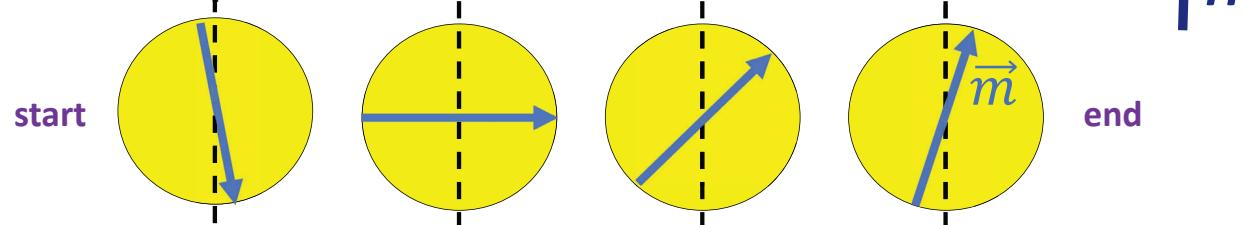
## Dynamics to reach a steady state = “relaxation”

1. **Magnetization relaxation** →  $\vec{M}$  moves towards a steady value
2. **Physical relaxation** → Particle density/microstructure moves towards a steady state

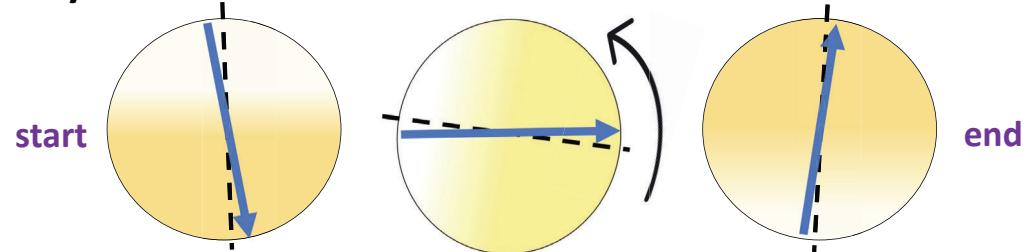
29

## Magnetization relaxation mechanisms

1. **Macrospin rotation** – called Néel relaxation



2. **Physical rotation** – called Brownian relaxation

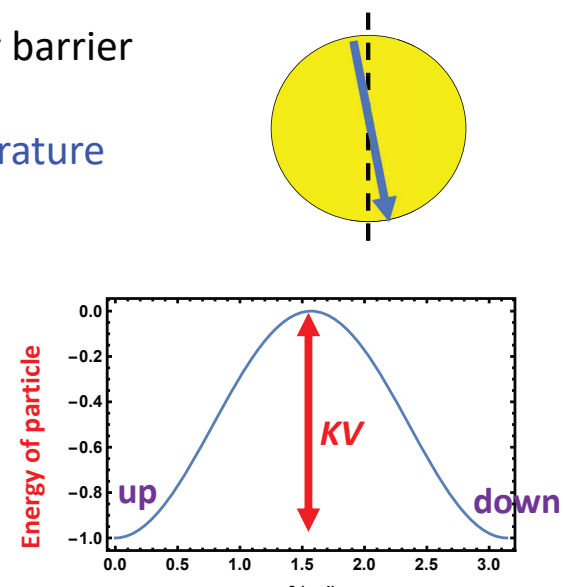


30

## Macrospin rotation – Néel relaxation time

- Macrospin must surmount energy barrier
- Small particles and/or high temperature
- A **stochastic** process!  
So we can only talk about  
“average time” to relax  
for a nanoparticle sample

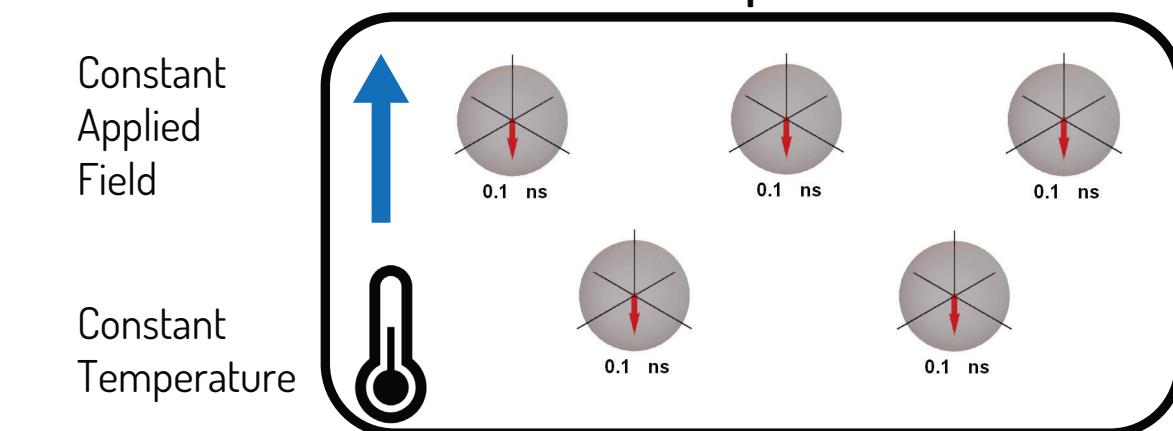
Deutsch and Evans, JMMM 354 (2014)  
Brown, Phys. Rev. 130, 1677 (1963)



31

## Average Néel relaxation time

Sample of many thousands or millions  
of nanoparticles

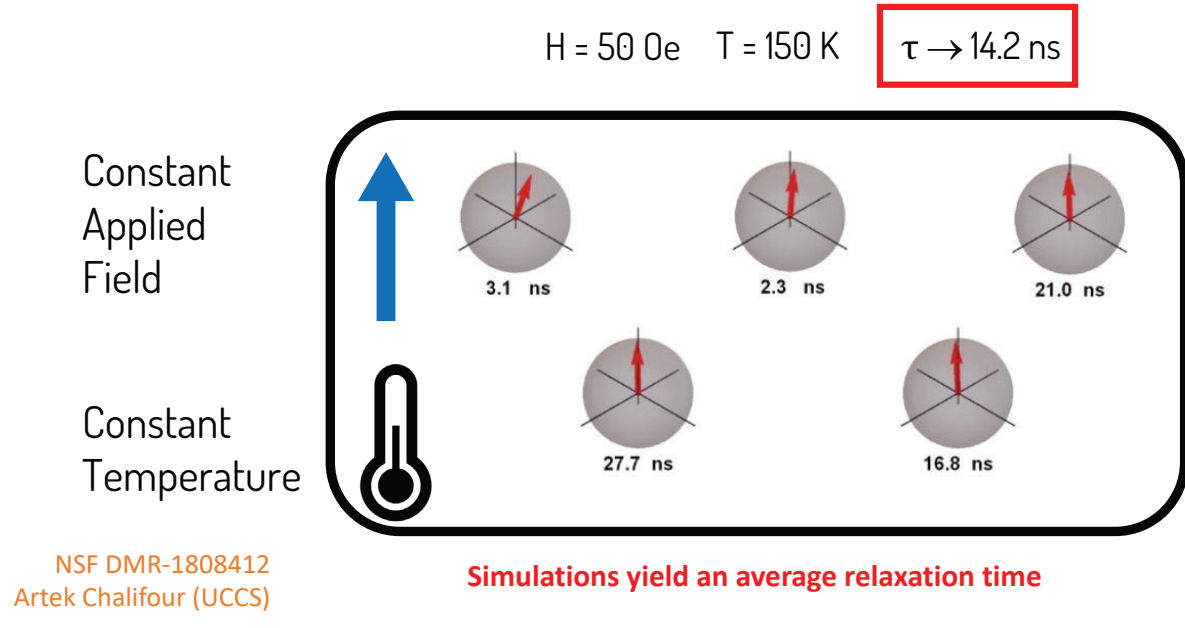


NSF DMR-1808412  
Artek Chalifour (UCCS)

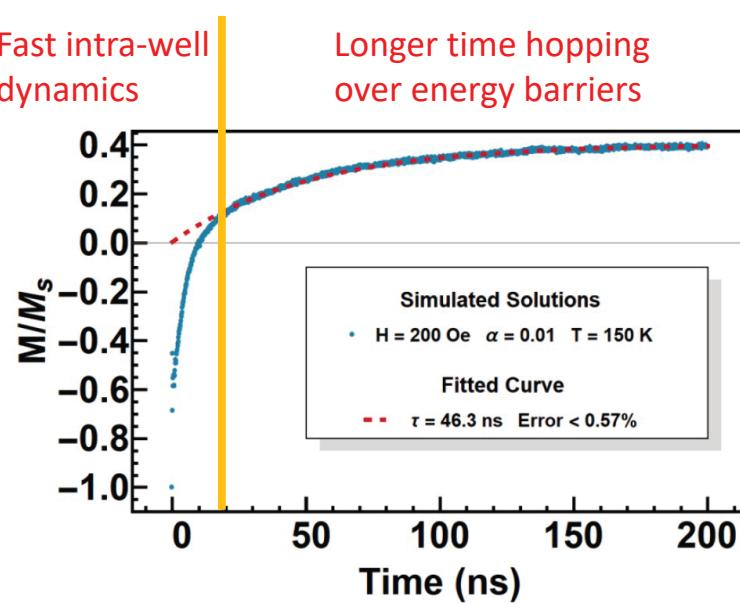
VIDEO: Thermal Landau-Lifshitz equation simulations

32

## Average Néel relaxation time



## Average Néel relaxation time



5000 particles  
5 nm radius magnetite

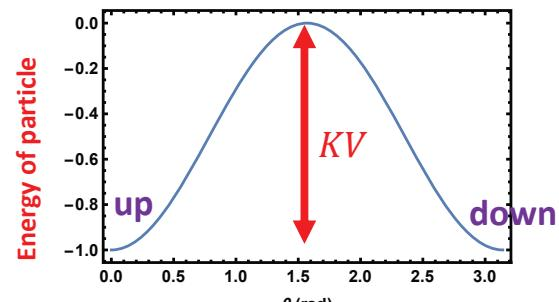
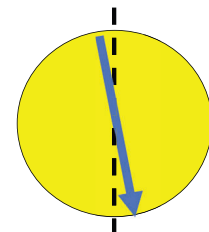
Chalifour et al. Phys. Rev. B  
104 (2021)

## Macrospin rotation – Néel relaxation time

- Analytic estimate:

Average time depends on barrier height ( $KV$ )  
compared to thermal energy ( $k_B T$ )

$$\tau_N = \tau_0 e^{\left(\frac{KV}{k_B T}\right)}$$

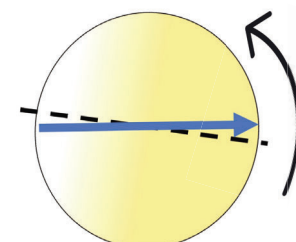


Deutsch and Evans, JMMM 354 (2014)  
Brown, Phys. Rev. 130, 1677 (1963)

35

## Physical rotation – Brownian relaxation time

- Whole particle rotates in a fluid (driven by field or diffusive)
- Larger particles and/or lower temperature
- Average time depends on fluid viscosity ( $\eta$ ) and hydrodynamic volume ( $V_h$ )  
compared to thermal energy ( $k_B T$ )



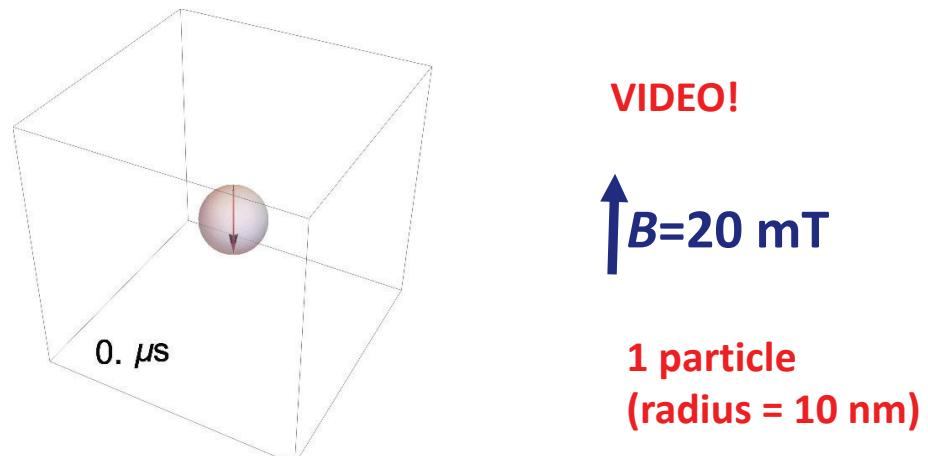
$$\tau_B = \frac{3\eta V_h}{k_B T}$$

Frenkel, Kinetic Theory of Liquids (1955)

36

## Physical rotation – Brownian relaxation time

- Whole particle rotates in a fluid (driven by field or diffusive)



- Brownian translations are seen here, as well as rotations

37

## An aside on units



- I am using **Standard International (SI)** here... mostly, rather than Centimeter-Gram-Second (CGS)

38

## An aside on units

- Magnetic field (**H**) and Magnetic induction (**B**) have SI units of  
[A/m] [T]

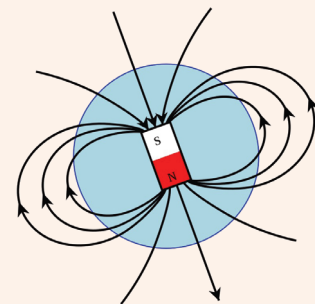
In a vacuum,  $B = \mu_0 H$ , where  $\mu_0$  is the vacuum permeability

$$1.6 \times 10^4 \text{ A/m} = 20 \text{ mT}$$

= 400 X larger than Earth's magnetic field in London

= 100 X smaller than in a Magnetic Resonance Imaging machine

= insufficient to dominate Brownian rotations



39

## An aside on units

- Magnetic field (**H**) and Magnetic induction (**B**) have SI units of  
[A/m] [T]

In a vacuum,  $B = \mu_0 H$ , where  $\mu_0$  is the vacuum permeability

- Volume magnetization has units [A/m].

- Mass magnetization (total moment per unit mass) has units [ $\text{Am}^2/\text{kg}$ ].

You may see emu/g (CGS) regularly...  
...I'm sorry.

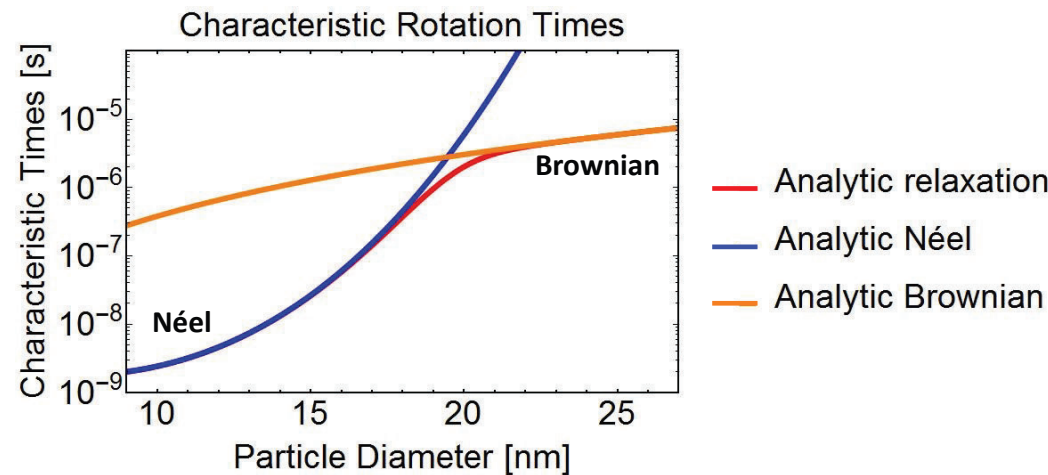


40

## Combined magnetic relaxation time

- Fastest process dominates relaxation.

$$\frac{1}{\tau} = \frac{1}{\tau_N} + \frac{1}{\tau_B}$$



41

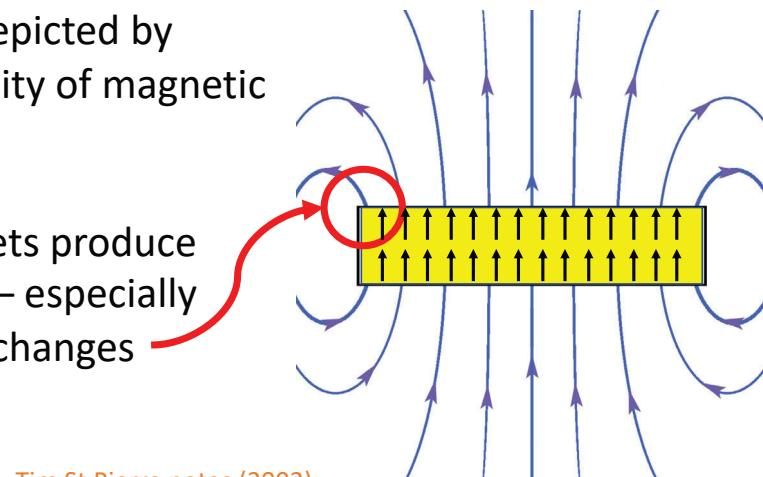
## Dynamics to reach a steady state = “relaxation”

1. Magnetization relaxation  $\rightarrow \vec{M}$  moves towards a steady value
2. Physical relaxation  $\rightarrow$  Particle density/microstructure moves towards a steady value

42

## Physical relaxation mechanism

- Macrospins feel a **force due to magnetic field gradients**
- Gradients are depicted by a changing density of magnetic field lines
- Most bar magnets produce a gradient field – especially at sharp edges/changes

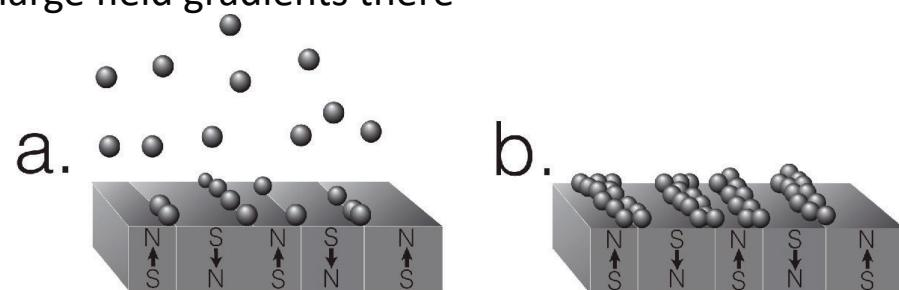


Tim St Pierre notes (2002)

43

## Self-assembly by magnetic field gradients

- e.g. magnetic substrate with magnetization transitions produces large field gradients there



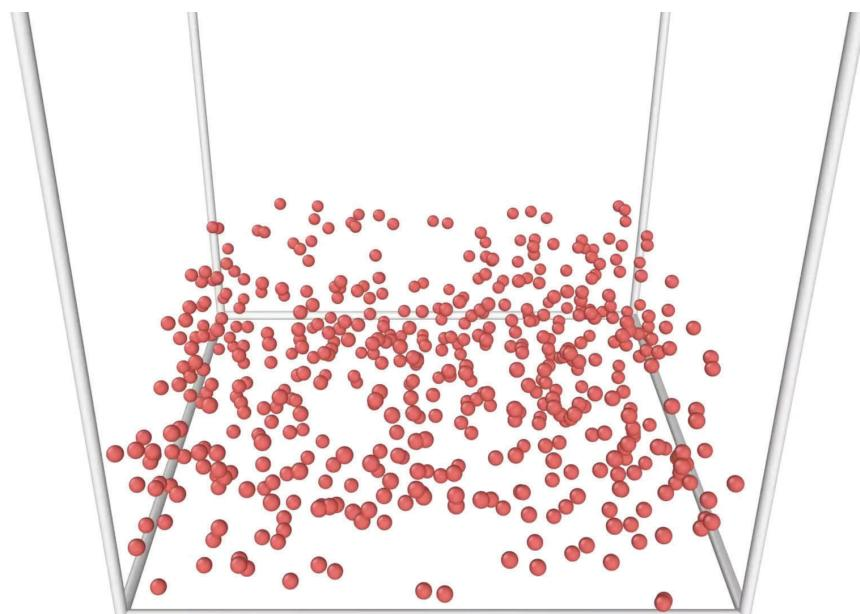
National Science Foundation DMR-1808412  
Prof. Crawford (Uni. South Carolina)

44

## Video: Simulation of self assembly in a fluid

- Field gradient generated by 2 magnetic transitions

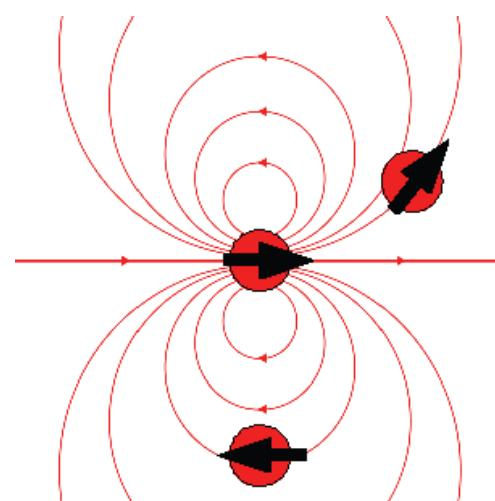
NSF DMR-1808412  
Jonathon Davidson (UCCS)



45

## Dipolar interactions

- Particles are attracted/repelled by the field gradients of others
- Presence of a static OR oscillating applied field can aid in the formation of chains



46

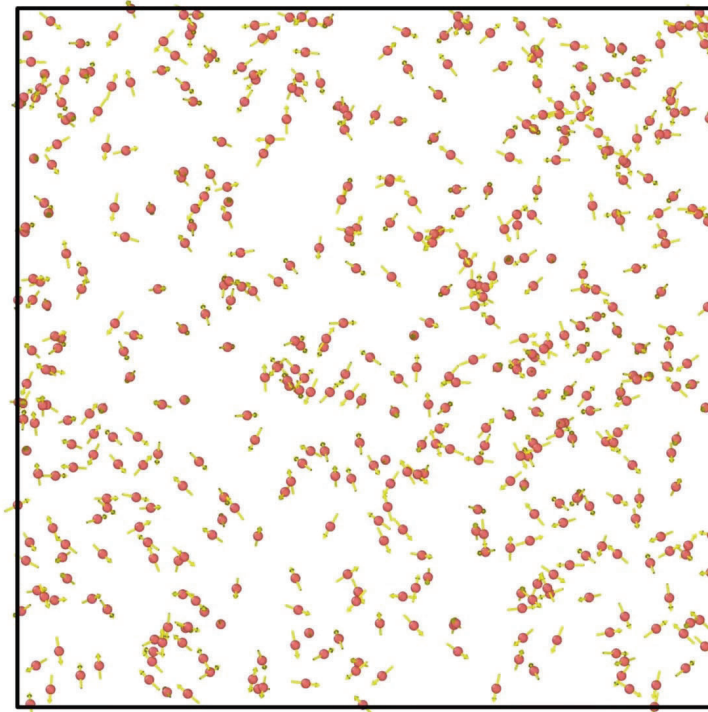
## Chain formation

VIDEO!

25 nm radius particles

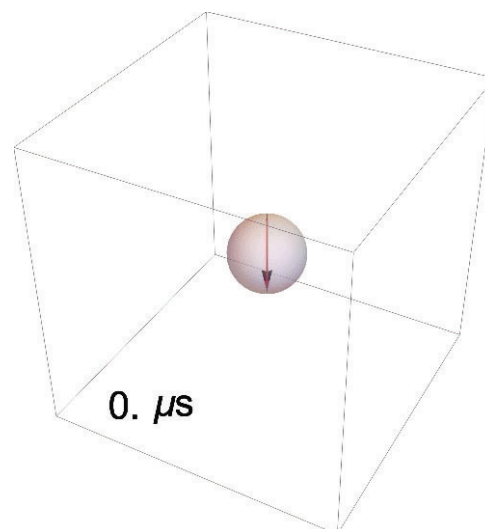
1.25 kHz field of  
100 kA/m

Anderson et al., Nanomaterials  
11 (2021)



47

## Physical structures affect magnetic relaxation



VIDEO!

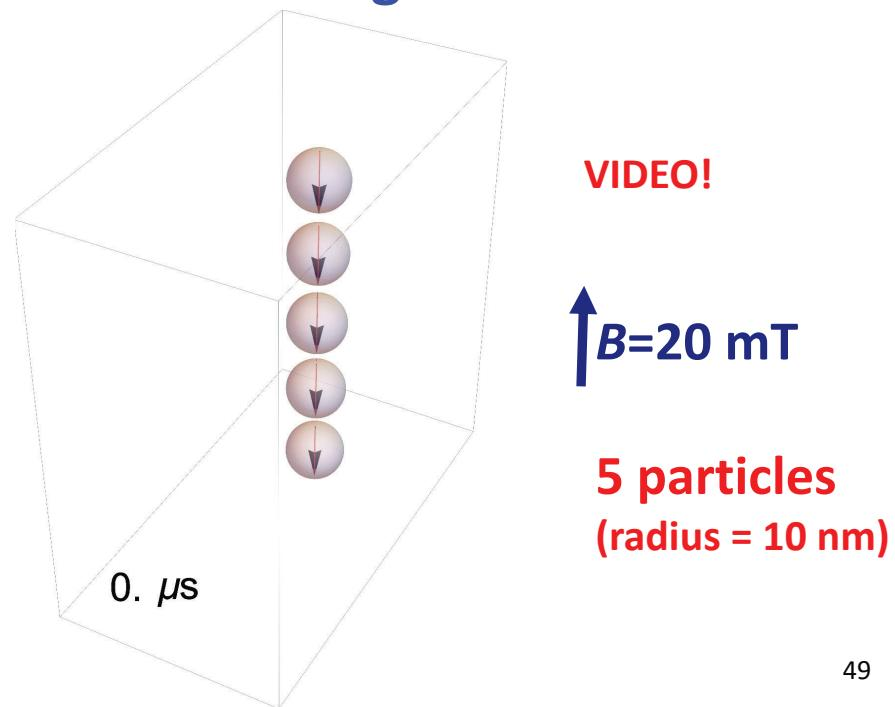
↑  
 $B=20 \text{ mT}$

1 particle  
(radius = 10 nm)

48

## Physical structures affect magnetic relaxation

Magnetization relaxation takes much longer than for the isolated particle



49

## Dynamics summary

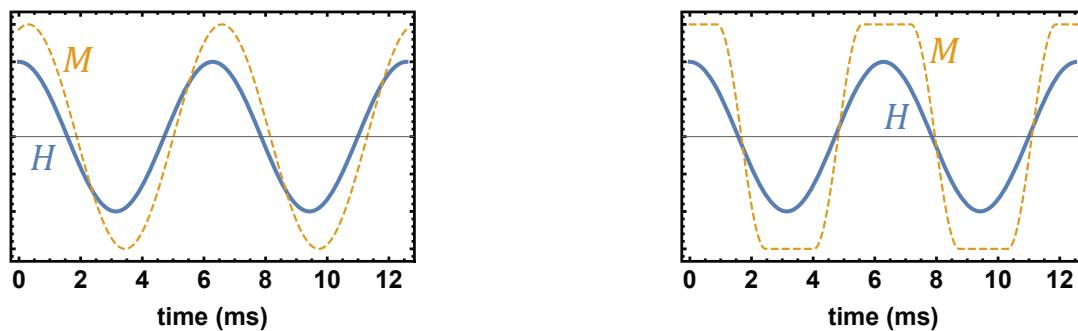
- **Magnetization relaxation** →  $\vec{M}$  moves towards a steady value  
**Brownian and Néel mechanisms**
- **Physical relaxation** → Particle density/microstructure moves towards a steady value  
**Magnetic field gradients**
- **Relaxation times over 10 orders of magnitude!!!**  
**1 nanosecond (Néel) to**  
**1 minute (self-assembly)**

50

## Dynamics – implications

- **Hyperthermia example:** maximize energy produced by oscillating the field with a period that matches the magnetic relaxation time.

Then particles can just keep up (left), and there is less static waiting (right).



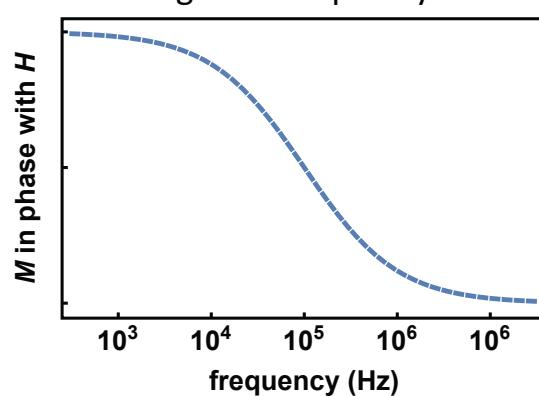
51

## Dynamics – implications

- **Characterization methods rely on relaxation processes:**  
***Dynamic Magnetic Susceptibility measurements***

How the magnetization keeps up with an oscillating field frequency

- tells us the relaxation time
- tells us the nanoscale energy barriers



52

# Basics of Magnetic Nanoparticles

Karen Livesey

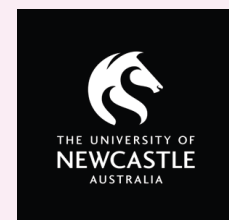
End of part 2

More on **characterization** tomorrow!

53

# Basics of Magnetic Nanoparticles

Karen Livesey



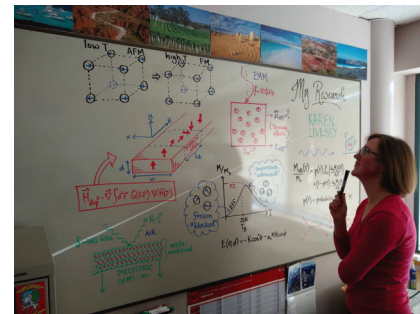
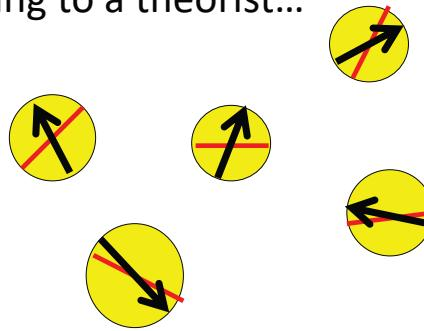
Three tutorials

1. Basics and energies
2. Magnetic nanoparticle dynamics
3. Characterizing magnetic nanoparticles

54

# Experiments and what they tell us

- According to a theorist...



- Some useful articles:

Maldonado-Camargo, Unni and Rinaldi-Ramos, In *Biomedical Nanotechnology*, pp. 47-71.  
(Humana Press, New York, 2017).

Sandler, Fellows and Mefford, *Anal. Chem.* **91**, 22, 14159–14169 (2019)

55

## What we may want to know

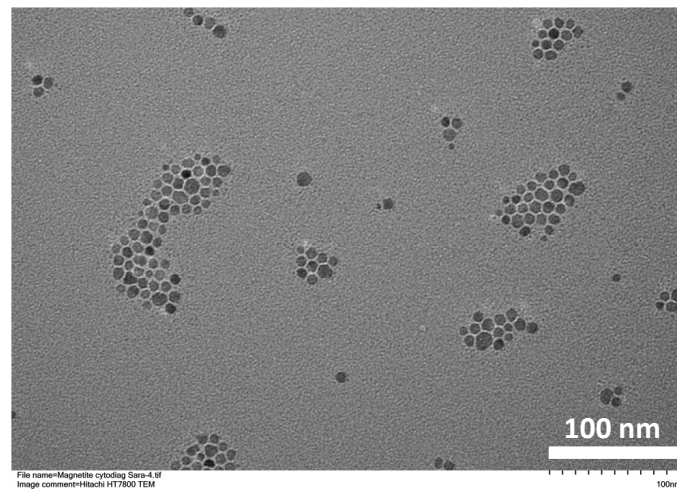
1. Particle size
2. Saturation magnetization
3. Particle interaction strength and sign
4. Anisotropy barriers

e.g. Hyperthermia: want a large saturation magnetization and  
moderate anisotropy to generate the most heat.  
Interactions may help or hinder!

56

## Particle size

- **Transmission Electron Microscopy (TEM) or Scanning Electron Microscopy (SEM)**



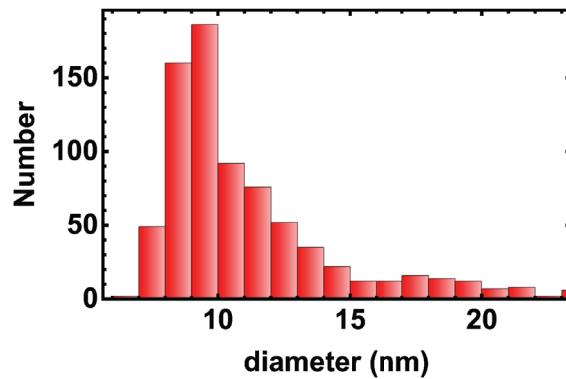
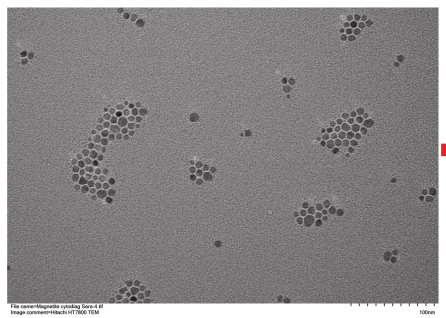
e.g. TEM image  
Immobilized particles

FitzGerald PhD dissertation,  
University of South Carolina  
(2021). Fig. 4.2

57

## Particle size from TEM

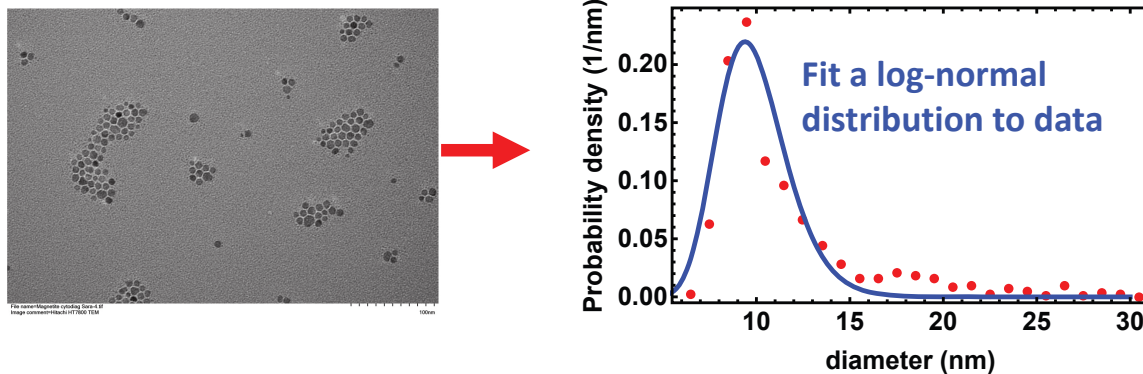
- From images, measure each particle and construct histogram of diameters



58

## Particle size from TEM

- From images, measure each particle and construct histogram of diameters



- Option: fit analytic function to particle size distribution

59

## Particle size from TEM: notes

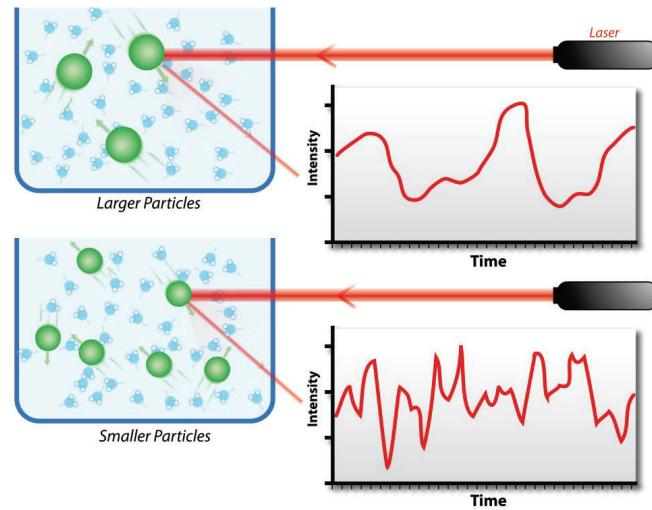
- The immobilized particles may be different to when in fluid
- It's possible to measure magnetic core size, subtracting ligands
- Beware the log-normal size distribution!
  - Mean and mode size are different*
  - Diameter distribution is different from the volume distribution*

60

## Particle size

- Dynamic light scattering (DLS) of fluids
- Measures the “hydrodynamic” size of particles
- Relies on their Brownian motion in solution

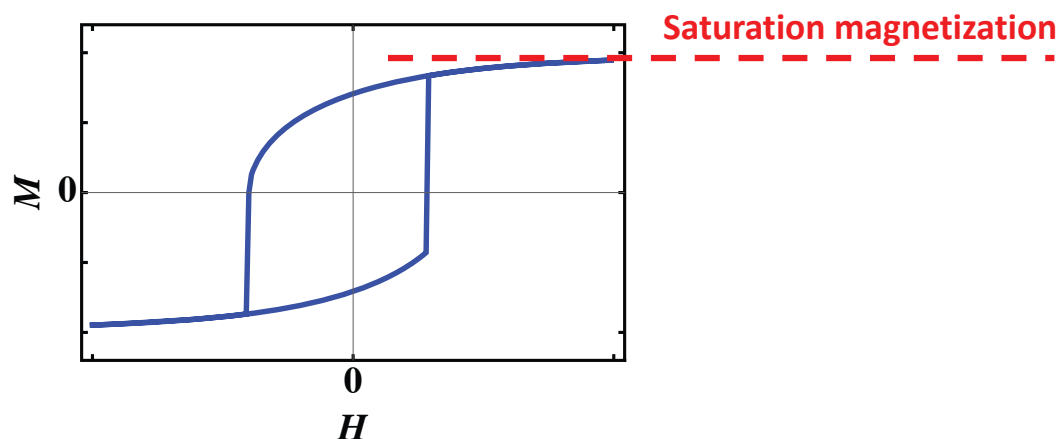
Wikipedia ‘‘Dynamic Light Scattering’’ (Image by Mike Jones)



61

## Saturation magnetization $M_s$ [A/m]

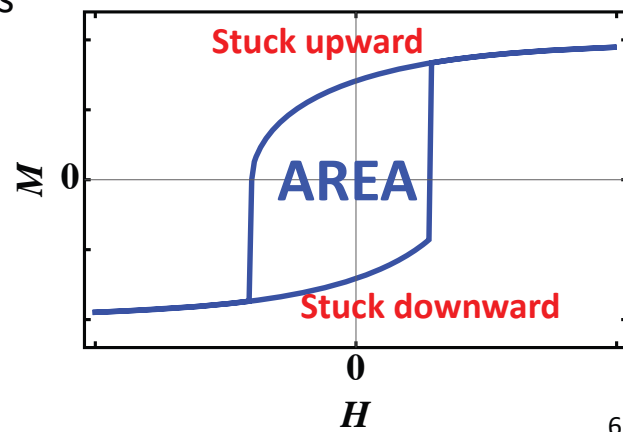
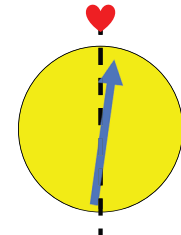
- Magnetization versus static applied field measurement
- Performed using a SQuID or VSM magnetometer



62

## M vs H – Low temperature

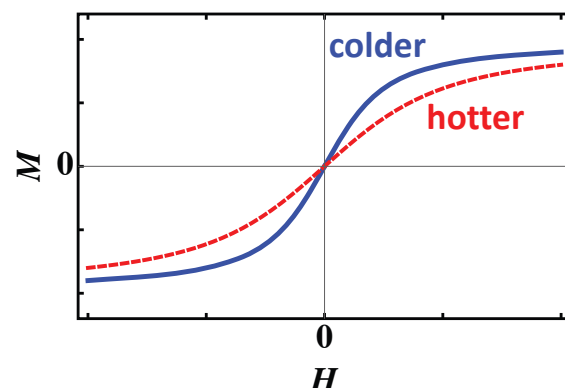
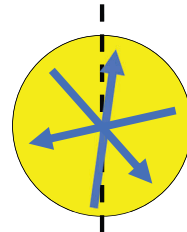
- The system has a **memory** ... “Hysteresis loop”
- Macrospins are “**blocked**” at low temperature and for fast field sweep rates
- **Area** inside loop = magnetic work done by the field (heat?)



63

## M vs H – High temperature

- The curve is now **reversible** – no memory
- Macrospins are “**superparamagnetic**” at high temperature and/or slow field sweep rates
- The net moment follows the field



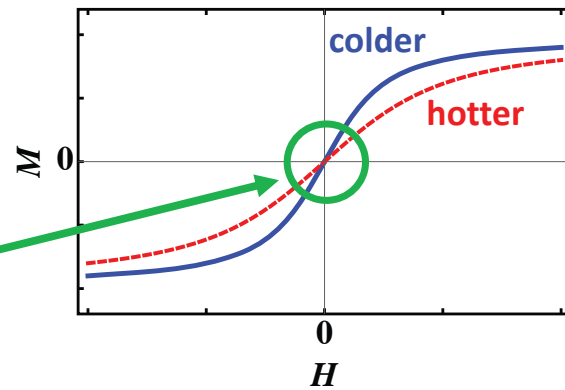
64

## M vs H – High temperature – Langevin function

- Superparamagnetic magnetization can be predicted using the Langevin function (not given)  
Assumes anisotropy barriers negligible & particles are non-interacting

- For small fields,  $M$  has linear behaviour

$$\frac{M}{M_s} \sim \left( \frac{\mu_0 M_s V}{3k_B T} \right) H$$

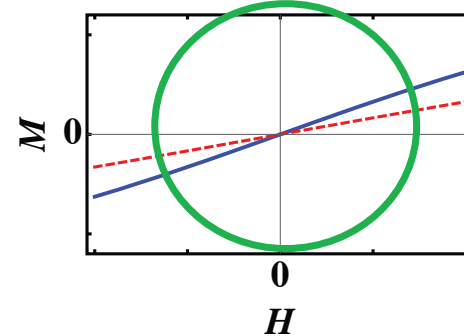


65

## Low field susceptibility $\chi$ – High temperature

- Susceptibility = the rate of magnetization  $M$  increase with an increase in field  $H$  (unitless **slope**)

$$\chi = \frac{M}{H} \sim \frac{\mu_0 M_s^2 V}{3kT}$$



66

## Low field susceptibility $\chi$ – High temperature

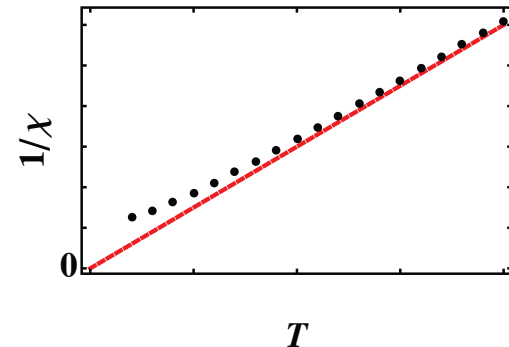
- Susceptibility = the rate of magnetization  $M$  increase with an increase in field  $H$  (unitless **slope**)

$$\chi = \frac{M}{H} \sim \frac{\mu_0 M_s^2 V}{3kT}$$

- A plot of  $1/\chi$  versus  $T$  should be linear and should extrapolate to origin...

$$\frac{1}{\chi} \sim \frac{3k}{\mu_0 M_s^2 V} T$$

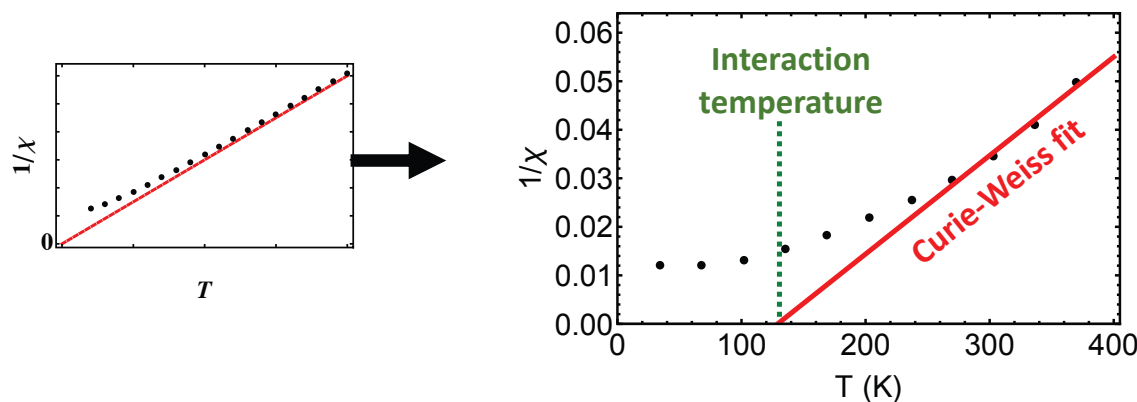
**Curie's Law**



67

## Interaction temperature

- Often  $1/\chi$  versus  $T$  does **not** go through the origin!!!!



- Due to dipolar interactions
- Can tell their strength and sign

68

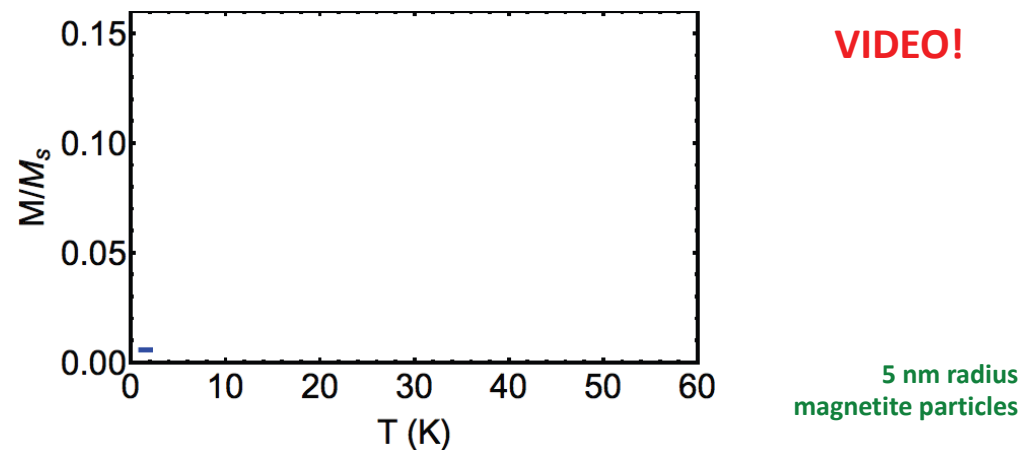
## Anisotropy barriers

- Zero-field cooled (ZFC) and field cooled (FC) magnetization versus temperature measurements
- Dynamic Magnetic Susceptibility measurements

69

## Zero field cooled measurement

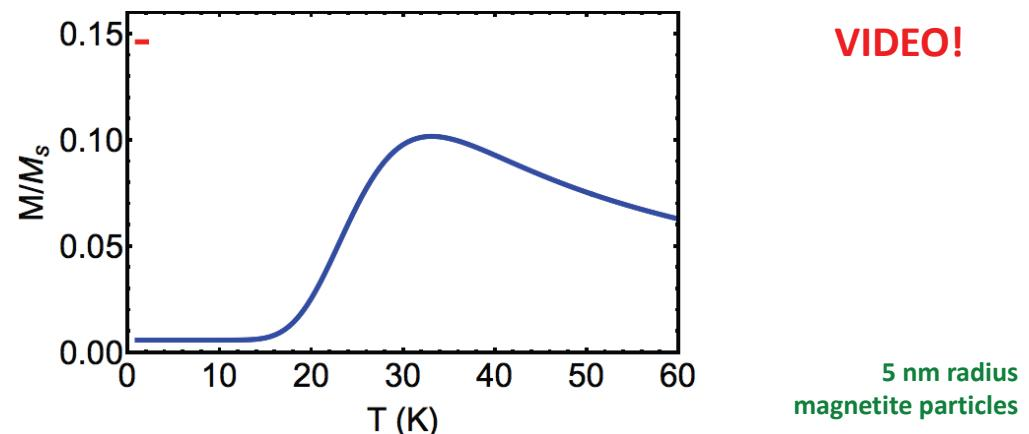
- Cool sample in zero field, then heat back up in a weak field  $H \sim 10$  Oe (CGS) or  $\mu_0 H \sim 1$  mT (SI)



70

## Field cooled measurement

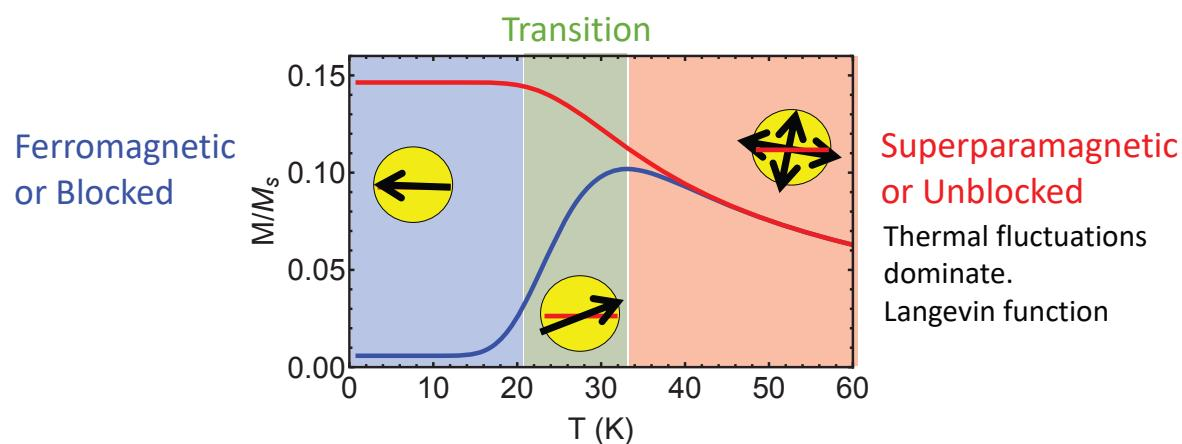
- Cool sample in weak field, then heat back up in a weak field



71

## Mean “Blocking temperature” $T_B$

= The average temperature at which particles become unblocked.



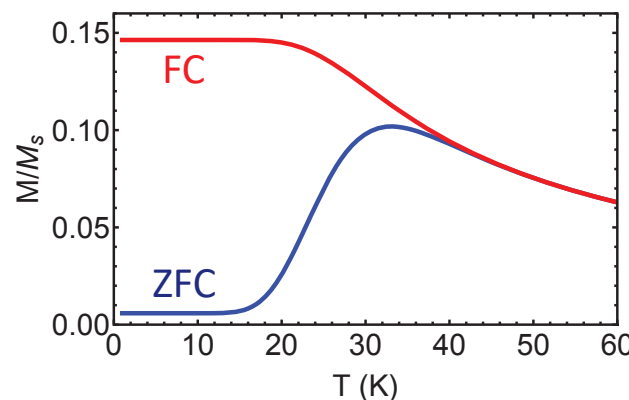
- Transition region is smeared because of particle size distribution

72

## Audience poll: Where is the mean Blocking temperature?

- a) At the ZFC peak, you idiot!
- b) To the right of the ZFC peak
- c) To the left of the ZFC peak

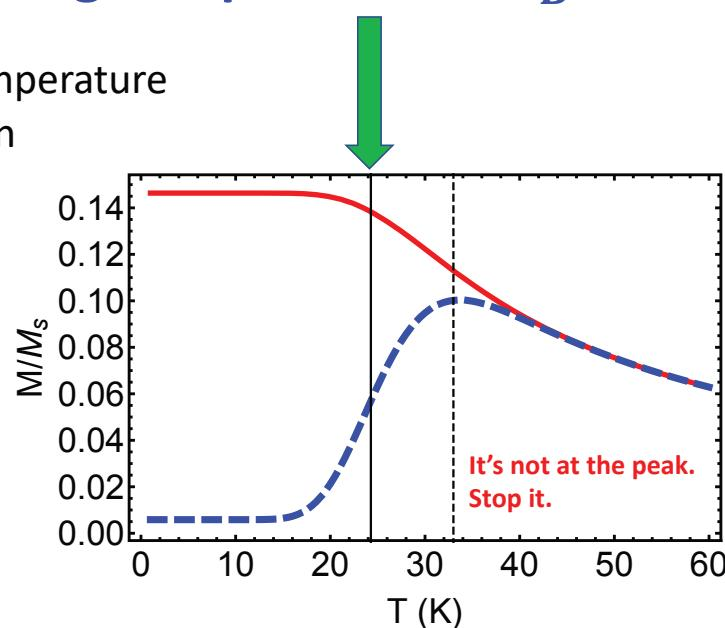
Vote now!



73

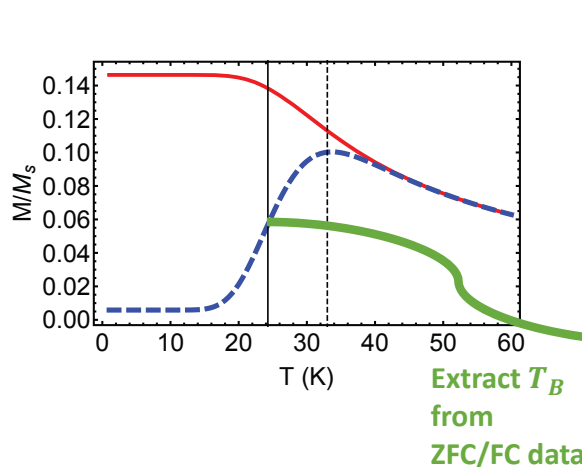
## Left of peak = “Blocking temperature” $T_B$

- The mean Blocking temperature tells us about the mean energy barrier  $KV$
- Recall the Néel relaxation time formula



74

## Extracting anisotropy constant $K$ [J/m<sup>3</sup>]



- Important for choosing materials for hyperthermia and other applications!

$$T_B = \frac{KV}{k_B \ln(\tau_m/\tau_0)}$$

Volume distribution  
Measurement time  $\sim 100$  s  
Attempt time  $\sim 1$  ns

Livesey et al. Sci. Reports 18 (2018)

75

## Summary of characterization

### 1. Particle size

Electron Microscopy and Dynamic Light Scattering

### 2. Saturation magnetization

Magnetization versus applied field

### 3. Particle interaction strength and sign

Low field susceptibility

### 4. Anisotropy barriers

Magnetization vs temperature (ZFC and FC) and Dynamic Susceptibility

76

# Thank you for listening

Karen Livesey

[Karen.Livesey@newcastle.edu.au](mailto:Karen.Livesey@newcastle.edu.au)



13<sup>th</sup> Magnetic Carriers Meeting, London, 2022



@KarenLivesey

77

## Thanks to all collaborators!

Nicholas Anderson  
Casey Chalifour  
Jonathon Davidson  
Robert Camley



Thomas Crawford  
Sara FitzGerald  
Rahman Mohtasebzadeh



David Serantes  
Daniel Baldomir  
Cristina Munoz-Menendez



Roy Chantrell  
Sergiu Ruta  
**THE UNIVERSITY of York**

Oksana Chubykalo-Fesenko



Ondrej Hovorka  
**UNIVERSITY OF Southampton**

David Cortie  
  
Australian Government



O. Thompson Mefford



78

# Sponsors and Exhibitors



## Micromod Partikeltechnology GmbH

<https://www.micromod.de/>

micromod Partikeltechnologie GmbH is the reliable supplier of particle-based system components for in vitro diagnostics, high-throughput screening, magnetic bio-separation, cell labeling as well as a partner in R&D of novel components for diagnosis (MPI, MRI) and cancer therapy (hyperthermia). A modern quality management according to EN ISO 13485:2016 ensures a high quality standard in the development and production of micro- and nanoparticles.



## Imagion Biosystems Limited

<https://imajionbiosystems.com/>

Imagion's purpose is to find and eliminate cancer. Treatments are more successful and survival rates improve with early detection. By combining high sensitivity imaging technologies with nanoparticle technology, we aim to make the detection of diseases like cancer better and safer for patients as well as provide new methods for therapeutic intervention.



## nanoTherics Ltd.

<http://www.nanotherics.com/>

Nanotherics are the market leader in products for nanoparticle heating and hyperthermia studies utilizing AC magnetic fields. The magneTherm™ system is a totally unique, very competitively priced bench top device which enables magnetic fluid and nanoparticle hyperthermia testing. It operates at a wide range of user-configurable frequencies and field strengths in one system with no hidden extras needed. The magneTherm™ allows users to study magnetic nanoparticle and material heating effects calorimetrically, in-vitro and in-vivo. The magneTherm™ offers internal/external solenoid/pancake coils, options for water jackets (in vivo) plus capabilities to expose cells to AMF on a microscope stage for time lapse studies.



## Chemicell

<http://www.chemicell.com>

Chemicell develops and produces magnetic nano- and microparticles for innovative bioseparation, gene transfection and detection systems. Focus of our product development is to design particles for high quality customer-oriented „ready to use“ kits with special orientation towards the compatibility for labor automatisation. It is chemicell's policy to be open for cooperations with other companies or scientific institutes to maximize the chances and opportunities that evolve from the rapid development of biotechnological procedures and to distribute innovative new products.



## nB nanoScale Biomagnetics

<https://www.nbnanoscale.com/>

We are a technology based company dedicated to the production of scientific and biomedical instruments for **Magnetic Hyperthermia** and other experiments based on **magnetic heating of nanostructured materials**.



## Nanotech Solutions

[www.ntsol.es](http://www.ntsol.es)

Nanotech Solutions develops and manufactures advanced instrumentation for characterising magnetic properties under alternating magnetic fields. Our instrumentation performs AC magnetization measurements of magnetic nanoparticles dispersed in liquids (aqueous or organics), gels, or inside biological matrices at room temperature. Magnetic losses and Magnetization harmonic parameters (amplitude and phase) can be determined for field frequencies from 1 kHz to 350 kHz and field intensities up to 150 kA/m.



## Bruker Biospin Gmbh

<https://www.bruker.com>

With more than 6000 employees in over 90 locations on all continents, Bruker is one of the world's leading companies for analytical instrumentation and

measurement technology. The Bruker BioSpin Pre-Clinical Imaging (PCI) division is a renowned provider of state-of-the-art preclinical imaging technologies, ranging from Magnetic Resonance Imaging (MRI), Computed Tomography (CT), Positron Emission Tomography (PET), Single Photon Emission Computed Tomography (SPECT) to its youngest imaging technology, Magnetic Particle Imaging (MPI).



**MSI Automation, Inc.**  
<https://www.msiautomation.com/>

MSI Automation, Inc. provides superior power to heat difficult to heat nanoparticles. Power Range available is 3.0 KW to 12.0 KW. Frequency Range is 100-450/800 kHz. Heating coils of the round type are available from 40-150 mm. Magnetic Field measurement and Frequency are displayed on the color touch screen. Special Petri Dish Coil is offered for studying the effect of heating while videoing the heating reaction live. A light weight Hand Unit and flexible 3-Meter Cable is available to treat near surface tumors as; Infant Brain, Bone, Thyroid, Breast and Skin.

For more info, check out this [link](#).



Taylor & Francis Group  
an informa business

**Taylor & Francis**  
<https://www.routledge.com/>

Taylor & Francis is one of the leading research publishers in the world. Its key components include Taylor & Francis, Routledge, CRC Press, F1000 Research and Dovepress. Our work as a leading publisher champions the knowledge-maker: serving, connecting and sustaining communities of scholars, instructors, and professionals.



**Quantum Design**  
UK AND IRELAND

**Quantum Design UK and Ireland Ltd**  
<https://qd-uki.co.uk/>

Quantum Design UK and Ireland is part of the [Quantum Design International](#) (QDI) group. The company distributes scientific and industrial instrumentation through an international network, with subsidiaries in every major technological centre around the world. QDI's success in distributing scientific products comes from more than 30 years' experience in manufacturing and distributing its own industry-leading [materials characterisation](#) systems. We also offer the DynoMag instrument which enables determination of the dynamic magnetic properties of liquids, powders and solid samples.



**Sepmag®**  
<https://www.sepmag.eu/>

SEPMAG manufactures **constant force biomagnetic separation equipment**. Its systems enhance the **reproducibility of diagnostic kits** eliminating assay variability, **recover the maximum of beads** and facilitate the validation process through a full **scale up technology**.



**FerroTec**  
<https://www.ferrotec.com/>

Ferrotec provides customers with advanced technology solutions that make their products work better, more precisely, and more reliably. Founded in 1968 on a technology core of FerroFluid magnetic liquid and Ferrofluidic® sealing products, the company and their product portfolio have grown to meet the evolving customer needs



**Magnet Sales & Service Limited**  
<https://magnetsales.co.uk/>

Magnet Sales & Service Limited provides magnetic solutions to a wide variety of markets and applications. Over many years we have worked closely with leading magnetic bead manufacturers, developers and users in providing both standard and bespoke separation devices. Whether you're looking for a rapid or improved separation device for a tube, vessel or plate, or if you require a magnetic separation process as part of your automated equipment or production, then Magnet Sales can help.

# PrecisionMRX® Superparamagnetic Iron Oxide Nanoparticles

The highest quality iron oxide magnetite ( $\text{Fe}_3\text{O}_4$ ) nanoparticles commercially available.

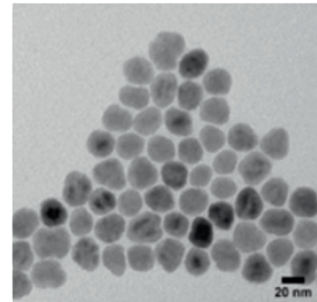
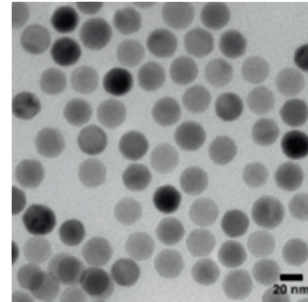
## PRECISE, UNIFORM, CONSISTENT

PrecisionMRX® nanoparticles are superparamagnetic iron oxide nanoparticles with uniform spherical morphology, narrow size dispersity, and high magnetic relaxivity.

To achieve the highest quality, Imagion Biosystems uses the thermal decomposition process, which allows precise control over size, shape, and magnetic properties of the nanoparticles. The manufacturing process is robust and produces high-quality magnetite ( $\text{Fe}_3\text{O}_4$ ) core nanoparticles with minimal batch-to-batch variability.



Conventional Suppliers



### Key Applications

- Superparamagnetic Relaxometry
- Magnetic Resonance Imaging
- Magnetic Particle Imaging
- Magnetically Induced Hyperthermia

### Other Applications

- Vaccine Adjuvant
- Drug Delivery
- Magnetomotive Ultrasound Imaging
- Theranostic Application
- Magnetic Immunoassays
- Magnetic Cell Enrichment Assays



PrecisionMRX nanoparticles are made specifically for the demands of biomedical applications and are available with a variety of coatings to facilitate their uses.

- ▶ Carboxylic Acid Functionalized PrecisionMRX® Nanoparticles
- ▶ Dextran-Coated PrecisionMRX® Nanoparticles
- ▶ mPEG Coated PrecisionMRX® Nanoparticles
- ▶ Oleic Acid Coated PrecisionMRX® Nanoparticles

PrecisionMRX nanoparticles are manufactured by Imagion Biosystems, Inc., a developer of non-invasive, non-radioactive diagnostic imaging technology. Combining nanotechnology and biotechnology, the company aims to use PrecisionMRX nanoparticles to support clinical research and other biomedical applications.

Contact us for bulk quantities or custom orders.

**IMAGION**  
BIOSYSTEMS  
[imaginbiosystems.com](http://imaginbiosystems.com)  
[info@imaginbio.com](mailto:info@imaginbio.com)  
PH: (855) 564-5264



Specialists in Magnetic Nanoparticle Heating

## Magnetherm Systems & Accessories

The **magneTherm™** system has been purpose built for this application for over 16 years and is now the most flexible, affordable, reliable and fit for purpose bench top system available.

*Installed on 5 Continents and over 28 Countries*

The best-selling, purpose designed systems for Nanoparticle Heating studies including: Hyperthermia, Calorimetry, In Vitro & In Vivo studies, Drug Release & Drug Delivery Research.

The New Magnetherm System is available with Full Software control and display of all operating parameters. Method Storage and recall with full data analysis and display of SAR/SLP/ILP.



Software Controlled Option



Our wide range of accessories makes the **Magnetherm** the most flexible System for all your **Nanoparticle Heating Studies**.



Water Jacket Options



Live Cell Exposure Option



Customised & Large Format Coil Options



Drug Release/Delivery Option

Visit our website for further details – [www.nanotherics.com](http://www.nanotherics.com)

Tel. +44 1925 812554 E-mail. [enquiry@nanotherics.com](mailto:enquiry@nanotherics.com)

# chemicell

NEW TOOLS IN BIOSCIENCES

Chemicell develops and produces magnetic nano- and microparticles for innovative bioseparation, gene transfection and detection systems. Focus of our product development is to design particles for high quality customer-oriented „ready to use“ kits with special orientation towards the compatibility for labor automatisation.

It is chemicell's policy to be open for cooperations with other companies or scientific institutes to maximize the chances and opportunities that evolve from the rapid development of biotechnological procedures and to distribute innovative new products.

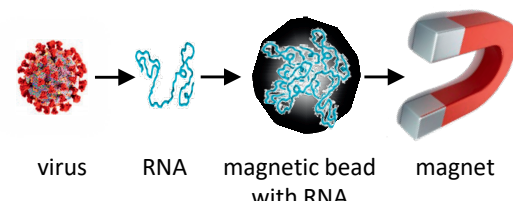


### Fast and efficient isolation of DNA and RNA by means of magnetic SiMAG-DNA particles not only in SARS-CoV-2 times.

**SiMAG-N-DNA** particles have been successfully used to isolate SARS-CoV-2 RNA for rapid large scale testing by RT-qPCR and RT-LAMP.

*Steffen Klein et al. - July 2020 - SARS-CoV-2 RNA extraction using magnetic beads for rapid large-scale testing by RT-qPCR and RT-LAMP.*

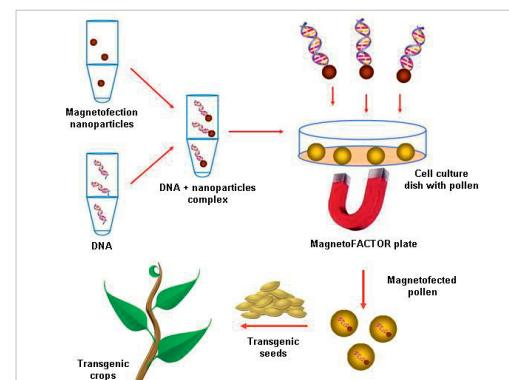
<https://www.mdpi.com/1999-4915/12/8/863>



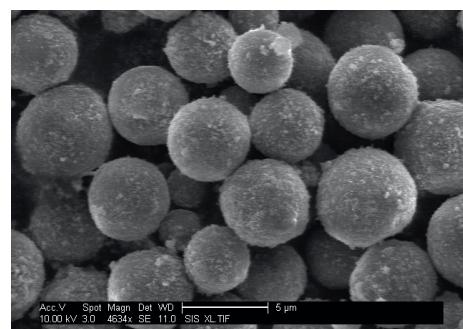
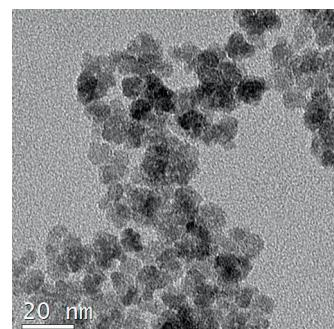
### Magnetofection – magnetic transfection of pollen

The simple and efficient Magnetofection technology was successfully applied to the transfection of pollen. This opens the possibility of the rapid and efficient generation of new variations of transgenic crops.

*Zhao et al. 2017 Pollen magnetofection for genetic modification with magnetic nanoparticles as gene carriers Nature Plants 3, 956–964 (2017).*



### SiMAG / fluidMAG - magnetic nano- and microparticles



### Contact

**chemicell** GmbH  
Eresburgstrasse 22-23  
12103 Berlin  
Germany

info@chemicell.com  
www.chemicell.com



**nanotech  
SOLUTIONS**

PROVIDING INSTRUMENTATION  
FOR EXPLOITING NANOMAGNETICS

## About us

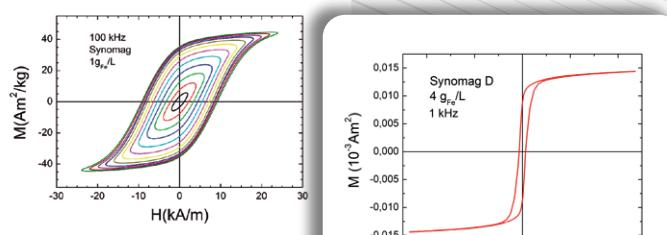
Nanotech Solutions S.L. is an innovation company founded on January 2019 and composed by experts in instrumentation and nanomagnetics research, development and manufacturing.

NTSOL focuses its commercial activities on the development and manufacturing of instrumentation for AC/DC magnetic field generation, or Magnetometry. These Systems are used for characterising the magnetic properties of nanomaterials and for its applications in different areas.

A tight interaction with customers to satisfy their requirements is our major fingerprint as manufacturer.

We are committed with magnetic nanomaterial's users to provide the best to benefit their research and/or industrial activities. NTSOL offers commercial alternatives to suit customer requirements and purchase capabilities: Sales or renting ?

For achieving this goal, "flexibility" guides our actions concerning the design, development, manufacturing and commercialization of NTSOL advanced instrumentation.



### Nanotech Solutions

**Headquarters:**  
C/Miguel Unamuno, 2 3ºB  
40150 Villacastín, Spain

**Commercial office:**  
C/Tomás Bretón, 50-52 4º  
Nave 7, 28045 Madrid, Spain  
+34 609 411 812  
+34 921 124 860  
+34 915 060 293

## AC Magnetometry

**AC Hyster series** are inductive magnetometers that perform calibrated magnetization measurements of magnetic nanoparticles dispersed in liquids, or inside biological matrices under alternating magnetic fields.

We have 3 different models measuring under AC magnetic fields at different field frequency ranges:

- **LF AC Hyster** is an inductive magnetometer whose performance is close to quasistatic conditions: single field frequency (1 kHz) and intensities up to 150 kA/m.
- **SENS AC Hyster** is an inductive magnetometer working in a field frequency range between 10 and 100 kHz up to 24 kA/m with sensitivity down to 300 nano Am<sup>2</sup>.
- **ADVANCE AC Hyster** is an inductive magnetometer working in a field frequency range between 25 and 350 kHz up to 24 kA/m.



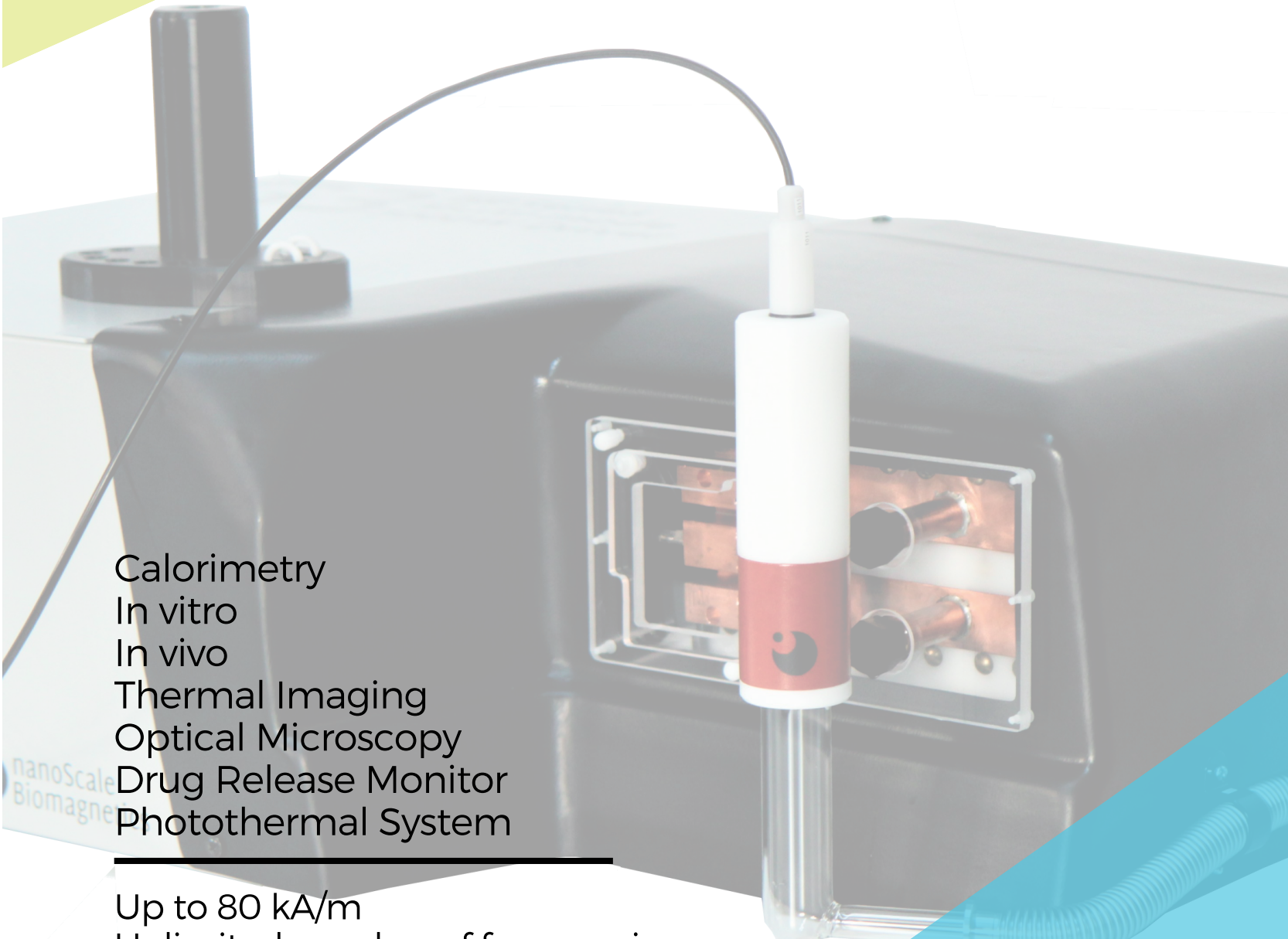
[www.ntsol.es](http://www.ntsol.es)

# D5 series

Instruments for  
Magnetic nanoHeating

Check out this video and find out all the possibilities our magnetic heating equipment can offer you!

 SCAN ME



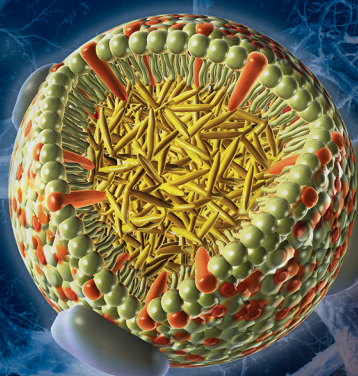
Calorimetry  
In vitro  
In vivo  
Thermal Imaging  
Optical Microscopy  
Drug Release Monitor  
Photothermal System

Up to 80 kA/m  
Unlimited number of frequencies  
Advanced Software integration  
Easily expandable

 nB  
nanoScale  
Biomagnetics  
Experts in Magnetic nanoHeating



# The World's First MPI System, Only from Bruker



The Bruker BioSpin Pre-Clinical Imaging (PCI) division is a renowned provider of state-of-the-art preclinical imaging technologies, ranging from Magnetic Resonance Imaging (MRI), Computed Tomography (CT), Positron Emission Tomography (PET), Single Photon Emission Computed Tomography (SPECT) to its youngest imaging technology, Magnetic Particle Imaging (MPI). Preclinical imaging plays an important role in the understanding of biological processes in both healthy and diseased states and of responses to pharmacological, physiological, or environmental challenges. The use of state-of-the-art analytical technologies can significantly advance clinical diagnosis and therapy routines. With our mission to develop each imaging technology to its best, Bruker drives innovation in new methodologies and solutions for scientists enabling ground-breaking discoveries. Bruker constantly advances Magnetic Particle Imaging in the preclinical area, paving the translational way to clinical perspectives. The use of nanomaterials and their specific response to external magnetic fields is not only crucial for molecular imaging but opens the door to the development of novel theranostic strategies, which in turn can improve patient outcomes and save lives.

To learn more please visit [www.bruker.com/mpi](http://www.bruker.com/mpi)

Innovation with Integrity



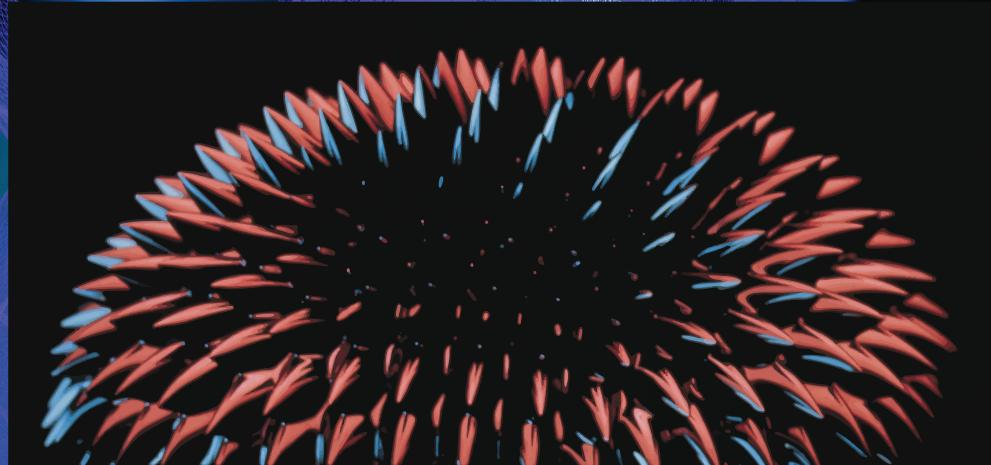
## FERROFLUIDS AND FUNCTIONALIZED BEADS/NANOPARTICLES FOR BIOMEDICAL APPLICATIONS

**FERROBEADS - SILICA COATED MAGNETIC NANOPARTICLES**

**PBG SERIES - PEG COATED MAGNETIC NANOPARTICLES**

**EMG SERIES - WATER-BASED FERROFLUIDS**

**CUSTOMIZED MAGNETIC NANOPARTICLES/BEADS - CARBOXYL, AMINE, OTHER COATINGS**



**FERROTEC (USA) CORPORATION \* 33 CONSTITUTION DRIVE \* BEDFORD, NH 03110**

**603-472-6800 \* [WWW.FERROTEC.COM](http://WWW.FERROTEC.COM) \* [FLUIDSCS@FERROTEC.COM](mailto:FLUIDSCS@FERROTEC.COM)**

# MAGNETIC HYPERTERMIA INSTRUMENT

## Features:

- A. RF Power Supply: 5.0-12.0 kW / 150-450 kHz
- B. Magnetic Power Intensity: 350-1200 Gauss / High SAR Values
- C. Round and Planar Heating Coils: 40-130 mm

### Hand Heating Unit is designed for Hyperthermia Treatment.

The 3.5 kg hand heating device applies hyperthermia heating energy downward and thru the skin to a depth of 30-40 mm. A 3-5 meter flexible cable allows the technician to easily position the heating anywhere over the body's surface. Heating can be concentrated in one area or heating can scan a larger area. Tumors that can be treated are bone, infant brain, thyroid and breast.



MSI Portable Power Supply is Free-Standing and on Wheels. (See Details)

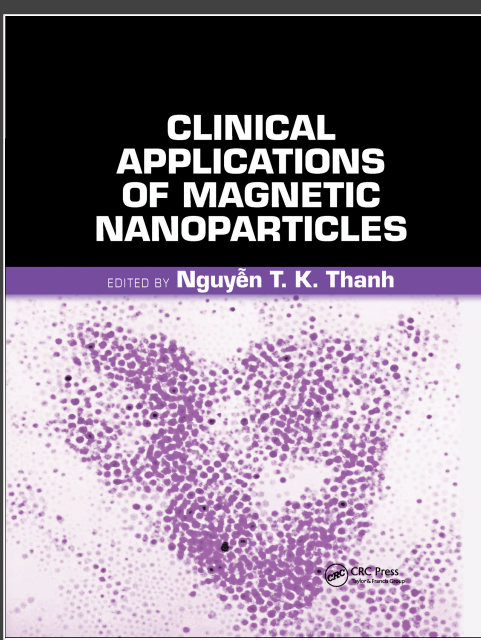
**MSI AUTOMATION, INC.**

Wichita, Kansas 67220 USA

Website: [www.msiautomation.com](http://www.msiautomation.com) / Email: [dave@msiautomation.com](mailto:dave@msiautomation.com)

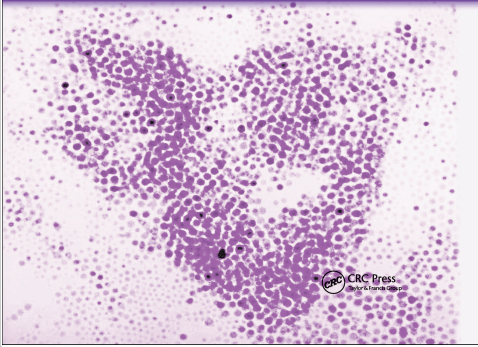
**International Representatives:**

Hong Kong/Shanghai: [www.worldwide-china.com](http://www.worldwide-china.com) / Romania: [www.pro-tehnici.ro](http://www.pro-tehnici.ro)  
Singapore: [www.dmxasia.com](http://www.dmxasia.com)



## CLINICAL APPLICATIONS OF MAGNETIC NANOPARTICLES

EDITED BY **Nguyễn T. K. Thành**



March 2020: 516pp  
358 illustrations

Hb: 978-1-138-05155-3 | \$375.00  
Pb: 978-0-367-90193-6 | \$140.00  
eBook: 978-1-315-16825-8

**20% discount with this flyer!**

# Clinical Applications of Magnetic Nanoparticles

From Fabrication to Clinical Applications

Edited by **Nguyen TK Thanh**, University College London,  
UK

Offering the latest information in magnetic nanoparticle (MNP) research, this book builds upon the success of the first volume and provides an updated and comprehensive review, from synthesis, characterization, and biofunctionalization to clinical applications of MNPs, including the diagnosis and treatment of cancers. The book captures some of emerging research area which was not available in the first volume. This volume, also written by some of the most qualified experts in the field, incorporates new developments in the literature, and continues to bridge the gaps between the different areas in this field.

**20% Discount Available - enter the code FLE22 at checkout\***

Hb: 978-1-138-05155-3 | \$300.00  
Pb: 978-0-367-90193-6 | \$112.00

\*Offer cannot be used in conjunction with any other offer or discount and only applies to books purchased directly via our website.

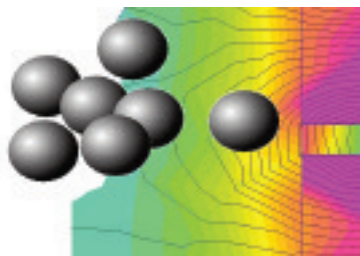
*For more details, or to request a copy for review, please contact:*



CRC Press  
Taylor & Francis Group

For more information visit:  
[www.routledge.com/9780367901936](http://www.routledge.com/9780367901936)

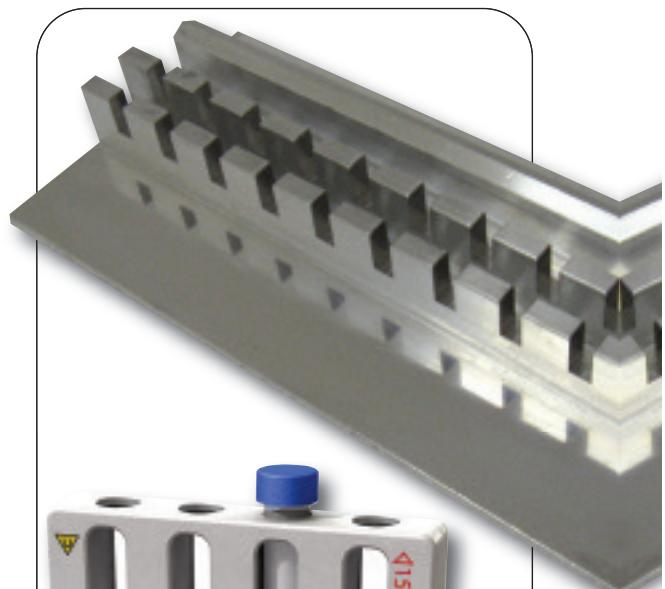
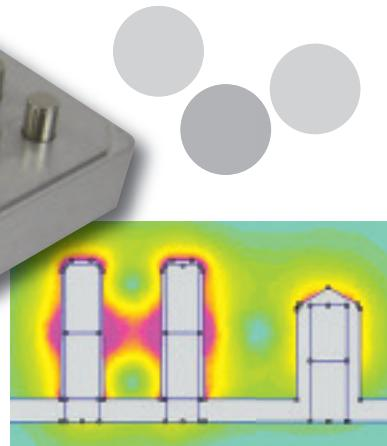
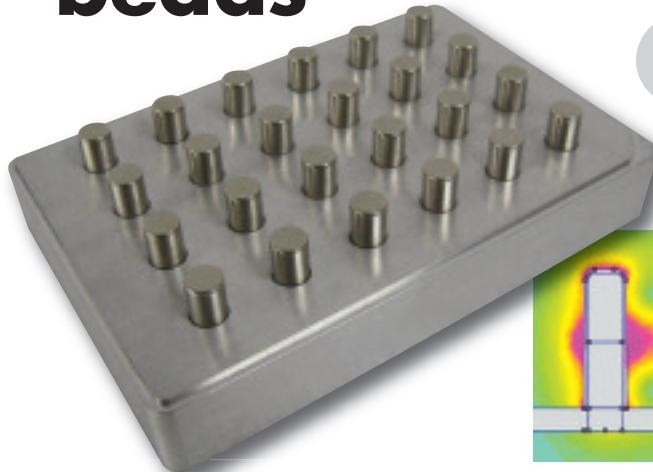
# magnetsales



and service limited

## Providing separation solutions for magnetic beads

**Magnet Sales & Service Limited** provides magnetic solutions to a wide variety of markets and applications. Over many years we have worked closely with leading magnetic bead manufacturers, developers and users in providing both standard and bespoke separation devices. Whether you're looking for a rapid or improved separation device for a tube, vessel or plate, or if you require a magnetic separation process as part of your automated equipment or production, then Magnet Sales can help.



### Magnet Sales & Service Limited

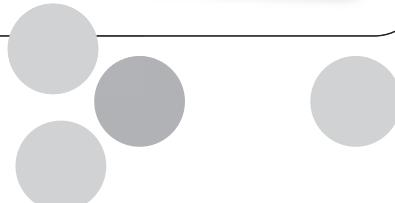
Unit 31 Blackworth Industrial Estate  
Highworth, Swindon, Wiltshire  
SN6 7NA UK

T +44 (0)1793 862100

F +44 (0)1793 862101

E sales@magnetsales.co.uk

[www.magnetsales.co.uk](http://www.magnetsales.co.uk)



# magnetsales

and service limited

# Keeping you at the front of the quantum revolution

**The most extensive range of low temperature  
physics instrumentation**



- Fully automated temperature and magnetic field testing platforms for materials characterisation
- Helium Liquefiers
- Measurement and control solutions for materials characterisation under extreme temperature and magnetic field conditions
- High-precision electrical, optical, and cryogenic systems

## Solutions for R&D and small volumes: monitor your biomagnetic separation process

Developing a magnetic bead-based process is a laborious task. Users often need to work with a wide range of volumes, starting with small tubes and increasing the sample size. Sepmag® proprietary technology generates constant magnetic force at their inner bore, with minimum stray fields. Processes are monitored and recorded, which enables the operator to explore the effects of bead size, concentration, or buffer conditions on the separation time.

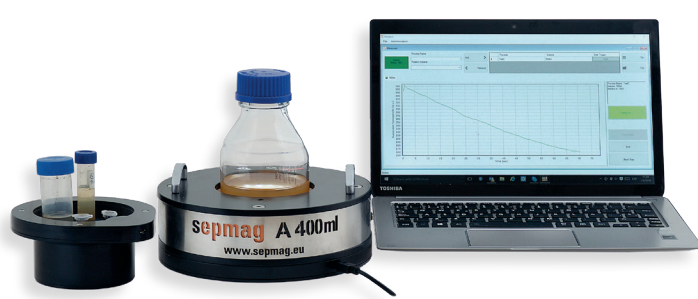
- **Real-time monitoring.** Our **Monitor** - software and hardware - measures optical changes in the suspension, displaying its behavior and comparing different compositions.
- **Well-defined magnetic separation conditions.** Applying a well-defined magnetic force to the entire sample means variations are restricted to suspension characteristics (particles, buffer, ...).
- **Safe System.** Large magnets can be dangerous. Our systems are designed to operate near computers and to protect operators from risks.

### Sepmag® LAB, especially suited to viscous media and/or small magnetic beads/particles

Model	Use
Sepmag® LAB	For small tubes (1.5-50 ml), filled up to 50 mm
Sepmag® LAB L	For small tubes (1.5-50 ml), filled up to 90 mm



### Sepmag® A, for the first steps with commercial magnetic beads and water buffers



Model	Use
Sepmag® A200ml	For 250 ml bottles
Sepmag® A200ml	For 500 ml bottles

Most popular adaptors	
MA211	2x 2ml + 1x 15ml + 1x 50ml
MA022	2x 15ml, 2x 50 ml
MA003	3x 50ml

Any questions? Do you need customized systems? Contact us at [contact@sepmag.eu](mailto:contact@sepmag.eu)



Trusted quality in a new design

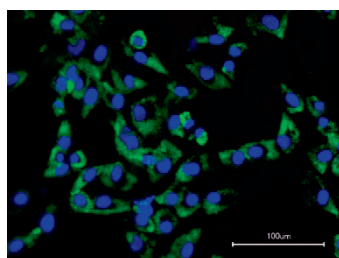


- operating internationally
- more than 25 years experience in particle synthesis and modification
- certified according to ISO 13485 since 2007

### Frontier research with high-quality products

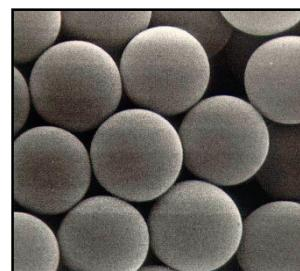
#### perimag®

- for Magnetic Particle Imaging (MPI) and Magnetic resonance Imaging (MRI) research
- for homing and tracking of stem cells in regenerative medicine<sup>[1]</sup>



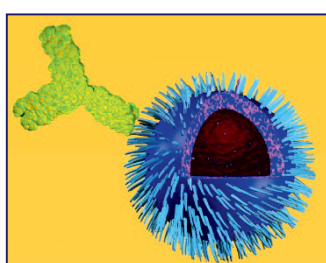
#### micromer®-M

- high magnetomobility and selectivity for cell separation
- components in biosensor and lab-on-chip applications



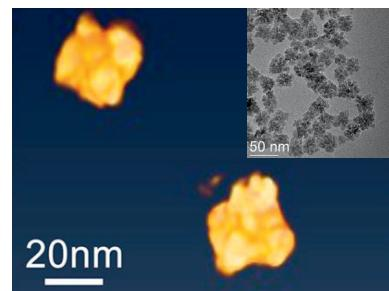
#### nanomag®-D

- high-throughput nucleic acid separation
- components in diagnostic kits and biosensors<sup>[2]</sup>



#### synomag®-D

- for MRI and MPI research
- for hyperthermia applications<sup>[3]</sup>



- Do you require particle design and modification in compliance with ISO 13485?

Get in contact with us: [info@micromod.de](mailto:info@micromod.de) or [www.micromod.de](http://www.micromod.de)

#### References:

- [1] Labeling of hMSC with fluorescent perimag® (nucleus: blue; perimag® in cytoplasm: green) , T. Kilian et al. *Nanomedicine* 2016, 11 (15) 1957-1970.
- [2] Viability assessment of Salmonella cells with nanomag®-D particles, E. Fernandez et al. *Biosensors and Bioelectronics* 2014, (52) 239-246.
- [3] TEM tomography image of synomag®-D, L.J. Zeng, Chalmers University of Technology, Göteborg.



**micromod**  
MODULAR DESIGNED PARTICLES